
Bismuth-mediated Arylation

Author:
Mark Jurrat

Supervisor:
Dr Liam T. Ball

Thesis submitted to the University of Nottingham for the degree of Doctor of Philosophy,
June 2019

Contents

Abstract	III
Acknowledgment	IV
List of Abbreviations	VI
1 Introduction	1
1.1 Motivation	2
1.2 The State of the Art in Directed C_{ortho} -H Activation of Phenols	3
1.3 Direct Arylation using Organobismuth Reagents	6
1.4 Bismuth – The White Matter	7
1.5 Bismuth in Organometallic Chemistry	8
1.6 The Chemistry of Ar_3BiX_2	12
1.7 Strategy	18
2 Arylation mediated by simple Triarylbismuthines	21
2.1 Exploration of Bismuth Sources	22
2.2 Creation of an Organobismuth(III) Library	22
2.3 Electrochemical Investigation	24
2.4 Extension of the Library towards Organobismuth(V) Compounds	26
2.5 Oxidative Arylation using Ar_3BiX_2 Reagents	27
2.5.1 Arylation of 4-Fluorophenol	28
2.5.2 Decomposition of Tri(4-fluorophenyl)bismuth Diacetate	31
2.5.3 Identification of the Decomposition Product	34
2.5.4 Optimisation of Reaction Conditions	36
2.5.5 Assay of Substrates	40
2.6 Kinetic Investigation	42
2.6.1 Naphthol Competition Experiments	43
2.6.2 Influence of Transferred Aryl Groups	45
2.6.3 Influence of Counter Ions	46
2.7 Arylation of Diarylbismuth Species	52
2.7.1 Transmetallation Using Organoboron Reagents	54
2.7.2 Solvent Dependency of the Transmetallation	55
2.7.3 Investigation into the Rate Determining Step	56
2.8 Oxidation and Combination of the Individual Steps	58
2.8.1 Halonium Reagents	59
2.8.2 Peroxo Reagents	61
2.8.3 Quinones	62

2.8.4	Miscellaneous Oxidants	63
2.8.5	Electrochemical Oxidation	64
2.9	Conclusion	65
3	Arylation mediated by Bismacycles	67
3.1	Identification of Appropriate Bismacycle	68
3.2	Optimisation of Individual Segments	77
3.2.1	Creation of a Thiabismine Dioxide (<i>Pseudo</i>)halide Library	77
3.2.2	Transmetallation	78
3.2.3	Influence of Base	78
3.2.4	Influence of Solvents	79
3.2.5	Optimized Conditions and Screen of Boronic Acids	81
3.2.6	Extention of the Transmetallation Methodology	83
3.2.7	Crystallographic Analysis of Aryl/Heteroaryl Thiabismine Dioxides	84
3.2.8	Mechanistic Investigation	86
3.2.9	Assessment of Bpin Transmetallation Reagents	87
3.3	Identification of Suitable Oxidants	88
3.4	Arylation of 2-Naphthol	90
3.5	Combination of the Individual Steps in a One-Pot-Protocol	91
3.6	Establishing Substrate Scope	92
3.6.1	Variation of the Boronic Acid	92
3.6.2	Application to Naphthol-like Substrates	95
3.6.3	Application to Phenolic Substrates	98
3.6.4	Expansion of Methodology to Thiophenols	104
3.7	Mechanistic Investigation	104
3.7.1	Investigation of Oxidation/Arylation	104
3.7.2	Identification of Aryl Thiabismine(V) Dioxide Reagents	106
3.8	Large Scale Access to Thiabismine Dioxide Tosylate Precursor	112
3.9	Recovery and Recycling of Thiabismine Dioxide Co-product	113
3.10	Conclusion	114
4	Future Projects	116
4.1	Tuning the Backbone	116
4.2	Extension Scope	117
4.3	Elevation to a Catalytic Regime	118

Abstract

Initial efforts were focused on the development of a catalytic protocol for the arylation of hydroxyarenes using Ar_3BiX_2 reagents. The individual steps oxidation, arylation and transmetallation were investigated separately to be combined in the final step. While the arylation of phenolic substrates results in low overall yields and selectivities, switching to 2-naphthol improved yields drastically, allowing for a mechanistic investigation into the rate and selectivity determining step of the oxidative arylation, the role of electronic properties of substrate and transferred aryl group, as well as the counter ion on the bismuth centre. The diaryl bismuth reaction product was identified and conditions for transmetallation from organoboron reagents to result in a Ar_3Bi compound were developed. While oxidation of the Bi(III) reagent could be achieved efficiently with a variety of oxidising agents, a combination of the three steps proved unsuccessful due to the inherent incompatibility of the necessary reagents, precluding development of a catalytic application of bismuth. For a stepwise stoichiometric approach, a variety of bismacyclic compounds have been prepared and tested concluding in a thiabismine dioxide core. Different bismacycle (*pseudo*)-halide salts of the thiabismine dioxide core have been prepared and their capability for transmetallation have been investigated. The reaction proceeds *via* a μ -oxo intermediate under basic conditions using readily available boronic acids. With a scope involving electron rich to electron poor aryl motifs as well as sterically demanding and even heterocyclic rings, a simple and robust transmetallation protocol has been developed. The subsequent oxidation and arylation was achieved using *m*CPBA as the oxidant with 2-naphthol as the initial substrate. Notably, no base is required in the arylation process. The scope was extended to numerous naphtholic and phenolic substrates. Mechanistic investigations of all significant processes have been conducted allowing for unprecedented insight into bismuth-mediated arylation, that provide a deeper understanding and provides *a priori* prediction for untested substrate combinations.

Acknowledgment

If there is anyone to acknowledge in this thesis, it's probably bismuth. Thank you for being such an interesting, surprising, yet frustrating element to work with. I spent so many hours trying to figure you out, but every time I thought I understood you, you showed me a new side of you. You have truly been the trouble of my life the last 3 years, of which are none that I would want to miss.

Also thanks to Claude Fraucious Geoffroy for proving it distinct from lead. Good job there.

Prof. Sir Derek Barton needs to be acknowledged at this point because he is the root of all evil finding bismuth's unique reactivity and inspiring Liam to pursue this research. Also thank you for settling for one Nobel Prize leaving the mysteries of organobismuth chemistry for me to unravel.

Thank you Alastair Lennox for bringing me in contact with Liam. This would have never happened without you.

And to the man of the hour, or better my last 3 years, Dr Liam Thomas Ball: Thank you for choosing me as your first PhD student in your newly established research group. Thank you for teaching me, advising me and always making me feel like we can do this, no matter how grim the results. Thank you for this opportunity, I am and was well aware of the implications it held. I appreciate the challenge this project entailed. That was exactly what I wanted: starting something from nothing, something hard, something new, something that is worth pursuing. Despite the sentimentality writing these lines, I have to say overall I enjoyed this project not although, but because it required the best of me. I know it was all guts and no glory, but I knew what I was getting into. I hope I was what you imagined a PhD student in your group would be like and set the bar where it needs to be for everyone following me.

Thank you Lorenzo, for enduring the time spent with me. I know it wasn't easy at times and you had to spend the most with the grumpiest member of the Ball Group.

Thank you Tom, for providing an extra level of Britishness to my days and helping me to narrate them with the weirdest song lyrics. Thank you for providing your Gutenbergian talents at the bitter end.

A special thanks goes out to Simon Woodward and his research group with which I had the pleasure of sharing a lab and office with. Especially, Ryan Nouch with whom I was always able to bounce off ideas and shuttlecocks. And Murdau - truly the main man. I would like to thank all the master's and summer student, who I had the pleasure of working with: Jamie and Michele, Björk, Ellie and Evie, and James, red James and the other James

(Charlie). Thank you to all the late additions to the Ball Group as well. You truly made this a unique experience.

The Walsh and O'Reiley groups have to be acknowledged for their support and helping me working with bismuth as well as awarding me with the honor member status.

No work would have been done without the analytics department (Neil Barnes, Mark Guyler, Tom Clayton, Adrienne Davies, Kevin Buttler, Mick Cooper, Ben Pointer-Gleadhill, William Lewis). And thank you Shaz for teaching me valuable life lessons. Also thank you Pete Licence for showing me that there also is a different approach to success.

Gratitude belongs to Lian Tze Lim, who helped me understand the mystery that is Latex. Thank you East Midlands Airport for providing me with easy access to the Vaterland.

Thank you to Andrew and Beth Gomm for their hospitality and making me feel home in this foreign land of Britain. And thanks David Cameron for this glorious Brexit that you brought to your country. It was a great time to see the tragedy unfold, while still being able to leave the shit show at any point.

Thank you Cullin, Gareth, Charlotte, Ed, Katharina and Tom for distracting me from work by going on amazing quests with me.

Thank you Robby and Daniel Aminati for showing me that anything is possible if you put your mind to it.

Thank you Julia, for supporting me through the last leg of this thesis and the following tedious write-up. It was tough for me, but surely having to keep up with me must have been even tougher.

And since there is a little more space, let's fill it with a picture of Enrique Echidna:



List of Abbreviations

18-Crown-6	1,4,7,10,13,16-Hexaoxacyclooctadecane
Alk	Alkyl
Ar	Aryl
ATR	Attenuated total reflection
BTMG	2- <i>tert</i> -Butyl-1,1,3,3-tetramethylguanidine
CAN	Ceric ammonium nitrate
DABCO	1,4-Diazabicyclo[2.2.2]octane
DBU	1,8-Diazabicyclo(5.4.0)undec-7-ene
DMF	<i>N,N</i> -Dimethylformamide
DMP	Dess–Martin periodinane, 1,1,1-triacetoxy-1,1-dihydro-1,2-benziodoxol-3(1 <i>H</i>)-one
DMPU	<i>N,N'</i> -Dimethylpropyleneurea
DMSO	Dimethylsulfoxide
EI	Electron ionization
EMIM-Cl	1-Ethyl-3-methylimidazolium chloride
EPR	Electron paramagnetic resonance
ESI	Electrospray ionization
Et ₂ O	Diethyl ether
HFIP	1,1,1,3,3,3-Hexafluoroisopropanol
HMPT	Hexamethylphosphorus triamide

HOMO	Highest occupied molecular orbital
HRMS	High resolution mass spectrometry
HSAB	Hard and soft acid and base
IUPAC	International Union of Pure and Applied Chemistry
KIE	Kinetic isotop effect
LUMO	Lowest unoccupied molecular orbital
M	Metal
MALDI	Matrix Assisted Laser Desorption/Ionization
<i>m</i> CBA	<i>meta</i> -Chlorobenzoic acid
<i>m</i> CPBA	<i>meta</i> -Chloroperbenzoic acid
MeCN	Acetonitrile
MeTHF	2-Methyl tetrahydrofuran
NBS	<i>N</i> -Bromosuccinimide
neo	Neodecanoate
NFSI	<i>N</i> -Fluorobenzenesulfonimide
NMR	Nuclear magnetic resonance
OAc	Acetate
OTFA	Trifluoroacetate
OTf	Trifluoromethanesulfonate
OTs	Tosylate
OXONE [®]	2KHSO ₅ ·KHSO ₄ ·K ₂ SO ₄
Selectfluor [®]	1-(Chloromethyl)-4-fluoro-1,4-diazoniabicyclo[2.2.2]octane ditetra-fluoroborate
SI	Supporting Information
ssce	sodium saturated calomel electrode

TBA	Tetrabutylammonium
TBACl	Tetrabutylammonium chloride
TBHP	<i>tert</i> -Butyl hydroperoxide
TEMPO	(2,2,6,6-Tetramethylpiperidin-1-yl)oxyl or (2,2,6,6-tetramethylpiperidin-1-yl)oxidanyl
THF	Tetrahydrofuran
TLC	Thin layer chromatography
TMG	1,1,3,3-Tetramethylguanidine
TRIP	2,4,6-Triisopropylphenyl
UV light	Ultraviolet light

1 | Introduction

Abstract: 2-Hydroxybiphenyls are a valuable motif in biologically relevant compounds. Current protocols for their synthesis suffer from insufficient atom economy, a multi-step procedure, uncontrollable selectivity, the use of expensive, toxic metal catalysts, overarylation and harsh reaction conditions to a limited scope, making them impracticable protocols for a mass audience and industrial application.

Organobismuth chemistry is a field that was widely investigated during the 1980s with the ground breaking work of Barton *et al.* with a specific focus on organobismuth reagents for the arylation of a wide range of substrates. However, since then not much research has been carried out in this field due to the low atom efficiency, substrate controlled selectivity and the overall lack of understanding of the mechanism in general.

This chapter will lay the ground work for the establishment of organobismuth chemistry in the Ball research group by giving an introduction to organic bismuth reagents as well as their specific reactivity. A particular focus will be the bismuth-mediated oxidative arylation of phenols as well as the traditional approaches to perform this transformation in order to set the scene for following investigations.

1.1 Motivation

The 2-hydroxybiphenyl motif can be identified as the core structure of numerous biologically-active and synthetically relevant molecules including more than 4000 natural products. Many of these demonstrate antimalarial, anti(retro)viral or cytotoxic properties.^{2,3}

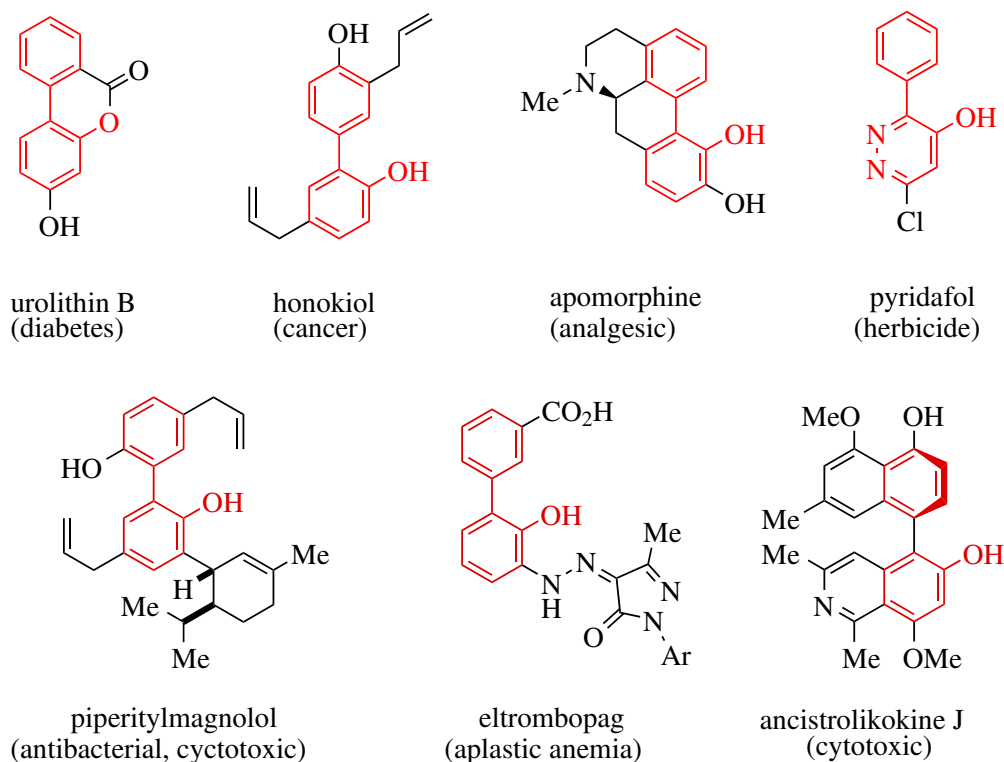
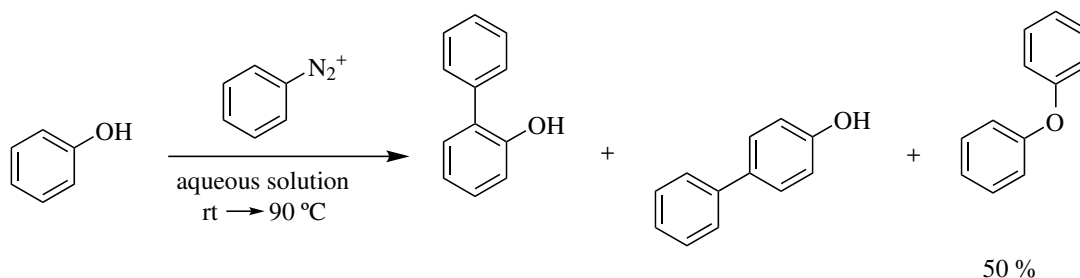


Figure 1.1.1: Selected examples of biologically active substances carrying a 2-hydroxybiaryl motif

Given this broad significance, methods for the preparation of 2-hydroxybiaryls are highly valued and have been the subject of much research effort. Classic preparative pathways involve metal-catalyzed arylation of a hydroxyarene-derived substrate *via* either cross-coupling or C–H functionalisation. However, expedient methods for the synthesis of 2-hydroxybiaryls remain scarce due to various disadvantages of the individual protocols. This includes bismuth-mediated direct arylation of phenols, which offers a unique reactivity, but is deprived with regards to atom- and step economy, reactivity and mechanistic insight. This thesis will lay out the opportunity provided within organobismuth chemistry and will address the issues of current protocols. This work will enable bismuth-mediated arylation as an attractive tool for late stage functionalisation and industrial application.

1.2 The State of the Art in Directed C_{ortho} -H Activation of Phenols

The earliest examples of activation of the C-H bonds of phenol by arylation have been reported as early as the late 19th century. These reports exploit the relatively easy access to cationic phenyl species *via* phenyl diazonium reagents. Upon elimination of N₂ the resulting Ph⁺ species were used to perform an electrophilic aromatic substitution on phenol (Scheme 1.1).^{4,5}

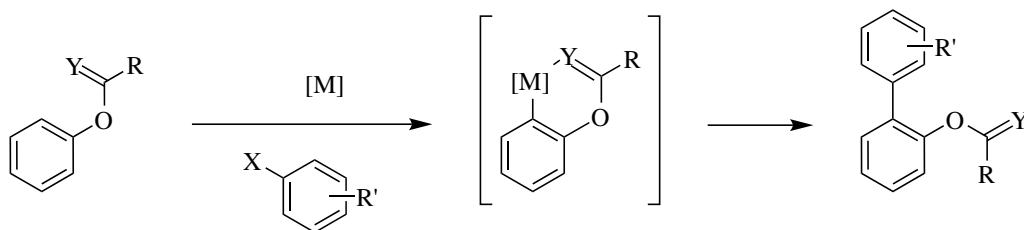


Scheme 1.1: Direct arylation of phenols using phenyl diazonium species. Ratio of the C -arylation products has not been specified.⁵

As can be seen in Scheme 1.1 this procedure occurs with low chemoselectivity resulting in 3 observed products. The phenylation products in *ortho* and *para* position of the phenolic ring obey the trends that have been established for S_{EAr} and S_N reactions before. The lack of selectivity renders this methodology inefficient and it has therefore not been employed further for non-*para*-substituted phenols.⁶

This overarching problem of poor regioselectivity on phenolic substrates has been predominant since these first cases of electrophilic aromatic substitution.⁷ Palladium-catalyzed direct arylation of phenols with aryl iodides has been established with the same problem. There, selectivity can be tweaked towards directed arylation at the *para* position,⁸ but the selective access to the *ortho* could only be achieved with the *para*-position blocked, rendering this methodology unfeasible for our endeavours.

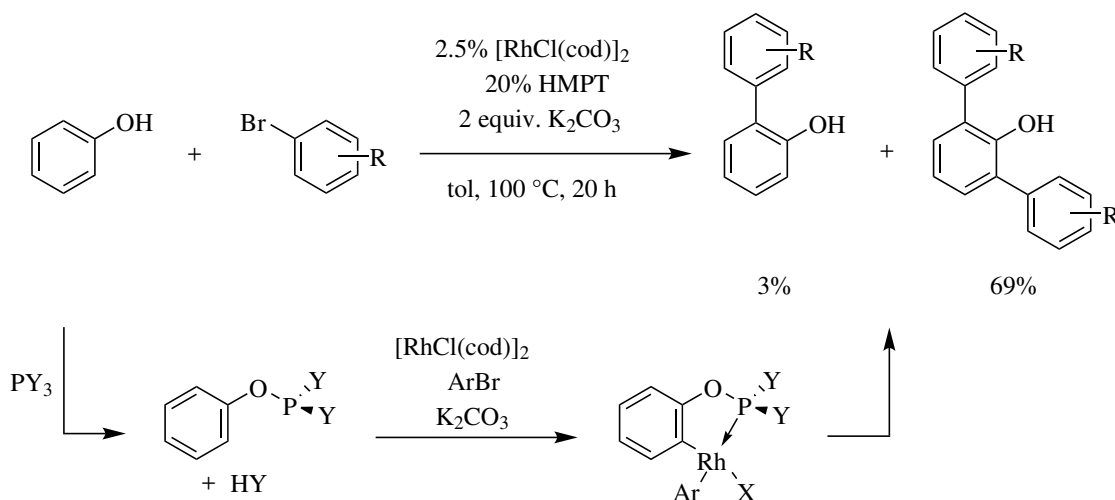
In order to facilitate *ortho* functionalisation, the use of directing groups has been exploited. Hereby, the phenol group is functionalised to allow a pre-coordination of the metal catalyst to ensure a selective C-H bond activation. Used methods include the prefunctionalisation of phenols as carbamates,^{9,10} pivalates,¹¹ and ethers of pyridines¹² and pyrimidines¹³ to render them directing groups for ruthenium or palladium (see Scheme 1.2). These groups, although excellent in directing the arylation, implicate the need for preinstallation and post reaction removal. This results in a less time, step and atom economic process.



Scheme 1.2: Selective *ortho* arylation of phenols enabled by directing groups, with Y = N, O and R, R' = aryl, alkyl

In the following selected examples of directed arylation will be presented, where the directing group is installed and cleaved *in situ*, allowing an easy access of the desired 2-hydroxyphenol from phenol without the need for additional steps.

A key example of this methodology is a rhodium-HMPT-catalyzed protocol using aryl bromides.¹⁴ In the first step hexamethylphosphorus triamide (HMPT) reacts with the phenol substrate to create a mixed PhOPY_2 species, where Y is either NMe_2 or a phenoxy species (see Scheme 1.3).

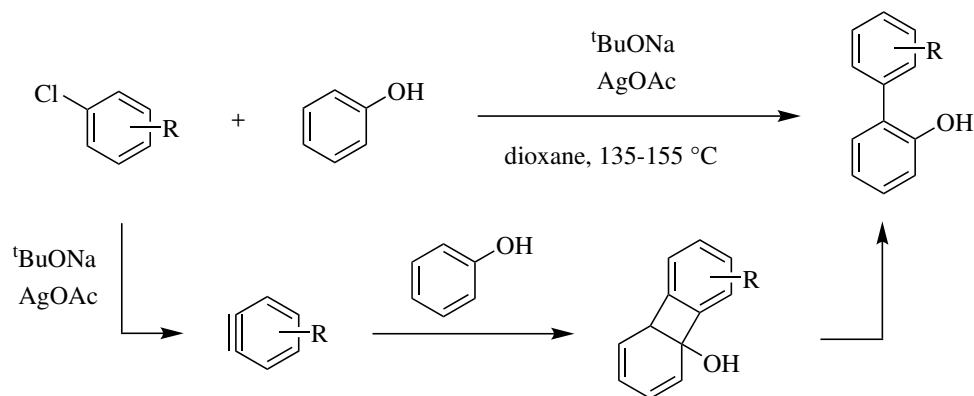


Scheme 1.3: Rh catalysed *ortho* arylation of phenols using HMPT as a directing group. With Y = NMe_2 , OPh, Obiphenyl; R = any and X = Cl, Br

The lone pair of the phosphorus is subsequently used as a directing group for the rhodium to enable the selective C-H activation in *ortho* position of the phenol. Unfortunately, isolation of the desired product obtains low yields despite excellent conversion of the aryl bromide. The major product of this transformation has been identified as the diarylation product. This overarylation effect might be explained by an accelerated reactivity of the rhodium centre with the increasing steric bulk of the phosphorus ligand throughout its arylation or simply the physical proximity of the substrate on the phosphine following the arylation.¹⁵

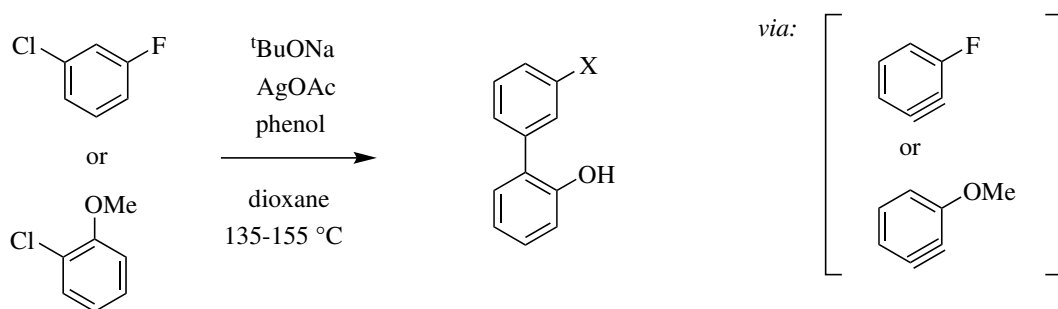
The arylation of phenols in a metal-catalyst-free procedure has been reported through an aryne pathway (see Scheme 1.4).¹⁶ Here an aryl chloride is treated with a silver salt

and base under harsh conditions (155 °C, dioxane) which is proposed to force the generation of an aryne, that can undergo a [2+2] cycloaddition with the phenolate. The resulting biphenylene intermediate can be quenched with H₂O to result in the desired 2-hydroxybiphenyl motif. While this procedure shows good yields for neutral and electron-deficient aryl chlorides, electron-rich representatives show no observable conversion.



Scheme 1.4: Arylation of phenol *via* an aryne intermediate mechanism

Regioselectivity of the aryl chloride component is equally limited as 1-chloro-3-fluorobenzene results in 3'-fluoro-[1,1'-biphenyl]-2-ol while 1-chloro-2-methoxybenzene equally results in the 3' substituted 3'-methoxy-[1,1'-biphenyl]-2-ol (Scheme 1.5). Together with with harsh conditions, this methodology can be considered non-viable as a general protocol for late stage functionalisation.

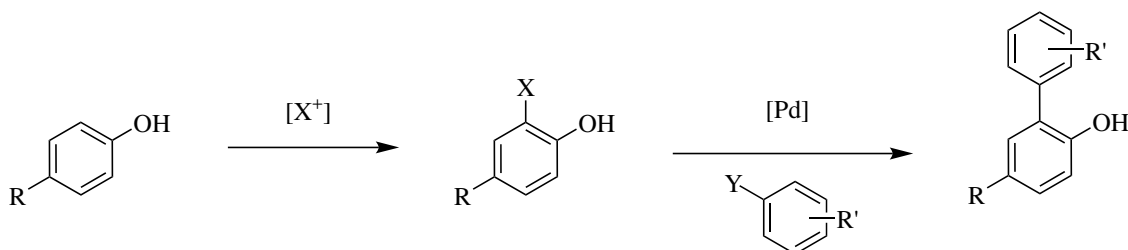


Scheme 1.5: Selectivity determination by the formation of the aryne intermediate, with X = F, OMe

The previously examined examples represent the contemporary knowledge on direct C-H activation for a direct C-C bond formation in the *ortho* position of phenols. While this appears surprising given the importance of this motif, an easy explanation can be found looking at the current approach in today's synthetic planning.

Methods for the bromination and a subsequent Suzuki-type cross-coupling have been the norm in current strategic synthesis approaches (see Scheme 1.6). However, methods for the

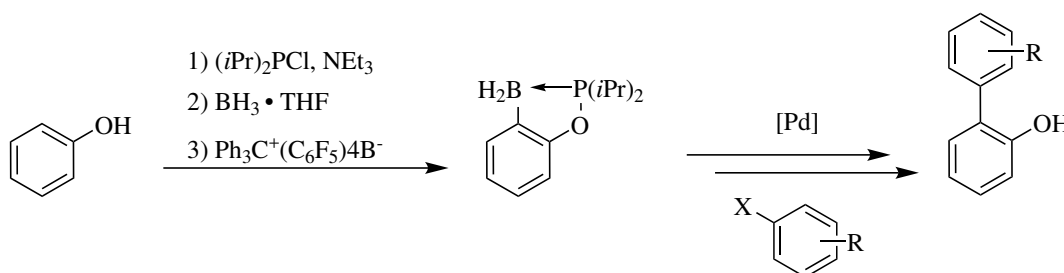
bromination on unfunctionalised phenol do not show promising results,^{17,18} but functionalised examples with good selectivity are ubiquitous.^{19–22} The subsequent Suzuki/Stille cross-coupling reactions have probably been some of the most well studied reactions at this point in time.^{23–26} Both reactions have been proven reliable, robust and high yielding, making the extra effort of going through a 2-step process the viable option.



Scheme 1.6: 2 step protocol using a halogenation followed by a Suzuki/Stille coupling. With R, R' = any, X = I, Br and Y = boronic acids, organostannanes

The less common approach of using the phenols as the boronic acid component is enabled by borylation of the phenol substrate. While most boronic acids derive from their halogenated counterparts^{27–29} in good yields, a direct lithiation followed by a borylation of phenols traditionally shows low yields.³⁰

Direct borylation of the *ortho* position of phenols can be achieved in a similar fashion to the examples used for direct C–H activation (*vide supra*). Di-isopropyl arylphosphinite allows for precoordination of a borane species. Upon addition of a hydride acceptor, a borenium cation is formed that undergoes electrophilic aromatic substitution in the *ortho* position of the phenol. The reaction product can subsequently be used as a transmetalation reagent in a Suzuki coupling reaction.³¹

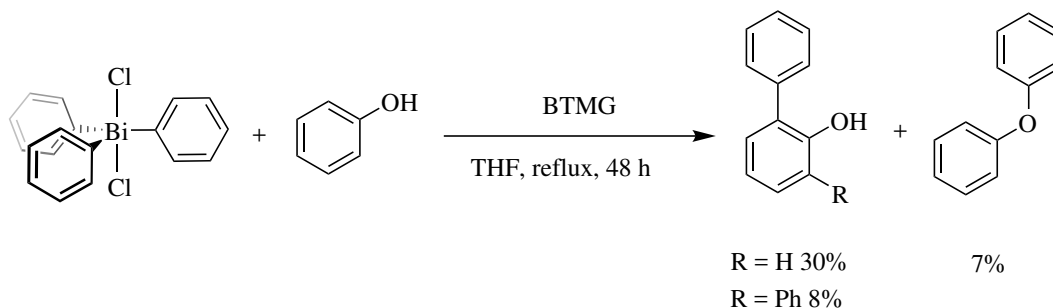


Scheme 1.7: Direct borylation of phenol with subsequent cross-coupling to form the 1-hydroxybiaryl motif. With R = any and X = I, Br

1.3 Direct Arylation using Organosbismuth Reagents

The direct arylation of phenols using organobismuth(V) reagents has been reported by Barton *et al.* in the 1980s (see Scheme 1.8). Here triphenylbismuth dichloride is reacted

with phenol in the presence of base to create 2-hydroxybiphenyl without the need for prior functionalisation. Despite overall yields and selectivities being low, this reaction offers a single-step approach to this valuable structural motif.



Scheme 1.8: Phenylation of phenol with 1.5 eq. of Ph_3BiCl_2 and 2.0 eq. of BTMG,³³ 8% biphenyl homocoupling product observed

Bismuth itself has no appreciable toxicity or negative environmental impact.³⁴ Combined with the low cost of the element, and the unique reactivity of its compounds, bismuth offers huge potential in synthetic organic chemistry. Given their oxidative nature, Bi(V)-mediated arylations are tolerant of the synthetically valuable halide functionality, rendering them orthogonal to the transition-metal catalysed cross-coupling methods commonly used to access these important molecular architectures.³⁵ However, the intrinsic appeal of the bismuth methodology is diminished by a) the need for stoichiometric amounts of the heavy metal, b) the limited commercial availability of different triarylbismuth(III) reagents, the synthesis of which typically employs highly reactive organometallic species, and c) the incorporation of only one of the three aryl groups into the product, representing poor atom economy. Overcoming these intrinsic disadvantages of bismuth-based redox arylations will greatly enhance application of this novel reactivity.

1.4 Bismuth – The White Matter

Bismuth (from German *Wismuth* meaning *white matter*) is a soft, heavy and lustrous metal that has been known to human kind since ancient times. While first being mentioned in the 1450s,³⁶ it took until 1753 for Claude Geoffroy the Younger to finally prove it to be distinct from lead.³⁷

Bismuth is the 69th most abundant element in the earth's crust with an estimated content of 0.008 ppm,³⁸ which makes it twice as abundant as gold.³⁹ While bismuth can be found in its native state, it is more commonly found in *bismuthinite* (Bi_2S_3) and *bismite* (Bi_2O_3) which naturally accompany ores of lead, copper, tungsten, tin, silver and gold.⁴⁰ The mate, slag, flue dust and fume discharged in the smelting process of these metals as well as the slime from electrorefining contain high amounts of bismuth, that are recovered in the Betterton-Kroll^{41,42} and the Betts processes.⁴³ This makes bismuth a common by-product

of the currently more desired metals, allowing for a relatively cheap price of 11 £/kg despite its low natural abundance. The world's production is estimated at 13.6 Mt in 2015, coming from China (55%), Vietnam (37%), Mexico, Russia and Bolivia.³⁹ The metal is commonly known for the large brittle crystals with a multi-coloured gleam that molten bismuth creates upon slow cooling. As a metal, bismuth possesses extraordinary properties: it has the highest diamagnetism, the lowest thermal conductivity (except mercury) and the highest Hall effect of all metals.³⁷ Given its half-life of radioactive decay of $1.9 \pm 0.2 \cdot 10^{19}$ years,⁴⁴ which is more than the current age of the universe, bismuth is considered the heaviest stable element.

Bismuth's properties are also outstanding with respect to its location in the periodic table. In contrast to its direct neighbours, and despite its heavy metal status, it is considered non-toxic and non-carcinogenic.³⁴ Hence, it finds use in medicine and veterinary practice and cosmetics. Bismuth subnitrate and subcarbonate are used in medicine; Pepto-Bismol (bismuth subsalicylate) for the treatment of stomach disorders and diarrhoea⁴⁵ as well as syphilis.^{46,47} Bismuth oxychloride is used to impart a pearlescent effect to lipstick, nail varnish, eye shadow and make-up powder. Accidental intoxication has only been reported by large doses of medical products rather than by exposure at the workplace.³⁶ The effects of acute intoxication include gastrointestinal disturbance, dark coloured stool and/or tongue, anorexia, headache and dislocation of the mucous membrane.^{36,48}

In industrial organic synthesis bismuth is used in the manufacturing of acrylonitrile and acrolein in heterogeneous Co-Bi-Mo or Pb-Bi-Mo systems.^{36,49} Bismuth is the environmentally friendly substitute to lead in fishing weights, ammunition, lubricating greases and alloys.³⁹ With other metals such as tin and cadmium, bismuth forms low melting alloys which find their application in fire detection and extinguishing systems.³⁷

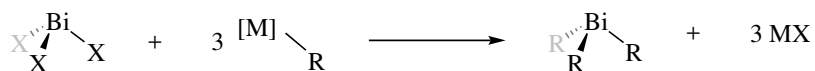
1.5 Bismuth in Organometallic Chemistry

Bismuth, the 83rd element of the periodic table, is the heaviest member of the pnictogens. Consistent with its ground state configuration of $[\text{Xe}] 4f^{14} 5d^{10} 6s^2 6p^3$, its most common oxidation states are +3 and +5.

Organobismuth(III) Compounds

While the role of inorganic bismuth(III) salts is limited to their use as Lewis acids,^{50–52} their organometallic counterparts show a more diverse chemistry.

BiEt_3 was the first reported representative of this class.⁵³ Since then, the preferred method of synthesis has shifted towards accessing organobismuth(III) reagents through a transmetallation reaction of an inorganic bismuth(III) salt ($\text{BiCl}_3/\text{BiBr}_3$) and a metallorganic reagent such as Grignard- and organolithium (Scheme 1.9).^{54–57}



Scheme 1.9: Synthetic pathway to organobismuth(III) compounds, with X = Cl, Br; R = aryl, alkyl, MX = MgX₂, LiX and M = MgX, Li

The procedure described in Scheme 1.9 forms the basis of nearly all organobismuth chemistry. Trialkyl bismuthines show sensitivity towards air while stable being stable in degassed water, with the lighter members showing pyrophoric properties.^{53,54,58} Given the challenges associated with their synthesis and handling, trialkyl bismuthines are less investigated than their aryl analogues with as few as 10 structurally described compounds.⁵⁹ Triaryl bismuthines are considered bench stable and show little to no sensitivity towards air- and moisture-induced decomposition.³⁶ The simplest member of this group is triphenyl bismuth. As displayed in Figure 1.5.1 it adopts a trigonal pyramidal conformation with bismuth-carbon bond lengths of 2.25(2) Å. The long bismuth-carbon bond in combination with the disparity of their individual orbital sizes leads to a poor orbital overlap, resulting in a highly polarised bond (Bi^{δ+}-C^{δ-}). With 137 kJ/mol, the resulting Bi-C bond strength is the weakest in comparison with the lighter pnictogen-carbon bonds.⁶⁰ The high degree of *s* character of the lone pair is due to the lack of hybridisation with the bonding 6*p* orbitals and is reflected in the smaller C-Bi-C angle of 94(1)° in comparison to the lighter pnictogens.⁶¹⁻⁶⁴

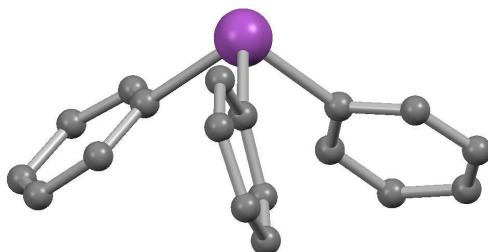
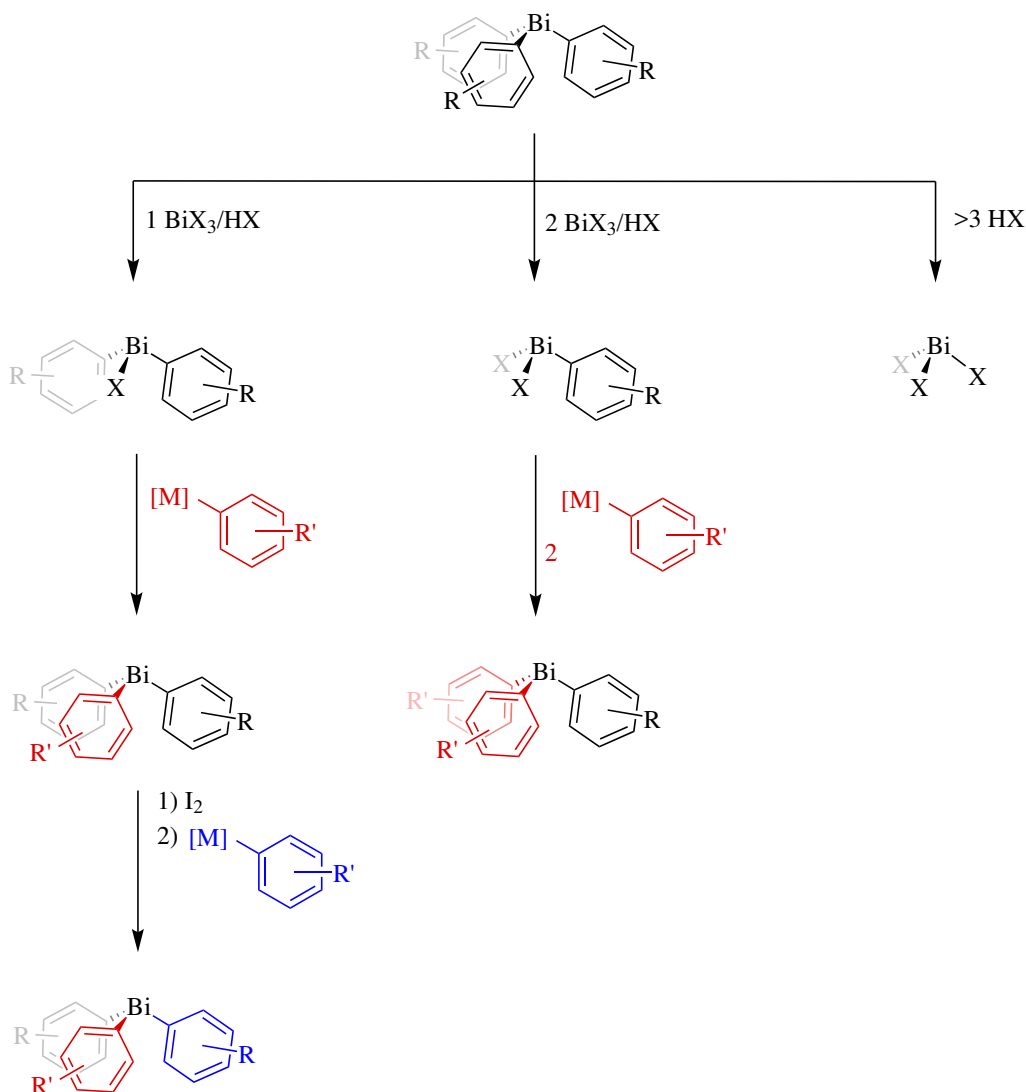


Figure 1.5.1: Molecular structure of triphenyl bismuth⁶⁵ (Ball and Stick, hydrogen atoms omitted for clarity)

Due to their preparation method, homoleptic triaryl bismuthines represent the vast majority of reported space. The generation of heteroleptic triaryl bismuthines traditionally involves the synthesis of the aryl bismuth halides as intermediates which is subsequently reacted with a 2nd/3rd organometallic reagent.^{66,67} Due to the low solubility of Ar₂BiX and ArBiX₂ and their hydrolytic sensitivity these species are traditionally generated *in situ*. Here either a comproportionation of triaryl bismuthines with either one or two equivalents of inorganic bismuth salt BiX₃ (with X = Cl, Br; see Scheme 1.10) or the protodebismuthation using acids (X = Cl, Br, OTs) have been reported.^{66,68-71}



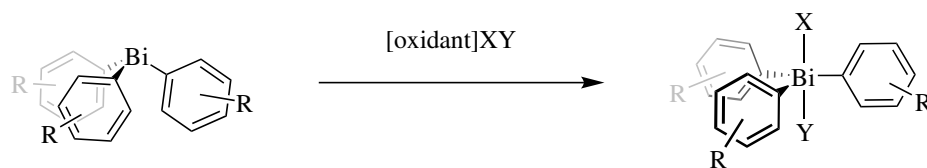
Scheme 1.10: Synthesis of unsymmetrical organobismuthines, $\text{M} = \text{MgX}, \text{Li}$

The preparation of triaryl bismuthines bearing three different aryl groups was first achieved by Matano *et al.* in 1996.⁷² Here, the mentioned unsymmetrical triaryl bismuthines of type $\text{Ar}_2\text{Ar}'\text{Bi}$ were treated with iodine. The most electron-rich aryl group is eliminated to result in $\text{ArAr}'\text{BiI}$ which can then be arylated by previously describe methods to result in the desired $\text{ArAr}'\text{Ar}''\text{Bi}$.⁷³

Organobismuth(V) Compounds

Just like their lower oxidation state equivalents, many aryl-based organobismuth(V) reagents are thermally stable and can be stored indefinitely, making them practical and convenient reagents for organic chemistry.⁷⁴ Traditionally they have been accessed from their triaryl bismuth(III) equivalents by oxidation with molecular halogens.⁷⁵ This practice nowadays has almost been fully replaced by more convenient oxidizing reagents such as sulfuryl

chloride,⁷⁶ xenon difluoride,⁷⁷ peracids⁷⁸ and hypervalent iodine reagents⁷⁹ or ozone⁸⁰ to result in triarylbismuth dihalides/dicarboxylates (Ar_3BiXY)(Scheme 1.11).



Scheme 1.11: Oxidation of triarylbismuthines to the corresponding organobismuth(V), with X, Y = F, Cl, Br, carboxylates

In most cases the ligands X and Y (see Scheme 1.11) are equivalent, resulting in penta-coordinate organobismuth(V) compounds of type Ar_3BiX_2 which typically adopt a trigonal bi-pyramidal geometry (see Figure 1.5.2). Herein, the aryl groups position equatorially, due to the higher apicophilicity of the X group. The apical arrangement creates a delocalised 3c-4e bond between the bismuth centre and the two apical ligands.⁸¹ The hypervalent nature of the X-Bi-X linkage renders the bismuth(V) centre electrophilic.

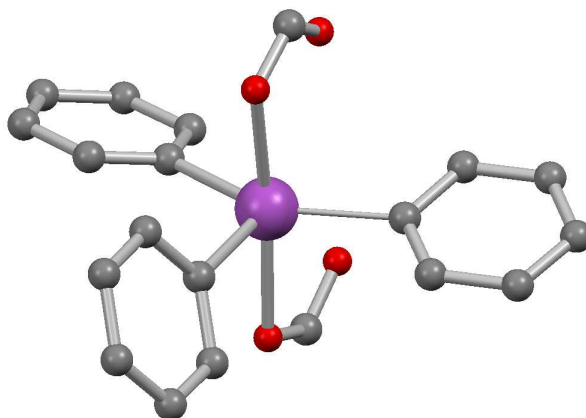
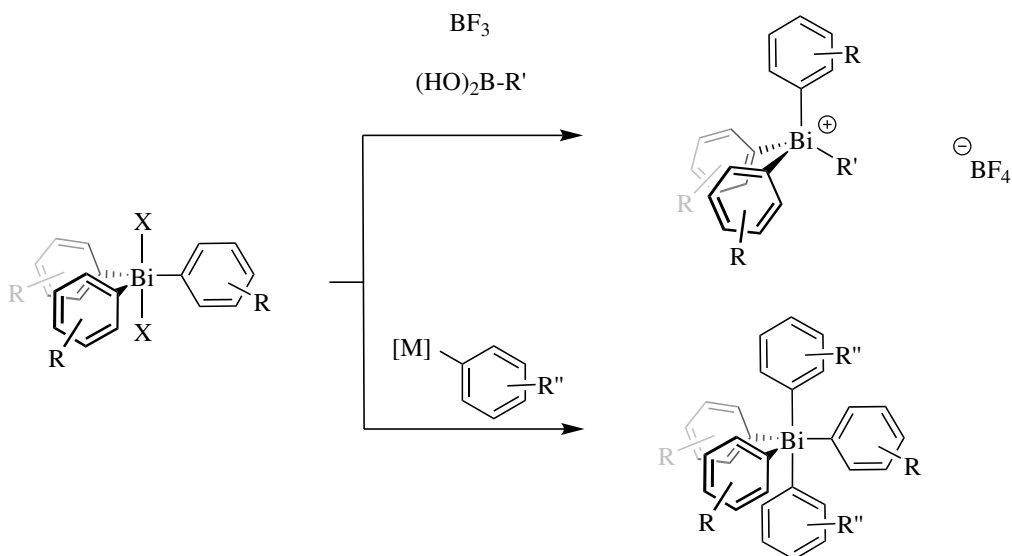


Figure 1.5.2: Molecular structure of triphenylbismuth diformate⁸⁰ (Ball and Stick, hydrogen atoms omitted for clarity)

While the following work will focus on compounds of the type Ar_3BiX_2 , other organobismuth(V) compounds must be mentioned for completeness.

Tetraaryl bismuthonium species can be prepared from Ar_3BiF_2 by Lewis-acid-promoted metathesis with boronic acids⁸²⁻⁸⁴ (see Scheme 1.12) or organosilicon compounds,⁸⁵ or by metathesis with silver salts starting from Ar_3BiCl_2 .⁸⁶ Hereby, BF_3 or Me_3SiOTf enhance the electrophilicity of the bismuth centre through coordination to an apical fluorine atom. The highly electrophilic bismuth center is able to perform a transmetalation with the boronic acid resulting in a bismuth center carrying four organic substituents. With abstraction of the second fluoride the bismuth center through BF_3 or Me_3SiOTf becomes tetravalent orienting the four aryl groups in a tetrahedral formation. Following

this methodology, a variety of organyl substituents such as methyl,⁸² 2-oxoalkyl,^{87,88} 3-oxoalkyl,⁸⁵ allyl,⁸⁹ alkenyl,⁹⁰ alkynyl⁹¹ and aryl^{83,92,93} have been introduced in the past. The ionic nature of these compounds make them even more electrophilic than Ar_3BiX_2 compounds. The tetravalent Ar_4Bi^+ featuring non coordinating counter ions (BF_4^- , OTs^- , ClO_4^-)⁹⁴ show a good shelf life, while coordinating Cl^- , Br^- , I^- , NO_2^- , CN^- decompose to give Ar_3Bi and the coupling product of one aryl group and the counter ion.⁹⁵



Scheme 1.12: Synthesis of tetraaryl bismuthonium and pentaaryl bismuth compounds, with $\text{X} = \text{Cl}, \text{Br}, \text{F}$ and $\text{M} = \text{MgBr}, \text{Li}$

Pentaaryl bismuth reagents can be accessed from the Ar_3BiX_2 in a single step reaction, using aryllithium or Grignard reagents at low temperatures.⁷⁴ This synthesis opens a pathway to homoleptic as well as heteroleptic organobismuth(V) compounds.⁷⁷ Homoleptic pentaaryl bismuth reagents orientate in a tetragonal pyramidal arrangement, while unsymmetrical substitution results in a distorted tetragonal pyramid towards trigonal bipyramidal with greater electronic and steric difference of the substituents.⁷⁷ Electron-deficient aryl groups result in a higher apicophilicity, favouring the trigonal bi-pyramidal geometry, while sterically demanding groups favour an equatorial orientation facilitating a tetragonal geometry.⁹⁶

1.6 The Chemistry of Ar_3BiX_2

Organobismuth(V) compounds have been employed in organic chemistry as potent oxidants due to the relatively high potential of the corresponding $\text{Bi(III)}/\text{Bi(V)}$ redox pair (*vide infra*). In contrast to their lower oxidation state equivalents a reversed bond polarisation is observed. The electrophilicity of the Bi(V) centre in combination with the relatively weak Bi-C bond renders the Ar^+ motif a potent leaving group and Ar_3BiX_2

species Ar^+ -surrogates. In the following a brief description into the reactivity of Ar_3BiX_2 will be given.

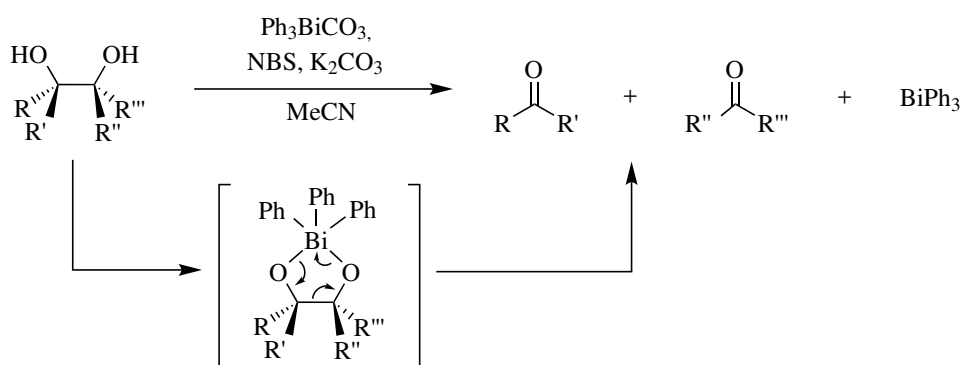
The use of organobismuth(V) reagents in combination with other metals has flourished into a variety of transformations. In most cases the organobismuth reagents have been used simply as an Ar^+ reagent or oxidant with the added metal performing the actual transformation. In combination with palladium, Heck-type arylations,⁹⁷ cross-coupling with iodonium salts⁹⁸ and aryl-, heteroaryl-, or styryltributylstannanes⁹⁹ as well as carbonylative couplings^{99,100} have been reported.

The combination of Ar_3BiX_2 reagents with copper enabled C-phenylation of 3-unsubstituted indoles¹⁰¹ and terminal alkynes.¹⁰² The following section will focus on transformations where bismuth is the sole organometallic reagent and its own unique reactivity has been exploited.

Oxidative Cleavage of α -Glycols

Upon addition of Ph_3BiCO_3 to vicinal aliphatic alcohols, cleavage of the bond between the alcohols has been observed to result in the corresponding aldehydes or ketones.

It has been proposed that the oxidation of α -glycols occurs *via* the formation of a pentacyclic intermediate as has been proposed for the oxidation using manganese¹⁰³ and vanadium.¹⁰⁴ In a similar fashion to this stoichiometric transformation the reaction can be performed catalytically when NBS is used as an oxidant (see Scheme 1.13). This allows a subsequent oxidation of the organobismuth(III) reagent to organobismuth(V), hence turning over the catalyst.¹⁰⁵

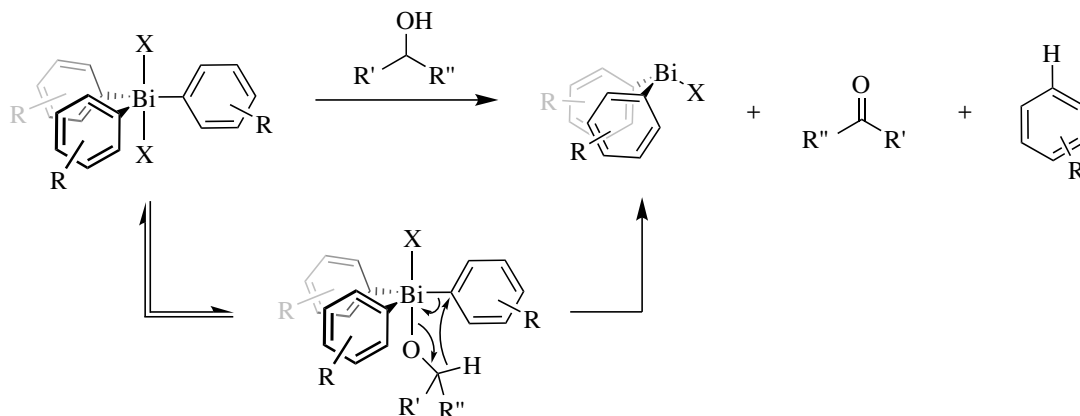


Scheme 1.13: Oxidative cleavage of glycols catalysed by Ph_3BiCO_3 (1 mol%) with R , R' , R'' , $\text{R}''' = \text{Ar}$, Alk , H

Oxidation of Alcohols

One of the earlier examples of the use of Ar_3BiX_2 species is the oxidation of primary and secondary alcohols resulting in aldehydes and ketones.^{106,107} As can be seen in Scheme 1.14, these reactions are postulated to involve the reversible formation of an alkoxytriarylbismuth(V) intermediate that subsequently undergoes a β -hydride elimination at the alcohol

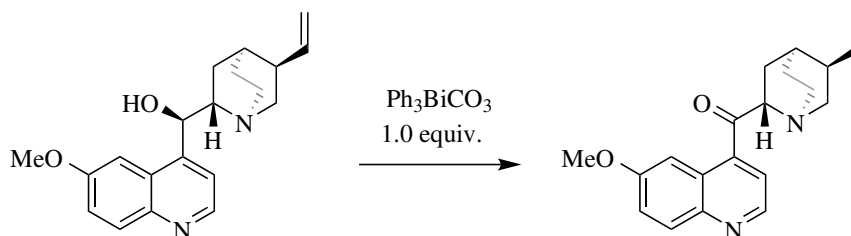
carbon to result in the desired aldehyde/ketone and ArH .^{108,109}



Scheme 1.14: Oxidation of alcohol to the corresponding aldehydes and ketones

During kinetic studies general trends could be established that hint towards a mechanism similar to a Meerwein–Ponndorf–Verley reduction.¹¹⁰ Sterically demanding or electron-deficient aryl rings enhance the overall rate of the reaction. Aryl rings carrying an *ortho*-methyl group enhance the rate of hydride transfer due to the relief of steric congestion at the bismuth centre as well as the increased bond polarisation of the $\text{Bi}-\text{C}$ through its steric elongation making the carbon *ipso* to Bi a more potent electrophile. Electron-deficient aryl groups increase the electrophilicity of the bismuth centre facilitating the nucleophilic attack of the alcoholate and presumably transfer of the nucleophilic hydride.¹⁰⁹ The oxidation of alcohols proceeds in almost quantitative conversions, and over-oxidation of primary alcohols to carboxylic acids has not been observed. Allylic and benzylic alcohols are not just well tolerated, but show a significantly higher activity. The chemoselectivity towards benzylic and allylic alcohols is considerably higher than is observed with DMP.^{108,111}

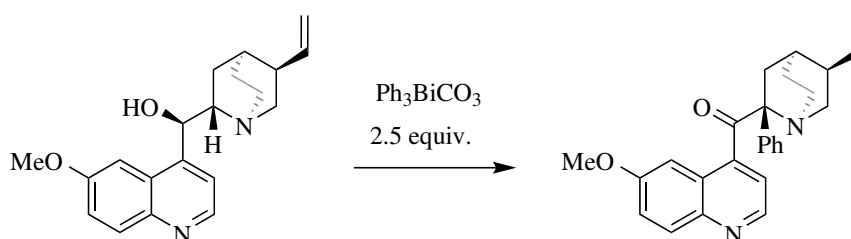
A prominent example for the application of organobismuth chemistry is the selective oxidation of quinine to quinone with one equivalent of Ar_3BiCO_3 (Scheme 1.15). In the presence of a variety of oxidatively sensitive functional groups the secondary alcohol of quinine is oxidised to the corresponding ketone.¹¹²



Scheme 1.15: Oxidation of quinine to quinone using one equivalent of Ph_3BiCO_3

Arylation of Nucleophilic Substrates

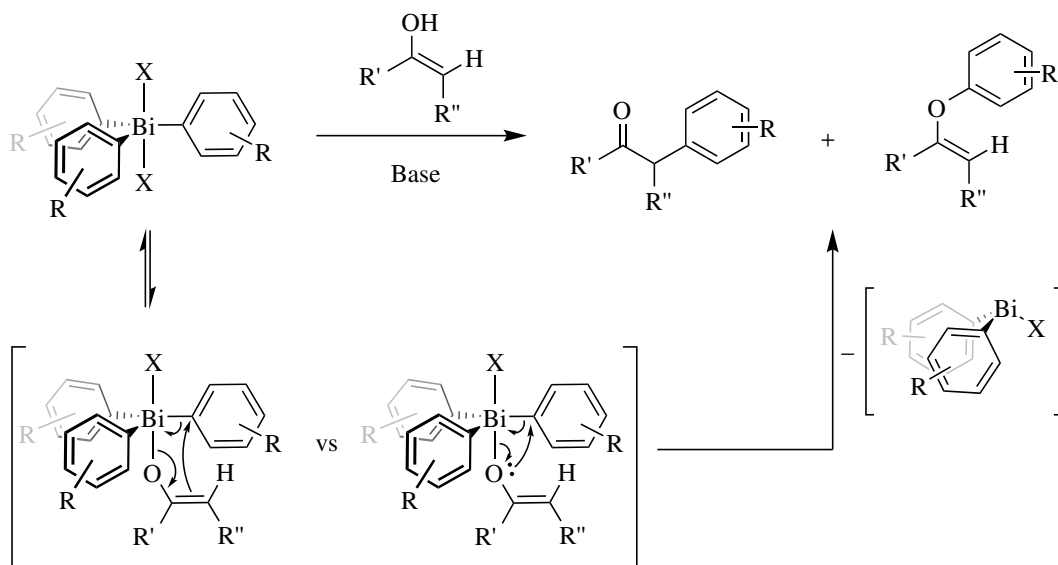
The reaction displayed in Scheme 1.15 has shown a specific reactivity of Ar_3BiCO_3 , but generally results in a low yield.¹¹² With closer investigation a second reaction product was identified. It was observed that the quinone reaction product undergoes phenylation of the aliphatic carbon α to the ketone. With the use of more than one equivalent of Ar_3BiCO_3 the formation of this phenylated product could be achieved selectively with α -phenyl quinone as the exclusive product. The functionalisation of this C–H bond had not been reported previously, the mechanism of which will be discussed (*vide infra*).



Scheme 1.16: Oxidation and subsequent phenylation of quinone to quinone using 2.5 equiv. of Ph_3BiCO_3

This reactivity of organobismuth(V) reagents for arylation reactions was investigated extensively and systematically by Barton and co-workers in the 1980s.^{1,113–115} These transformations have been reported for stoichiometric and metal-catalysed protocols, and prove to be effective for the phenylation of enols,^{116–118} phenols,^{119,120} alcohols,¹²¹ amines,¹²² amides,^{73,123} thiols⁸¹ and sugars.¹²⁴

A general distinction has been made between two types of arylation products that have been reported to originate from a similar general mechanism. In an analogous fashion to the oxidation of alcohols, the formation of a Bi–substrate bond represents the first step of the reaction and precedes a mechanistic divergence (Scheme 1.17). The formation of this bond is facilitated by the addition of base, enabling the substrate to function as a nucleophile. Traditionally, NaH , Et_3N , 1,1,3,3-tetramethylguanidine (TMG), 2-*tert*-butyl-1,1,3,3-tetramethylguanidine (BTMG) and 1,8-diazabicyclo(5.4.0)undec-7-ene (DBU) have been employed to deprotonate the substrate.



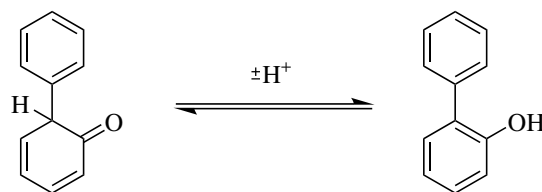
Scheme 1.17: Proposed mechanism for bismuth-mediated arylation¹²⁵ of enols with $\text{X} = \text{Cl}, \text{Br}, \text{O}_2\text{CR}$ and $\text{R}/\text{R}'/\text{R}'' = \text{aryl/alkyl}$

In the following the mechanism of arylation will be discussed on the example of an enol substrate as it provides both possible arylation products. In the first step the enolate has been proposed to perform nucleophilic attack on the bismuth centre to create a organobismuth enolate adduct. Subsequently, two possible elimination processes have been proposed to account for formation of two different products.

In first case, nucleophilic attack originates from the double bond of the enolate onto the *ipso* carbon of the aromatic ring. This creates a new C–C bond resulting in a α -aryl-ketone that can rapidly undergo keto-enol-tautomerism to form an α -aryl-enol.

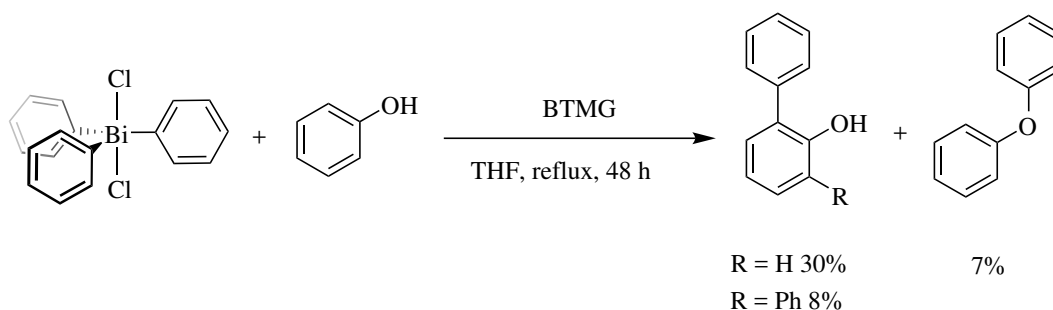
In the second case, the reductive elimination process is proposed to initiate from the oxygen of the enolate to result in the *O*-arylation to an aryl-enol-ether (See Scheme 1.17).

While methodologies for *O*-arylation are ubiquitous^{126–130} and α -*C*-arylation of ketones have been well established,^{131–133} the direct α -arylation of phenols with their enol motif embedded in the aromatic ring remains more of a challenge.^{134–138} Their potential to de-aromatise during the arylation process, resulting in a 2-phenyl-cyclohexa-2,4-dien-1-one intermediate only to tautomerise to the more favourable aromatic 2-hydroxybiaryl makes them a desirable class of substrates (Scheme 1.18). This methodology opens the pathway for direct *ortho* functionalisation of this class of compounds.



Scheme 1.18: Equilibrium of 2-phenyl-cyclohexa-2,4-dien-1-one and 2-hydroxybiphenyl through keto-enol-tautomerism

Barton *et al.* worked extensively on the arylation of phenolic substrates, as can be seen in Scheme 1.19. Here a triphenylbismuth dichloride was used for the arylation of phenol. While the desired product 2-hydroxybiphenyl was acquired, a degree of *O*-phenylation and di-*ortho-C*-phenylation as well as homocoupling was observed.



Scheme 1.19: Phenylation of phenol with 1.5 eq. of Ph₃BiCl₂ and 2 eq. of BTMG,³³ 8% biphenyl homocoupling product observed

The outcome of this reaction is characteristic for arylation using organobismuth(V) reagents. The observed yields, *C_{ortho}*/*O*-selectivities and degrees of overarylation differ from poor to excellent. The outcome depends on the nature of the organobismuth reagent, the reaction conditions and the electronic properties of the phenolic substrate¹³⁹ although an absence of mechanistic detail prevented an *a priori* prediction of the outcome.

A study investigating the influence of the nature of the phenol involving triphenylbismuth dichloride under basic conditions revealed that electron-deficient phenols were predominantly *O*-arylated, while phenols bearing electron-donating substituents undergo *C_{ortho}*-arylation predominantly.³³ Electronically neutral reagents afford complex mixtures of *O*-phenyl- and *C_{ortho}*-phenyl-phenols (as seen in Scheme 1.19).³³

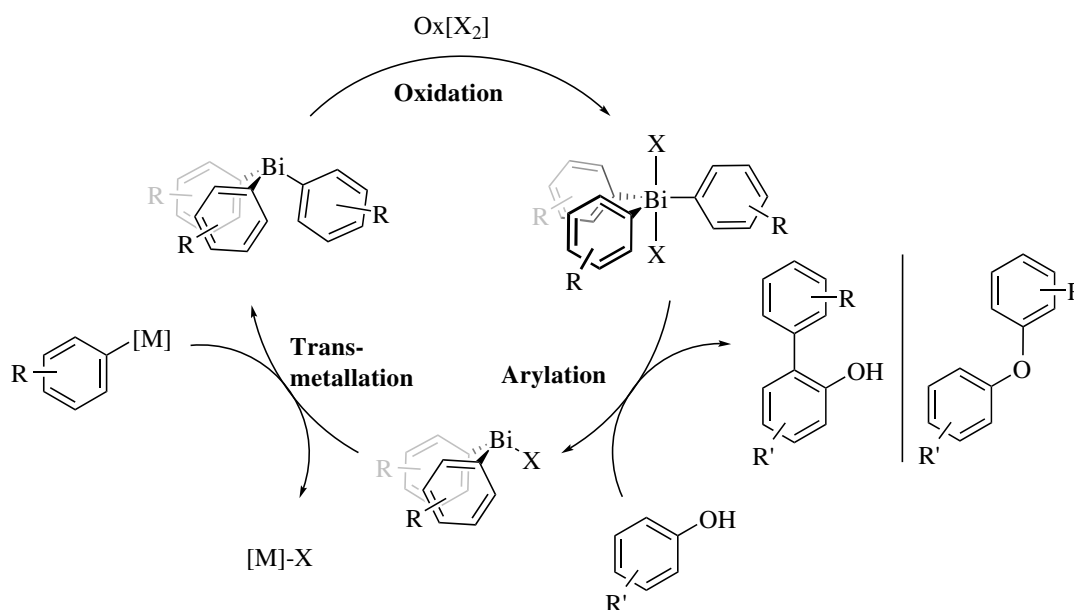
This substrate controlled selectivity has previously rendered organobismuth(V)-mediated arylation inferior to existing methodologies as a route to the 2-hydroxybiphenyl motif.

1.7 Strategy

In order to overcome the inherent disadvantages of organobismuth chemistry two different strategies have been pursued.

Catalytic Approach (Chapter 2)

In order to address atom and step efficiency, an elevation of the current stoichiometric protocol towards a catalytic methodology will be investigated. Here, a potential catalytic cycle has been identified.



Scheme 1.20: Proposed catalytic cycle

In one plausible catalytic cycle, three elementary steps were identified for a potential catalytic approach. In the first step an Ar₃Bi(III) species is oxidised to Bi(V) in order to access the active arylating reagent. Phenol subsequently reacts with the Bi(V) species *via* a Bi-phenoxy intermediate (*vide supra*) which undergoes reductive elimination to result in the desired 2-hydroxyphenyl or phenylether product and an Ar₂BiX species. The diaryl bismuth reagent is recovered by transmetalation from an arylmetallic reagent. Crucially for the goal of making this methodology attractive for a general lab scale or industrial application, both the oxidant ([Ox]) and the terminal aryl source ([M]) must be cheap and non-toxic, and sufficiently mild as to maintain high chemoselectivity.

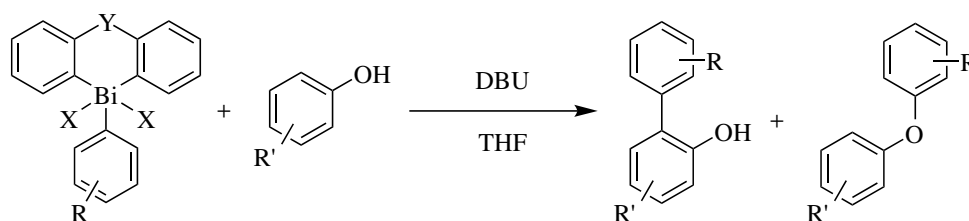
In order to achieve this objective, the individual steps are investigated sequentially. These investigations are accompanied by mechanistic studies allowing for additional insight into reaction mechanism and sensitivities. This allows for an assessment of the compatibility of the individual steps as well as a potential for *a priori* prediction of the reaction outcome of future substrates. The individual steps will subsequently be combined sequentially in

order to establish the possibility of a full catalytic cycle.

Sequential Stoichiometric Approach (Chapter 3)

The key to a functioning catalytic system relies on the compatibility of the individual steps and reagents in a single pot. In order to circumvent this limitation a stoichiometric approach was developed, performing each individual step (transmetalation, oxidation, arylation) in a consecutive fashion. By using one equivalent compatibility issues were rendered irrelevant.

Whilst both Bi-O and Bi-C bonds undergo facile intramolecular migration and intermolecular exchange, the latter can be rendered stable by incorporation into a chelating framework.⁷⁶ Examples of such frameworks include the bismole,¹²⁵ bismine⁷⁶ and bismocene¹⁴⁰ motifs (Scheme 1.21). The organobismuth(V) derivatives of these scaffolds have been shown to transfer solely the exocyclic aryl moiety in arylation reactions of phenols¹²⁵ (Scheme 1.21).



Scheme 1.21: Transfer of only the exocyclic group in the arylation of phenolic substrates with bismacyclic reagents

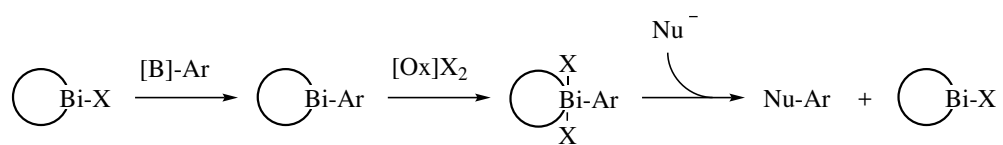
This observation renders the cyclic aryl groups practically inert allowing them to act as a constant backbone that can be tuned to increase reactivity and stability of the organobismuth reagent. This chemistry is therefore less dependent on the transferred exocyclic aryl group.

Access to these reagents requires multi-step synthesis from commercial starting materials, even before the actual arylation reaction can occur, creating a synthetic obstacle to this unique chemistry. Quick access to these reagents had to be found in order to increase the practicality of bismacycle-mediated oxidative arylation.

The approach involves the creation of a uniform bismacyclic precursor that can easily be functionalised with a variety of differently substituted exocyclic aryl groups. Organoboron reagents have been chosen as a target transmetalation reagent due to the ubiquitous availability and easy handling. This provides fast and convenient access to a number of different aryl groups that can be transferred in subsequent steps.

The insight gained from previous studies will be used to determine a suitable oxidant to a bismacycle(V) reagent. With the following addition of the nucleophilic substrate, an arylation using the previously transferred exocyclic aryl group can be performed, resulting in the arylated nucleophile and a bismacyclic co-product. Recovery and recycling will be

attempted in order to increase atom efficiency. Following this approach, a stepwise protocol similar to the one displayed in Scheme 1.22 will be developed.



Scheme 1.22: Modular system for oxidative arylation using a bismacyclic precursor

2 | Arylation mediated by simple Tri-arylbismuthines

Abstract: This chapter features the initial efforts for the development of a catalytic protocol for the arylation of hydroxyarenes using Ar_3BiX_2 reagents.

In order to understand all occurring processes and ensure compatibility of all reagents present in the proposed catalytic system, the individual steps oxidation, arylation and transmetallation were investigated separately to be combined in the final step. After identification of a bismuth source, a library of Ar_3Bi and Ar_3BiX_2 reagents have been created. Arylation of phenolic substrates initially resulted in low yields and selectivities. A variety of reaction parameters (purity, electronic properties, and stoichiometry of reagents, solvents, light, temperature) have been investigated but the base-induced decomposition of the Ar_3BiX_2 reagent remained dominant.

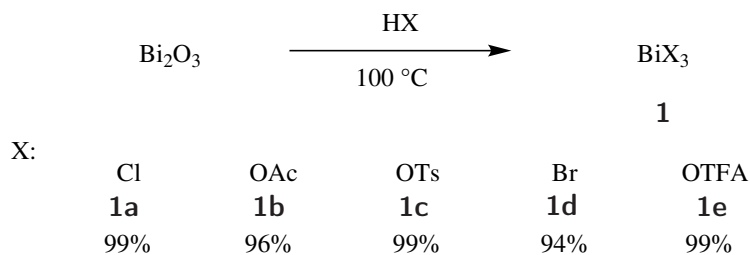
Upon switching the substrate to 2-naphthol yields improved drastically, allowing for a mechanistic investigation into the rate and selectivity determining step of the oxidative arylation, the role of electronic properties of substrate and transferred aryl group, as well as the counter ion on the bismuth centre.

The diaryl bismuth reaction product was identified and conditions for transmetallation from organoboron reagents to result in a Ar_3Bi compound were developed.

While oxidation of the Bi(III) reagent could be achieved efficiently with a variety of oxidising agents, a combination of the three steps proved unsuccessful due to the inherent incompatibility of the necessary reagents, precluding development of a catalytic approach.

2.1 Exploration of Bismuth Sources

Classic substrates for the synthesis of organobismuth(III) compounds are BiCl_3 and BiBr_3 . Due to their sensitivity to hydrolysis they have to be stored and handled under anhydrous conditions. Commercially available sources are provided in standard screw top bottles and were found to be of dubious purity. Therefore it was decided to access inorganic bismuth(III) salts from an alternative feedstocks: the cheap, available and stable Bi_2O_3 . Following the procedure shown in Scheme 2.1 a variety of bismuth(III) compounds have been prepared in high yields. BiCl_3 **1a** and BiOAc_3 **1b** are colourless crystalline solids that do not show any solubility in common organic solvents. $\text{Bi}(\text{OTs})_3$ **1c** is soluble in DMSO and DMF, exculsively, while BiBr_3 **1d** and $\text{Bi}(\text{OTFA})_3$ **1e** can be dissolved in MeCN, THF and Et_2O . This renders them better candidates for organic synthesis. Their hygroscopic properties and hydrolytic sensitivity still persist, requiring a certain level of caution regarding handling and storage.

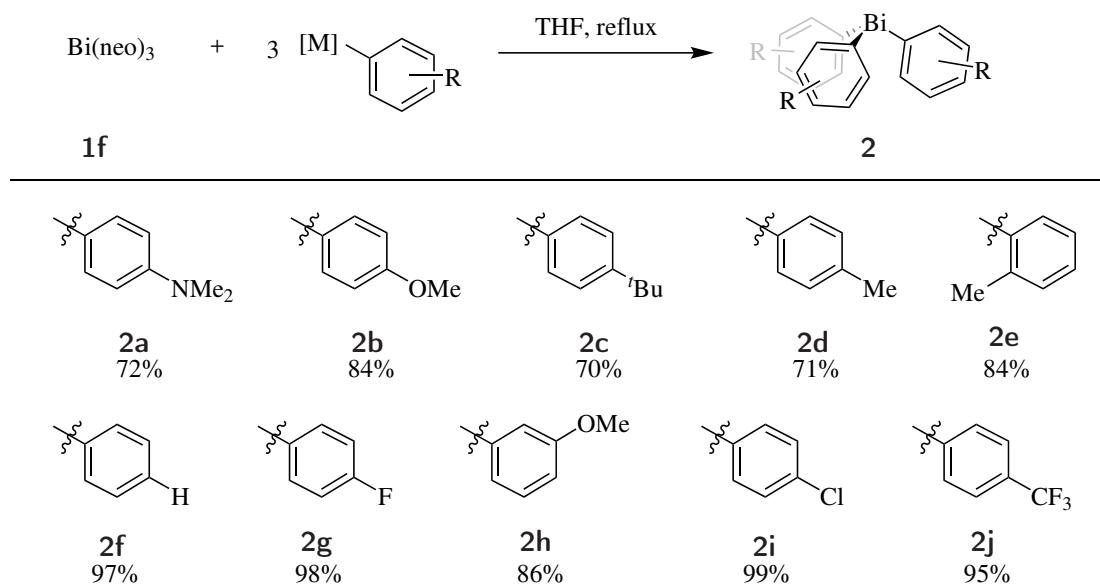


Scheme 2.1: Synthesis of BiX_3 with $\text{X} = \text{Cl}, \text{Br}, \text{OAc}, \text{OTFA}, \text{OTs}$, removal of water by use of Dean-Stark conditions or anhydride (see SI)

In contrast, commercially available Bi(III) neodecanoate ($\text{Bi}(\text{neo})_3$) **1f** offers an insensitive alternative. The long alkane chains of the carboxylate counter ions allow a for a low sensitivity towards atmospheric moisture due to their hydrophobic properties and excellent solubility in organic solvent. Hence, it has been employed for the preparation of the initial organobismuth(III) reagents.

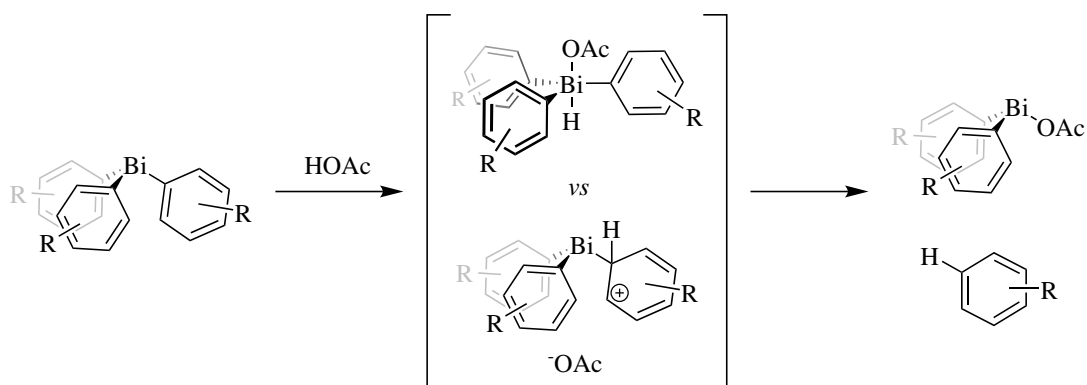
2.2 Creation of an Organobismuth(III) Library

In order to access organobismuth chemistry a variety of Ar_3Bi reagents were prepared. This library allows access to quantitative investigation of two key elementary steps: the oxidation of Ar_3Bi and the following arylation using the corresponding Ar_3BiX_2 species. Compounds **2a-j** were prepared from $\text{Bi}(\text{neo})_3$ in good to excellent yields (Scheme 2.2). While the majority of compounds were synthesised following the addition of the appropriate Grignard reagent, $(p\text{NMe}_2\text{-C}_6\text{H}_4)_3\text{Bi}$ **2a** was not achieved by this pathway but rather with the organolithium equivalent.



Scheme 2.2: General synthesis of compounds **2a-j**, with M = MgCl, MgBr, Li

The bismuthines **2a-j** were obtained as colourless crystalline bench-stable solids and possess a wide range of electronic properties. A determination of steric effects was enabled by (*o*-tol)₃Bi **2e**. In the solid state these Ar₃Bi compounds proved stable to light, air and moisture with no noticeable decomposition over the course of 3 years. While being stable to neutral and basic conditions in solution, a significant increase in acid sensitivity was observed for electron-rich representatives. While **2d** and **2f** only showed a slow decomposition upon treatment with HOAc, **2a** and **2b** suffered from major decomposition. This trend can be explained by the increased affinity towards protodebismuthation that in its extremes can be described as either an oxidative addition/reductive elimination process or electrophilic aromatic substitution process (see Scheme 2.3). Both processes are promoted by electron-rich bismuth centre/aryl rings.^{71,75}



Scheme 2.3: Possible decomposition mechanisms of organobismuthines with acetic acid

2.3 Electrochemical Investigation

With a library of Ar_3Bi reagents at hand the (re)-oxidation segment of the proposed catalytic system (Scheme 1.20) was investigated. It was anticipated that this insight could be used to tailor the required oxidant to the oxidation potential of the bismuth species, allowing for the most mild reaction conditions possible. A dependency of the oxidation potential of these compounds with different aryl groups on the bismuth centre has been suspected but not been investigated previously. The electrochemical potential (E^{Ox}) of Ph_3Bi has been reported as 1.6 V in acetonitrile.¹⁴¹ These data were acquired using a platinum anode with a 0.1 M NEt_4OTf electrolyte solution against a sodium saturated calomel electrode (ssce). Since the use of ssce has not been recommended by the IUPAC^{142,143} for non-aqueous solvents, a ferrocene based reference with a platinum disc working electrode, a platinum counter electrode and a silver wire *pseudo* reference electrode in NBu_4PF_6 was used in the present investigation. The peak oxidation potential (E_P^{Ox}) of 1.5 V measured with this system for Ph_3Bi is similar to that reported previously. Figure 2.3.1 shows a typical cyclic voltammogram of a triaryl bismuth compound. As illustrated for **2g** (Figure 2.3.1), the oxidation of tri(4-fluorophenyl)bismuth occurs at 1.66 V with respect to ferrocene, and is non-reversible.

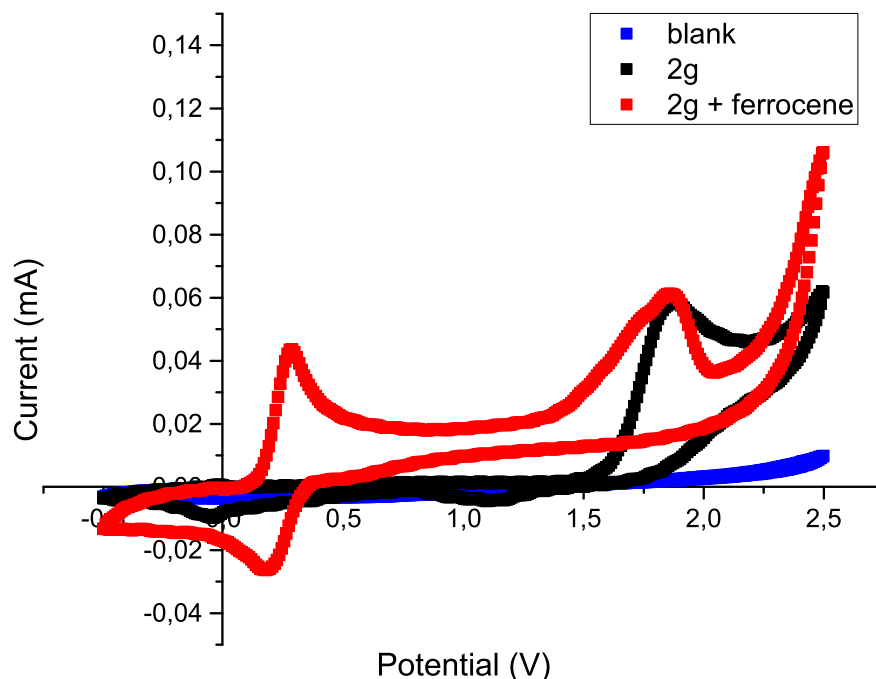


Figure 2.3.1: Cyclic voltammogram of **2g** with $[\text{NBu}_4\text{PF}_6] = 0.1 \text{ mM}$, $[\mathbf{2g}] = 1 \mu\text{M}$, $[\text{ferrocene}] = 1 \mu\text{M}$ in acetonitrile at 25 °C at a scan rate of 100 mA/s.

The investigation of E_P^{Ox} for the different Ar_3Bi showed a good correlation to the σ -values of the corresponding substituents (Figure 2.3.2). This indicates that the oxidation takes place at the bismuth centre rather than the adjacent aryl group, as **2b** and **2h** have similar

values attributed to them. The positive correlation indicates that with decreasing electron density on the bismuth centre provided by the substituents on the surrounding aryl groups the ionisation energy increases, *i.e.* a higher potential is required for the oxidation process. While this was expected the intensity of this trend is significant, even when considering that the influence is tripled by the three aryl groups surrounding the bismuth centre. While **2a** posses an oxidation potential of 0.33 V, the electron-poor equivalent **2j** has a 7-fold greater oxidation at 2.2 V.

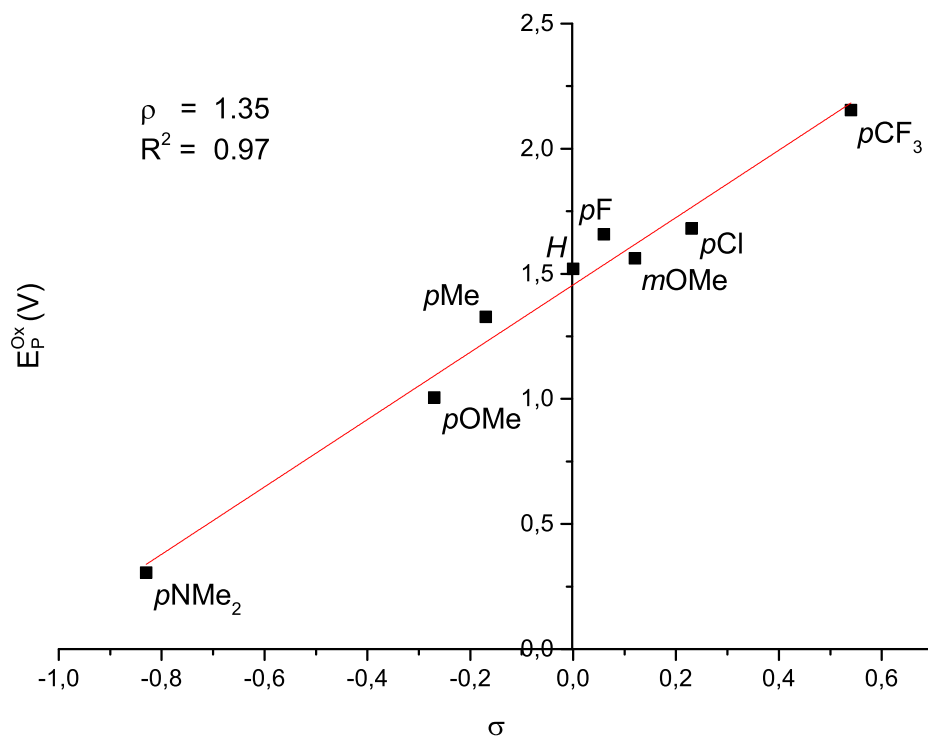
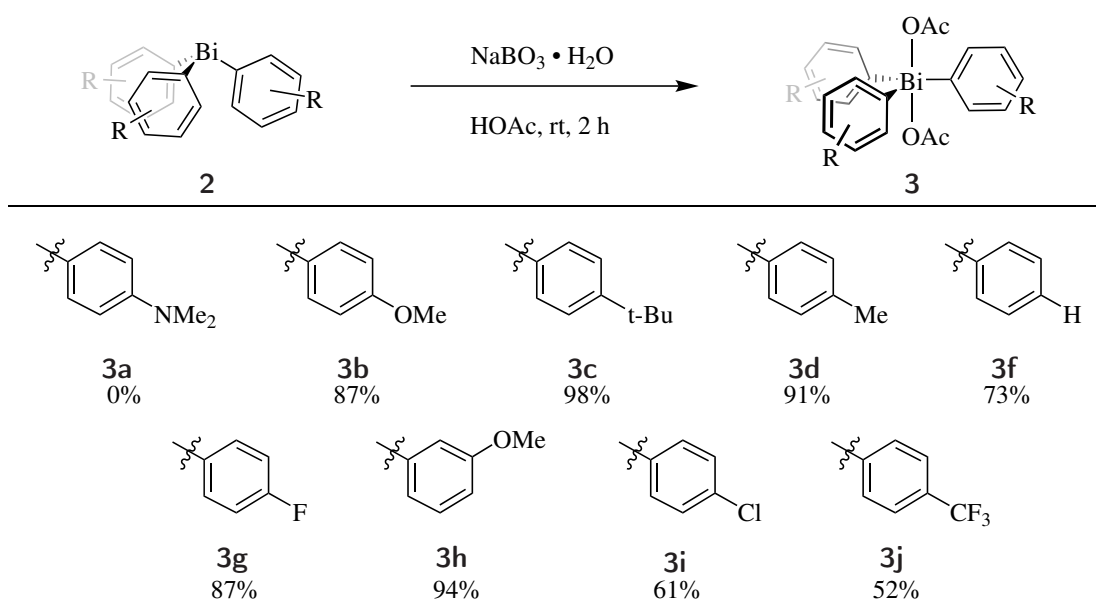


Figure 2.3.2: Correlation of σ values and peak potential of triaryl bismuthines **2** relative to ferrocene

E_P^{Ox} does not provide any information about the nature of the oxidation happening at the electrode surface. Since a two electron oxidation is required for the catalytic system the number of transferred electrons needed to be verified. A simple approach to access the number of transferred electrons is the use of the Randles-Sevcik equation for irreversible electron transfer processes (see 4.3.1).¹⁴⁴ Unfortunately the oxidation process is not just irreversible on the electrode surface, but also results in the passivation of its surface. Despite the use of a variety of different electrode materials and electrolytes, we were not able to prevent the passivation process, preventing the determination of the number of transferred electrons in the oxidation step. The absence of the secondary peak in the cyclic voltammogram hints towards a two-electron process, but is by no means conclusive.

2.4 Extension of the Library towards Organobismuth(V) Compounds

The first reports of organobismuth(V) compounds originate from the reaction of Ar_3Bi reagents with molecular halogens.⁷⁵ Current approaches rely on the use of strong oxidants such as sulfonyl chloride, XeF_2 or *m*CPBA.⁸¹ Despite them being a major improvement in relation to safe and easy handling, an even easier protocol was employed in the following. Herein, the cheap, readily available, and bench stable oxidant sodium perborate was used to perform the transformation without the need for exclusion of air and water. In combination with HOAc, sodium perborate is able to create the highly reactive peracetic acid, that is responsible for the oxidation to Bi(V) to form $\text{Ar}_3\text{Bi}(\text{OAc})_2$ compounds.¹⁴⁵



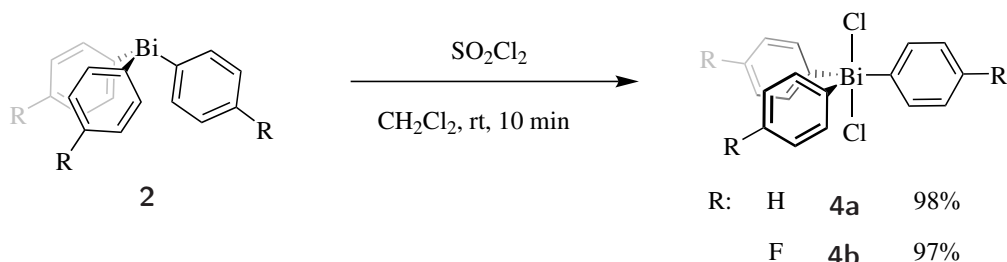
Scheme 2.4: Oxidation of Ar_3Bi to the corresponding $\text{Ar}_3\text{Bi}(\text{OAc})_2$ using sodium perborate in acetic acid

This procedure proved to be appropriate for the oxidation of a wide range of Ar_3Bi compounds. The transformation of the very electron-rich **2a** to **3a** did not result in the desired product, but showed decomposition of the starting material. This result can be attributed to the increased acid sensitivity of the electron-rich $(p\text{NMe}_2\text{-C}_6\text{H}_4)_3\text{Bi}$ species as has been discussed above.

While electron-poor Ar_3Bi species possess greater stability towards acid, lower yields were obtained for increasingly electron-poor aryl rings attached to the bismuth centre. Lower rates of oxidation for electron-poor aryl groups may have led to reactions being terminated before completion resulting in lower yield.

Since recent literature focused mostly on the use of the Ar_3BiCl_2 derivatives, the most simple member Ph_3BiCl_2 **4a** as well as a fluorinated equivalent **4b** have been prepared. As displayed in Scheme 2.5, the reaction proceeds within minutes using sulfonyl chloride as

an oxidant, yielding highly pure crude mixtures that can easily be recrystallised from cyclohexane.

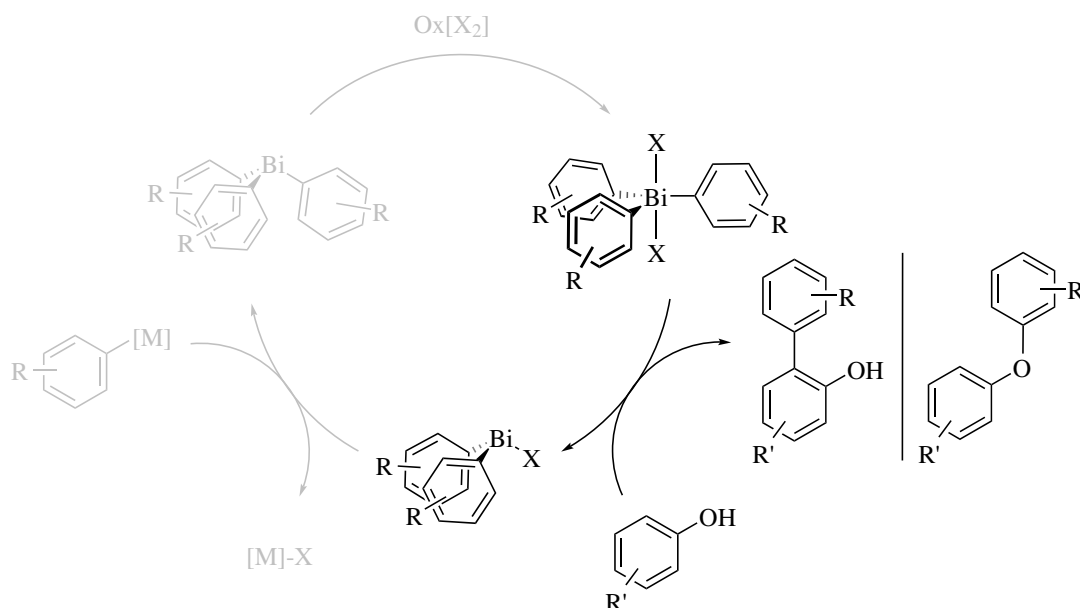


Scheme 2.5: Oxidation from Bi(III) to Bi(V) using sulfonyl chloride

In the beginning, the investigation will focus on the product forming arylation step of the proposed catalytic cycle. A closer investigation into different oxidants capable of performing the transformation from Bi(III) to Bi(V) will be addressed later (*vide infra*). The prepared library of Ar_3BiX_2 species detailed above will provide initial insight used for the arylation of phenolic substrates in the following.

2.5 Oxidative Arylation using Ar_3BiX_2 Reagents

The proposed catalytic cycle consists of three elementary steps: oxidative arylation of the substrate, regeneration of the Ar_3Bi species *via* transmetalation, followed by the oxidation to Bi(V). While each of these steps have been reported before, a simple combination of the reagents required for all the steps results in marginal chances of success. *A priori* prediction of the interactions between the components in the reaction mixtures would be extremely challenging. Additionally, unraveling the effects of changing reaction conditions (temperature, concentration, reagent, solvent...) on a combined system would become a torturous conundrum. Hence, each of the individual steps will be investigated individually in the following.



Scheme 2.6: Arylation of phenols using Ar_3BiX_2 compounds in the proposed catalytic cycle

The initial focus was set on the investigation of bismuth-mediated arylation, as it is the crucial step involved in the generation of the desired product (Scheme 2.6). The reaction conditions are based on studies by Barton *et al.* (see Scheme 1.19), which furnished both C_{ortho} and O -arylation of phenols with poor selectivity and moderate yields. While several studies investigating the influence of different parameters^{114,146} on the overall yield of the arylated products exist, coherent data into the chemoselectivity (C_{ortho} vs O) have not been reported.

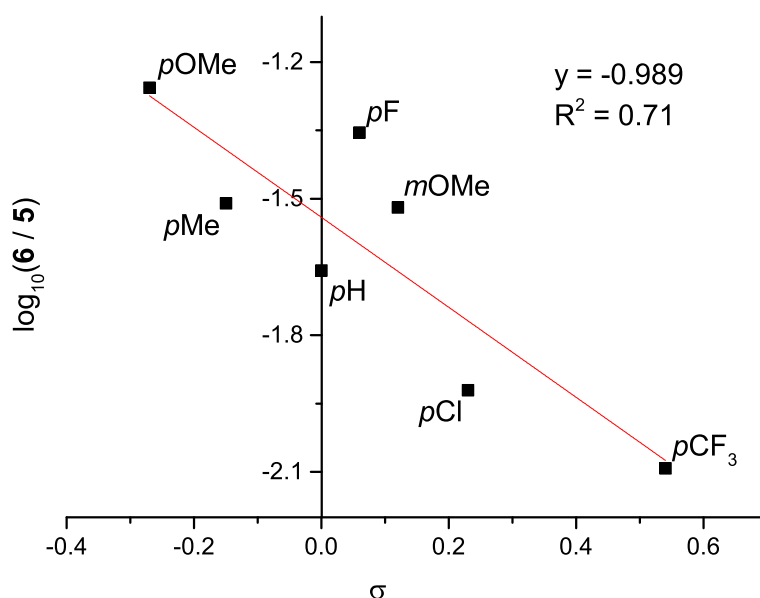
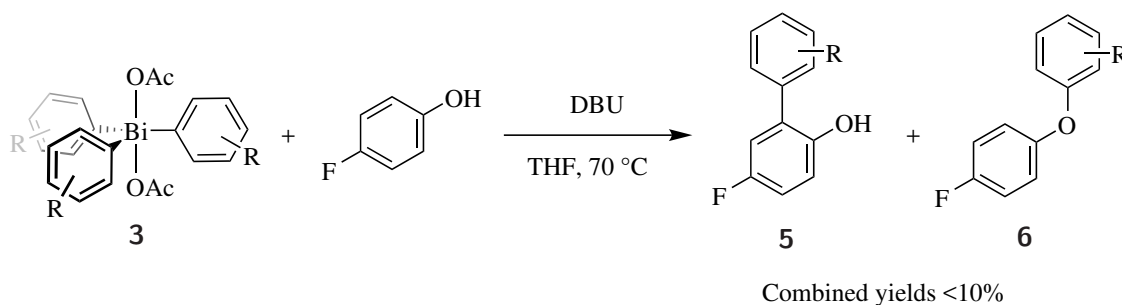
Since the ability to control and predict this selectivity is desired, a number of the previously prepared organobismuth(V) reagents are used to investigate electronic and steric effects.

2.5.1 Arylation of 4-Fluorophenol

In the first instance general alterations have been made to Barton's original protocol. The report by Barton *et al.* relied on the phenylation of phenol using Ph_3BiCl_2 with *tert*-butyl tetramethyl guanidine (BTMG) in refluxing THF for 2 d. Preliminary investigations allowed for the use of more compelling reagents and reaction conditions.

In the original conditions BTMG was used as a base for the deprotonation of phenol. The specific use of BTMG can be traced back to its trivial name "Barton's Base", which made it the obvious weakly coordinating base for this chemistry for Barton *et al.* in their investigations. In our work, DBU was found to be a viable alternative base to BTMG, leading to comparable results. Since DBU is cheaper and more widely applied in industry and research, it was used in the following investigation. The classic substrate phenol has been exchanged for 4-fluorophenol so that ^{19}F NMR spectroscopy could be used for *in situ* reaction monitoring. Notably (Scheme 2.7), the 4-fluoro substituent exerts only a marginal

electronic effect ($\sigma_p = 0.06$).¹⁴⁷



Scheme 2.7: Arylation of 4-fluorophenol; Conditions: [4-fluorophenol] = 12.7 mM, $[\text{Ar}_3\text{BiX}_2] = 19.1$ mM and $[\text{DBU}] = 31.9$ mM, R = pOMe, pMe, pF, H, pCl, pCF₃ and Ar = C₆H₄-pOMe, C₆H₄-pMe, C₆H₄-pF, Ph, C₆H₄-pCl, C₆H₄-pCF₃, respectively

Using the previously prepared $\text{Ar}_3\text{Bi}(\text{OAc})_2$ reagents the arylation of 4-fluorophenol was performed in J. Young's tap NMR tubes under inert conditions with distilled/recrystallised reagents to avoid any effects that could be attributed to contaminants. The crude reaction mixture was analysed by ¹⁹F NMR spectroscopy. The individual peaks were assigned following isolation of the reaction products *via* preparative TLC.

Differently substituted aryl rings allow an insight into the electronic impact of the organobismuth(V) compounds on the chemo selectivity of the arylation. The conducted Hammett investigation (Scheme 2.7) indicates a product selectivity towards *C_{ortho}*-arylation with more electron-poor aryl rings on the bismuth centre.¹ This is consistent with a previously proposed non-synchronous concerted mechanism.¹⁴⁸ However, in contrast to this previ-

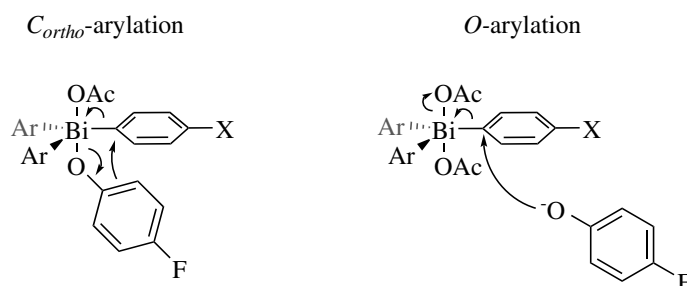
¹The low R² value can be attributed to the low overall yields of the arylation products, which result in significant error in integration of the NMR signals.

ously stated mechanism we propose an alternative mode of action.

C_{ortho} -arylation proceeds through nucleophilic attack of the phenolate onto the Bi(V) centre resulting in a phenoxy-bismuth intermediate (see Scheme 2.8). This species subsequently undergoes a reductive elimination process featuring a nucleophilic attack of the *ortho*-carbon of the phenoxide onto the *ipso* carbon of the aryl group on the bismuth(V) centre to result in the desired C_{ortho} arylation product.

For the O -arylation on the other hand, we propose a $\text{S}_{\text{N}}2$ -type pathway that involves a nucleophilic attack of the phenolate directly onto carbon *ipso* to bismuth resulting in the phenolic ether.¹⁴⁸

A classical free-radical mechanism was eliminated by Barton *et al.* using EPR spectroscopic investigations and quantitative chemical trapping.^{105,146}



Scheme 2.8: Proposed mechanisms for C_{ortho} - and O -arylation of phenols

Time-resolved Investigation

Although insight into the influence of the electronic properties of the arylbismuth(V) compounds was achieved, the reported yields of Barton *et al.* could not be reproduced. While prior distillation or recrystallisation of all substrates resulted in a slight increase of yield, no single cause of the low yield could be determined. Even using Ph_3BiCl_2 **4a** and phenol under exactly the same conditions as previously described by Barton *et al.*, similar results to the ones reported have not been achieved. Thus, a more detailed investigation of the reaction profile was performed, using **3g** and 4-fluorophenol *via in situ* ^{19}F NMR spectroscopy in order to understand the processes taking place during the reaction.

As can be seen in Figure 2.5.1 **3g** is consumed within approximately 6 h. This appears in strong contrast to the 48 h reaction time of Barton *et al.*. With the consumption of **3g** a number of peaks arise in the spectrum being identified as fluorobenzene (PhF), tri(4-fluorophenyl)bismuth(III) **2g** and an unidentified species **7**. Additionally, the appearance of precipitate in the NMR tube was noted. As can be seen in Figure 2.5.1, **2g** is produced within the 2 hours, reaction followed by a slow decay over time, while the concentration of fluorobenzene increases constantly. These components were expected as they have been reported as side products before.³³ The unexpected peak associated with **7** is the dominant species after 5 hours. Identification of this compound as well as the origin of fluorobenzene and **2g** were therefore undertaken (*vide infra*).

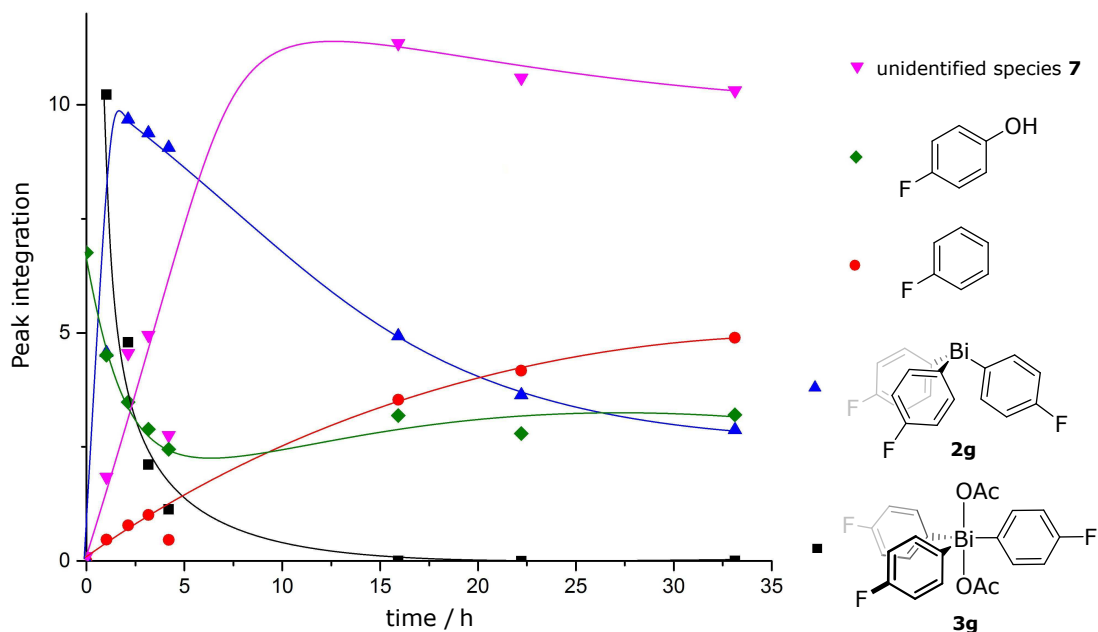
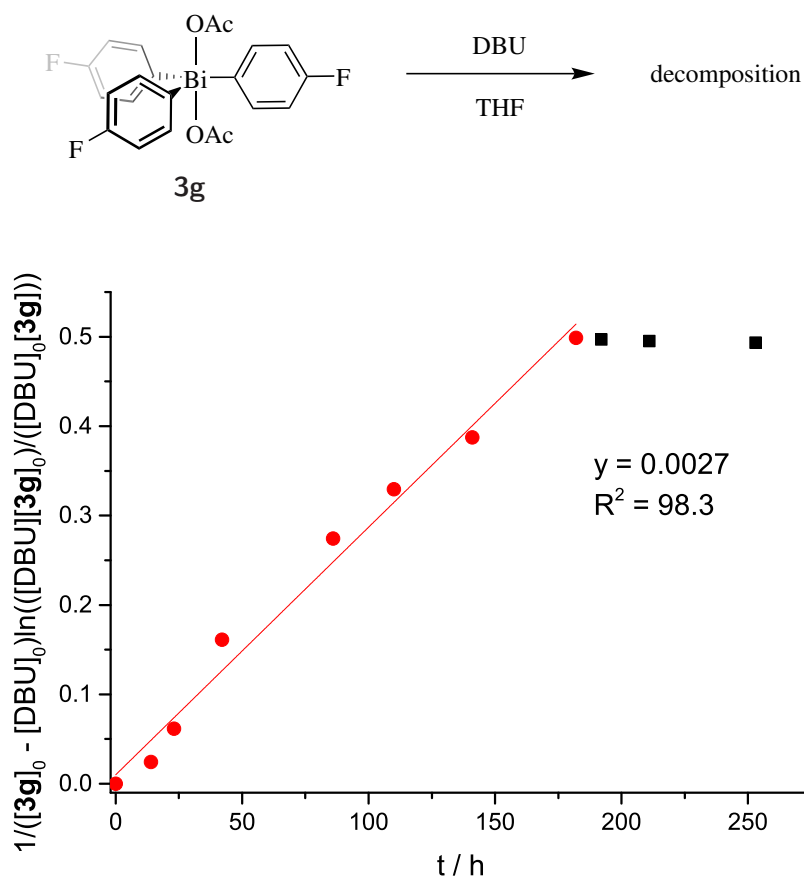


Figure 2.5.1: Reaction profile of the arylation of 4-fluorophenol monitored by ^{19}F NMR spectroscopy, $[\text{4-fluorophenol}]_0 = 12.7 \text{ mM}$, $[\mathbf{3g}]_0 = 19.1 \text{ mM}$ and $[\text{DBU}]_0 = 31.9 \text{ mM}$ in THF at 70°C . The peak integral has been used as the y-axis, as the number of fluorophenyl groups per molecule of the unidentified compounds is not known. The lines between data points are provided for a guide to the eye only.

2.5.2 Decomposition of Tri(4-fluorophenyl)bismuth Diacetate

Upon sequential addition of the individual reagents, it has been found that the decomposition of **3g** appears independently from the presence of phenol, but instead is induced by the addition of base (Scheme 2.9).

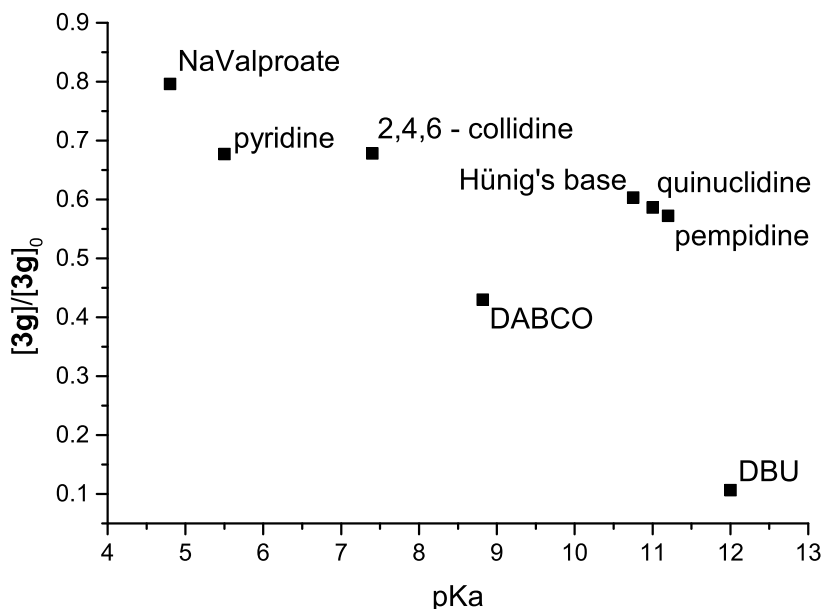
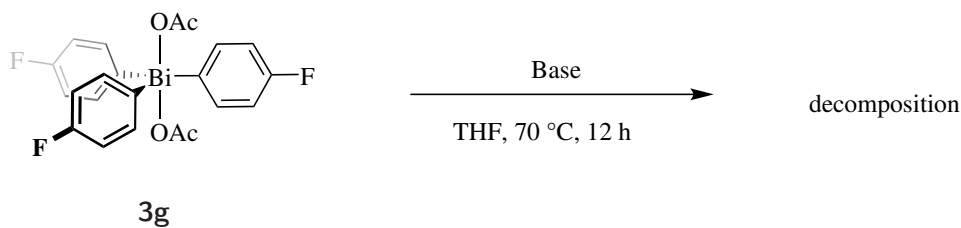
Further investigation reveal that the decomposition proceeds in a similar time frame even in the absence of 4-fluorophenol. This indicates that the decomposition kinetically outcompetes the desired arylation. In order to gain control over this effect a closer investigation into this previously unreported decomposition was conducted. Therefore, the decay of **3g** was investigated with exclusively base and solvent present. With the reduction of the reaction temperature to 25°C , the rate of decomposition was significantly reduced enabling a kinetic observation *via* ^{19}F NMR spectroscopy (Scheme 2.9). Additionally, the composition of the reaction products is dominated by the unidentified species **7**. The decomposition proceeds in a second order fashion, which is first order in both DBU and **3g**. Surprisingly, during the reaction progression $[\text{DBU}]$ decreased almost twice as fast as $[\mathbf{3g}]$ and comes to a halt upon full consumption of DBU. This implicates that the decomposition proceeds *via* a second order decomposition followed by the use of a second equivalent of DBU (For further discussion see 2.5.3).



Scheme 2.9: 2^{nd} order kinetics of DBU-induced decomposition of **3g**; Conditions: $[\text{DBU}]_0 = 77.1 \text{ mM}$, $[\mathbf{3g}]_0 = 83.3 \text{ mM}$ at 25°C in THF

Investigation into the Nature of the Applied Base

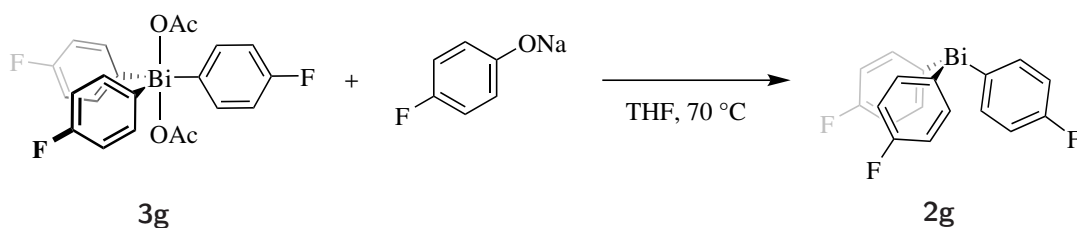
In order to prevent the decomposition, and allow for an unimpeded arylation of the phenol substrate, a variety of bases have been employed to investigate the influence of the nature of the base on the decay of the organobismuth(V) reagent (Scheme 2.10).



Scheme 2.10: Remaining **3g** after 12 h at 70 °C with a variation of organic bases; $[\mathbf{3g}]$, $[\text{base}] = 27.2 \mu\text{M}$, with base = pyridine, 2.4.6-collidine, pempidine, DABCO, quinuclidine, Hünig's base, DBU, sodium valproate

In this investigation the residual organobismuth(V) species has been used as a measure to quantify the influence of the base on the decomposition mechanism. A rough trend between the pK_aH of the individual base and the degree of decomposition was observed. The decay always involves the production of fluorobenzene, **2g** and a unassigned peak **7**, the chemical shift of which differs depending on the base, indicating an involvement in the species. The only exception is Na-Valproate, where additionally to the expected products two distinct peaks in the Bi(V) region were observed, suggesting the exchange of the acetate group of **3g** with one or two valproate groups, respectively. This hints to the mechanism in which the unidentified peak is formed: the bases with a higher pK_aH may be coordinating to **3g** forming an unstable intermediate, that decays to the unidentified species.

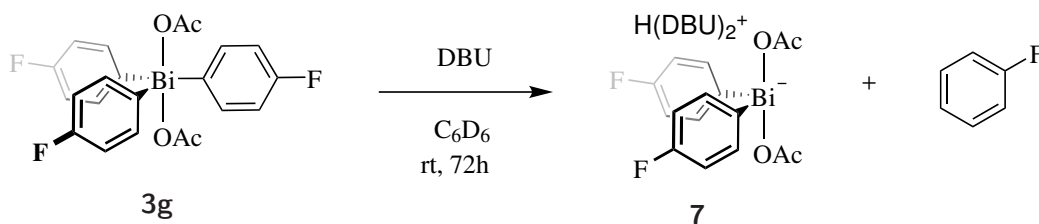
In order to overcome the base-induced decomposition, the role of the base had to be reevaluated. The original conditions proposed by Barton and Finet required for the base to deprotonate of the phenol, enabling its nucleophilic coordination to the bismuth as a phenoxide. Therefore we decided to generate the phenoxide prior to the addition to the organobismuth(V) compounds, using NaH (Scheme 2.11).

Scheme 2.11: Reduction of **3g** to **2g** with sodium (4-fluorophenoxide)

The reaction of sodium 4-fluorophenoxide with **3g** resulted in an initial creation of three peaks in the organobismuth(V)- (around -105 ppm) and three peaks in the phenol region (around -128 ppm), resembling the non-, mono- and di- phenoxy substituted organobismuth(V) species as well the free phenoxide. Under reaction conditions these species decay almost exclusively into **2g** with only trace amounts of phenoxide. No arylation products could be observed. An oxidation of the 4-fluorophenol to polyphenolic species can explain the loss of signal in the ^{19}F NMR spectrum in the phenolic region with polymeric peak broadening into the baseline. Notably, none of the previously found decomposition products fluorobenzene or **7** were observed. ^{II}

2.5.3 Identification of the Decomposition Product

The information acquired into the decomposition mechanism provided insight into factors effecting the rate of consumption of **3g**, but no leads into the nature of the main product **7** of this reaction. With the developed reaction conditions of moderate temperatures we set out to identify and isolate this key species.

Scheme 2.12: Identification of the product of the base mediated decomposition of **3g**

As can be seen in Scheme 2.12 the decomposition of **3g** results in an anionic bismuth(III) species of type $[\text{Ar}_2\text{BiOAc}_2]^-$. Related species such as $[\text{HDBU}][\text{Ar}_2\text{BiCl}_2]$ have been reported before as products from the oxidation of alcohols^{108,109} and disproportionation reactions.^{94,151} While the observed decomposition product stands in contrast to previous reports on bismuth-mediated arylation reactions, the isolated species is a logical reaction

^{II}The lack of arylation product is surprising considering Fedorov *et al.*¹⁵⁰ were able to arylate phenols using NaH.

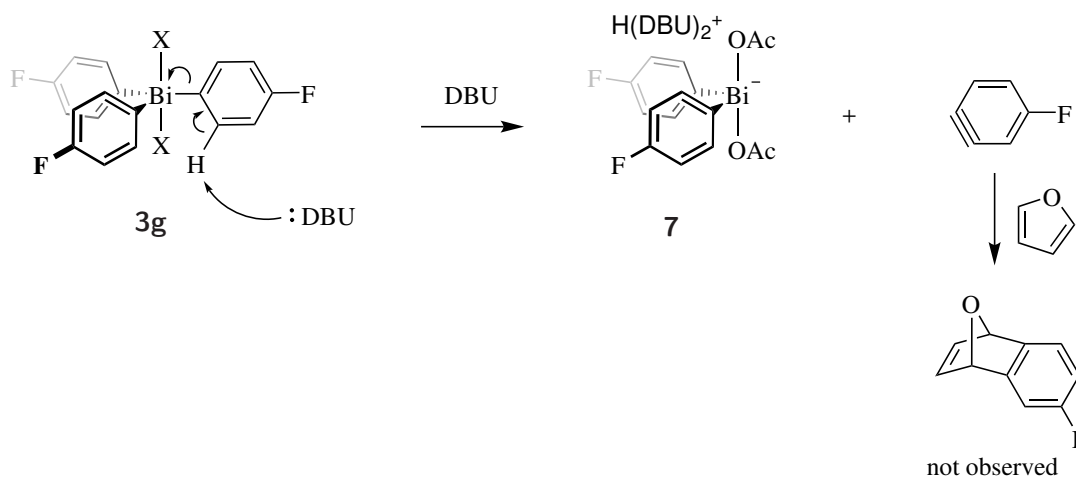
product of the kinetic investigation performed in 2.5.2, where a second order rate determining decomposition led to the consumption of 2 equivalents of DBU.

Proposing a mechanism for the observed transformation remains complicated. As can be seen one aryl group attached to the bismuth centre in **3g** is cleaved to afford in fluorobenzene, requiring a hydrogen source. Equally, the $[\text{HDBU}_2]^+$ obtained a proton. No obvious source of these hydrogen units could be found, as the only reagents in the reaction mixture have been stated in Scheme 2.12.

Identifying the Hydrogen Source

While the reagents themselves do not possess easily abstractable protons, a different source of hydrogen had to be identified. The use of a deuterated solvent in C_6D_6 ruled out the solvent as the hydrogen source as no deuterated fluorobenzene has been observed by either $^1\text{H}/^{13}\text{C}$ NMR spectrometry nor mass spectrometry.

As discussed in recent literature¹⁵² a decomposition mechanism involving an aryne intermediate would provide a proton source (Scheme 2.13). In order to capture any aryne intermediates and therefore identify the proton source, furan was added to the standard reaction mixture. No Diels-Alder product was found, dismissing this mechanism for the proton source.

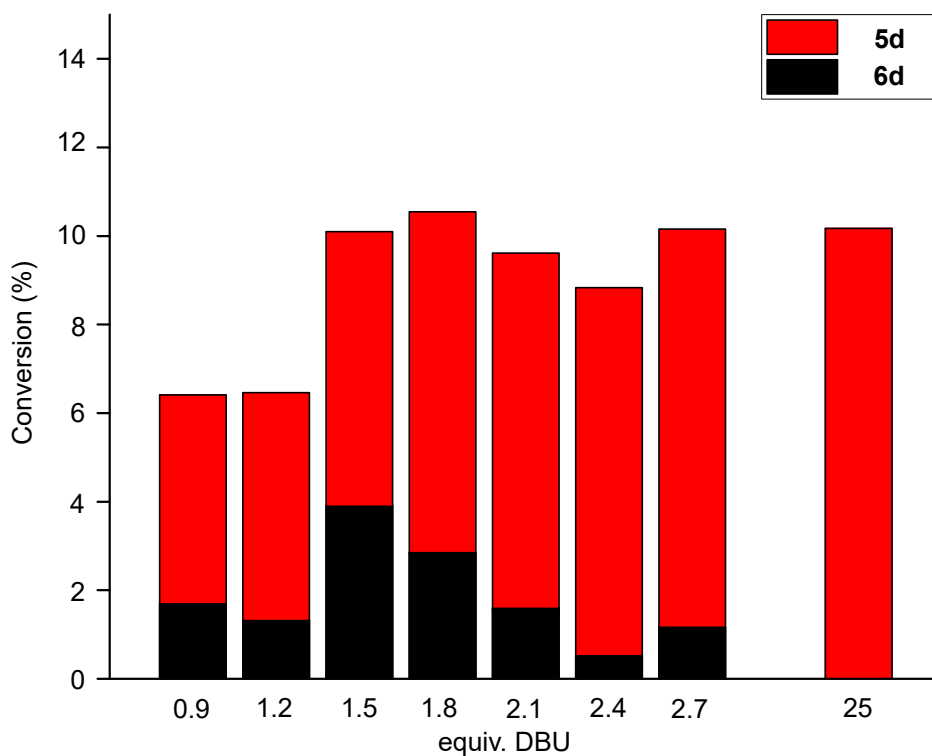
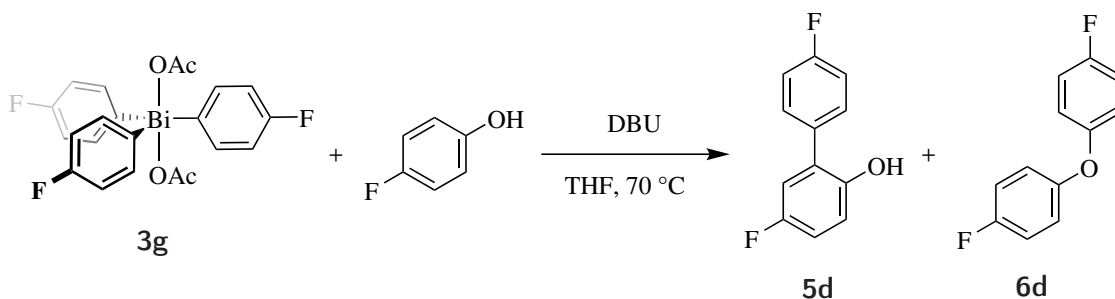


Scheme 2.13: The absence of Diels-Alder products argue against a benzyne mechanism for the liberation of a proton¹⁵²

With no mechanistic explanation for the base-induced decomposition of the organobismuth(V) reagents and no solution to prevent this process occurring, a path facilitating the desired process of phenol arylation over decomposition by acceleration of the desired process will be used in the following.

2.5.4 Optimisation of Reaction Conditions

The purpose of the base to deprotonate the phenol does not explain its use in excess in previous literature. Therefore the effect of different ratios of base *vs* **3g** has been investigated with respect to both the overall yield as well as the product composition.



Scheme 2.14: Product mixture of arylation with different equivalents of DBU; 20 h at 70 °C, [**3g**], [4-fluorophenol] = 23.0 μM in THF

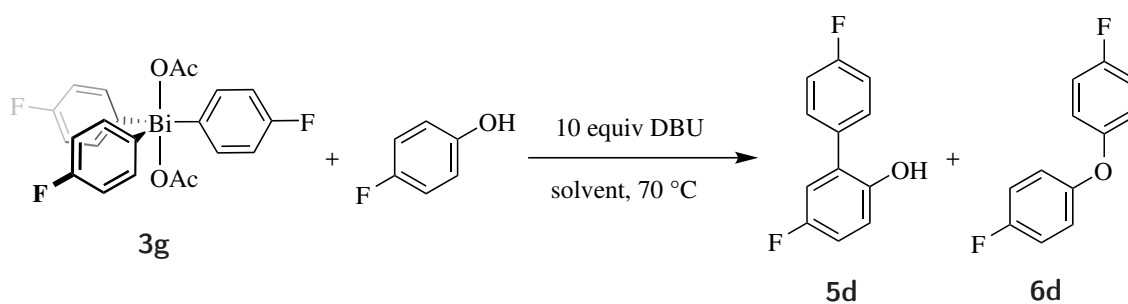
Technically, the base is required to improve nucleophilicity of the phenol as the phenoxide in order to facilitate the nucleophilic attack onto the bismuth centre. Since deprotonation even with strong bases can be considered a reversible process and the hydroxy group is present in product as well as starting material a substoichiometric use of DBU remains viable. With fewer equivalents of base the decomposition reaction would be decelerated, resulting in higher yields. As can be seen in Scheme 2.14 an almost stoichiometric amount of base results in a significantly lower overall yield. With the use of 1.5 equivalents the overall yield levels at around 10%.

When comparing chemoselectivities of the arylation reaction using different equivalents of

DBU a clear trend can be observed. With the increase in relative base concentrations the selectivity between C_{ortho} and O -arylation changes to favour C -arylation with an exclusive selectivity towards 2-hydroxy-5-fluoro-biphenyl product **5d** with high excess of base. The excess of base allows for a higher concentration of the active phenoxide nucleophile. This condition facilitates both arylation processes and should not lead to a change in selectivity. This observation implies that the nucleophilic attack is not the selectivity determining step under these conditions.

Solvent Screen

As the influence of solvents on yield and selectivity of reactions has been reported briefly before,^{153–155} an assessment of different solvents for the arylation of 4-fluorophenol has been conducted.



Entry	Solvent	Yield [%]	
		C_{ortho} -arylation product 5d	O -arylation product 6d
1	Toluene	-	traces
2	THF	10	-
3	THF (air)	3.3	1.5
4	2-Me-THF	1.5	1.4
5	CDCl_3	-	traces
6	MeCN	-	traces
7	DMF	-	5.0
8	DMPU	-	-
9	DMSO	0.6	1.3

Scheme 2.15: Arylation of 4-fluorophenol in different solvents; Conditions: [**3g**] = 23.1 mM, [4-fluorophenol] = 15.4 mM, [DBU] = 231 mM in THF at 70 °C under anhydrous and inert conditions unless stated otherwise.

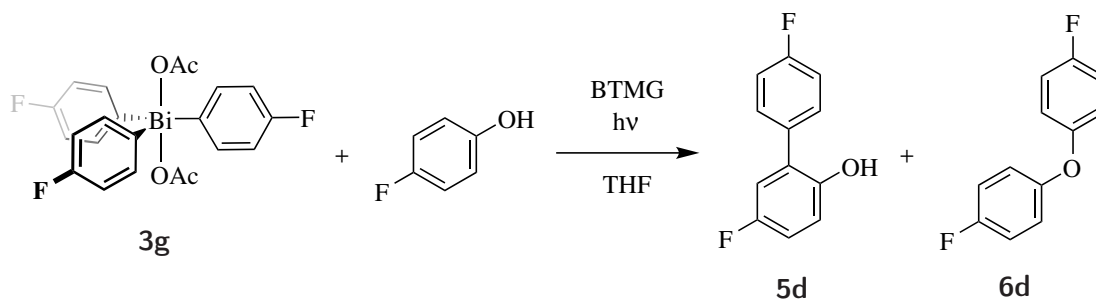
Exploiting the results of the base concentration study, the reactions were performed with a high excess (25 eq.) of DBU (Scheme 2.15). The yields observed in different solvents proved not to deliver higher yields than the THF that was used in our previous studies.

It was observed that anaerobic condition result in higher yields. This observation implies that the presence of air and/or moisture contributes to both selectivity as well as overall yield.

The use of DMF surprisingly resulted in a complete reversal of the selectivity towards the *O*-arylated product. This observation might be attributed to the coordination of the DMF onto the bismuth centre in a mechanism similar to the one reported *vide supra*. The competition of DMF with the phenoxide would then favour the direct nucleophilic attack onto the carbon centre of the aryl ring *ipso* to bismuth, resulting in the *O*-arylated product.

The Influence of Light

Organobismuth(V) compounds generally do not possess visible colour, but show absorption in the UV region below 350 nm (see SI). With the addition of base and phenol a colour change towards yellow is observed, indicating an absorption shift into the visible region. Therefore, an investigation into the dependence of irradiation on overall yield and *C_{ortho}*/*O*-selectivity with visible and UV-Vis light was conducted (Scheme 2.16).



Entry	Light	Yield 25 °C [%]		Yield 70 °C [%]	
		5d	6d	5d	6d
1	none	12	5	9	3
2	Vis (450-700 nm)	19*	2*	11	3
3	UV-Vis (150-700 nm)	16	6	10	4

Scheme 2.16: Light-assisted bismuth-mediated arylation of 4-fluorophenol; [phenol] = 15.4 mM, [**3g**] = 23.14 mM, [BTMG] = 38.6 mM in THF after 20 h, * after 48 h in Pyrex glass equipment.

As can be seen in Scheme 2.16 the reaction was performed with the complete exclusion of light (entry 1), as well as upon irradiation with light in the visible and UV-Vis range. In order to identify a potential light induced acceleration of the reaction's rate, investigations were also conducted at both 25 and 70 °C.

The fact that previously observed yields were reproduced even in the complete absence of light shows that the reaction is not light dependent. The arylation is, however, facilitated

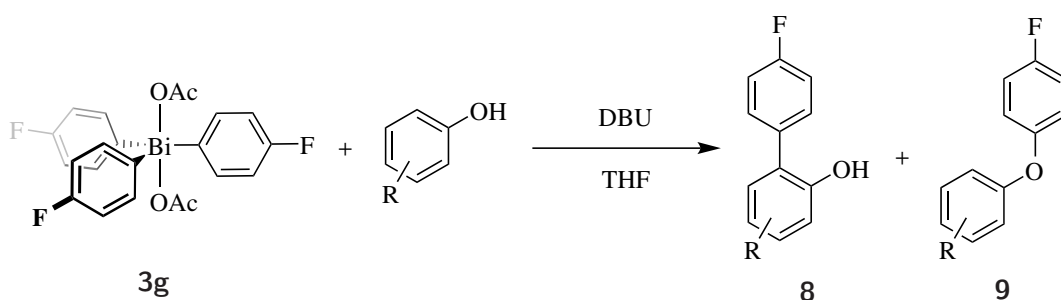
by light as can be seen in Scheme 2.16 (entries 2 and 3). While the trend is close to negligible when the reaction proceeds at 70°C , a clear acceleration of the product forming arylation pathway over decomposition has been observed at 25°C . The negative effect of higher temperatures has been noted once before,¹⁵⁶ but was dismissed by most researchers post and prior.

The samples irradiated with additional light in the UV region showed a black precipitate suspected to be metallic bismuth. Equally a large amount of fluorobenzene has been observed hinting towards the two decomposition products of **2g**. For use in a potential catalytic system, irradiation with visible light appears a plausible option to enhance yields. Regardless of this discovery the observed yields proved inadequate.

2.5.5 Assay of Substrates

While the development of a general protocol for the arylation of all phenols is desired, certain limitations might apply. In order to investigate whether the chosen substrate 4-fluorophenol was such a limiting factor, a variety of different substrates were tested for their reactivity towards bismuth-mediated arylation.

A number of differently substituted phenols have been tested in order to investigate their electronic effects on both yield and chemoselectivity. Electron donating substituents on the phenol such as a methoxy group did not result in detectable yield, but decomposition of **3g** (entry 1 and 3). With electron-neutral as well as slightly electron withdrawing substituents equally no observable yield was detected with the exception of 4-fluorophenol (entry 4). In contrast, electron withdrawing substituents led to significantly different results. Starting from 4- CF_3 -phenol (entry 6) the decomposition of **3g** appears massively decelerated. While our previous investigations show a rapid full decomposition of the Bi(V) species at 70 °C, when using the 4- NO_2 -phenol 92% of **3g** remains present after 20 h (entry 9). Equally the chemoselectivity is rendered reversed with exclusively *O*-arylated products observed.



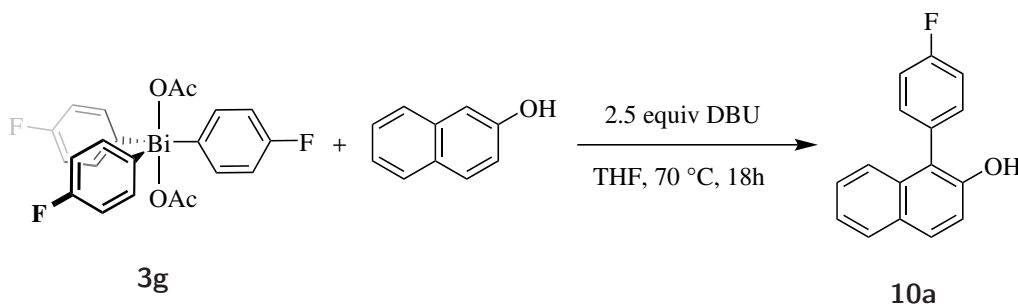
Entry	R	σ	Conversion [%]	<i>O/C_{ortho}</i>	Temp [°C]
1	4-OMe	-0.27	0	-	70
2	4-F	0.06	10	1/9	70
3	3-OMe	0.12	0	-	70
4	3-F	0.34	0	-	70
5	4-Br	0.39	0	-	70
6	4- CF_3	0.54	6	<i>O</i> exclusively	70
7	3,5-F	0.64	20	-	70
8	4-CN	0.66	21	<i>O</i> exclusively	100
9	4- NO_2	0.78	6	<i>O</i> exclusively	70
10	4- NO_2	0.78	67	<i>O</i> exclusively	100
11	2,3,4,5,6-F	-	0	-	70
12	2-F-4- NO_2	-	0	-	70
13	2-F-4- NO_2	-	3	-	100

Scheme 2.17: Arylation of differently substituted phenols; Conditions: [phenol] = 15.4 mM, [**3g**] = 23.14 mM, [BTMG] = 38.6 mM in THF.

While initially surprising these results remain consistent with our previously proposed mechanism. The inherent increase in stability of the Bi(V) species in the presence of phenols bearing an electron withdrawing group can be associated with their decreased pKa (from 10 in phenol to 7.2 in 4- NO_2 -phenol in water). This leads to an increased degree of deprotonation reducing the concentration of free DBU. In accordance to our previous investigations this decrease results in a significantly lower rate for the decomposition of **3g**.

The high chemoselectivity towards *O*-arylation is consistent with previously discussed mechanism (*vide supra*) as well. While electron-poor phenols are deprotonated more easily, they are also worse nucleophiles rendering the competition with the acetate group of **3g** less favourable. While an attack on the *ipso* carbon of the aryl ring remains equally disfavoured it maintains a significant advantage. The *O*-arylation consists of a singular elementary step in the proposed mechanism while the *C_{ortho}* is disfavoured in the nucleophilic attack of the oxygen onto the bismuth centre as well as the nucleophilic attack of the *C_{ortho}* onto the *ipso* carbon of the aromatic ring.

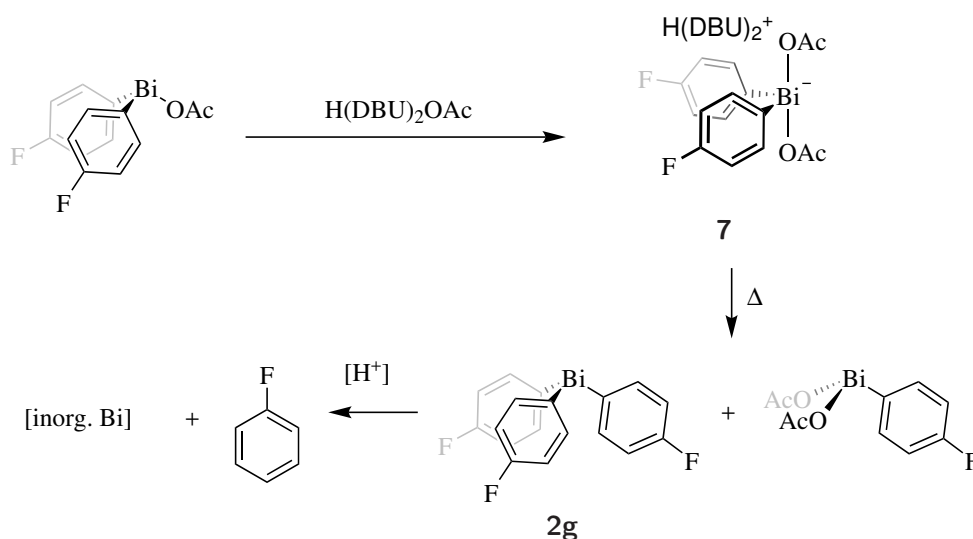
2-Naphthol showed an quantitative conversion to 1-(4-fluorophenyl)-2-naphthol *via C_{ortho}* arylation in the 1 position in almost quantitative yields (Scheme 2.18). As these results have been reported for similar reaction conditions,^{32,157} this result confirmed the trustworthiness of previous reports that identified 2-naphthol as an appropriate substrate for bismuth-mediated arylation reactions. In contrast to previous substrates 2-naphthol converts into the desired product a clean and rapid fashion with perfect chemoselectivity.



Scheme 2.18: Arylation of 2-naphthol

Reaction times could be lowered to 1 hour at 70 °C while maintaining almost quantitative conversion. The use of fluorinated bismuth reagents allowed for an *in situ* observation of the outcome of this reaction. Here, three other previously identified species could be observed: **2g**, fluorobenzene and **7**. The formation of **7** is easily rationalised by the addition of an acetate to the expected Ar_2BiOAc co-product of the arylation proposed by Barton and co-workers¹⁵⁸ (Scheme 2.19). The source of the other reaction products however needed to be investigated.

The relative amount of fluorobenzene and **2g** increased with longer reaction times, hinting towards their nature as decomposition products. A plausible mechanism involves disproportionation to the mono- and tri-aryl bismuth species. The Ar_3Bi species is prone to protodebismuthation, especially under these harsh conditions, resulting in fluorobenzene.

Scheme 2.19: Thermal decomposition of **7** to **2g** and ArBiOAc₂

Upon performing this reaction with 2,6-di-*tert*-butylpyridine, no species of type **7** could be observed, while still maintaining full conversion to the arylated product. This suggests that steric hindrance of the base impedes the formation of this species.

2.6 Kinetic Investigation

As observed in the previous section, and as previously reported,^{105,125,156,157} 2-naphthol undergoes selective arylation at the 1 position in excellent yields. Therefore it was chosen as a substrate to investigate the reaction mechanism of bismuth mediated arylation in greater detail.

In order to understand the reaction mechanism by which triaryl bismuth(V) reagents operate, an investigation of the kinetics of arylation of 2-naphthol derivatives has been conducted. For convenience an *operando* observation using ¹⁹F NMR spectroscopy has been chosen, requiring fluorinated reagents. Thus, a fluorinated 2-naphthol derivative **11c** was prepared (See SI) and reacted with the **3g** rendering both reaction partners observable by ¹⁹F NMR spectroscopy.

As can be seen in Figure 2.6.1, the reaction is considered to occur in a 2 step process. First, nucleophilic attack of the naphtholate onto the Bi(V) centre creates intermediate **12**. This intermediate is assumed to subsequently undergo oxidative arylation of 2-naphthol resulting in the desired product **13c** and the bismuth co-product **7**. No intermediate was observed *via* ¹⁹F NMR spectroscopy. Therefore, if the reaction undergoes a pathway involving an intermediate, its formation must determine the rate of this transformation, with the subsequent oxidative arylation proceeding much more rapidly. Figure 2.6.1 displays the reaction progression plotted in a 1st and 2nd order fashion. As can be seen, the reaction correlates to a 2nd order plot. In the context of the proposed reaction mechanism this indicates a bimolecular interaction in the rate determining step that can be achieved in

the nucleophilic attack of the naphtholate onto **3g**. This appears in good agreement with the absence of intermediate **12**. Hence, the C–C forming reductive elimination proceeds significantly faster than the nucleophilic attack.

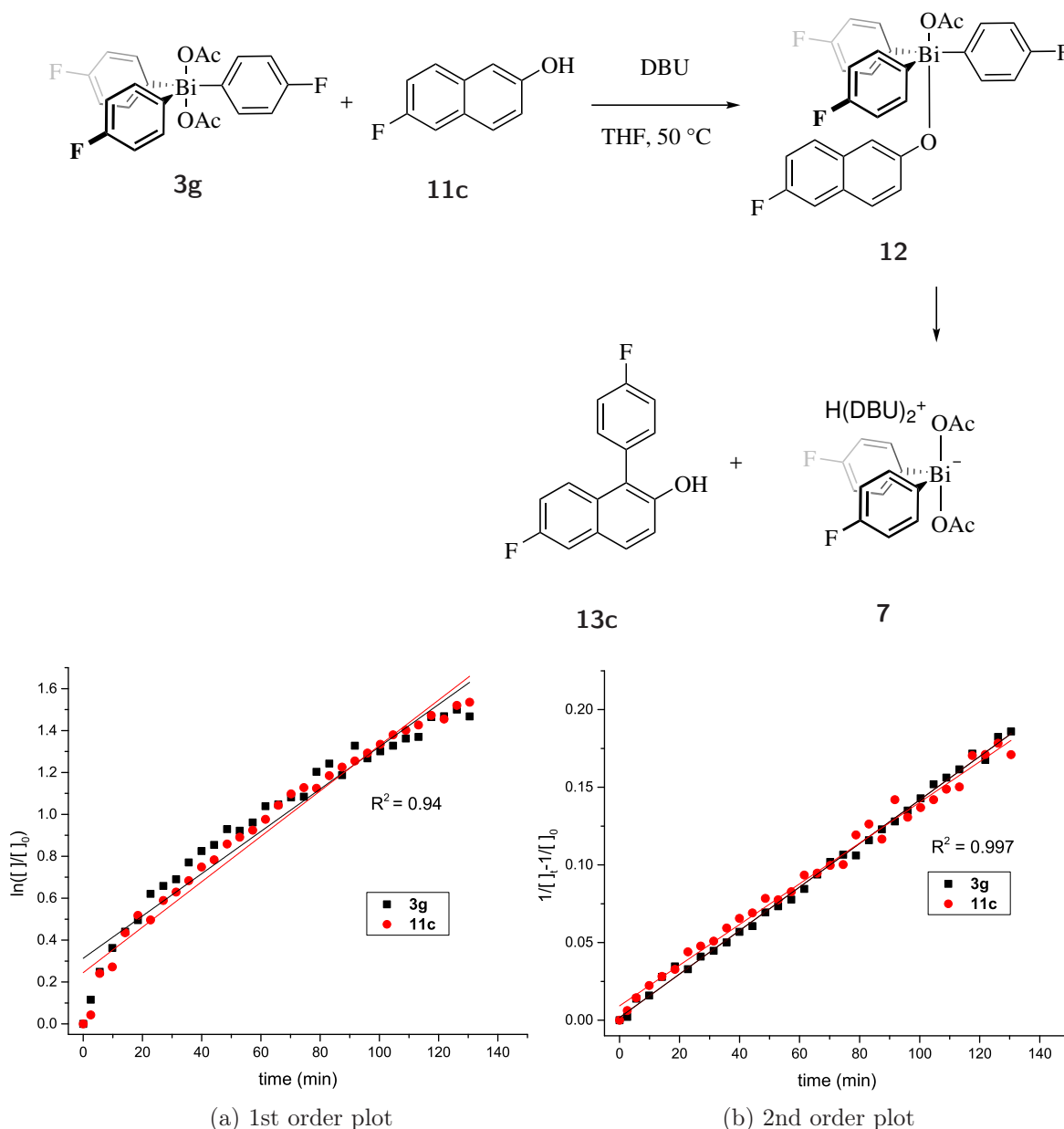


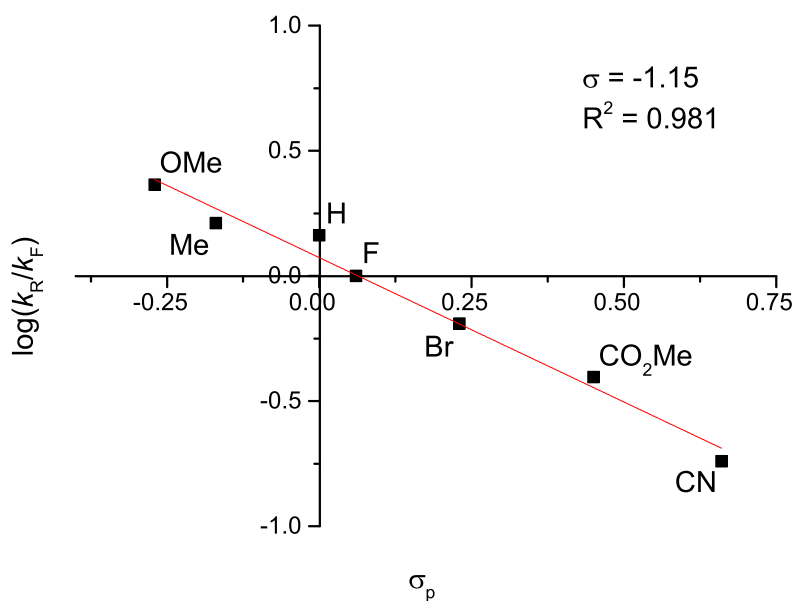
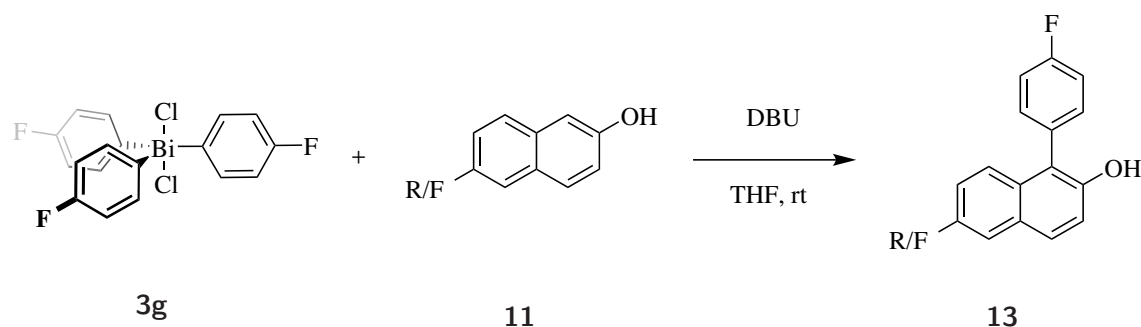
Figure 2.6.1: Reaction progression plotted for a first (left) or second order (right) process; Conditions: [**3g**], [**11c**] = 23.3 mM, [DBU] = 52.9 mM in THF/ C_6D_6 (99/1) at 50 °C.

2.6.1 Naphthol Competition Experiments^{III}

In order to gain insight into the proposed mechanism a detailed investigation into the dependencies of the rate determining step of bismuth-mediated arylation of 2-naphthols was conducted. Given that the formation of the bismuth-naphtholate is the rate deter-

^{III}The experiments detailed in section 2.6.1 have been performed by James Gillespie, a final year masters student, under my supervision.

mining step of the naphthol arylation and that this step is likely to control the selectivity between different naphthols, an intermolecular competition experiment would interrogate the influence of substrate electronics on both selectivity and ratio. To this end competitive experiments between two different 2-naphthols have been performed (Scheme 2.20) with 5.0 equivalents of each 2-naphthol in order to enforce a *pseudo*-1st-order dependency in the bismuth reagent **3g**. The ratio of the individual products must therefore resemble the ratio of the individual rate constants in product determining step of nucleophilic attack.



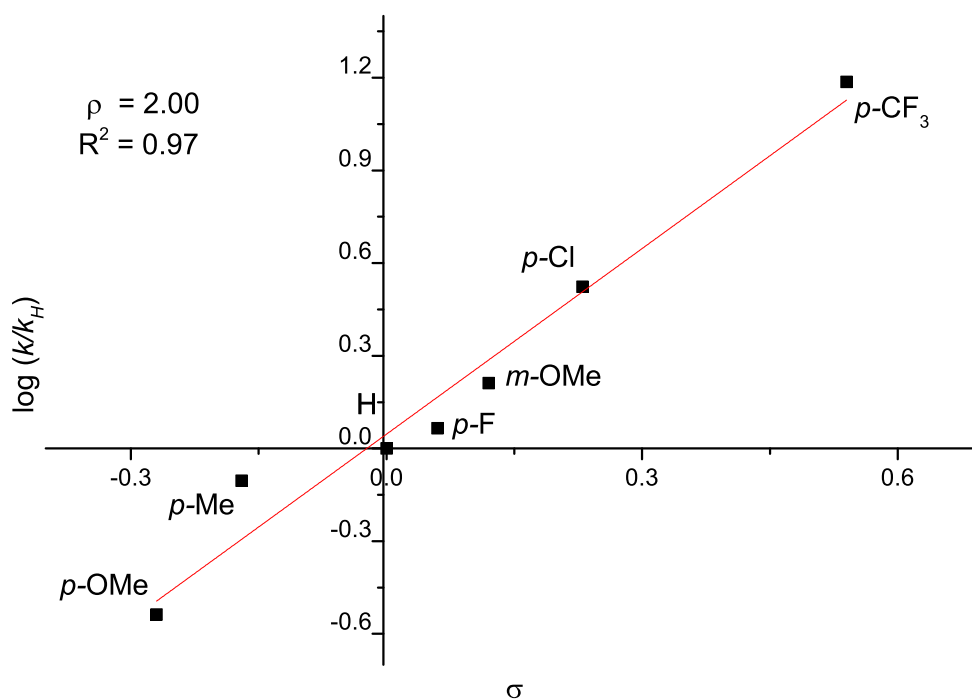
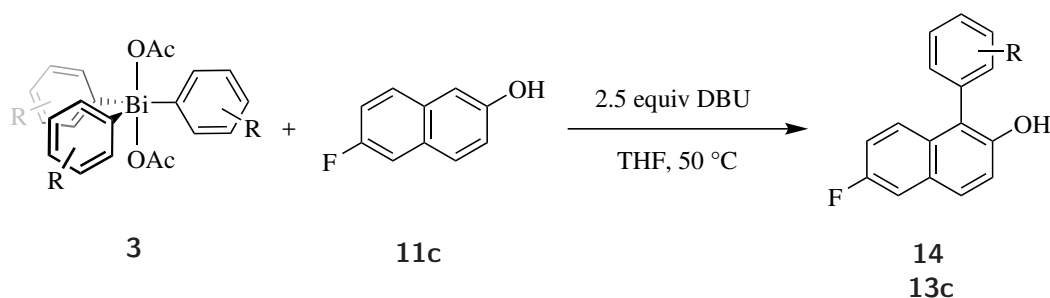
Scheme 2.20: Competitive arylation of 6-fluoro-2-naphthol and 6-substituted-2-naphthol using **3g**; Conditions: [2-naphthols] = 116.7 mM, [**3g**] = 23.3 mM, [DBU] = 583 mM at room temperature in CDCl₃

The use of a fluorinated bismuth(V) reagent allowed the use of ¹⁹F NMR spectroscopy for the direct integration of the ratio of the reaction products. A Hammett-type plot of k_R/k_F vs σ_p yielded in a negative correlation $\rho = -1.15$ as can be seen in Scheme 2.20. This indicates a build up of a positive charge in the 2-naphthol upon transition from a free naphtholate towards a coordination to the Bi(V) centre. This result is consistent with the proposed mechanism, suggesting that the selectivity determining step is also being the

rate determining step of this reaction.

2.6.2 Influence of Transferred Aryl Groups

In order to investigate the influence of the electronic properties of the aryl substituents attached to the bismuth centre, a Hammett study using direct observation of arylation rates of different $\text{Ar}_3\text{Bi}(\text{OAc})_2$ species **3** with 6-fluoro-2-naphthol **11c** was conducted. The resulting second order rate constants were used to construct a Hammett-type plot using relative rates k_{rel} of the differently substituted Bi-species against their electronic properties represented by their Hammett values σ (Scheme 2.21).

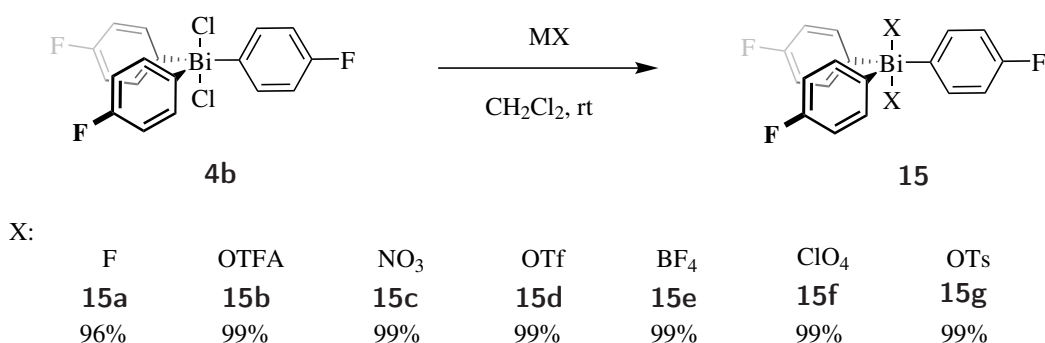


Scheme 2.21: Arylation of 6-fluoro-2-naphthol **11c**; Conditions: $[\mathbf{3}] = 29.1 \text{ mM}$, $[\mathbf{11c}] = 26.4 \text{ mM}$, $[\text{DBU}] = 52.9 \text{ mM}$ in THF/ C_6D_6 (99/1) at 50°C .

The ρ value of 2.00 indicates a build up of negative charge in the reactive centre during the rate determining step. This again is consistent with rate limiting attack by the naphtholate which would lead to an increase in electron density at the bismuth(V) centre (Scheme 2.22).

has been conducted to allow for a holistic understanding of bismuth-mediated arylation. The nature of the anions attached to the bismuth(V) centre in Ar_3BiX_2 influences the reactive centre in two regards. For one, more acidic/weakly coordinating anions donate less electron density to the bismuth centre allowing for a more electrophilic centre and driving force for the nucleophilic attack. On the other hand, weakly coordinating counter ions represent better leaving groups.

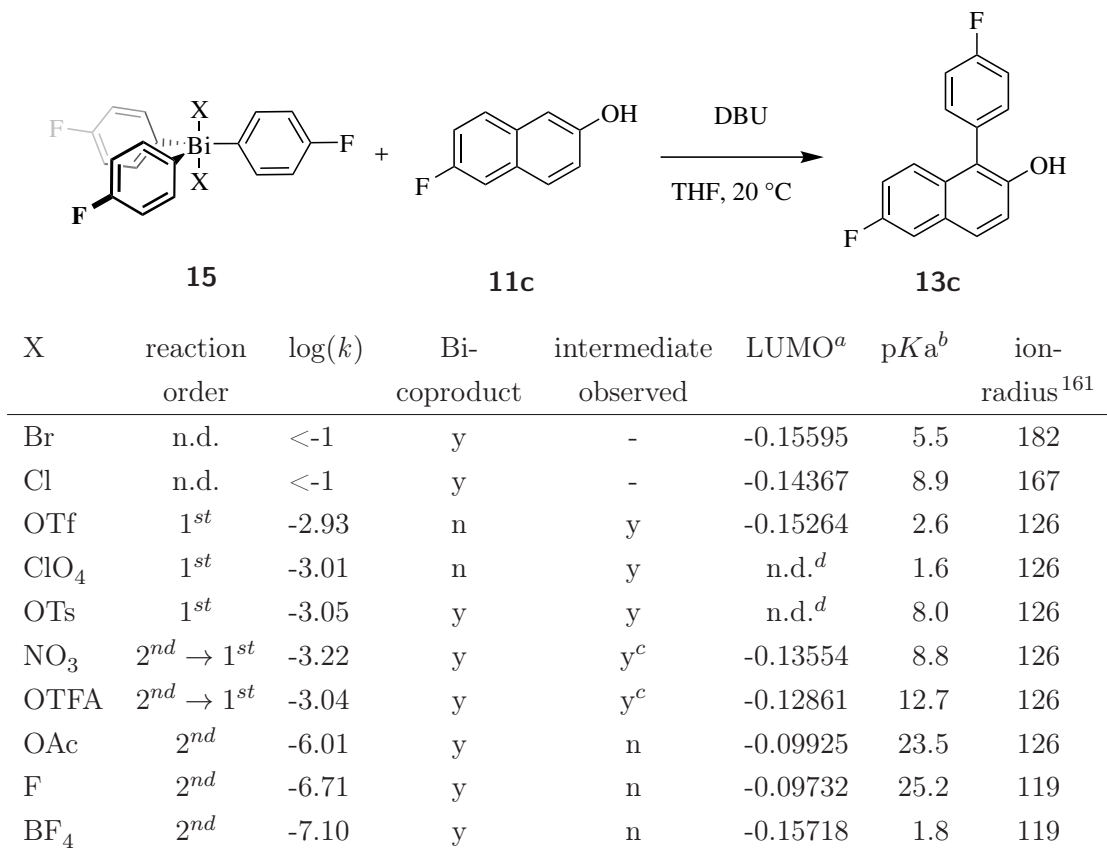
In order to investigate the influence of differently substituted bismuth centres a variety of Ar_3BiX_2 species has been prepared. While counter ions Cl^- , Br^- , OAc^- are readily accessible through oxidation of the corresponding Ar_3Bi species, other counter ions had to be accessed from Ar_3BiCl_2 by salt metathesis using the corresponding silver salts or in the case of F^- sodium fluoride.



Scheme 2.23: Exchange of the counter ion of Ar_3BiCl_2 **4b** *via* salt metathesis; M = Ag, Na

Other derivatives, in particular the ones using weakly coordinating anions, have not been studied previously in great detail. The iodide or thiocyanate derivatives have been reported to undergo spontaneous decomposition to give the Ar_2BiX and ArX .^{159,160} When oxidation was performed with using IBr , the decomposition products were exclusively determined as aryl iodide. This intramolecular competition shows that the softer counter ion undergoes the elimination process.

Derivatives featuring F, OAc, Cl, OTFA, NO_3 , Br, BF_4 , OTf, ClO_4 and OTs counter ions have been prepared. The resulting Ar_3BiX_2 -species were used for the arylation of 6-fluoro-2-naphthol **11c** in order to establish their kinetic behaviour.



Scheme 2.24: Arylation of 6-fluoro-2-naphthol **11c**; X = F, Cl, Br, OTf, ClO₄, OTs, NO₃, OTFA, OAc, BF₄; ^a calculated B3LYP LANL2DZdp ECP, ^b measured in MeCN,¹⁶² ^c slow build-up, ^d a stable conformation could not be found.

Monitoring the reaction profiles using ¹⁹F NMR spectroscopy allowed for the observation of a variety of species and trends. While the counter ions OAc⁻, F⁻ and BF₄⁻ showed classical 2nd order reaction profiles with a direct conversion from starting material to the arylated 2-naphthol product **13c** and the Ar₂BiX₂⁻ species, other anions showed a more complex behaviour. For NO₃⁻ and ⁻OTFA the reaction mixture changed from the starting materials towards a multitude of reactive intermediates within the first minutes of observation. Upon complete conversion of the starting materials a classic 1st order profile was observed (Figure 2.6.3).

The reaction profiles of the arylation reactions using ⁻OTs, ClO₄⁻ and ⁻OTf show a more rapid build up of the intermediate species. A 1st order conversion to the arylated 2-naphthol product **13c** was observed.

For the Ar₃BiX₂ species with an Cl⁻ and Br⁻ counter ion no reaction profile could be obtained as the reaction concluded before the first ¹⁹F NMR spectrum could be taken (58 s).

This indicates a significantly higher rate of reaction than for the other counter ions.

The bismuth-coproduct Ar₂BiX₂⁻ has been observed for most counter ions. ClO₄⁻ and ⁻OTf showed no observable bismuthate species, but a significant amount of precipitate built-up over the course of the reaction.

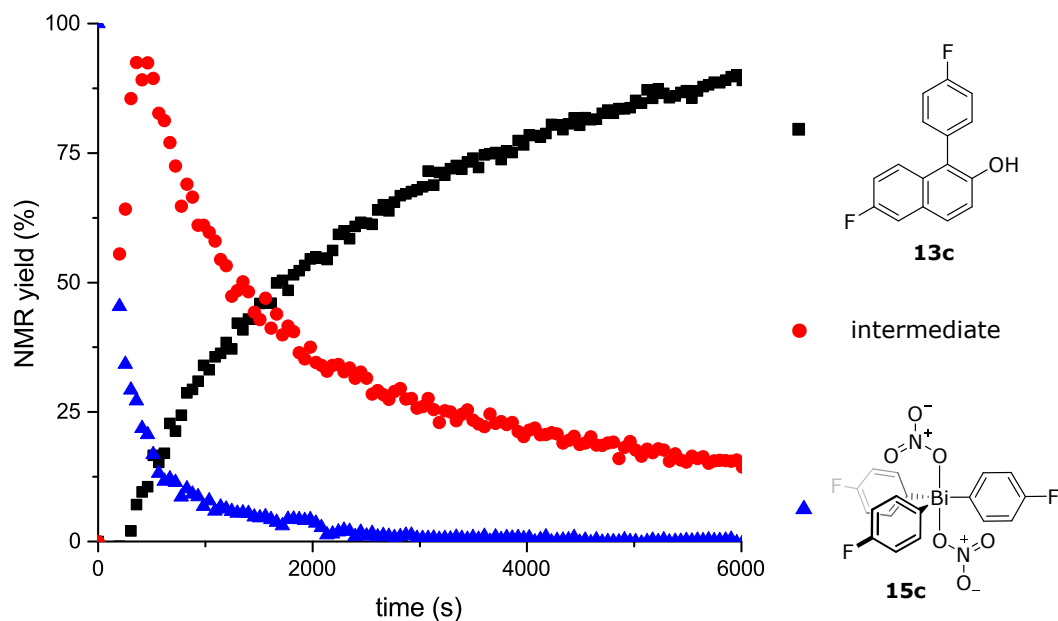
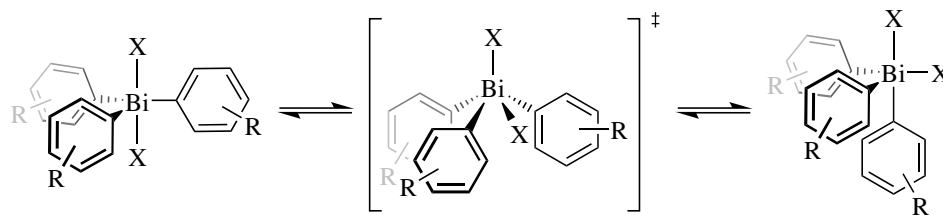


Figure 2.6.3: Kinetic profile of **15c** and 6-fluoro-2-naphthol **11c** with initial build-up of the Bi-ONaph intermediate species

In order to explain the trends observed a variety of parameters were considered. First of all, a distinction between three trends needs to be made: the rate of nucleophilic attack, the rate of reductive elimination and the stabilisation of the $\text{Ar}_2\text{BiX}_2^-$ bismuth-coproduct. In order to explain the effects on the nucleophilic attack, a classical measure to evaluate the coordinating properties of counter ions was considered; the pKa. Strong acids produce weak conjugate bases due to a better charge distribution in the corresponding anionic form. Following this principle the Ar_3BiX_2 -species with anions of increasingly stronger acids possess an increasingly higher rate of the nucleophilic attack. This can be observed with F^- and OAc^- . As the counter ions become less coordinating the rate increases until the nucleophilic attack becomes faster than the reductive elimination as can be seen in the other examples. NO_3^- and $^- \text{OTFA}$ show a slow build up of the bismuth-naphtholate species as the rate of formation and reductive elimination are similar. The bismuth reagents featuring the conjugate base of the stronger acid show a considerably higher rate of formation, making this build-up too fast to observe.

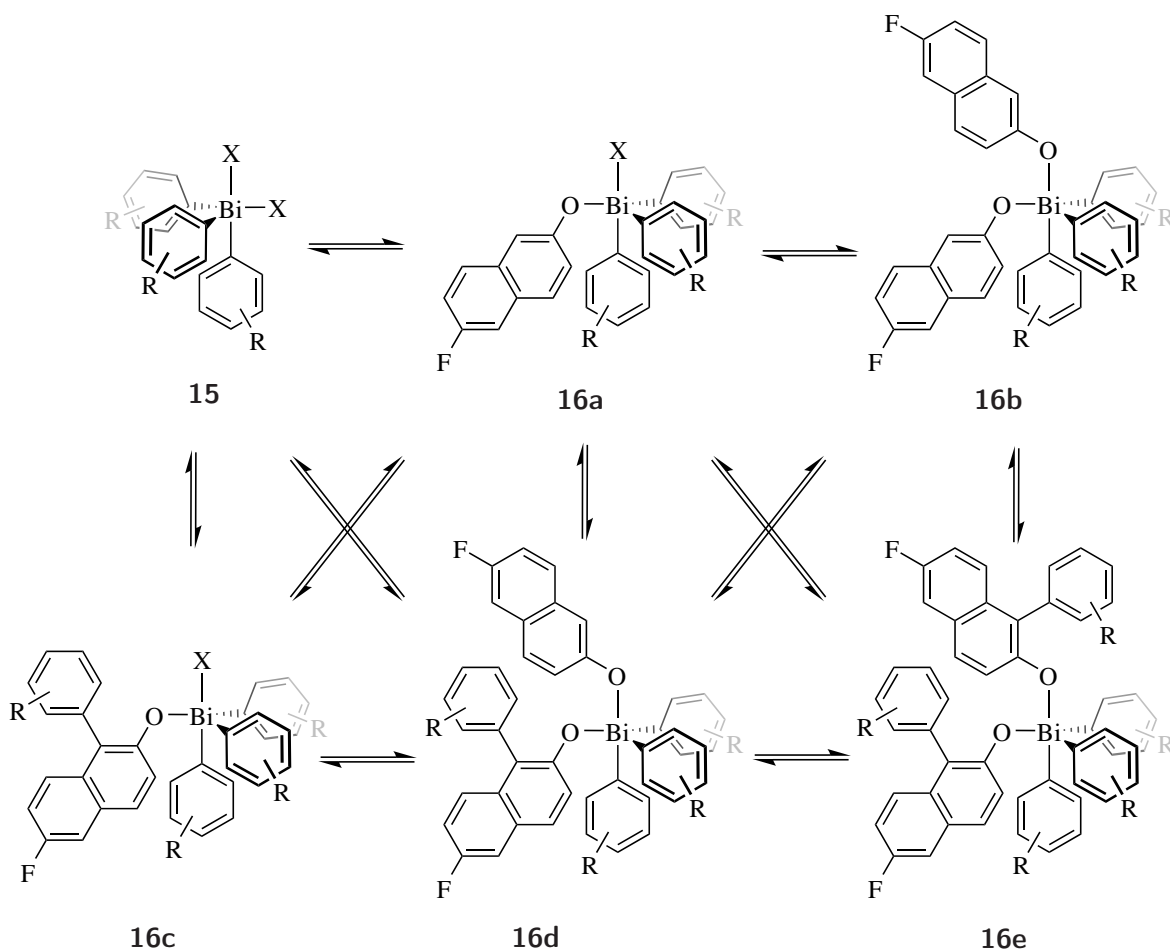
Another explanation for the same trend can be found in a more theoretical approach. As the nucleophilic attack proceeds by population of the of the electrophiles LUMO, the position of these orbitals can be considered. A nucleophilic attack in an $\text{S}_{\text{N}}2$ type mechanism traditionally involves the σ^* of the Bi-X bond. With the standard representation the anionic ligands are usually described in an apical position due to their higher apicophilicity such that the Bi-X σ^* is blocked due to the linear hypervalent 3c-4e of the bismuth centre and the apical counter ions. In order to render the LUMO/ σ^* accessible, Ar_3BiX_2 species must undergo a Berry *pseudorotation* (Scheme 2.25).¹⁶³

Scheme 2.25: Berry *pseudorotation* of Ar_3BiX_2

Following this process the LUMO/ σ^* is exposed in the equatorial position rendering a nucleophilic attack possible. The energy of the orbital was calculated by DFT (See SI), revealing that the counter ions that show rate limiting nucleophilic attack possess a significantly lower LUMO energy.

For the bismuth species where the counter ions result in a rate limiting reductive elimination the identification of a trend is more complicated. Neither pKa nor LUMO energies result in a good correlation to the observed rates. Especially the significantly faster Cl^- and Br^- don't fit any previous trends.

The most compelling explanation can be found in the classical HSAB concept.¹⁶⁴ With respect to the atom binding to the bismuth centre a rough trend can be observed. While the $^- \text{OTFA}$, NO_3^- , $^- \text{OTs}$, ClO_4^- , and $^- \text{OTf}$ possess significantly different electronic properties, the overall observed rates do not show a significant difference. This might be explained by the one thing they have in common: a coordination through the oxygen. Cl^- and Br^- possess much larger radii and the rates of both attack on bismuth and subsequent reductive elimination are also much higher. This observation might indicate that a soft-soft interaction between bismuth and the counter ion X promotes the reductive elimination of the naphtholate-bismuth-X intermediate. This hypothesis is supported by previous attempts to make Ar_3BiX_2 species with even softer anions, X (I^- or SCN^-). The soft character of these counter ions promotes the reductive elimination to the point that Ar_3BiX_2 species themselves become unstable even without 2-naphthol present resulting in Ar_2BiX and ArX . The naphtholate-bismuth(V) intermediate species have been observed for the reaction of 2-naphthol with Ar_3BiX_2 where X = $^- \text{OTFA}$, NO_3^- , $^- \text{OTs}$, ClO_4^- or $^- \text{OTf}$. While only the naphtholate-bismuth-X species was expected, a multitude of peaks was observed. These peaks were attributed to organobismuth(V) species, as can be seen in Scheme 2.26.



Scheme 2.26: Proposed intermediates for the arylation of 6-fluoro-2-naphthol, with R = 4-fluoro.

At the beginning of the arylation, free Ar_3BiX_2 is present in equilibrium with the mono- and di-2-naphthol substituted organobismuth(V) species **16a** and **16b**. As the reaction progresses the peak of Ar_3BiX_2 disappears and new peaks arise that were assigned to organobismuth(V) species substituted with the 1-aryl-2-naphthol reaction product **16c**, **16d** and **16e**. The species involved in the production of the reaction product could not be identified as all species exist in a fast equilibrium and the sum of all peaks decays in a 1st order fashion.

It is interesting to note that the organobismuth(V) species substituted with two 2-naphthol substituents does not undergo a destructive reduction process resulting in Ar_3Bi and oxidised 2-naphthol, as has been observed for phenols (*vide supra*).

It was noted that the soluble anionic $\text{Ar}_2\text{BiX}_2^-$ Bi-coproduct can be observed for all examples except the OTf and ClO_4 species. Presumably the weakly coordinating nature of these anions prevents the formation of the ate-species, resulting in the precipitation of the bismuth-containing co-product.

As this investigation was not the prime objective of this project, additional work has not

been conducted on this mechanistic investigation. It was noted that the exchange to weakly coordinating anions resulted in a change in the rate determining step towards the reductive elimination and that the use of heavier halogens results in a almost instantaneous reaction progression.

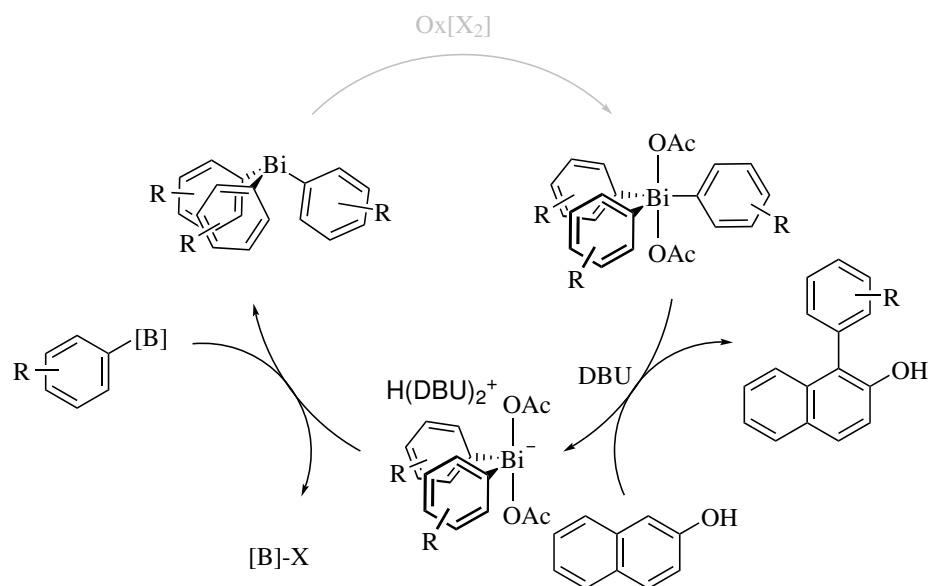
These trends can be used as guidelines for a future, more in depth investigation into the mechanism of this reaction, as well as potentially in the design of more effective arylation protocols.

2.7 Arylation of Diarylbismuth Species

In order to achieve the catalytic application of bismuth the re-arylation of diarylbismuth species **7** to triarylbismuth was investigated. Transmetallations onto a bismuth centre using organometallic reagents have been reported before employing highly reactive organolithium⁷⁸ or Grignard-reagents.^{66,72,109,165} The need for these powerful reagents is based on the weak Bi–C bond (137 kJ/mol⁶⁰) creating a weak thermodynamic driving force for its formation.

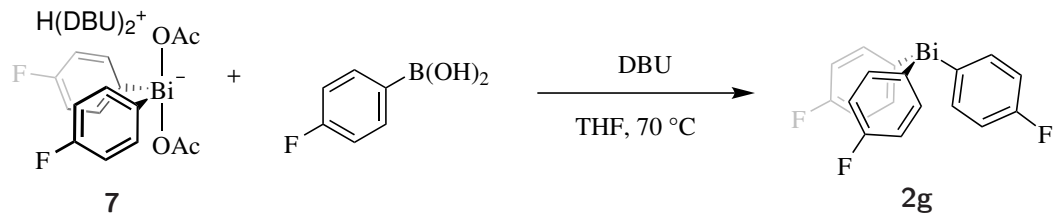
In the context of the proposed catalytic cycle (Scheme 2.27), however, the use of reactive organometallics is not possible due to their incompatibility with substrate, oxidant and/or other reagents. Therefore it was decided to attempt to use the much milder, more readily available aryl boron species as a transmetallation reagents. These have been applied to transmetallation with a vast number of metals, including bismuth.⁹² While the transmetallation to Bi(V) compounds using organoboron reagents has been used extensively by Matano *et al.*,¹⁶⁶ the transmetallation of Bi(III) has been proven to the best of our knowledge only using NaBPh₄¹⁶⁷ for conversion of bismuth tricarboxylates to Ar₃Bi, and using boronic acids *via* aryl group migration.¹⁶⁸

The required diarylbismuth reagent Ar₂Bi(OAc)₂[−] was accessed through the previously investigated arylation of 2-naphthol. Since Ar₂Bi(OAc)₂[−] showed a poor bench stability they were freshly prepared prior to transmetallation studies and used in a one pot protocol, providing insight into the compatibility of the individual reagents.



Scheme 2.27: Arylation of phenols using Ar_3BiX_2 compounds and subsequent transmetalation in the proposed catalytic cycle

In order to investigate the transmetalation capabilities of boronic acids in the context of the proposed catalytic cycle, we initially considered transmetalation protocols that have been successfully applied to the transmetalation to precious metals¹⁶⁹ (Scheme 2.28).



Scheme 2.28: Transmetalation to **7** from 4-fluorophenyl-boronic acid

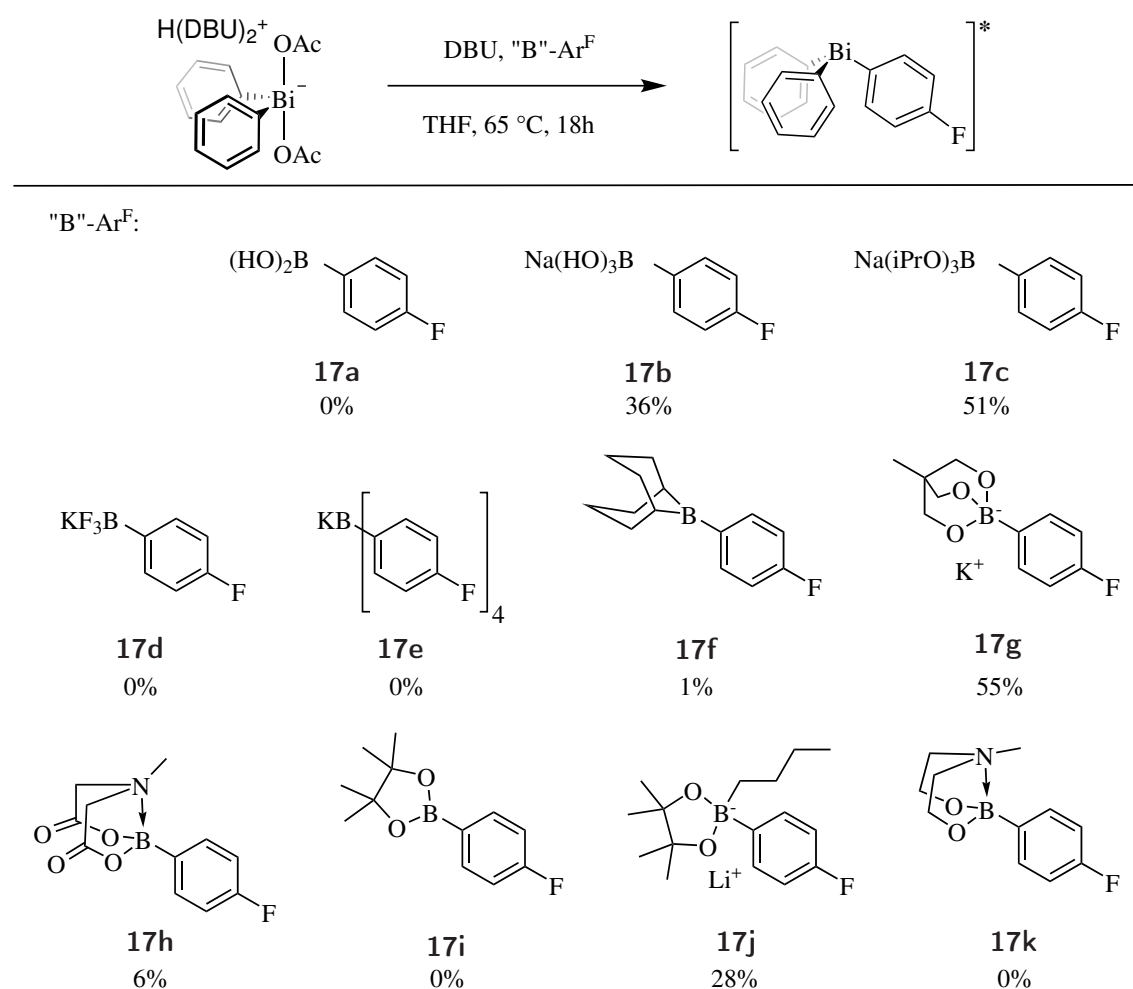
Using ^{19}F NMR spectroscopy, conversion from $\text{Ar}_2\text{Bi}(\text{OAc})_2^-$ **7** to Ar_3Bi **2g** was observed, although full mass balance of this transformation could not be accounted for. As discussed above, the diaryl bismuth(III) species undergoes a disproportionation reaction to result in the desired product as well. Therefore, a distinction between decomposition product and transmetalation product remains challenging.

In order to overcome this challenge a non-fluorinated $\text{Ph}_3\text{Bi}(\text{OAc})_2$ has been used for the arylation of 6-fluoro-2-naphthol rendering the diaryl bismuth(III) co-products undetectable by ^{19}F NMR spectroscopy. Using 4-fluorophenyl boronic acid as the transmetalating reagent, the product should therefore be the sole detectable species, allowing for an easy quantification.

2.7.1 Transmetallation Using Organoboron Reagents

The initial attempts for the transmetallation of $\text{Ph}_2\text{Bi}(\text{OAc})_2^-$ showed no conversion to the desired $\text{Ar}^F\text{Ph}_2\text{Bi}$ product ($\text{Ar}^F = 4\text{-fluorophenyl}$). To enhance the reactivity of organoboron reagents for the transmetallation to bismuth(III) reagents, a variety of different 4-fluorophenyl boron reagents was prepared and subjected to the transmetallation conditions.

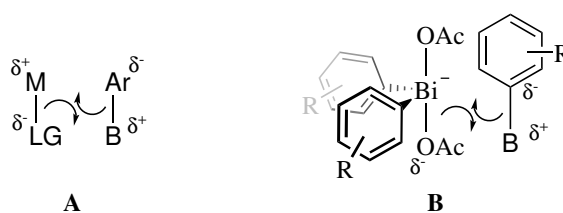
During this study the expected transmetallation product of type ArPh_2Bi was not identified as the exclusive product. Instead, a multitude of peaks were observed. A combination of ^{19}F NMR spectroscopy and mass spectrometry allowed for the identification of products with varying amounts of Ar^F groups (Ph_3Bi , $\text{Ar}^F\text{Ph}_2\text{Bi}$, Ar^F_2PhBi , Ar^F_3Bi , $\text{Ar}^F\text{PhBiX}_2^-$ and $\text{Ar}^F_2\text{BiX}_2^-$). Migration of aryl groups between bismuth centres has been observed before,¹⁵² but it can clearly be stated that the Ar^F groups originate from an arylation with the boron derivative.



Scheme 2.29: Transmetallation to $\text{Ph}_3\text{Bi}(\text{OAc})_2$ from organoboron reagents, *mixture of different species of $\text{BiAr}_n^F\text{Ph}_{3-n}$ with $n = 0-3$ and $\text{Ar}^F = 4\text{-fluorophenyl}$; $[\text{Ph}_2\text{Bi}(\text{OAc})_2^-] = 10.2 \text{ mM}$, $[4\text{-fluorophenyl boron reagent}] = 40.8 \text{ mM}$ in THF at 65°C for 18 h.

The use of different boron species (Scheme 2.29) employed aryl groups of varying nucleophilicity to this methodology. It was observed that while the charged boron species (**17b**, **17c**, **17g** and **17j**) result in a successful transmetalation, neutral boron species (**17a**, **17f**, **17h**, **17i** and **17k**) showed low or no conversion. The trifluoroborate **17d** and tetraarylborate **17e** proved exceptions to the trend, presumably due to their limited solubility.

Overall, the trend observed shows that more electron-rich and therefore nucleophilic boron derivatives show a higher activity towards transmetalation. Illustrated in Scheme 2.30 A is simplified mechanism in which the accepting metal (M) is typically electropositive with a partial positive charge. Aryl boron reagents have a bond polarisation towards an electronegative carbon atom adjacent to boron. This simplification enables a concerted mechanism in which the nucleophilic carbon of the boronic acid attacks the electrophilic metal.



Scheme 2.30: A: general mechanism transmetalation, B: Mismatched situation on $\text{Ar}_2\text{BiX}_2^-$

The negative charge of the $\text{Ph}_2\text{BiOAc}_2^-$ reduces the electrophilicity of the bismuth centre and renders the σ^* orbital occupied. In combination with the creation of the relatively weak Bi–C bond, the weak driving force for this transformation remains. An increased nucleophilicity of boronate compounds presumably allows for the reaction to occur despite the mismatched electronic properties of the reagents.

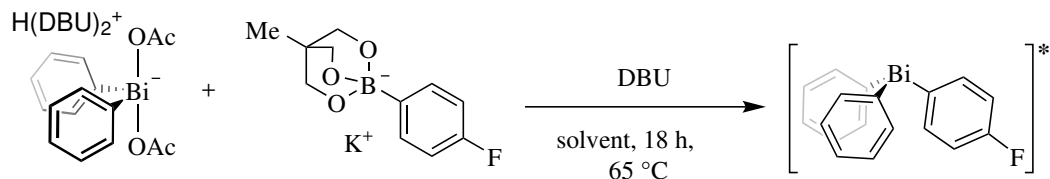
The best result was achieved using the potassium 4-fluorophenyl triol borate at 55% due its high nucleophilicity.¹⁷⁰ For this reason this boron species has been used in the following investigation.

As the proposed catalytic cycle involves the transmetalation as a key step, optimisation of this procedure was conducted. The reaction is heterogeneous with the boron reagent showing low solubility in THF as was confirmed using ^{19}F NMR spectroscopy. In combination with the absence of a rate increase upon the use of superstoichiometric amounts of the boron reagent, a 0^{th} order mass transfer limited reaction profile was assumed with a rate determination by low concentration of the boron reagent in solution.

2.7.2 Solvent Dependency of the Transmetalation

In order to overcome the inherent insolubility of the boron species a variety of solvents were tested for transmetalation. For this investigation solvents of varying polarity have been employed to the B-to-Bi transmetalation conditions that have been reported above. The polarity of different solvents can be quantified by their dielectric constant (ϵ_r). As

anticipated, more polar solvents such as DMSO or DMF result in a better/full solubility of the boron reagent.



Entry	Solvent	Conversion [%]	ϵ_r ^{171,172} []
1	Dioxane	77	2.3
2	Toluene	55	2.4
3	CDCl ₃	>99	4.8
4	MeTHF	>99	6.9
5	THF	65	7.5
6	EMIM-Cl	-	~12.9
7	HFIP	-	16.7
8	Ethanol	42	24.3
9	MeCN	7.9	37.5
10	DMF	-	38.0
11	DMSO	-	46.7
12	PC	-	64.0

Scheme 2.31: Transmetalation of $\text{Ar}_2\text{BiX}_2^-$ using potassium 4-fluorophenyl triol borate in different solvents, *mixture of different species of $\text{BiAr}_n^F\text{Ph}_{3-n}$ with $n = 1-3$ and $\text{Ar}^F = 4$ -fluorophenyl; $[\text{Ph}_2\text{Bi}(\text{OAc})_2^-] = 10.2 \text{ mM}$, $[\text{4-fluorophenyl triol boronate}] = 40.8 \text{ mM}$ at 65°C for 18 h.

As can be seen in Scheme 2.31, higher conversions can be observed with relatively non-polar solvents with no observed conversion for highly polar solvents such as DMF, DMSO and PC. This counter-intuitive effect may be explained by the absence of a driving force due to the solubility of KOAc in the more polar solvents or the coordination of the polar solvent to the bismuth centre. The use of MeTHF or CDCl₃ results in full conversion after 5 h. Less polar solvents result in worse conversion, most likely due to insufficient solubility of the organoboron species.

The use of HFIP resulted in the generation of quantitative amounts of fluorobenzene, indicating a protodeboronation mechanism mediated by the acidic solvent. The use of EMIM-Cl presumably proved unsuccessful due to the presence of Cl⁻ within the system, resulting in a more stable $\text{Ph}_2\text{BiX}_2^-$ species.^{94,109,151}

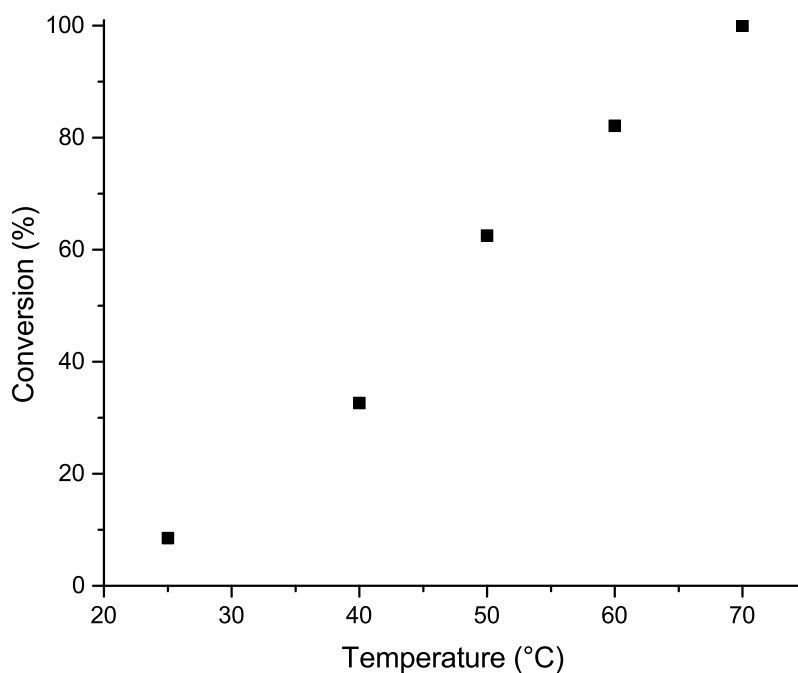
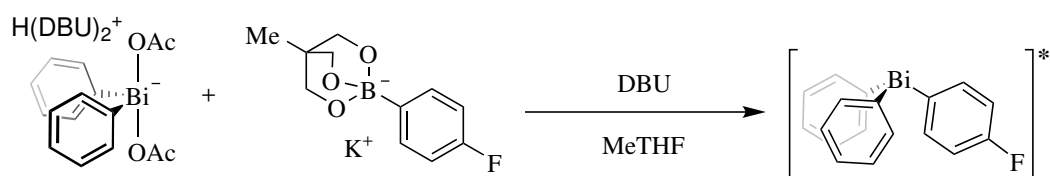
While both CDCl₃ and MeTHF result in full conversion after 5 h, MeTHF was identified for future studies, due to its smaller environmental impact.¹⁷³

2.7.3 Investigation into the Rate Determining Step

In order to further improve the rate of the reaction the rate limiting factor had to be identified. With previous indication pointing towards the solubility of the arylboron species

this hypothesis was investigated.

While the dependency of most reactions obey Arrhenius' law ($k = Ae^{-\frac{E_a}{RT}}$), a solubility dependent reaction should not show this behaviour. Therefore an Arrhenius-type plot was conducted for the transmetallation of the $\text{Ph}_2\text{BiOAc}_2^-$ species.



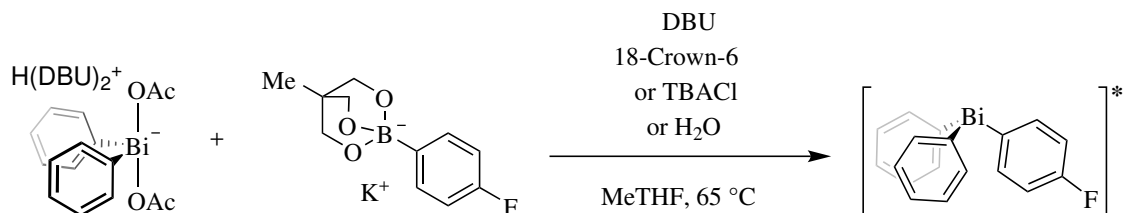
Scheme 2.32: Transmetallation of $\text{Ar}_2\text{BiX}_2^-$ using postassium 4-fluorophenyl triol borate at different temperatures; $[\text{Ph}_2\text{Bi}(\text{OAc})_2^-] = 10.2 \text{ mM}$, $[\text{4-fluorophenyl triol borate}] = 40.8 \text{ mM}$ at various temperatures for 5 h, *mixture of different species of $\text{BiAr}_n^F \text{Ph}_{3-n}$ with $n = 0-3$ and $\text{Ar}^F = 4\text{-fluorophenyl}$

The linear trend observed for this investigation (see Scheme 2.32) indicates a non Arrhenius-type behaviour, indicating a solubility dependency of the reaction. The increase in temperature results in an increased solubility of the bismuth species as well as an increased rate based on Arrhenius' equation, hindering the possibility of distinguishing between the two effects.

Traditionally, inherent insolubility of an reagent can be overcome by the use of phase transfer reagents. This methodology has been applied to this reaction due to the insolubility of the organoboron transmetallation reagents. The use of TBACl should allow for an increased solubility by the precipitation of KCl in MeTHF to form the more soluble TBA organoborate. However, instead of increased conversion, none of the desired product was

observed. This has been observed before as bismuth reagents result in insoluble precipitates in the presence of TBA cations.^{174,175}

When 18-crown-6 was employed as an additive to chelate the potassium cation of the borate no increase in solubility and conversion was observed.



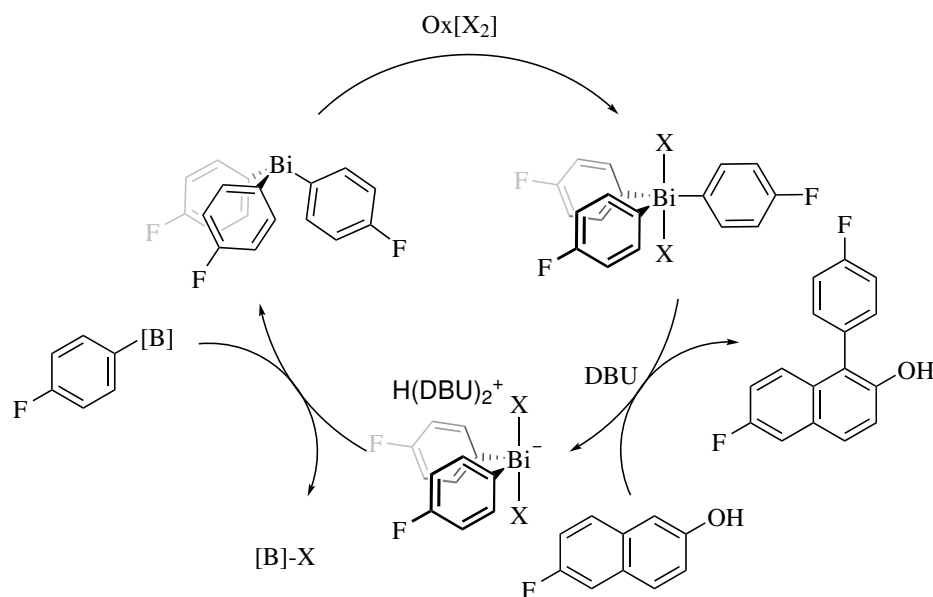
Scheme 2.33: Transmetalation of $\text{Ar}_2\text{BiX}_2^-$ using postassium 4-fluorophenyl triol boronate with different phase transfer reagents, reaction time = 5 h, *mixture of different species of $\text{BiAr}_n^F\text{Ph}_{3-n}$ with $n = 1-3$ and $\text{Ar}^F = 4\text{-fluorophenyl}$

Water was added to the transmetalation reaction in order to generate a biphasic system. While a biphasic system with complete solubility of all reagents in either of the phases was achieved an increase in conversion was not observed.

While an increase in rate of this reaction is a valuable premise, an extensive optimisation will be performed once all steps of the completed proposed catalytic cycle have been established (Scheme 2.34).

2.8 Oxidation and Combination of the Individual Steps

The oxidation is the remaining step step to complete the proposed catalytic cycle. The investigation was performed using **2g** as it allows for observation of the reaction progress *via* ^{19}F NMR spectroscopy.



Scheme 2.34: Proposed catalytic cycle

On top of the analytical advantages, **2g** is a good candidate as it possesses an oxidation potential in the middle of the electrochemical spectrum of Ar₃Bi species (*vide supra*).

While the starting compound **2g** can be easily identified by its shift of -112.76 ppm, the shifts of the previously prepared oxidation products **3g** and **4b** are shifted significantly down-field (-107.79 ppm and -106.36 ppm, respectively). In this investigation, the competence of an oxidant was established by consumption of the organobismuth(III) reagent and the subsequent creation of signals in the region of previously identified organobismuth(V) reagents, as well as the formation of known side products such as fluorobenzene and 1-substituted-4-fluorobenzenes.

In addition the compatibility of the oxidant with the other reagents (2-naphthol and aryl-boron reagent) were investigated as a incompatibility with any of the reagents would render the oxidant unusable.^{IV}

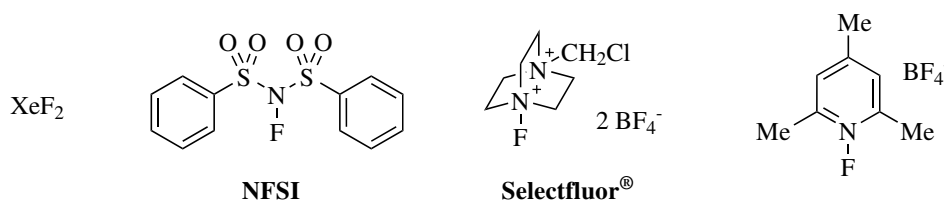
2.8.1 Halonium Reagents

As halogenating reagents have been reported before for the oxidation of Ar₃Bi species,⁸¹ a variety of oxidants containing a halonium motif have been investigated. While halonium reagents of fluorine, chlorine, and bromine were investigated, reagents based on iodine were excluded as they have been reported to cause spontaneous decomposition to the corresponding aryl iodides.^{159,160}

^{IV}A full list of the oxidants used and their compatibility with all necessary reagents can be found in the experimental part of this thesis.

Fluorination

Strong fluoronium reagents like XeF_2 , *N*-fluorobenzenesulfonimide (NFSI) and Selectfluor[®] perform the oxidation of **2g** rapidly and efficiently, setting them into a prime position for the use in a catalytic system.



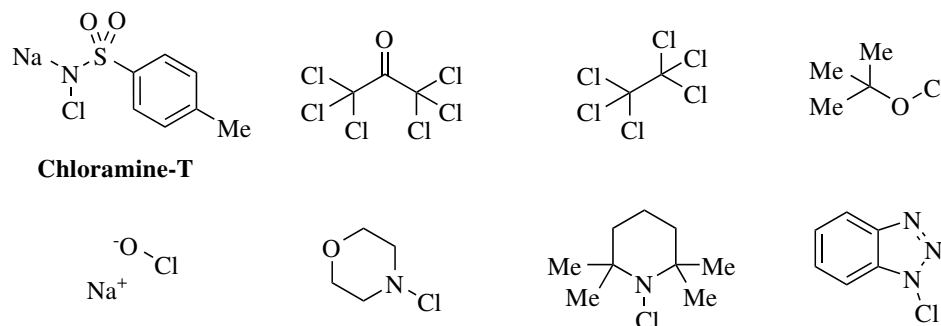
Scheme 2.35: Fluorination agents for the oxidation of **2g**

However, these reagents are not just excellent for the oxidation of Ar_3Bi , but also fluorinate 2-naphthol to result in the 1-fluoro-2-naphthol and 1,1-difluoronaphthalen-2(1*H*)-one.¹⁷⁶ This reactivity rules them out for the use in a catalytic approach.

Despite being as strongly oxidising as NFSI,¹⁷⁷ 1-fluoro-2,4,6-trimethylpyridinium tetrafluoroborate exhibited a significantly lower rate for the oxidation of **2g**. The oxidation of 2-naphthol was not observed, while the oxidation of the triol boronate was observed immediately, ruling even the weakest fluorinating reagents out for the application in a catalytic approach.

Chlorination

While sulfonyl chloride and chlorine gas have been investigated before as oxidants for Ar_3Bi species,⁷⁵ they have also been reported for the chlorination of 2-naphthol,^{178,179} rendering them inappropriate for a catalytic system. For this reason, weaker chlorinating agents have been applied in order to find a valid candidate (Scheme 2.36).



Scheme 2.36: Chlorination agents for the oxidation of **2g**

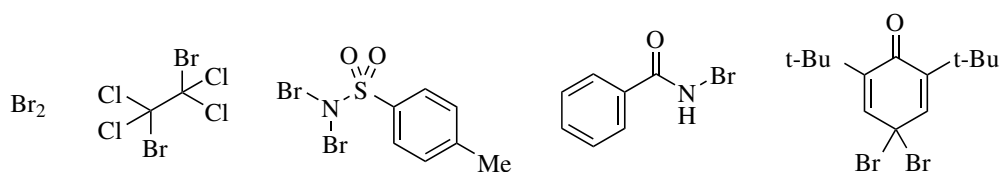
Chloramine-T performs the oxidation of **2g**, but also chlorinates 2-naphthol, which is not surprising as Chloramine-T derivatives have shown activity towards this transformation.¹⁸⁰

The same result can be achieved using NaOCl, *t*BuOCl and *N*-chlorobenzotriazole. The weaker oxidants *N*-chloromorpholine and *N*-chloro-2,2,6,6-tetramethylpiperidine showed no activity towards the oxidation of **2g**. In order to identify a chlorinating agent that performs the oxidation of Ar₃Bi but no chlorination of 2-naphthol, hexafluoroethane and hexafluoroacetone were tested. They offer a chlorine atom attached to a highly electron deficient carbon. Such reagents act as a chloronium source with highly nucleophilic reagents.^{181,182} In the case of **2g**, no oxidation was observed.

Bromination

In comparison to hexachloroethane (*vide supra*) the reagent Cl₂BrC–CBrCl₂ offers a softer electrophile in bromine, rendering an oxidation reaction more favourable. Unfortunately no reaction was observed. In contrast, Br₂, Bromamine-T and *N*-bromobenzamide oxidise **2g**, but also brominate 2-naphthol to 1-bromo-2-naphthol and 1,1-dibromonaphthalen-2(1*H*)-one.

4,4-Dibromo-2,6-di-*tert*-butylcyclohexa-2,5-dien-1-one contains a potential bromonium unit in the quinone type structure. The bromonium compound performs the oxidation reaction generating a hindered phenolate counter ion, which can not be oxidized or arylated. In reaction with **2g**, three distinct peaks in the expected region were observed. These can be explained as the dibromide, bromide-phenolate and diphenolate existing in a fast equilibrium with one another. Unfortunately this bromonium reagent also performs the bromination of 2-naphthol, rendering it unsuitable for the application in a catalytic system (Scheme 2.37).



Scheme 2.37: Bromination agents for the oxidation of **2g**

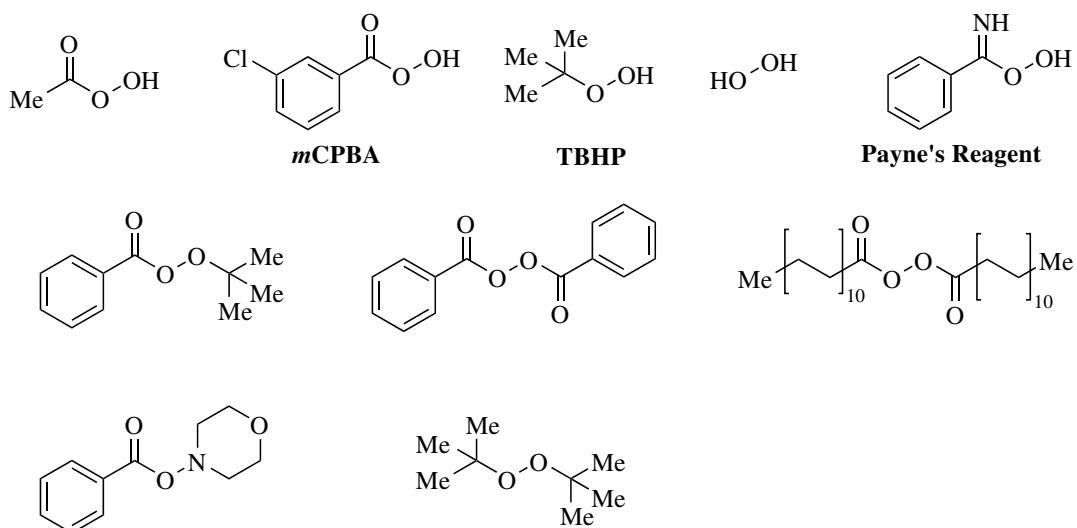
2.8.2 Peroxo Reagents

As peroxo-reagents have been exploited before in the oxidation of Ar₃Bi reagents,^{167,183,184} they have also been employed in this study (Scheme 2.38). They can be separated into peracids, and symmetrical or non-symmetrical peroxides.

Peracetic acid, *m*CPBA and TBHP are competent oxidants of organobismuth(III) reagents and do not react with 2-naphthol. In contrast the boronic acid undergoes oxidation to result in 4-fluorophenol, rendering this class of oxidant incapable for application in a catalytic approach. Additionally, the acid co-products (HOAc/*m*CPBA) are strong enough to protodeboronate the organoboron reagent resulting in fluorobenzene. As peracetic acid and *m*CPBA commercially come in mixtures of acid and peracid an additional complication

would arise when using these reagents.

In an attempt to overcome protodeboronation of the boronic acid, Payne's reagent (benzimidoperoxoic acid), generated from benzonitrile and hydrogen peroxide, has been employed. This reagent releases the corresponding amide as oxidation co-products, which are not acidic enough to protodeboronate the organoboron reagent. Unfortunately, this reagent was unable to oxidise **2g**.

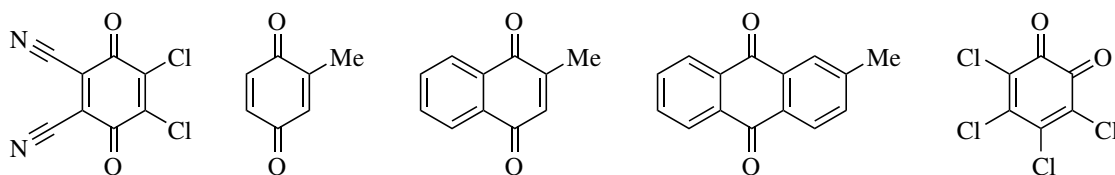


Scheme 2.38: Peroxo agents for the oxidation of **2g**

While *tert*-butyl perbenzoate, benzoyl peroxide and lauroyl peroxide oxidize the Ar_3Bi species, only the latter did not interact with 2-naphthol. Yet, lauroyl peroxide decomposes the arylboron reagent. Morpholino benzoate and di-*tert*-butyl peroxide did not show any signs of oxidation.

2.8.3 Quinones

Quinones have proven excellent oxidants for many organic oxidations.¹⁸⁵ Therefore they have been employed in this study as well. With a reported oxidation potential 3.18 V upon irradiation with light¹⁸⁶ an oxidation of **2g** should be possible. No oxidation of **2g** was observed though, even upon irradiation with light, for any of the quinone derivatives illustrated in Scheme 2.39.



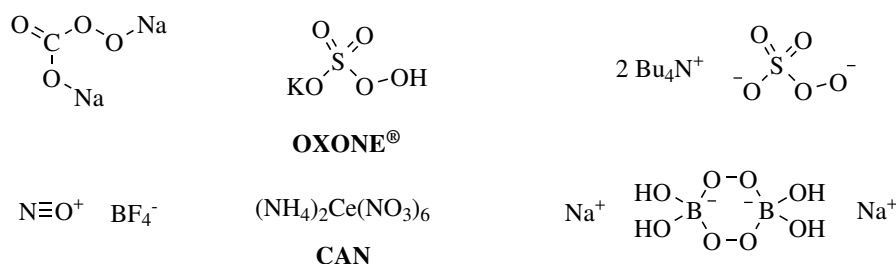
Scheme 2.39: Quinone oxidants employed for the oxidation of **2g**

2.8.4 Miscellaneous Oxidants

In order to identify a suitable oxidant numerous organic and inorganic reagents have also been explored.

Inorganic Oxidants

Sodium percarbonate showed good results in the oxidation of **2g** and did not lead to any oxidation of 2-naphthol. Unfortunately, oxidation of the arylboron reagent to the corresponding 4-fluorophenol was observed (Scheme 2.40).



Scheme 2.40: Inorganic oxidants for the oxidation of **2g**

OXONE[®] initially did not show any potential for the oxidation of **2g**. This could be attributed to its insolubility in MeTHF. A soluble (NBu₄)₂OXONE[®] derivative showed good bismuth oxidation capabilities, but consumed 6-fluoro-2-naphthol rapidly.

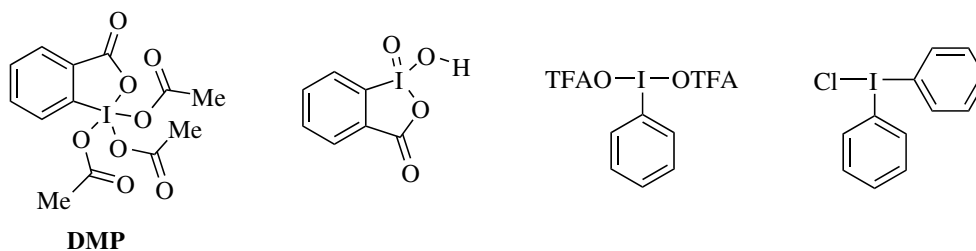
No oxidation of **2g** was observed with nitrosoium tetrafluoroborate.

Cerium ammonium nitrate showed good results in the oxidation of **2g**, but also oxidised 6-fluoro-2-naphthol.

While sodium perborate showed good results in the oxidation under acidic condition¹⁴⁵ (*vide supra*) no oxidation was observed under neutral conditions. This can be attributed to the *in situ* generation of peracids under acidic conditions, which have shown good results in oxidation.

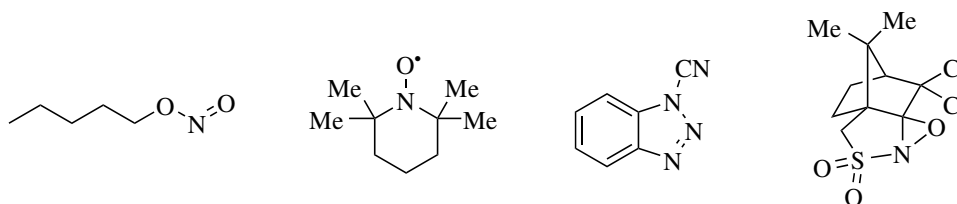
Hypervalent Iodine Reagents

Hypervalent iodine compounds have been employed as they have shown good results in a variety of oxidations.¹⁸⁷ For the oxidation of **2g** only diphenyl iodonium chloride showed oxidation products. While it didn't react with 6-fluoro-2-naphthol, the boronate was oxidized, rendering it unsuitable for the catalytic approach (Scheme 2.41).

Scheme 2.41: Hypervalent iodine reagents for the oxidation of **2g**

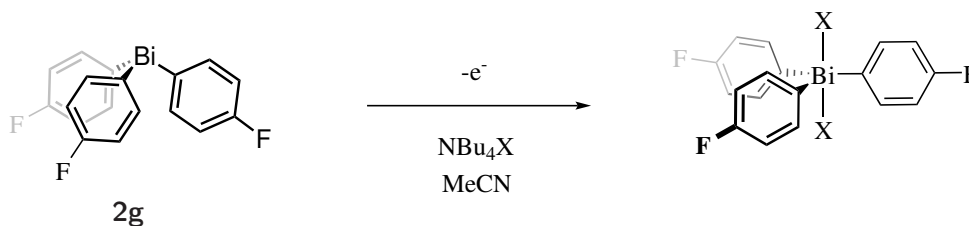
Other Oxidants

Amyl nitrite, TEMPO, *N*-cyano benzotriazol and (+)-(8,8-dichlorocamphorylsulfonyl) oxaziridine did not oxidise **2g** (Scheme 2.42).

Scheme 2.42: Reagents screened for the oxidation of **2g**

2.8.5 Electrochemical Oxidation

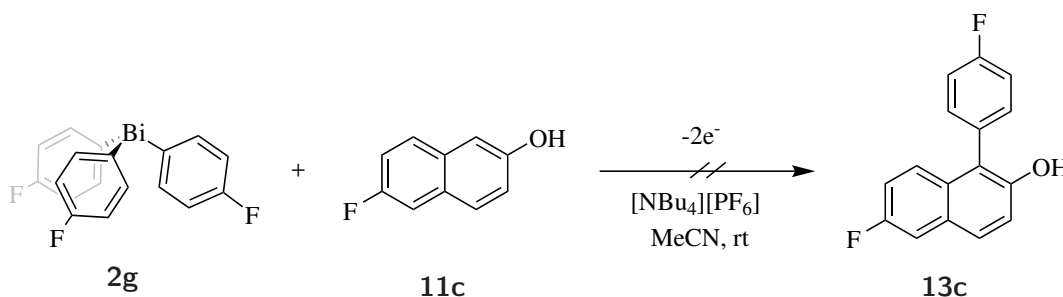
To overcome the inherent incompatibility of traditional organic and inorganic oxidants, an electrochemical approach was pursued to enable oxidation of the organobismuth reagent **2g** without the decomposition of substrate or transmetallation reagent (Scheme 2.43).

Scheme 2.43: Electrochemical approach for the oxidation of **2g**

Previous cyclic voltametric studies establishing the oxidation potential of Ar_3Bi species showed a non-reversible oxidation. This non-reversibility was attributed to the instability of the produced organobismuth(V) species. The electrochemical oxidation of bismuth from 3 to 5 requires the 2 anions necessary to balance the formal positive charge on the bismuth centre. These would be provided by the PF_6^- originating from the electrolyte ($[\text{NBu}_4][\text{PF}_6]$).

In order to overcome this instability $[\text{NBu}_4][\text{BF}_4]$ and $[\text{NBu}_4][\text{OTs}]$ have been used for the cyclic voltametric investigation. However, neither electrolytes provided a reversible oxidation.

Since the exchange of the counterion is an unnecessary step for the formation of the naphthol-bismuth adduct, an attempt was made to perform the electrochemical oxidation in the presence of 6-fluoro-2-naphthol. Therefore a system using a carbon sponge working electrode, platinum flag counter electrode and a silver reference electrode were employed for a solution of **2g**, 2-naphthol and $[\text{NBu}_4][\text{PF}_6]$ (0.1 M) in MeCN on a preparative scale. No product has been observed after work-up indicating that this approach is not viable (Scheme 2.44).



Scheme 2.44: Electrochemical approach for the *in situ* oxidation and arylation

2.9 Conclusion

The arylating abilities of organobismuth(V) reagents were reported more than 40 years ago. Ever since, its reactive potential has been largely overlooked and almost no systematic mechanistic investigations have been conducted.

In order to overcome the major challenges of oxidative organobismuth(V) chemistry a catalytic approach was proposed and each elemental step was investigated individually.

The oxidative arylation of phenol derivative proved unsuccessful as the process was competing with a base induced decomposition of the bismuth(V) reagent. While the decomposition product was identified the mechanism remains unsolved, a prevention of this pathway proved impossible. In order to out compete the decomposition in favour of the arylation process a variety of conditions and substrates were assessed allowing identification of 2-naphthol as a viable candidate.

Using 2-naphthol, unprecedented mechanistic insight was gained with the nucleophilic attack as the rate determining step on the $\text{Ar}_3\text{Bi}(\text{OAc})_2$ species. Further direct observation and competitive kinetic studies allowed for the determination of the influence of transferred aryl group, oxidation potential, substrate and counter ion. Here the latter has been identified as the most sensitive variable allowing for a massive rate acceleration of the nucleophilic attack until the reductive elimination of the naphtholate-bismuth intermediate becomes rate determining. The use of Br^- and Cl^- resulted in unobservably fast conversion.

The bismuth co-product was identified as $[\text{H}(\text{DBU})_2][\text{Ar}_2\text{Bi}(\text{OAc})_2]$ and a variety of organoboron reagents have been tested towards a rearylation to Ar_3Bi reagents. Potassium 4-fluorophenyl triol borate showed the best transmetallation results and was chosen for further studies. An optimisation of equivalents, temperature, solvents and reaction time allowed for a full transmetallation in less than 5 h. The rate of this reaction is determined by the low solubility of the organoboron reagent.

In order to complete the catalytic cycle the oxidation of Ar_3Bi has been approached using numerous oxidants. While a variety of reagents proved capable for the oxidation of organobismuth reagents, all of them also reacted with other reagents essential to the closing of the proposed catalytic cycle.

Since the incompatibility of naphthol, organoboron reagents and oxidant has been determined, a catalytic use of bismuth for oxidative arylation was not realised.

The gained fundamental insight into the mechanism of the arylation reaction, the identification of a capable transmetallation reagent on bismuth(III) centres and the capability of oxidants to perform the oxidation of Ar_3Bi species will aid in the development of the modular stoichiometric approach (outlined in chapter 3).

3 | Arylation mediated by Bismacycles

Abstract: This chapter covers the development of a modular bismacycle-based system for the arylation of phenolic substrates. In order to identify a suitable backbone scaffold, a variety of bismacyclic compounds have been prepared and tested for a) their stability as the bismacycle (*pseudo*)halide species, b) their properties towards transmetallation using an organoboron reagent and c) their arylation capabilities. A thiabismine dioxide core has been found to perform all steps, rendering it a viable candidate.

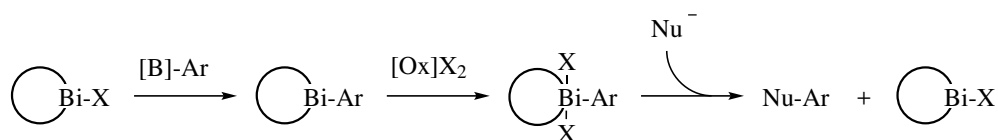
Different bismacycle (*pseudo*)halide salts of the thiabismine dioxide core have been prepared and their capability for transmetallation have been investigated. The reaction proceeds *via* a bismacycle-O-bismacycle μ -oxo intermediate under basic conditions using readily available boronic acids. With a scope involving electron-rich to electron-poor aryl motifs as well as sterically demanding and even heterocyclic rings, a simple and robust transmetallation protocol has been developed.

The subsequent oxidation and arylation was achieved using *m*CPBA as the oxidant with 2-naphthol as the initial substrate. No base is required in the arylation process. The scope was extended to numerous naphtholic and phenolic substrates.

Mechanistic investigations of all significant processes have been conducted allowing for unprecedented insight into bismuth-mediated arylation, that provide a deeper understanding and provides *a priori* prediction for untested substrate combinations.

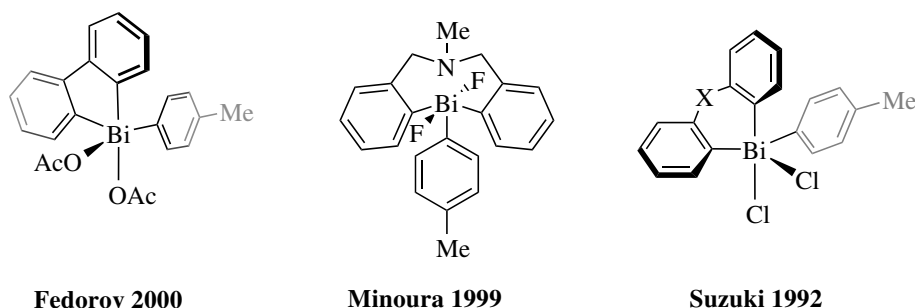
3.1 Identification of Appropriate Bismacyle

Due to the inherent incompatibility of the individual reagents in the proposed catalytic cycle (Scheme 1.20), a stoichiometric approach was developed, in which each individual step (transmetalation, oxidation, arylation) would be performed in a consecutive one-pot fashion (Scheme 3.1). In this way, the incompatibility of some of the individual reagents would be rendered irrelevant.



Scheme 3.1: Modular system for oxidative arylation using a bismacyle precursor

In contrast to their simpler triarylbismuth analogues, two of the aryl rings have been fused, resulting in an increased stability of the connected rings allowing them to act as a backbone that controls the reactivity and stability of the bismuth species. The simplest backbone is the biphenyl unit, which can be extended with a variety of groups in between the two aryl units (*e.g.* methylene,⁷⁶ ether,⁷⁶ thioether,^{47,76,188} amine,^{55,57,189,190} sulfone¹⁹¹).



Scheme 3.2: Reported bismacyle reagents. X = CH₂, O, S or SO₂

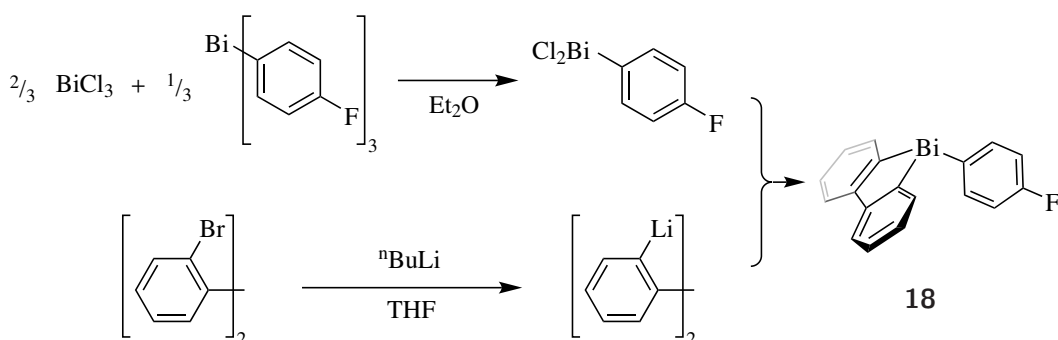
While a variety of bismacycles has been reported previously,⁷⁶ their application as arylation agents has so far been limited.^{113,192,193}

For generation of the desired bismacyle (*pseudo*)halide species two common preparative pathways can be chosen. Flexible electron donating groups such as (CH₂)₂NR and (CH₂)₂S allow for a transannular coordination that enables a stable bismacyle (*pseudo*)halide species to be formed directly from the corresponding BiX₃.¹⁹⁴ Rigid backbones (O, S, SO₂) lack this stabilising effect and result in bismacyle oligomers. Instead, in these cases the dilithiated backbone can be added to a ArBiX₂ compound to make the aryl bismacyle compound. The aryl group can be removed selectively using strong acids resulting in ArH and bismacyle (*pseudo*)halide, or soft oxidants resulting in Ar-X and bismacyle (*pseudo*)halide.

In the following, access to the individual bismacyles will be established and their capability to perform the proposed transformations (transmetallation, oxidation and arylation) will be tested.

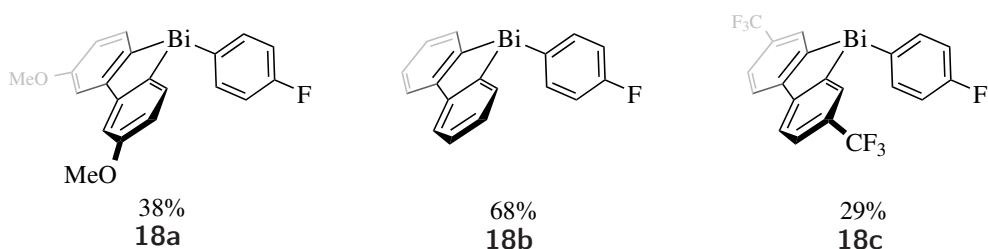
Bismoles

The simplest bismacyle of this type is a bismole that only consists of a backbone made from two directly fused aryl rings creating a 5-membered bismacyclic ring. These compounds can be accessed *via* lithium halogen exchange of the dibromobiphenyl and subsequent reaction with a ArBiX_2 species prepared from the comproportionation of BiX_3 and BiAr_3 (Scheme 3.3).



Scheme 3.3: Synthetic pathway towards bismole reagents

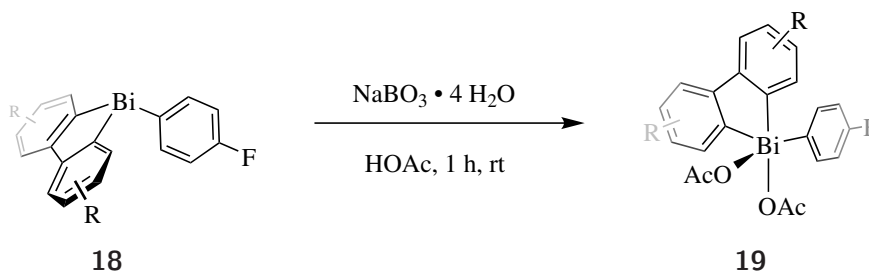
Since the rigid biphenylene backbone acts as a stable ligand, modifications to the electronic properties were made in order to investigate the impact that modulation of the backbone has on stability of the bismacyle and the rate of the individual reactions. Synthesis of these bismoles showed lower overall yields in comparison to the triaryl-bismuth reagents. This can be attributed to the inefficient con-proportionation of BiCl_3 and Ar_3Bi as the former shows very low solubilities in both Et_2O and THF.



Scheme 3.4: Bismols prepared carrying electron-rich, -neutral and -poor motifs on the aryl groups of the bismacyle

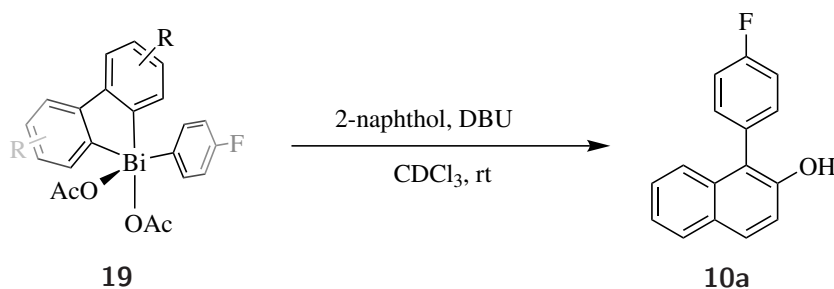
In order to compare the reactivity of aryl bismole(V) X_2 species and their Ar_3BiX_2 equivalents, the aryl bismole(V) acetates were prepared by previously established protocol

(Scheme 3.5). While the oxidation of **18a** and **18b** resulted in moderate to good yields no organobismuth(V) reagent has been observed for the electron deficient CF₃-substituted bismole. Investigations into the origin for this observation included the acquisition of the oxidation potential of the aryl bismole(III) reagents. Surprisingly, the oxidation potential shows only very minor differences with E_p^{Ox} (OMe→CF₃) = 2.1→2.3 V. This decreased sensitivity, as well as the generally higher oxidation potential, might be explained by the decreased orbital overlap of the bismuth's p orbitals with sp² orbitals of the aromatic rings due to the constrained conformation of the bismole motif.



Scheme 3.5: Oxidation of aryl bismole(III) reagents to aryl bismole(V) diacetates

An investigation into the capability of bismole(V) diacetates to perform the product generating arylation reaction was performed first. Under the same conditions used for the previous investigation, a rapid increase in the rate of the reaction has been observed. Indeed, observation *via* ¹⁹F NMR spectroscopy is rendered impossible as the reaction completed in less than 1 min.

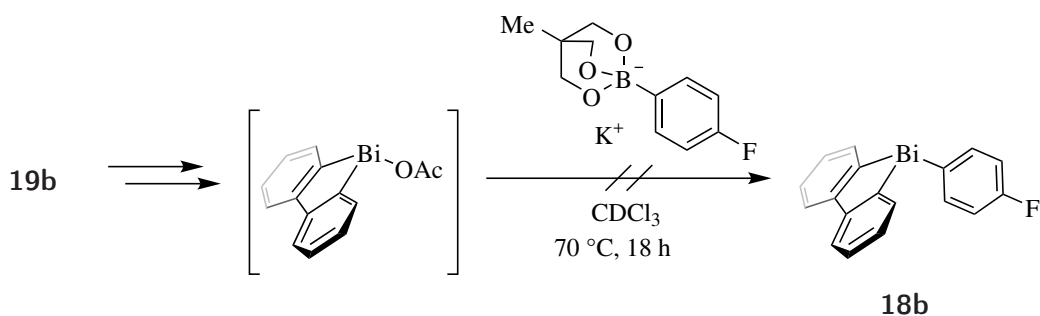


Scheme 3.6: Arylation of 2-naphthol using aryl bismole(V) diacetates under basic conditions

While an increase in rate was expected due to the increased electrophilicity represented by the higher oxidation potential, the completion in less than 1 min does not behave in accordance to the previously established rate *vs* E_p^{Ox} correlation (see Figure 2.6.2). A potential explanation can be found in the crystal structure of aryl bismole(V) X₂ reagents:¹⁹⁵ in contrast to bismuth reagents of type Ar₃BiX₂, aryl bismole(V) X₂ reagents do not arrange with both counter ions X in apical position, but with one of the aryl groups of the biphenyl unit located in an apical orientation. This arrangement allows easier access to the Bi–X σ* orbital which was identified as the rate limiting step before.

With the reaction proceeding too rapidly for observation for all three substituted bismoles,

no insight into the influence of electronics of the backbone scaffold can be made. The transmetallation step was investigated next. The traditional approach to remove the exocyclic aryl group from the bismuth centre is either oxidation/reductive elimination with iodine to produce the bismole iodide and aryl iodide or protodebismuthation using strong acids. While both methods have been applied resulting in aryl iodide or aryl-H, respectively, the corresponding bismole-X species could not be identified. Instead, insoluble precipitate was observed that could not be applied successfully to the previously established transmetallation protocol using 4-fluorophenyl triol borate. Similar observations were made with ArBiX_2^- and Ar_2BiX -species before. With the organoboron reagent also possessing a low solubility in THF, this approach to transmetallation was not productive. Therefore an alternative strategy was sought. Prior knowledge gained from the investigations into the catalytic approach was used to create a soluble bismole (*pseudo*)halide similar to the previously reported $\text{Ar}_2\text{BiX}_2^-$ (Scheme 3.7).



Scheme 3.7: Approach for the transmetallation of bismole acetate-type species created from the arylation of 2-naphthol using **19b**

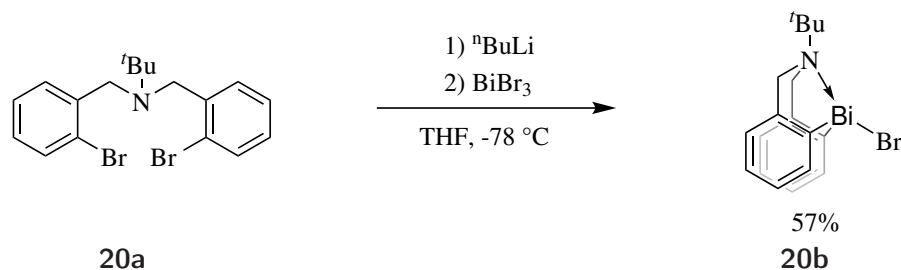
With respect to the proposed modular system (*vide supra*) this approach appears atom and step ineffective, but for a proof of concept an easy access a bismole-(*pseudo*)halide was utilised.

Unfortunately no transmetallation product was observed. This low reactivity towards transmetallation, as well as the lack of an atom-efficient access to the bismole (*pseudo*)halide-type species rendered the bismole scaffold unsuitable for the proposed modular strategy.

Azabismocines

Easy access to bismacyle (*pseudo*)halides is offered using a azabismocine scaffold. Here, the aryl groups on the bismuth centre are fused with a $-\text{CH}_2-\text{NR}-\text{CH}_2-$ linkage to form a 9-membered bismacyle. The lone pair on the nitrogen allows for a transannular dative interaction with the σ^* of the Bi-X bond, affording a stable azabismocine (*pseudo*)halide. These reagents were accessed by the reaction of the lithiated backbone and BiBr_3 .

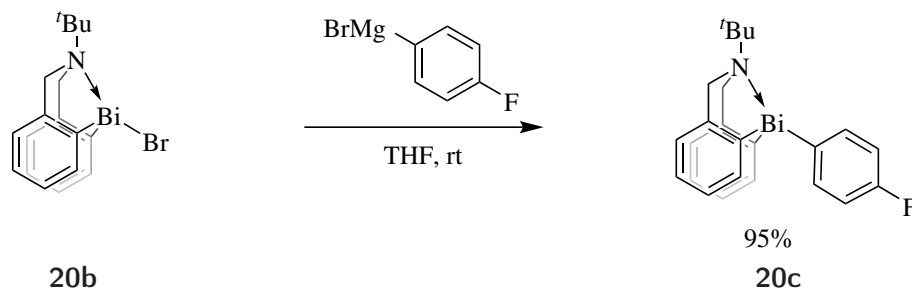
An azabismocine bromide was accessed from *N,N*-di(2-bromobenzyl)-2-methylpropan-2-amine and BiBr_3 allowing direct access to the desired bismacyle bromide precursor (Scheme 3.8).



Scheme 3.8: Synthetic route to azabismocine bromide through the reaction of a prelithiated backbone scaffold with BiBr_3

While access to these reagents is easy and atom efficient and their synthesis occurs in high yielding clean products, any further purification is complicated by their high sensitivity towards protic conditions including silica.

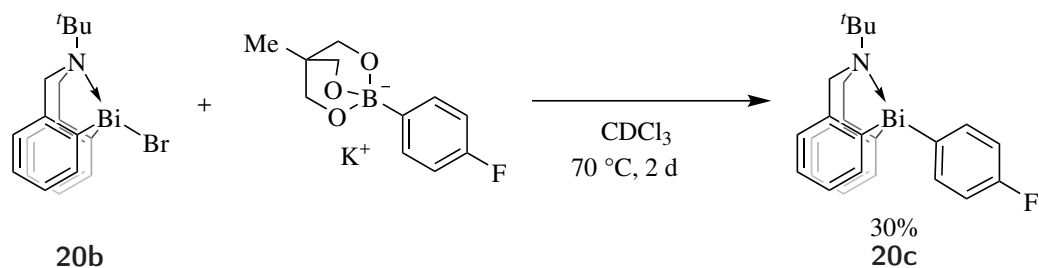
With the precursor in hand the subsequent transmetalation was attempted. Procedures for this transformation have been reported using organolithium and Grignard reagents.^{190,196} This route was initially used to produce the 4-fluorophenyl azabismocine in good yields.



Scheme 3.9: Functionlisation of azabismocine using organometallic aryl reagents

The procedure highlighted in Scheme 3.9 allows for the aryl azabismocine motif to be prepared easily. However, it still required the use of inert and anhydrous handling and reagents. As the aim of this project was the development of an easy to follow protocol the use of organoboron reagents for this transformation was investigated. With respect to previous studies, the transmetalation was attempted using organoboron reagents. While the transmetalation was observed to occur, the transformation progresses slowly with 30% transmetalation after 2 days under the same conditions that afforded full conversion in 5 h for $\text{Ar}_2\text{BiOAc}_2^-$ **7** (Scheme 3.10).

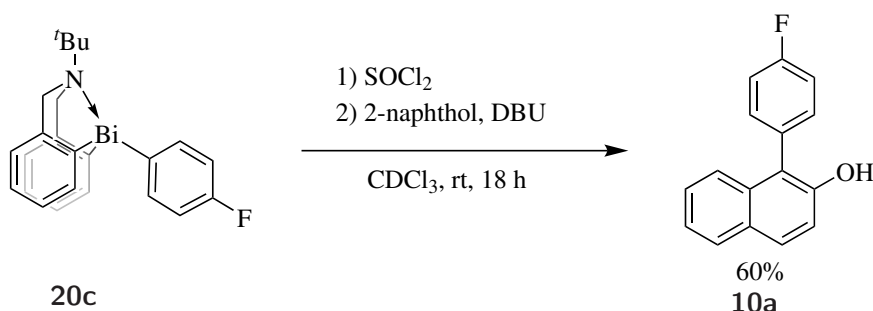
The low rate of this transformation can be explained by donation of the amine lone pair into the bismuth centre. The donation decreases the electrophilicity of the bismuth centre hindering the nucleophilic attack of the aryl group in the transmetalation. On the other side, the lone pair occupies the $\text{Bi}-\text{Br}$ σ^* orbital necessary for the transmetalation that might result in a lower rate. This influence can be seen in the crystal structure of these reagents.¹⁹⁶ In general, the ability of azabismocine-X species to perform transmetalation



Scheme 3.10: Functionlisation of azabismocine bromide **20b** using 4-fluorophenyl triol borate

reactions have been proven, but is insufficient to be practical.

In agreement with previous studies, the oxidation of azabismocines proceeds fully and cleanly to the azabismocine(V) species using a variety of oxidants. Therefore an *in situ* oxidation followed up with the subsequent arylation was attempted. 2-Naphthol was chosen, as it showed good results in the previous investigation. As complete conversion was previously observed with similar Ar_3BiCl_2 species within seconds, conversion was initially assessed after 5 min. Almost no conversion was observed *via* ^{19}F NMR spectroscopy.

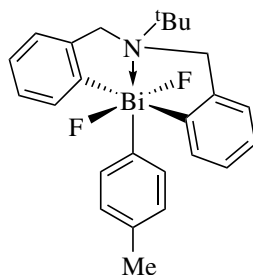


Scheme 3.11: Arylation of 2-naphthol using *in situ* generated aryl azabismocine dichloride

The reaction was allowed to progress for 18 h at room temperature, resulting in 60% conversion. Two factors have been taken into account to explain these observations.

The oxidation potential of aryl azabismocine **20c** has been determined at 0.96 V, rendering the bismuth centre significantly more electron-rich than the simple biphenyl backbone. This is attributed to both the donation of the nitrogen backbone as well as better orbital overlap of the more flexible backbone.

The assessment of the crystal structure of a similar azabismocene(V) species¹⁹⁰ equally allows for an explanation for the slow conversion (Scheme 3.12). While regular Ar_3BiX_2 species arrange in a penta coordinate trigonal bipyramid azabismocine(V) reagents assume a *pseudo* octahedral coordination with the nitrogen acting as the sixth coordination partner that places the backbone as tridentate ligand in a *mer*-orientation. This arrangement forces the X-type counter ions in a *trans* position to one another and impedes the rotation process that has been determined as involved in the rate limiting step.



Scheme 3.12: Arrangement of azabismocine(V) species¹⁹⁰ with the amine group acting as an additional coordination partner making this class of reagents hexacoordinate

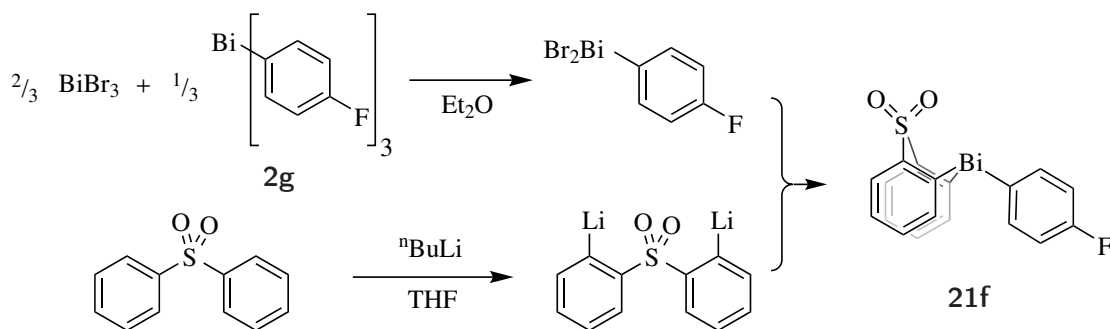
It has been shown that all steps of the proposed modular stoichiometric system are possible. However, while the donating nature of the amine backbone has proven useful for the synthesis of the azabismocine (*pseudo*)halide reagents, it retards the transmetallation and arylation steps. Additionally, practical work with these reagents was rendered unfavourable as they are unstable to column chromatography on silica, making purification difficult.

Thiabismine dioxides

Thiabismine dioxide reagents have been reported previously,^{197,198} with their use being limited to transmetallation for copper catalysis¹⁹⁹ and esterification of tosylates.¹⁹¹ In order to assess their potential for the arylation of phenolic substrates, access to thiabismine dioxide reagents had to be established.

While thiabismine dioxide (*pseudo*)halides have been reported before,¹⁹⁸ all routes involve the synthesis of aryl thiabismine dioxide species with subsequent debismuthation of the exocyclic aryl group by either protodebismuthation or oxidation with subsequent decomposition of the aryl thiabismine(V) dioxide species.

In the first instance, the aryl thiabismine dioxide species were prepared. While the synthesis of bismacyles have been reported with moderate to bad yields, the reports of Worrell *et al.* offered excellent yields due to the conscious choice of Et₂O as the reaction solvent and BiBr₃ as the bismuth reagent (¹⁹⁹).

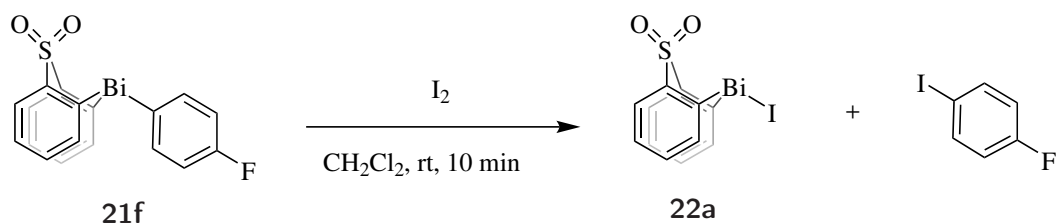


Scheme 3.13: Synthetic route to **21f** starting from commercially available starting materials

The first part of this reaction entails the comproportionation of Ar₃Bi and BiBr₃ to the

corresponding ArBiBr_2 , which is selectively accessed by precipitation in ethereal solution (Scheme 3.13). In the other part of the reaction, the diphenylsulfone backbone is selectively lithiated, circumventing the need for prior bromination as was the case for the other scaffold precursors. The combination of the two parts results in **21f** in almost quantitative yields, enabling easy access to this class of bismacyles.

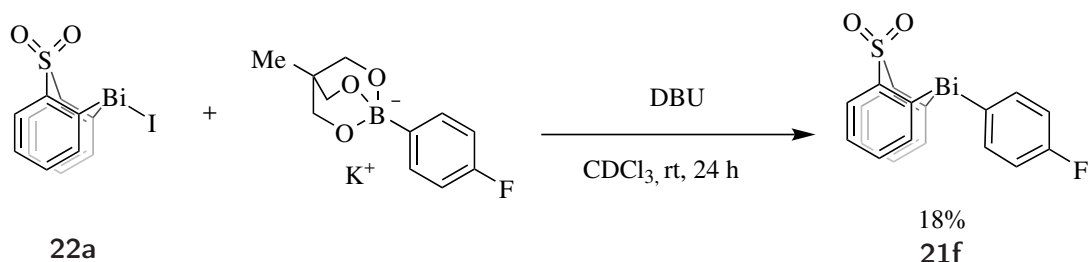
For an initial assessment of the backbone scaffold in transmetalation using organoboron-reagents, thiabismine dioxide iodide **22a** was prepared by oxidation with molecular iodine and the subsequent decomposition into the aryl iodide and thiabismine dioxide iodide (Scheme 3.14).



Scheme 3.14: Synthetic route to a thiabismine dioxide iodide precursor **22a** *via* oxidation and subsequent reductive elimination

This oxidation and subsequent decomposition of Ar_3Bi species using iodide has been observed before¹⁶⁰ and usually results in an ill-defined mixture of $\text{Ar}_{3-n}\text{BiI}_n$ products, that show a poor solubility in most common solvents. In contrast, the sulfone bridged bismacyle forms a distinct, soluble bismacyclic species.

The transmetalation was performed using the conditions established in the previous investigation. After 24 h at room temperature, a transmetalation of 18% to the corresponding **21f** was observed (Scheme 3.15).

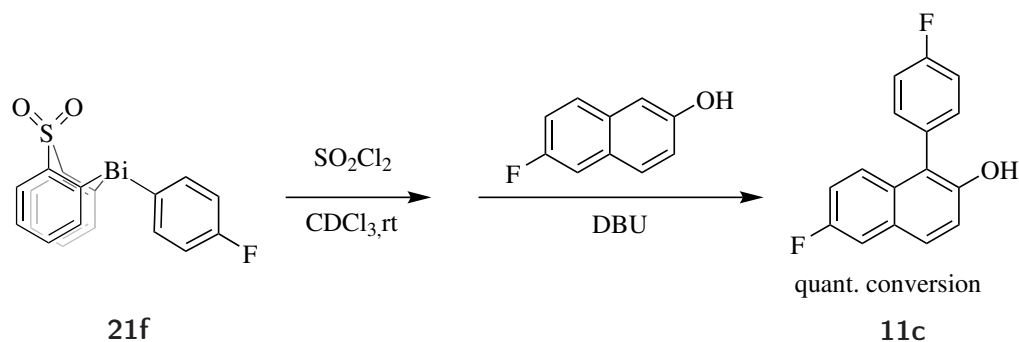


Scheme 3.15: Transmetalation of a thiabismine dioxide iodide precursor **22a** using potassium 4-fluorophenyl triol borate

While conversion was low, the concept of B-to-Bi transmetalation on thiabismine dioxides has been proven.

In the next step of the proposed modular system, the oxidation of **21f** and the subsequent arylation of 6-fluoro-2-naphthol was attempted. The degree of oxidation, as well as the progression of the arylation to the known arylation product **11c**, has been deter-

mined by ^{19}F NMR spectroscopy. Both steps showed quantitative conversion (Scheme 3.16).



Scheme 3.16: Oxidation of 4-fluorophenyl thiabismine dioxide using sulfuryl chloride and subsequent arylation of 2-naphthol

With these observations in hand, the preferred scaffold for further investigations has been identified in the thiabismine dioxide backbone. This structural motif performs all necessary reactions (B-to-Bi transmetallation, oxidation, arylation of 2-naphthol), while also being accessible in a high yielding process from commercially available starting materials.

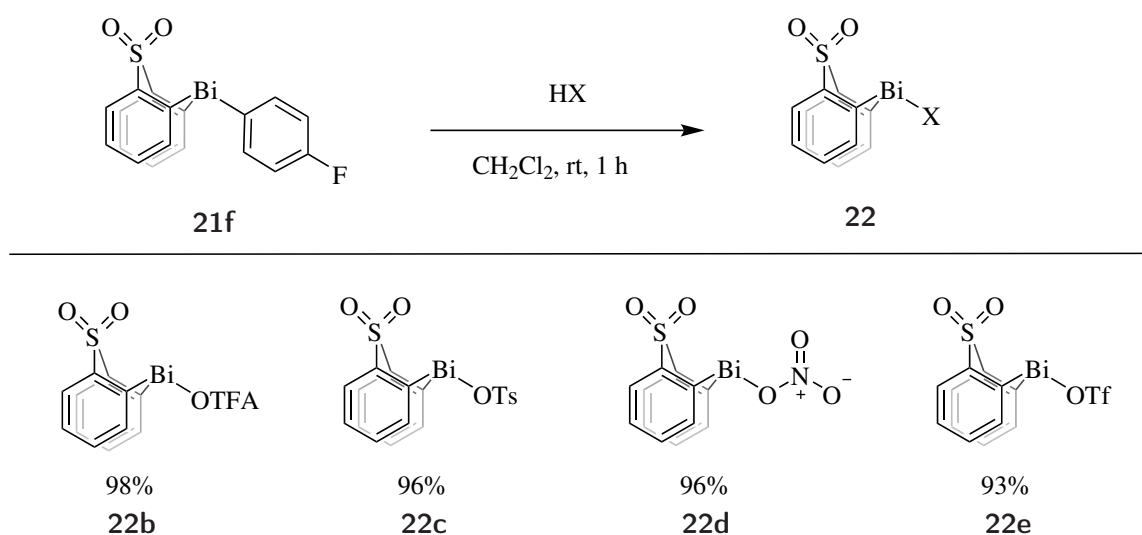
In the following an in depth investigation into each of the proposed steps will be performed to enable their combination into an easy-to-follow, accessible, modular protocol for arylation using a thiabismine dioxide scaffold.

3.2 Optimisation of Individual Segments

3.2.1 Creation of a Thiabismine Dioxide (*Pseudo*)halide Library

As a direct synthesis of thiabismine dioxide bromide by addition of BiBr_3 to the lithiated diphenylsulfone does not result in the the desired product but an ill defined polymeric mixture, the aryl thiabismine dioxide had to be prepared prior to the cleavage of the Bi-Ar bond to result in the desired precursor.

In prior studies thiabismine dioxide iodide **22a** was obtained through a pathway with oxidation with molecular iodine followed by subsequent reductive elimination. As this methodology is restricted to soft oxidants, a protodebismuthation pathway was employed to create a library of differently substituted thiabismine dioxide (*pseudo*)halides (Scheme 3.17).



Scheme 3.17: Synthetic route to thiabismine dioxide (*pseudo*)halides through a protodebismuthation route, with $\text{X} = \text{OTFA}, \text{OTf}, \text{NO}_3$ and OTs

In contrast to triarylbismuth reagents, the addition of acid results in clean protodebismuthation of the exocyclic aryl group, affording the thiabismine dioxide (*pseudo*)halides. This methodology is viable for the creation of a library of potential precursors for the proposed modular protocol.

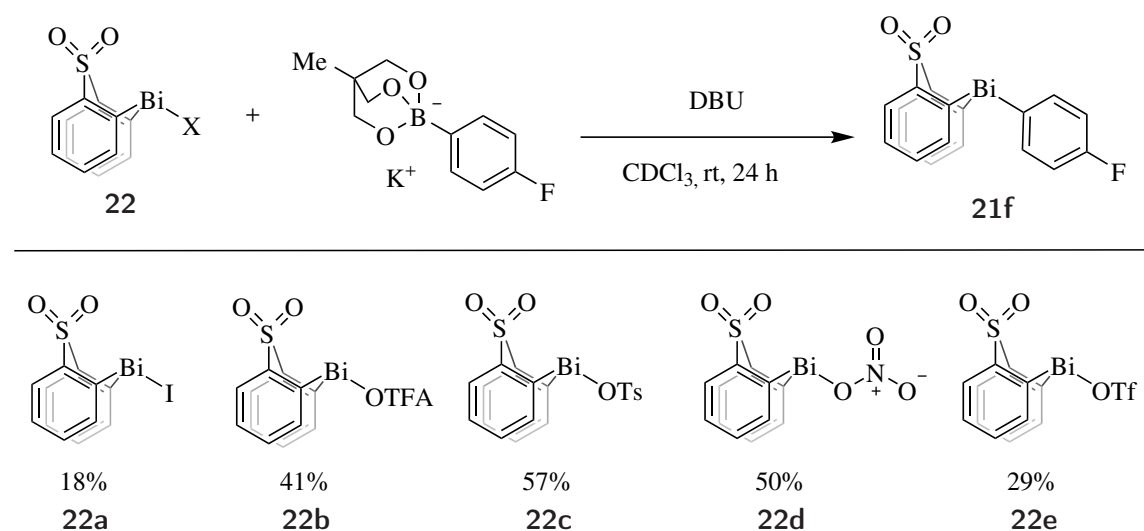
Additionally, an excess of acid could be used to provide the desired product in quantitative conversion, with residual acid and aryl-H removed *in vacuo*. In the case of thiabismine dioxide tosylate **22c** *in vacuo* removal of the acid was not possible, but separation was achieved by simple trituration in Et_2O .

3.2.2 Transmetallation

Influence of Counter Ions

The library of thiabismine dioxide (*pseudo*)halides were subjected to transmetallation conditions using organoboron reagents to establish the impact of the counter ion attached to the bismuth centre (Scheme 3.18).

It was observed that the iodine-derived thiabismine dioxide showed a lower conversion in the given time frame. This observation can be attributed to the lower thermodynamic driving force of this reaction with the creation of a B–I bond, which is significantly weaker than the corresponding B–O bond (384 vs 806 kJ/mol).⁶⁰ For the remaining thiabismine dioxide (*pseudo*)halide species a correlation to their pKa has been observed. With ⁻OTFA (-0.25) being the strongest base, a relatively strong bond to the bismuth is formed and the cleavage of this bond is presumably rate limiting. The weaker bases ⁻OTs (-0.6) and NO₃⁻ (-1.3) facilitate this process resulting in higher conversions.



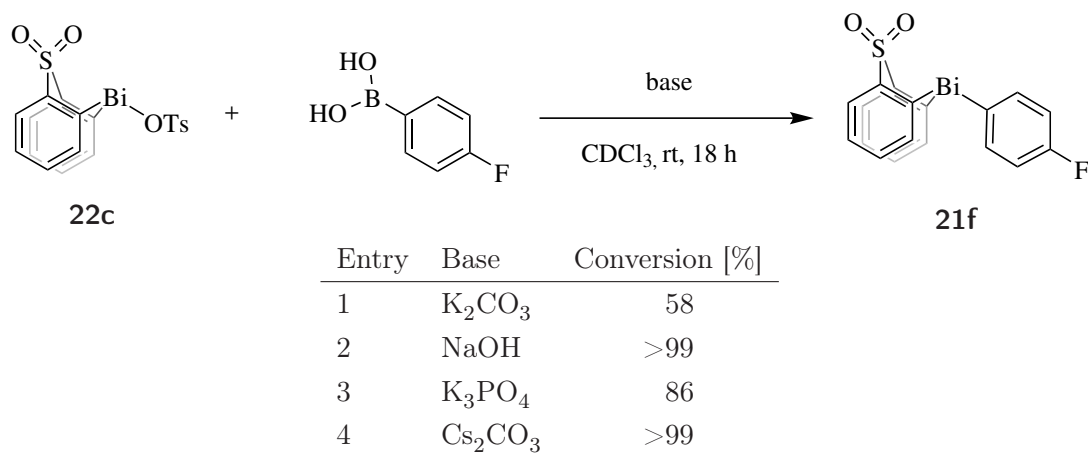
Scheme 3.18: Transmetallation of thiabismine dioxide (*pseudo*)halides with potassium 4-fluorophenyl triol borate

With a conversion of 57% after 25 h thiabismine dioxide tosylate **22c** showed the best result. Hence, **22c** was selected for further investigations.

3.2.3 Influence of Base

While potassium 4-fluorophenyl triol borate has proven a capable transmetallation reagent, the need for prior preparation renders it inconvenient for a widespread application. Therefore, the transmetallation was attempted using commercially available boronic acids as the B-to-Bi transmetallation reagents. In accordance to previously reported Suzuki-Miyaura protocols, inorganic bases were used due to their easy handling, low price and general insensitivity to oxidation in the later stages of the proposed system (Scheme 3.19).

In all cases transmetallation has been observed, enabling use of the more convenient boronic acids as the first example of B-to-Bi transmetallation using boronic acids on a Bi(III) centre. The addition of NaOH and Cs₂CO₃ resulted in full conversion to the desired **21f**, while K₂CO₃ and K₃PO₄ resulted in 58% and 86% conversion, respectively.

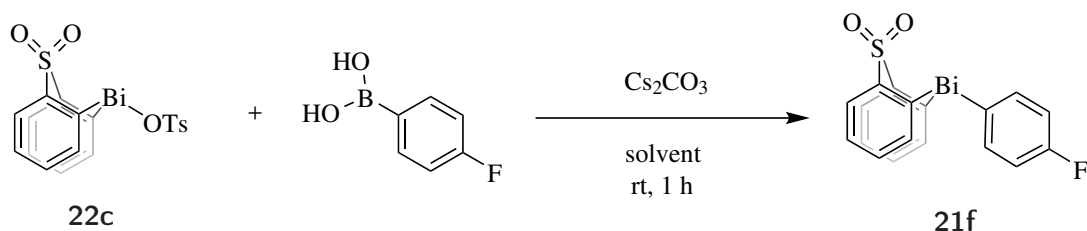


Scheme 3.19: Transmetallation of **22c** with different bases

3.2.4 Influence of Solvents

Several solvents were considered for the transmetallation, keeping Cs₂CO₃ constant as a mild but effective base. The reaction time was reduced to 1 h to allow a better interrogation of the reaction progression.

In the following, it was anticipated that the more polar solvents should allow for better results due to the increased Cs₂CO₃ solubility on the one hand and a better stabilisation of the polar transition state on the other.



Entry	Solvent	Conversion [%]
1	methanol-d ₄	0
2	MeCN	0
3	THF	0
4	acetone	0
5	CDCl ₃	20
6	toluene	27
7	CDCl ₃ /H ₂ O (9/1)	80
8	CH ₂ Cl ₂ /methanol (9/1)	0
9	toluene/methanol (9/1)	0

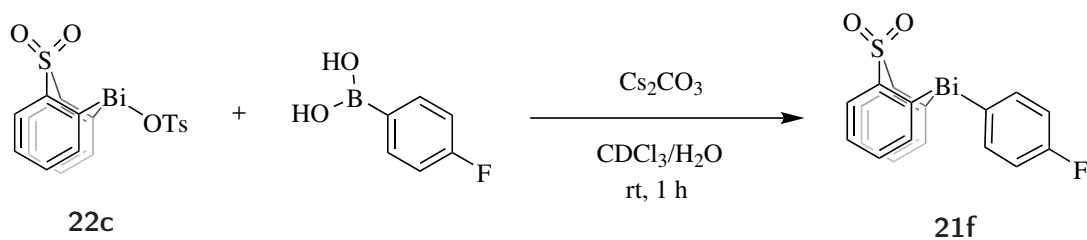
Scheme 3.20: Transmetalation of **22c** using 4-fluorophenyl boronic acid in different solvents

As can be seen in Scheme 3.20, the transmetalation appears highly dependent on the choice of solvent. CDCl₃ and toluene result in good yields, with the latter achieving 27% conversion in 1 h at room temperature. More polar solvents such as methanol, acetone, THF and MeCN were chosen to increase the solubility of both the boronic acid as well as Cs₂CO₃, but did not show any conversion to **21f**. Coordination of the polar solvents to the organobismuth reagent, hindering transmetalation, appears likely as coordination of DBU has been observed before (see SI). In order to increase the solubility of the boronic acid and Cs₂CO₃, the use of small equivalents of polar solvents such as water and methanol was tested. The addition of methanol exclusively prohibits transmetalation making a methoxide inhibition likely.

The addition of water to CDCl₃ resulted in biphasic system with the boronic acid and Cs₂CO₃ presumably in the aqueous phase. Here the rate of the reaction can easily be controlled by the stir rate.

Influence of Water

With the significant increase in conversion upon addition of water, a closer investigation into the role of the water has been conducted. Herein, different amounts of H₂O have been added to the reaction mixture. With the addition of 0.5 Vol% of water no residual solids were observed, resulting in a liquid biphasic system.



Entry	H ₂ O [Vol%]	Conversion [%]
1	0	20
2	0.1	53
3	0.5	56
4	1	65
5	5	83
6	10	84

Scheme 3.21: Transmetalation of **22c** with varying water content

Analysis of the data showed an increase of conversion with increase of water content up to 5 Vol%, and no further increase thereafter (see Scheme 3.21). Assuming a saturation concentration of both Cs₂CO₃ and 4-fluorophenyl boronic acid with solids present, a constant rate would be expected, regardless of the water content. Therefore the rate limitation must be found in the diffusion between the two phases. This holds true especially for the conversion after the solid reagents have been fully dissolved. The increase can be attributed to the increase in surface area of the organic and aqueous phase. This trend progresses until the increase of surface area is out competed by the reduction in concentration with further dilution by added water. This is likely to be the case around 10 Vol% as no further increase in yield can be observed.

3.2.5 Optimized Conditions and Screen of Boronic Acids

To establish a guideline that allows for full conversion in a convenient time frame a higher reaction temperature of 60 °C and an increased reaction time of 2 h was chosen.

With base solubility addressed through the addition of water, K₂CO₃ was selected as the cheaper alternative to Cs₂CO₃.

These optimised condition ensure full transmetalation within 2 h and have been chosen to establish the range and capability of B-to-Bi transmetalation.

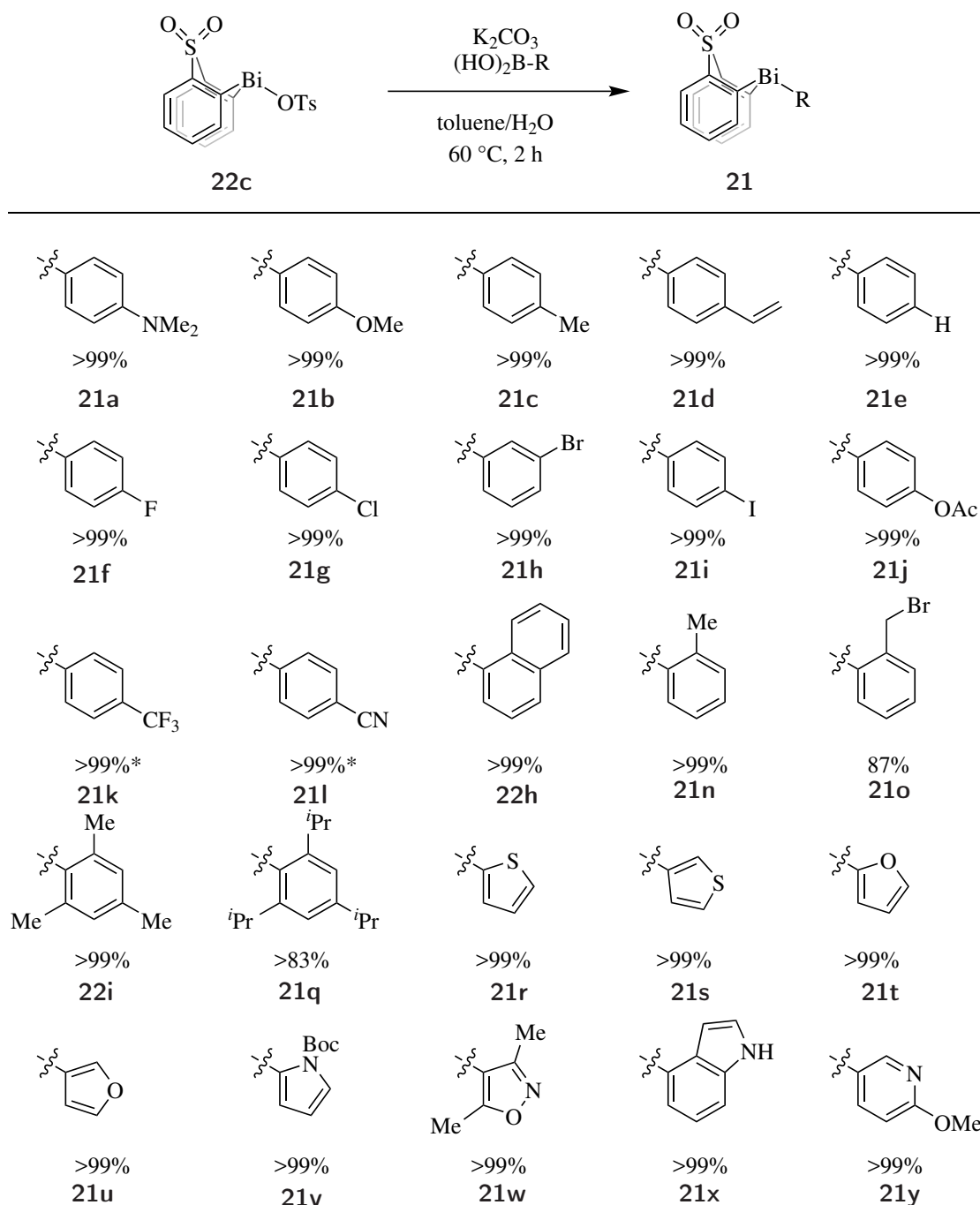
As can be seen in Scheme 3.22, the transmetalation of arylboronic acids carrying electron-rich and moderately electron-poor substituents (**21a-j**) can be performed with quantitative conversion. Aryl groups carrying very electron-poor substituents such as CF₃ (**21k**) and CN (**21l**) did not result in full conversion within the 2 h reaction time, but in a complex mixture of different products. Upon an extension to 6 h, full conversion was observed. 4-Nitrophenyl boronic acid did not result in the 4-nitrophenyl thiabisminium dication transmetalation product even after extended reaction periods.

Equally, aryl substituents carrying sterically demanding motifs have been introduced using this methodology. Transmetallation of the mesitylene group onto bismuth has been shown before with moderate yields using Grignard or lithium reagents,^{48,150,200} but can now be realised in a quantitative fashion using our methodology (**22i**). Even more impressive is the result of 2,4,6-triisopropylphenyl boronic acid (TRIP) (**21q**). Previous attempts to make the analogous TRIP₃Bi using Grignard or lithium reagents were widely unsuccessful or resulted in poor yields (4% isolated yield by Sasaki *et al.*²⁰¹), due to the high steric demand of three groups around a bismuth centre. The use of a backbone on the bismuth centre circumvents this problem and allows for a reduced steric congestion, that results in an 83% conversion in 2 h using the developed methodology.

Additionally, a variety of heteroaryl boronic acids showed excellent capabilities for B-to-Bi transmetallation, which have previously been prepared in poor to moderate yields as the triheteroaryl bismuth equivalents^{202,203} (**21r-y**).

The mild conditions used allowed for the installation of aryl groups carrying functional groups that can be used for further modification, such as vinyl, iodo, bromo, chloro and ester- motifs that were challenging to install previously,²⁰⁴ e.g. 21% yield of tri(4-iodophenyl)bismuth *via* an aryldiazonium salt.²⁰⁵

Initially, isolation of each bismuth reagent was performed through column chromatography on silica gel. It was observed that while most aryl thiabismine dioxide reagents are robust to these conditions, very electron-rich or sterically demanding aryl groups were prone to decomposition. This observation is not problematic as isolation in the proposed one-pot system is neither necessary nor desired.

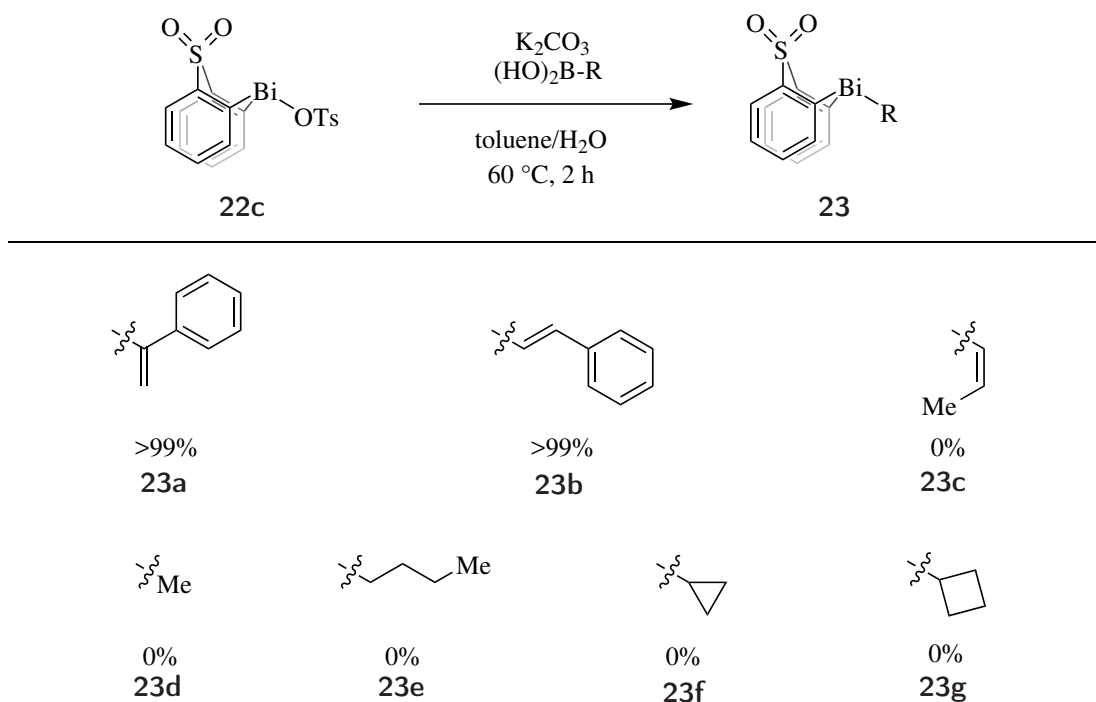


Scheme 3.22: Scope of boronic acids for the transmetalation of **22c**; Conversions have been determined by ^1H NMR spectroscopy; Conditions: [**22c**] = 4.2 mM, [K_2CO_3] = 5.0 mM, [boronic acid] = 4.6 mM in toluene/ H_2O (200/1), *reaction time was 6 h.

3.2.6 Extention of the Transmetalation Methodology

With general transmetalation conditions in hand, an extension of this methodology was attempted to include non-aryl boronic acids as potential coupling partners (Scheme 3.23). Phenylvinylboronic acids showed quantitative conversion to the corresponding phenylvinyl thiabismine dioxides. In contrast, methylvinyl boronic acid did not result in any transmetalation product. A pendant aryl ring motif appears necessary to provide better stabilisa-

tion of the developing charge in a transmetallation transition state.



Scheme 3.23: Transmetalation of vinyl and aliphatic boronic acids under the previously established transmetalation protocol; Conditions: $[\mathbf{22c}] = 4.2 \text{ mM}$, $[\text{K}_2\text{CO}_3] = 5.0 \text{ mM}$, $[\text{boronic acid}] = 4.6 \text{ mM}$ in toluene/ H_2O (200/1).

As trialkyl bismuth reagents have been reported to be pyrophoric^{53,54,58} alkyl thiabismine dioxide analogues were also expected to be sensitive. Indeed, no clear transmetalation products could be identified in the crude mixtures and purification *via* column chromatography.

With an already broad scope of aryl reagents in hand, further investigations have been focused on the aryl groups that show good transmetalation capabilities.

3.2.7 Crystallographic Analysis of Aryl/Heteroaryl Thiabismine Dioxides

A crystallographic investigation of the individual thiabismine dioxides has been conducted. All obtained crystal structures resulted in aryl thiabismine dioxide molecules similar to the one displayed in Figure 3.2.1.

The thiabismine dioxide scaffold can be seen to span out in a butterfly shape with a mirror plane in the Bi–S–O plane. The C–Bi–C angle of the bismacyclic carbons is significantly smaller than in Ar_3Bi with around 86° . The C–Bi–C angles of the exocyclic aryl group with the carbon of the bismacycle vary from 91 to 96° . The exocyclic aryl group orients in a slightly tilted fashion to the Bi–S–O plane.

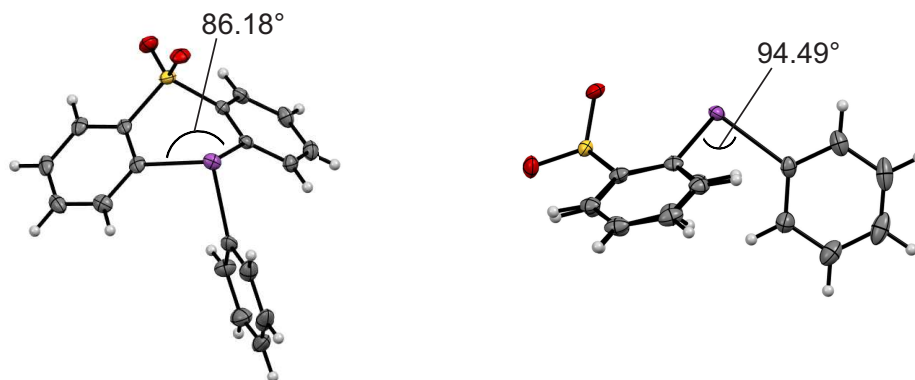


Figure 3.2.1: Crystal structure of **21e** in different orientations. Thermal ellipsoids with 50% probability

Among the differently substituted thiabismine dioxides only small variation were observed. Within these minor iterations the only trend that could be found is the extending Bi–C bond length of the exocyclic aryl ring. Here a rough correlation to the Hammett parameter of the individual substituents was observed (Figure 3.2.2).

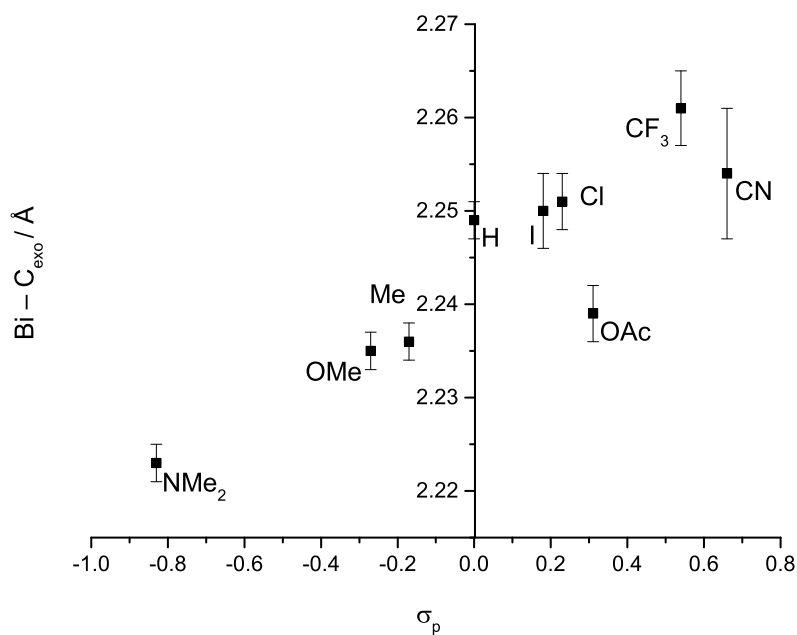


Figure 3.2.2: Correlation of the Bi–C bond length to the individual Hammett parameters of the substituents on the *para* position of the exocyclic aryl ring

Thiabismine species with a longer B–C bond show a greater stability towards decomposition on silica gel, which may be an indication of their potential to undergo protodebismuthation. While compounds up until a bond length of 2.25 Å show no sensitivity to silica, a shorter bond length results in decomposition.

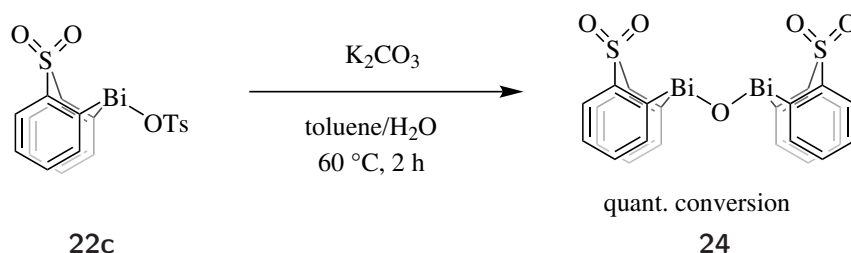
This observation is supported by the bond lengths of the isoxazol- (2.226(5) Å), 3-thienyl- (2.228(6) Å) and 2-furyl derivatives (2.2230(4) Å), which all decompose on silica gel.

The sterically hindered 1-naphthyl derivative possesses a bond length of 2.26(1) Å, which does not provide conclusive information about a steric influence. Equally 1-phenylvinyl- (2.283(5) Å and 2-phenylvinyl- 2.220(7) Å do not obey the observed trend by both being stable to silica gel, despite their widely different Bi–C bond lengths.

3.2.8 Mechanistic Investigation

B-to-Bi transmetallation performs significantly better for the thiabismine dioxide backbone than other bismacycles investigated as well as simple diaryl bismuth halides (see 2). In order to identify the cause of this increased activity a mechanistic investigation was conducted.

A first indication into the mechanism was obtained with the transmetallation of CF₃- and CN- substituted aryl boronic acids. Observation of ill defined species after 2 h, but full conversion after 6 h, hinted towards the existence of one or more intermediates. In order to identify this intermediate the bismacycle tosylate **22c** was exposed to the previously identified transmetallation conditions in the absence of aryl boronic acid (Scheme 3.24).



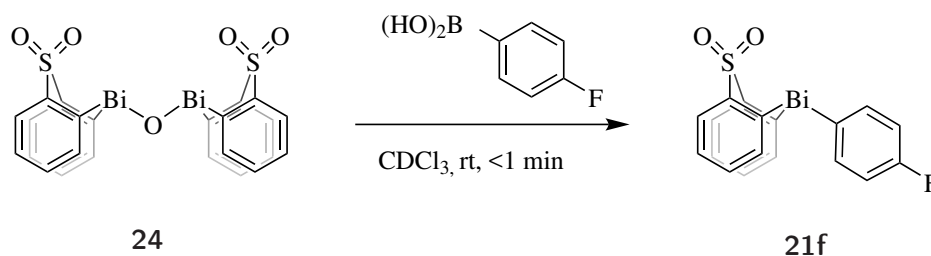
Scheme 3.24: Isolation of μ -oxo-bridged dimer **24** under transmetallation conditions in the absence of boronic acid

Under these reaction conditions, μ -oxo-bridged dimer **24** was isolated. **24** is likely the product of a dehydration of two thiabismine dioxide hydroxide species formed through an anion exchange of ⁻OTs through OH⁻ under basic aqueous conditions. Upon workup the water was removed, shifting the equilibrium towards the anhydride **24**.

The addition of H₂O to the dimer **24** resulted in an ill-defined reaction mixture similar to the one observed in the transmetallation with electron deficient aryl boronic acids, indicating a fast equilibrium between thiabismine dioxide hydroxide and the dimeric condensation product **24**. Related Bi-O-Bi-species have been reported before for triarylbismuth(V) reagents.²⁰⁶

Upon addition of 4-fluorophenyl boronic acid to the isolated **24** transmetallation occurred within seconds, rendering the formation of the intermediate the rate determining step for normal and electron-rich aryl boronic acids (Scheme 3.25). For very electron-poor aryl boronic acids B-to-Bi transmetallation is rate determining and accumulation of the inter-

mediate is observed.

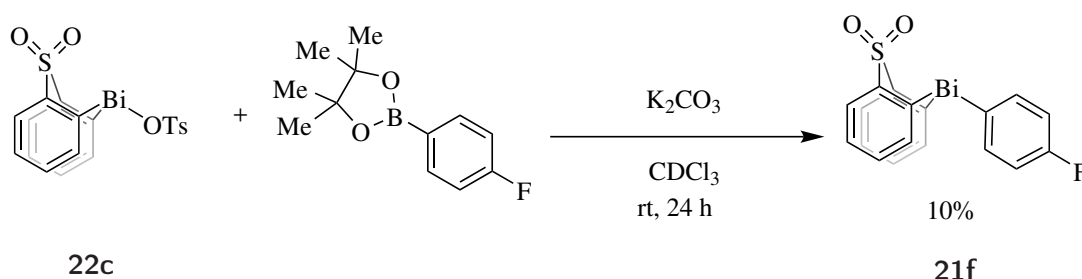


Scheme 3.25: Transmetalation of **24** using 4-fluorophenyl boronic acid

While clear identification of the elementary steps involved in transmetalation remains to be achieved, the mechanism is likely to involve a B–O–Bi bond, similar to the Pd-oxo pathway for transmetalation in Suzuki coupling reactions.^{169,207,208}

3.2.9 Assessment of Bpin Transmetalation Reagents

With easy synthetic access to pinacolato boron reagents (Bpin) through various methods,^{209–211} extension of the transmetalation scope was attempted. Hence, 4-fluorophenyl Bpin was subjected to the previously established transmetalation conditions.



Scheme 3.26: Transmetalation of **22c** using 4-fluorophenyl Bpin

Under the regular condition only 10% transmetalation was observed, despite the presence of the pre-transmetalation intermediates. This observation indicates that pinacolato boronic esters are not competent in the transmetalation reaction, indicating further that a B–OH bond is necessary for the transmetalation process. The low degree of transmetalation can be attributed to the slow hydrolysis of the boronic ester to the corresponding boronic acids, which readily undergoes the desired transformation.²¹²

This observation not only provides further detail to the transmetalation process, but also allows for greater synthetic variability as a molecule carrying both a boronic acid and ester could potentially be selectively functionalised.

3.3 Identification of Suitable Oxidants

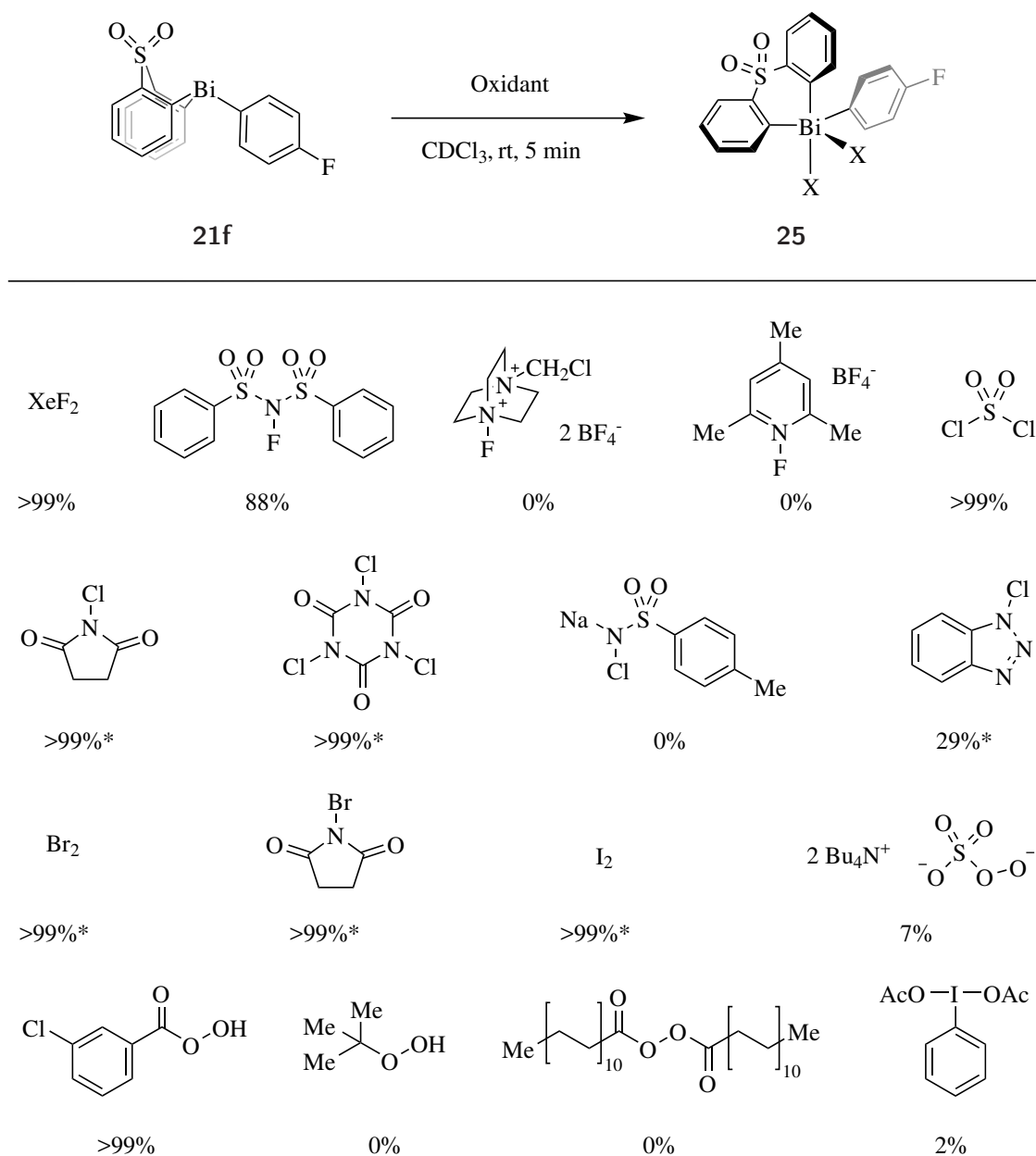
With a robust transmetallation protocol in hand, the next step of the proposed modular system was investigated. In agreement with the previous study, the fluorinated aryl thiabismine dioxide reagent **21f** was used to allow a fast and efficient screen of various oxidants *via* ^{19}F NMR spectroscopy.

Stable aryl thiabismine(V) dioxide species have been reported once before.¹⁹¹ The aryl thiabismine(V) dioxide di-*metachlorobenzoate* (*mCBA*) species was obtained *via* addition of *mCPBA* to the thiabismine(III) reagent and *mCBA*, which was subsequently thermally decomposed with HOTs to result in aryl tosylates.¹⁹¹

In order to establish the capability of various oxidants, screening reactions were analysed using ^{19}F NMR spectroscopy. While the starting compound **21f** can be found at -111.18 ppm, oxidation products are typically observed between -105 and -108 ppm.

With prior information about capable oxidants (see chapter 2) a small oxidant screen was conducted. In contrast to the previous investigation into a catalytic use of bismuth reagents, compatibility of the oxidant with substrates and transmetallation reagents are of minor concern: the sequential addition in the present strategy ensures full consumption of each reagent prior to addition of the next.

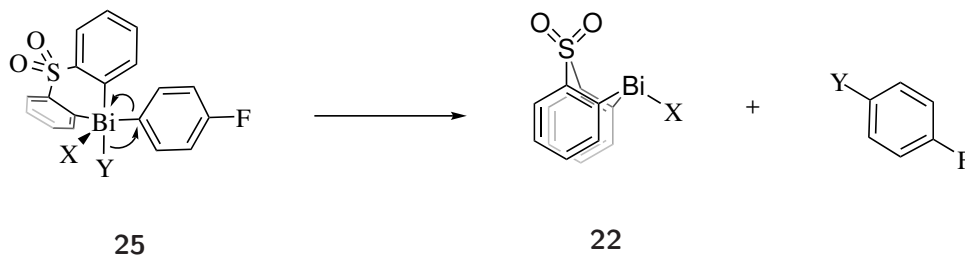
While the fluorination reagents XeF_2 and NFSI show good results in the oxidation of **21f**, no Bi(V) products were observed using selectfluor and 1-fluoro-2,4,6-trimethylpyridinium tetrafluoroborate.



Scheme 3.27: Conversion of **21f** using different oxidation agents in CDCl₃; Conditions: [21f] = 31.6 mM, [Oxidant] = 63.2 mM; *no aryl thiabismine(V) dioxido observed but decomposition products

The use of chlorinating reagents led to interesting results. Sulfuryl chloride, NCS and trichloroisocyanurate proved to be potent oxidants, resulting in full conversion to the Bi(V) species. 1-Chloro-benzotriazole showed moderate yields, and chloramine-T showed no conversion. With the exception of aryl thiabismine(V) dioxido species resulting from the oxidation by sulfur chloride, all Bi(V) products proved unstable, decomposing to thiabismine dioxido chloride and 1-chloro-4-fluorobenzene. Assuming a reductive elimination process similar to that observed for aryl triarylbismuth(V) dioxido isothiocyanates and iodides,^{159,160} the observation of these products is surprising considering the relatively hard character of the chloride anion (for proposed mechanism see Scheme 3.28). The

stable nature of aryl thiabismine(V) dichloride under ambient conditions (decomposition upon increased temperature¹⁹¹) is especially remarkable, and indicates that the reductive elimination is dependent on both the transferred and the remaining counterion. The significantly harder nitrogen of the succinimide presumably allows the softer Cl^- counter ion to undergo the reductive elimination to form the aryl chloride. This observation is consistent with previous reports of elimination of Bi(V) species bearing counterion of different softness.⁴⁸



Scheme 3.28: Proposed decomposition mechanism involving a reductive elimination to form a thiabismine dioxide (*pseudo*)halide species and an ArY , with X = succinimide, dichloroisocyanurate, benzotriazole and $\text{Y} = \text{Cl}$ or $\text{X} = \text{Br}$, succinimide and $\text{Y} = \text{Br}$ or $\text{X} = \text{Y} = \text{I}$

The bromination reagents bromine and NBS showed great potential for the oxidation of aryl thiabismine dioxide reagents, which was offset by the observation of a similar aryl bromide decomposition product. The decomposition of the NBS-derived Bi(V) product was expected with regards to the results using NCS, as bromide is significantly softer. The instability of aryl thiabismine(V) dioxide dibromide though contrasts the stability of Ar_3BiBr_2 , indicating an increased propensity towards reductive elimination provided by the thiabismine dioxide scaffold that can become useful in the reductive elimination step of the arylation of phenols in the proposed modular system.

The use of peroxide oxidants for **21f** shows mixed results. While *m*CPBA results in complete conversion, the OXONE-derivative and $\text{PhI}(\text{OAc})_2$ only result in minor aryl thiabismine(V) species. Other peroxy species such as TBHP and lauroylperoxide did not result in any observable oxidation products.

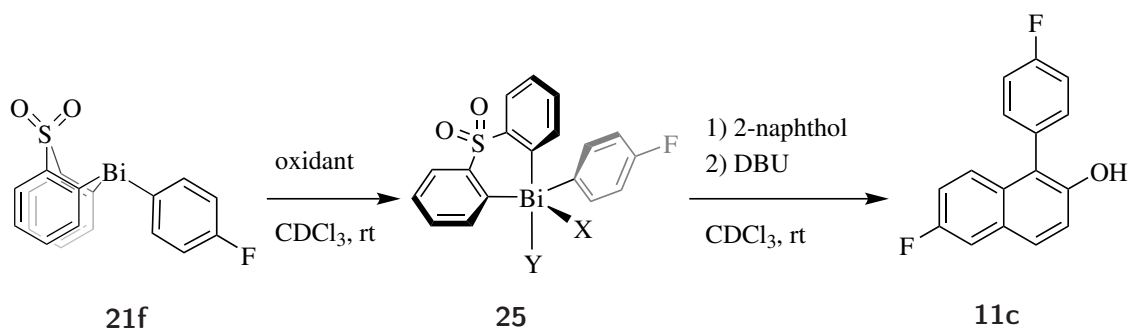
With XeF_2 being ruled out due to the desire to develop an affordable and convenient protocol, only NFSI, *m*CPBA and sulfuryl chloride remain viable candidates for the application to the oxidative arylation of the desired substrates.

3.4 Arylation of 2-Naphthol

Having identified suitable oxidising reagents, the resulting Bi(V) reagents were tested for their ability to perform the desired arylation of 2-naphthol. Considering the proposed modular approach, the prior isolation of the Bi(V) reagents appeared impractical and undesired. Therefore, the oxidation was carried out *in situ* followed by the addition of

2-naphthol. In a subsequent step base is added to promote the arylation reaction. The combined protocol for oxidation and arylation was monitored *via* ^{19}F NMR spectroscopy to ensure full oxidation of **21f** as well as compatibility of the Bi(V) reagent with 2-naphthol before the addition of base.

All aryl thiabismine(V) dioxide reagents showed a clean oxidation profile, as previously established, but only the ones emerging from SO_2Cl_2 and NFSI can be characterised as stable to the addition of 2-naphthol. Upon addition of DBU to create the naphtholate necessary for the arylation reaction, conversion to the desired arylation product was observed, rendering them viable candidates for the desired transformation (Scheme 3.29).

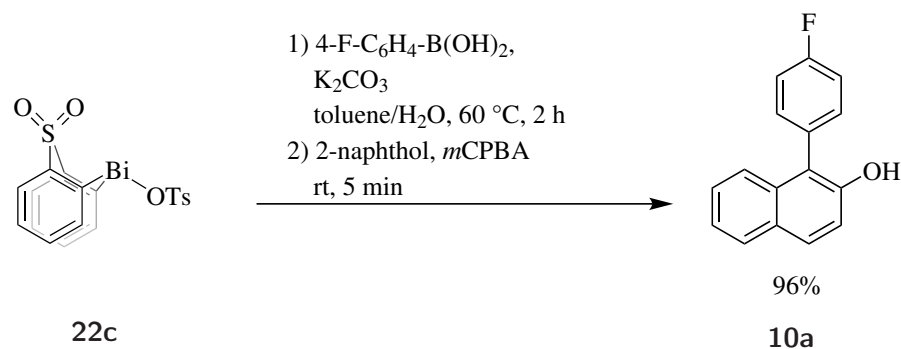


Scheme 3.29: Combined oxidation-arylation protocol with oxidant = SO_2Cl_2 , NFSI or *m*CPBA

The aryl thiabismine(V) dioxide reagent resulting from the oxidation with *m*CPBA did not prove stable upon addition of 2-naphthol. A full consumption of the bismuth(V) species was observed within seconds after the addition of 2-naphthol. Upon analysis of the reaction products, 6-fluoro-1-(4-fluorophenyl)-2-naphthol was identified as the major product in quantitative conversion. This represents base-free bismuth-mediated arylation, a never-reported protocol that provides a more atom and cost effective route to arylated products. Hence, further studies were performed using *m*CPBA as an oxidant. The mechanism of arylation under these conditions will be discussed separately.

3.5 Combination of the Individual Steps in a One-Pot-Protocol

With all individual reactions established, a combination of the individual steps has been performed to fully assemble the proposed modular protocol. Here the thiabismine dioxide tosylate precursor **22c** was exposed to the previously established transmetallation conditions using 4-fluorophenyl boronic acid. After 2 h the reaction mixture was allowed to cool to room temperature and 2-naphthol and *m*CPBA were added and the solution stirred for additional 5 min before working up the reaction.



Scheme 3.30: One-Pot-Protocol for the arylation of 2-naphthol

The desired 1-(4-fluorophenyl)naphthalen-2-ol **10a** was isolated in a 96% yield, proving the one-pot approach a viable system for the arylation of 2-naphthol.

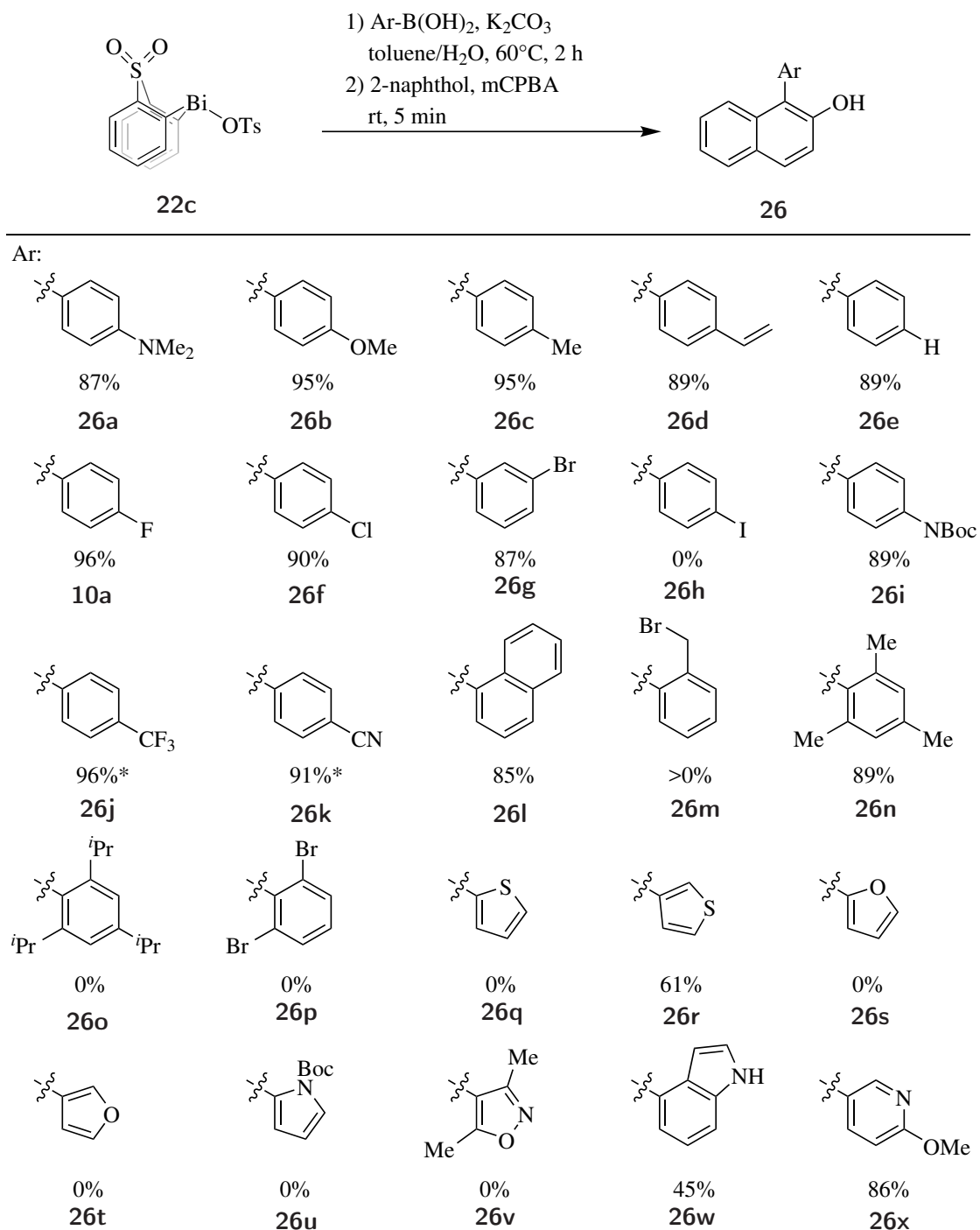
3.6 Establishing Substrate Scope

3.6.1 Variation of the Boronic Acid

With a working one-pot approach in hand, the range of substrates and coupling partners had to be established. With a scope of aryl boronic acids capable of transferring the aryl group onto the bismuth centre already investigated (Scheme 3.22) a full transmetallation was ensured allowing for investigation to focus on the aryl thiabismine dioxide's ability to be oxidised and transfer the aryl group onto 2-naphthol.

As portrayed in Scheme 3.31, the arylation of 2-naphthol proceeds in excellent yields for electron-poor to electron-rich aryl groups (**26a-26k**). Sterically demanding aryl rings have been applied to this methodology with 1-naphthyl (**26l**) and mesityl (**26n**) groups being successfully transferred onto the substrate. The extremely demanding TRIP group did not show observable conversion to the desired product. This result can be attributed to the steric demand of the isopropyl groups blocking the nucleophilic attack of the 2-naphthol onto the Bi(V) centre, as the oxidation product has been observed.

Using this methodology the first bismuth-mediated arylation using heterocyclic motifs has been achieved. Excellent yields have been observed for 4-methoxy-3-pyridyl and moderate yields for 3-thienyl and unprotected 5-indolyl substituents. While the reduced yields of the indolyl derivative can be attributed to the sensitivity of the indol motif to oxidation using *m*CPBA, a more complex explanation has to be offered for the other electron-rich heterocyclic motifs in the scope (*vide infra*).



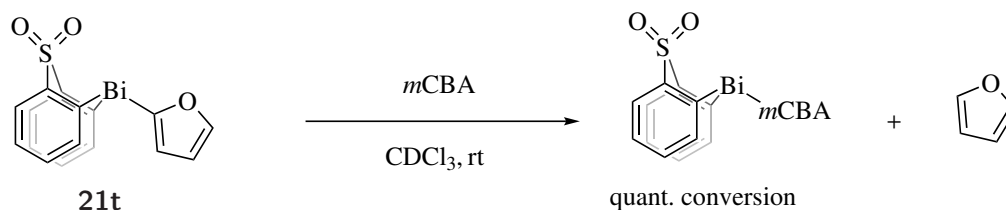
Scheme 3.31: Scope of one-pot protocol for the arylation of 2-naphthol, * = transmetalation time increased to 6 h

Investigation into the Behaviour of Heteroaryl Thiabismine Dioxides Featuring Electron-rich Heterocycles

As it was noted before, electron-rich aryl groups attached to bismuth show an increased sensitivity towards acid induced protodebismuthation. In order to establish their inability to transfer the heterocyclic motif onto 2-naphthol, their sensitivity towards *m*CBA was tested. The 2-furyl thiabismine dioxide derivative **21t** was used for this investigation as it

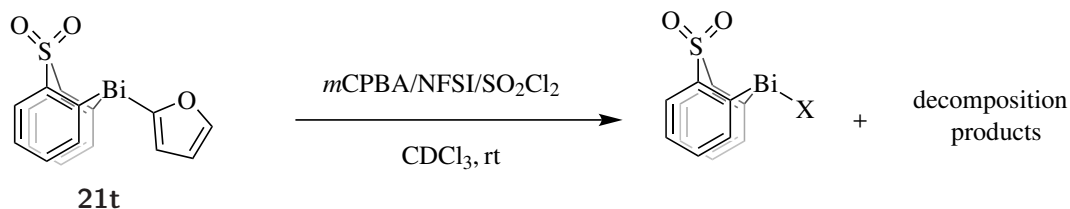
represents the most electron-rich member of the library.

As can be seen in Scheme 3.32, the addition of *m*CBA to **21t** results in protodebismuthation creating furan and the 2-furyl thiabismine dioxide *m*CBA species. With *m*CBA present in commercial *m*CPBA, this decomposition pathway can be considered to be the cause of the incapability of this transformation



Scheme 3.32: Protodebismuthation of the 2-furyl group of **21t** by *m*CBA.

In order to overcome this limitation a protocol was developed without the presence of acids, that could promote protodebismuthation. Therefore freshly purified *m*CPBA as well as SO_2Cl_2 and NFSI have been investigated as potential oxidants for **21t** (Scheme 3.33). The addition of purified *m*CPBA, as well as NFSI and SO_2Cl_2 did not result in stable Bi(V) reagents. NFSI resulted in furan as the reaction product despite the absence of a Brønsted acid under the reaction conditions.



Scheme 3.33: Oxidation of **21t** under non-acidic conditions, X = *m*CBA, Cl, F.

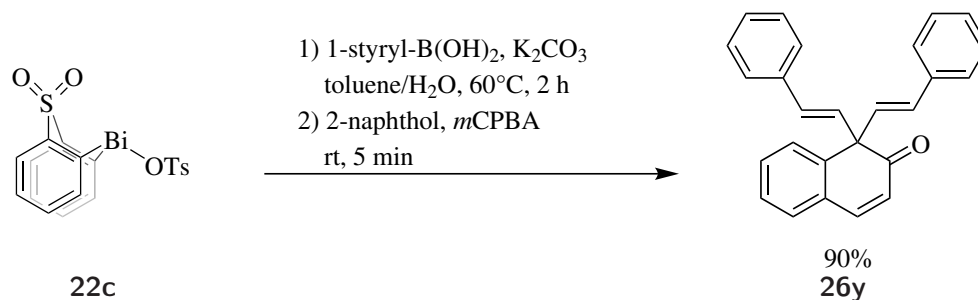
SO_2Cl_2 and *m*CPBA result in reaction mixtures that clearly show an intact thiabismine dioxide scaffold. However no furyl group is observable, indicating an inherent instability of 2-furyl thiabismine dioxide structures equipped with electron-rich heterocycles. The short Bi–C bond of these species can be an indicator for the factors that result in a faster elimination process.

The inherent instability of thiabismine dioxide derivatives with electron-rich heterocycles has been established and remains a limitation of the current modular approach.

Application of the One-Pot Protocol to Thiabismine dioxides Carrying the Styryl-Motif

Phenylvinylboronic acids showed excellent results in the transmetallation onto **22c**. Therefore the capability of the resulting thiabismine dioxides **23a** and **23b** to transfer the styryl motif to 2-naphthol was investigated in the one-pot procedure.

For the transmetallation of the 1-styryl group the unexpected product 1,1-di(*E*-styryl)naphthalen-2(1*H*)-one **26y** has been identified as the sole product of this transformation (Scheme 3.34).



Scheme 3.34: Transfer of 1-styryl motif onto 2-naphthol resulting in 1,1-di(*E*-styryl)naphthalen-2(1*H*)-one **26y** (yields based on bismuth)

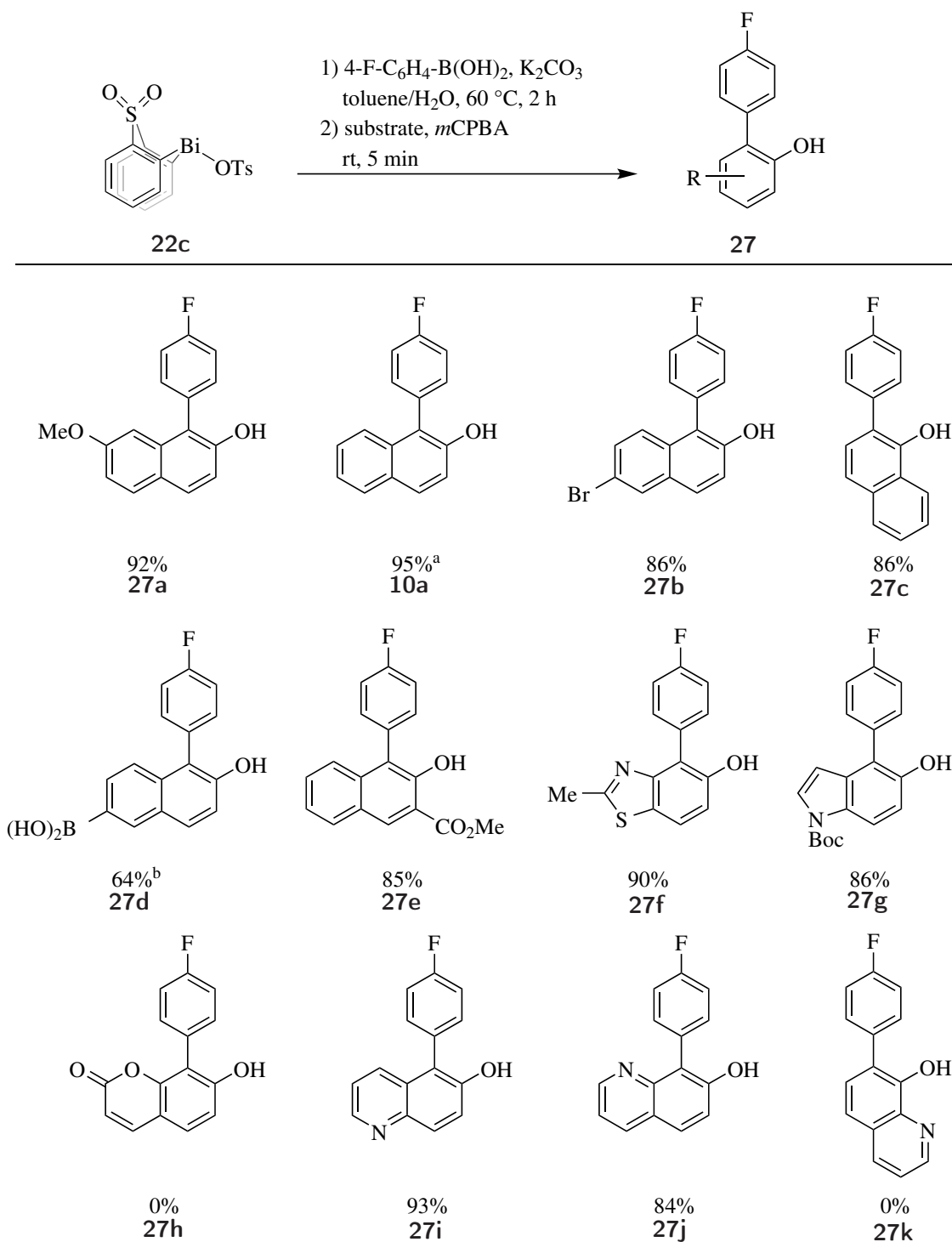
This reaction product is the result of a styryl group being installed at 2-naphthol followed by a subsequent addition of the second styryl equivalent. With an equimolar ratio of aryl thiabismine dioxide and 2-naphthol, the exclusive observation of the dearomatised product requires the first product to be a significantly better substrate than the original substrate. This can be accounted for by the extension of the π -system of 2-naphthol allowing for an increased susceptibility towards further modification.

Complementing the result of electron-rich heterocycle substituted thiabismine dioxides, no transformation of 2-naphthol has been observed for the 2-styryl thiabismine derivative. An intrinsic elimination out-competes the bimolecular arylation process, disallowing observation of the desired product.

3.6.2 Application to Naphthol-like Substrates

As the one-pot protocol has been established to selectively transfer a variety of aryl groups onto 2-naphthol, the range of suitable hydroxyaryl substrates was investigated. In the first instance 2-naphthol derivatives and close analogues have been tested as substrates.

In order to establish an easy to follow screening mechanism the previously prepared 4-fluorophenyl thiabismine dioxide **21f** was used for small scale testing of the individual substrates prior to the larger scale approach following the one-pot approach.



Scheme 3.35: One pot approach for the arylation of naphtho-like substrates, ^a starting material 1-bromo-2-naphthol, ^b isolated as the Bpin ester.

As displayed in Scheme 3.35, the developed methodology proved applicable to a variety of different naphthol derivatives. Electron-donating groups (OMe, **27a**) as well as electron-withdrawing groups (COOMe, **27e**) are readily tolerated on both the direct as well as the adjacent ring allowing for broad application.

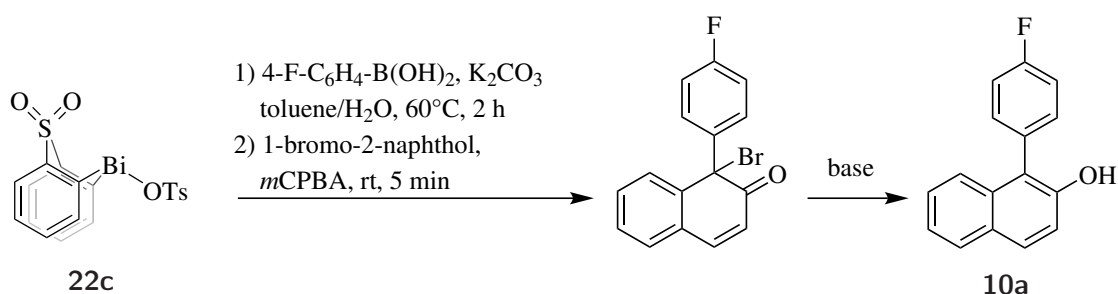
Notably, functional groups such as bromine and boronic acids are well tolerated, which

renders this methodology orthogonal to current cross coupling and C–H activation protocols that rely on these motifs to perform their transformation.^{213,214} A complementary use of the developed methodology with subsequent use of the already existing protocol would allow for new synthetic strategies.

Heterocyclic naphthol substrates that have previously been overlooked in Bi(V) chemistry have been assessed during this investigation. While several of these substrates were successfully engaged in this methodology (**27f–27j**), quinolin-8-ol did not result in an observable yield (**27k**). This can be attributed to a coordination of the adjacent basic nitrogen, locking the substrate onto the bismuth(V) centre of the aryl thiabismine dioxide rather than performing the arylation as it has been reported before by Barton *et al.*⁹⁴ for homoleptic Bi(V) reagents.

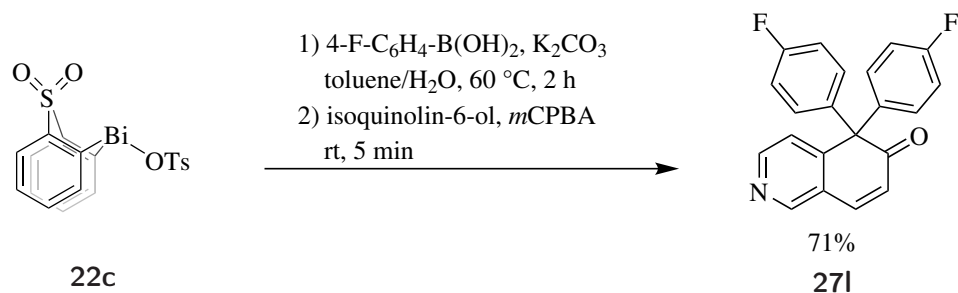
Umbelliferone proved unsuitable as a substrate not resulting in the arylation product **27h**, although the origins for this behaviour are unclear.

The selectivity of 2-hydroxy-substituted starting materials always prefers the the designated 1 position. In an effort to block this position 1-bromo-2-naphthol derivative was chosen to prevent arylation at the 1 position. Upon exposure to the arylation protocol an unidentified reaction intermediate was observed that decomposed into **10a** during basic work-up. It can be presumed that, despite blocking of the 1 position with a sterically demanding and electron withdrawing substituent, arylation of the 1 position has taken place resulting in a 1-bromo-1-(4-fluorophenyl)naphthalen-2(1*H*)-one intermediate (Scheme 3.36).



Scheme 3.36: One pot approach for the arylation of 1-bromo-2-naphthol resulting in a 1-bromo-1-(4-fluorophenyl)naphthalen-2(1*H*)-one intermediate that decomposes to **10a** in presence of base.

With a variety of quinolinol derivatives showing good activity in aryl thiabismine dioxide-mediated arylation isoquinolin-6-ol was chosen as a substrate (Scheme 3.37). Surprisingly, only the doubly arylated 5,5-bis(4-fluorophenyl)isoquinolin-6(5*H*)-one (**27i**) was observed. In accordance with the previously observed double functionalisation product **26y**, an increase activity of the mono-arylated product over the original substrate must be the basis of this observation.

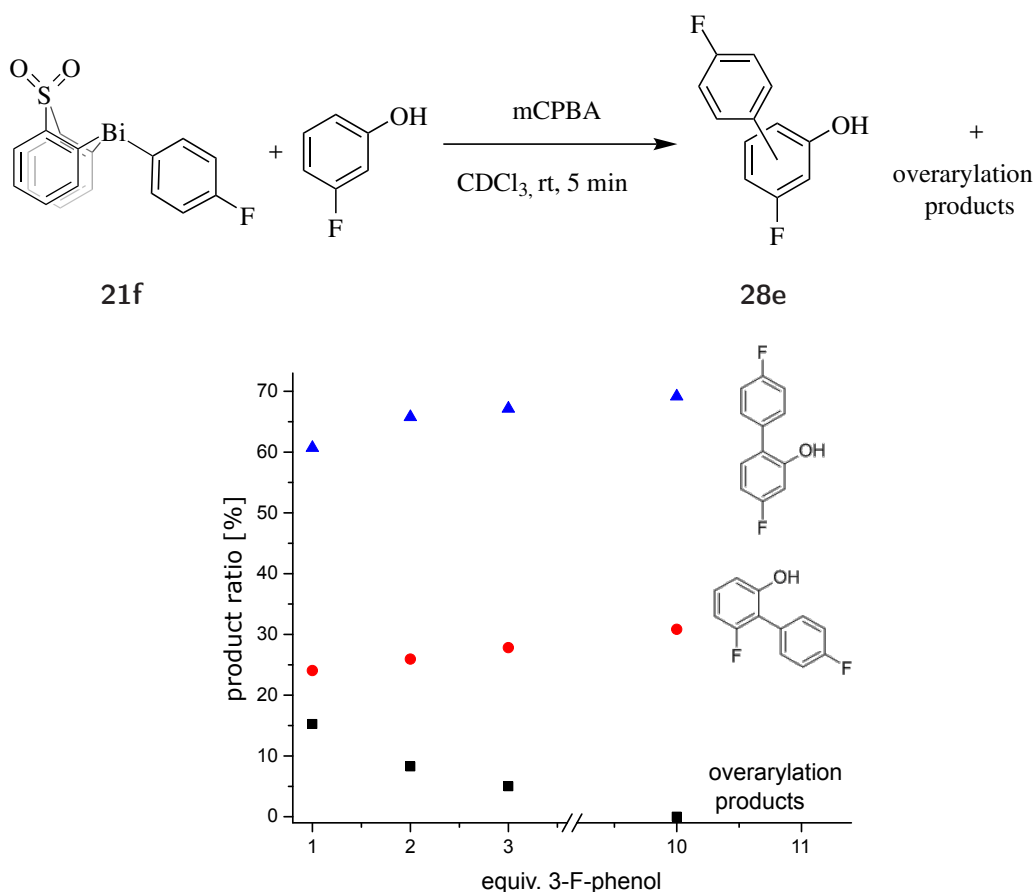


Scheme 3.37: Double arylation of isoquinolin-6-ol under standard conditions

3.6.3 Application to Phenolic Substrates

The excellent results of the arylation of naphthol-like substrates, encouraged us to extend the scope to phenolic substrates. These substrates have previously shown moderate to poor yields, with a substrate controlled *O*-*vs*-*C*_{ortho}-selectivity and a high degree of overarylation on phenol molecules featuring two unsubstituted *ortho* positions.

While initial results suggested a complete *C*_{ortho} over *O* selectivity using the developed system the problem of overarylation remained. It was anticipated that this limitation could be addressed by using a higher stoichiometry of phenol in relation to bismuth.



Scheme 3.38: Variation of the relative amount of 3-fluorophenol and its dependency on the degree of overarylation

The minimum excess of phenol necessary to prevent overarylation was assessed using 3-fluorophenol to enable analysis by ¹⁹F NMR spectroscopy.

It can be seen in Scheme 3.38 that the overarylation is reduced with an increasing relative ratio of the substrate with complete avoidance at around 10 equivalents. For further studies 3 equivalents were used as a compromise between selectivity (95% monoarylated products) and atom efficiency.

With the issue of overarylation solved, a screen of a variety of phenols was tested to establish substrate scope as well as to provide insight into the regioselectivity towards different non-symmetrical substrates (Scheme 3.39).

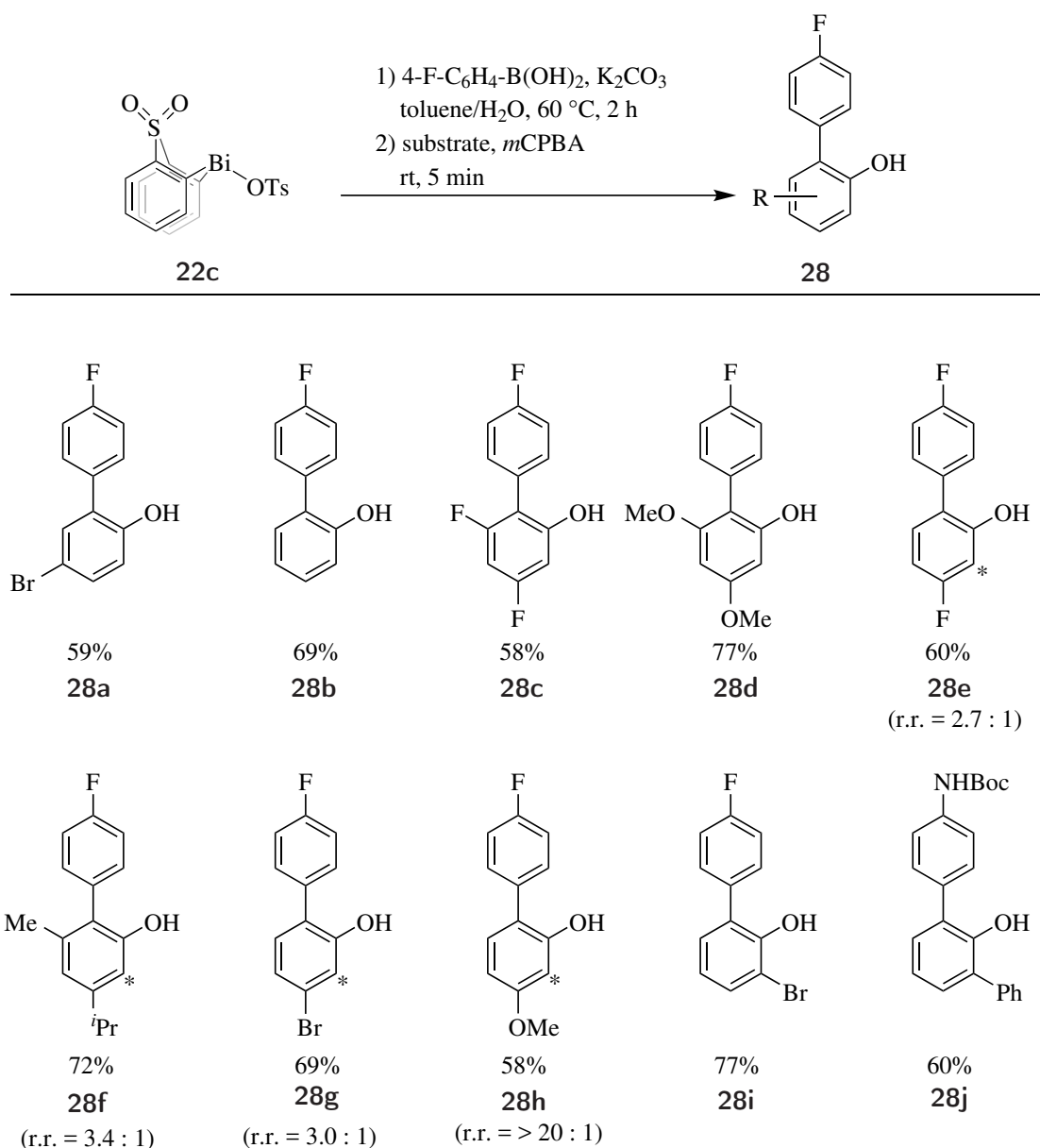
The arylation of phenols succeeded with moderate to good yields. More impressive is the increase in reactivity in comparison to the original conditions proposed by Barton *et al.*³³ which offer a maximum of 30% of the desired product and various side products. Our conditions allow for selective C_{ortho} arylation with no overarylation or O-arylation being observed.

The methodology proved applicable to electron-rich and -neutral phenols (**28b**, **28d**) and showed good activity towards moderately electron-poor rings (**28a**, **28c**). The use of highly electron withdrawing groups such as CF₃ and NO₂ did not result in any observable arylation product.

For the arylation of unsymmetrical phenols, regioselectivity towards the different C_{ortho} positions was observed. 3-Fluorophenol proved an adequate reagent to investigate these trends as this substitution creates two sterically equivalent, but electronically different, C_{ortho} positions. It was observed that the product resulting from arylation of the more electron-rich carbon centre (**28e**) dominated with a regioisomeric ratio of 2.7:1. This was expected following the proposed electrophilic nature of the transferred aryl group.

For the investigation of sterically in-equivalent but electronically similar substrate, 3-isopropyl-5-methylphenol has been chosen. Here a slightly more pronounced preference towards the sterically less demanding carbon centre (**28f**) was observed with a regioisomeric ratio of 3.4:1.

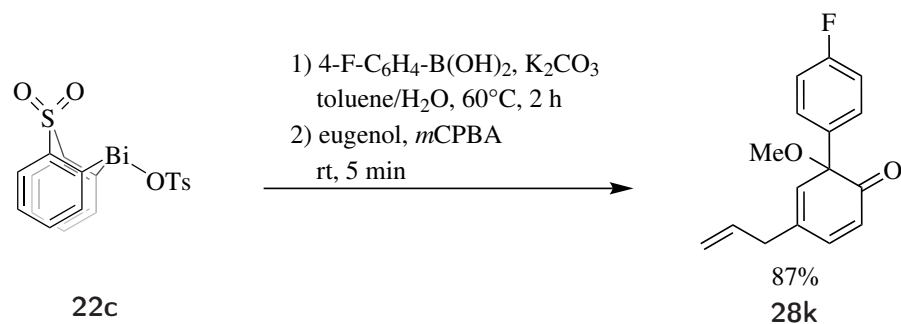
For examples with more complicated electronic and steric properties, prediction of selectivity proved less reliable. 3-Bromophenol results in a product ratio of 3.0:1 towards the sterically less demanding and more electron-rich carbon. 3-Methoxyphenol gave exclusive arylation at the 5 position, which is both sterically and electronically highly favoured. Again this methodology compares favourably to common procedures such as the Friedel-Crafts-type arylation using diazonium salts (Yield: 15%) that feature a significantly reduced functional group tolerance.²¹⁵



Scheme 3.39: Substrate scope for the arylation of phenols, *indicates the position of the aryl group on the minor isomer.

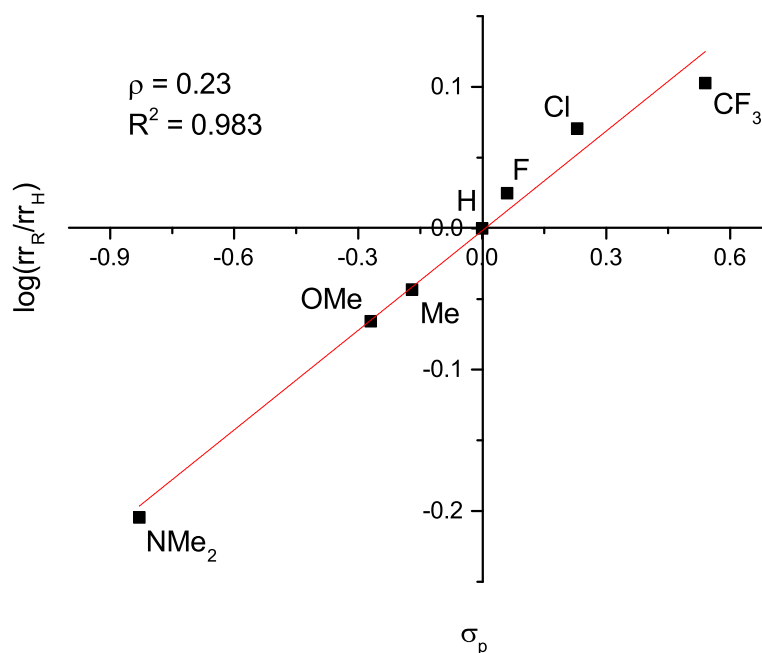
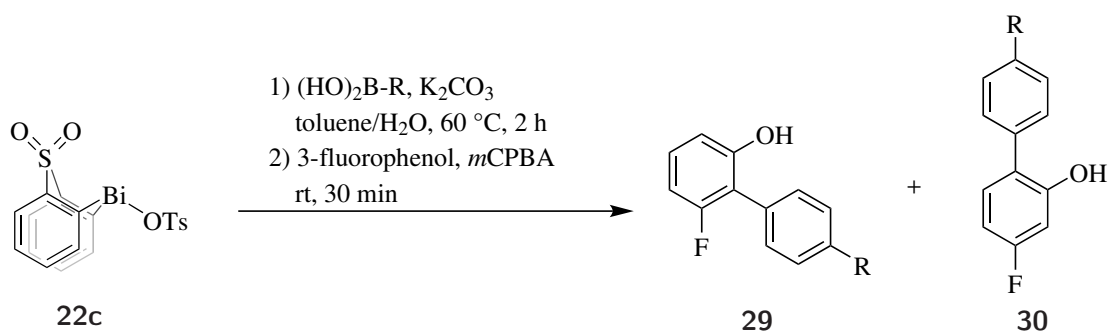
Arylation of 2-substituted phenols exhibits selectivity towards the unsubstituted position for 2-bromo or 2-phenyl phenols (**28i**, **28j**). For the arylation of phenols bearing more electron donating substituents selectivity shows a significant change. *o*-Cresol results in a variety of different products while the 2-methoxy substituted eugenol (4-allyl-2-methoxyphenol) resulted in exclusive arylation the 2 position *ipso* to OMe, resulting in a dearomatised reaction product carrying a [1,1'-biphenyl]-2(1*H*)-one motif (see Scheme 3.40). In this case arylation *ipso* to the sterically demanding methoxy group is preferred over a simple proton. As such, electronic effects are more significant than steric parameters. This methodology is superior to previous attempts to access this functionality starting from phenols that traditionally involve a 3-step synthesis.²¹⁶ Starting from 2-methoxy-1-naphthol the dearomatised product could be accessed in a 52% yield using

chlorodiphenyl- λ^3 -iodane.²¹⁷



Scheme 3.40: Arylation of eugenol resulting in 5-allyl-4'-fluoro-1-methoxy-[1,1'-biphenyl]-2(1*H*)-one **28k**

In order to further determine factors effecting the regioselectivity of arylation, a variety of aryl boronic acids of different electronic properties were investigated. 3-Fluorophenol was chosen as a substrate as in this case the selectivity is exclusively determined by electronic factors.



Scheme 3.41: Hammett-plot for the arylation of 3-fluorophenol with aryl groups of varying electronic properties. $R = \text{NMe}_2, \text{OMe}, \text{Me}, \text{H}, \text{F}, \text{Cl}, \text{CF}_3$

As can be seen in Scheme 3.41, the regioselectivity follows a trend towards a higher selectivity with electron-withdrawing substituents on the transferred aryl groups. However, the sensitivity of selectivity is low with a ρ -value of 0.23.

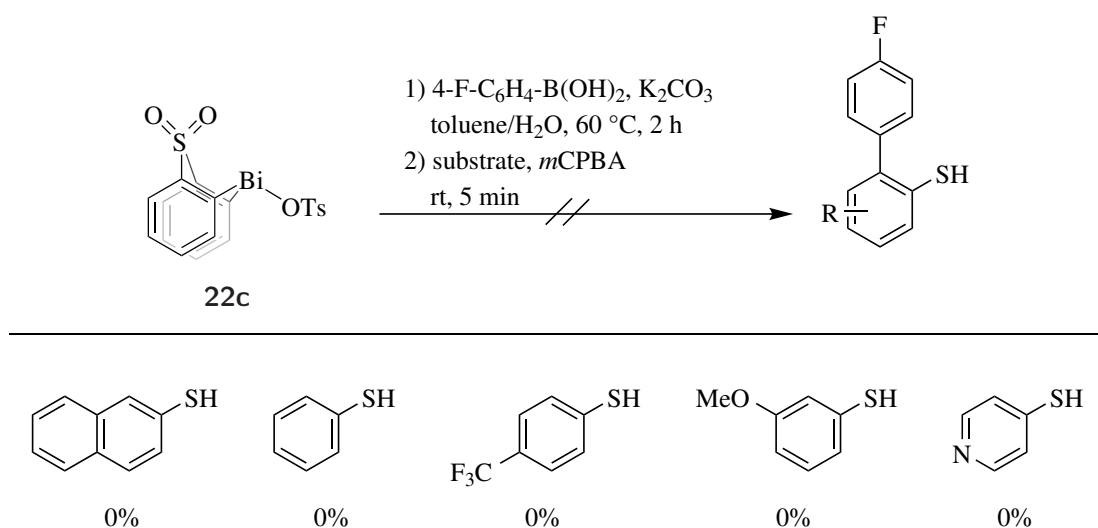
With similar investigations performed for temperature and solvent the selectivity does not appear dependent on these factors. Therefore the transition state/s leading to the different products must be similar and there is no difference in stabilisation of the different intermediates.

Overall the developed methodology can be applied to a range of different naphtholic and phenolic substrates. The observed yields and selectivities show a significant improvement over current protocols^{14–16,27,30} as well as previous results using bismuth mediated arylation (Chapter 2).

3.6.4 Expansion of Methodology to Thiophenols

With the arylation of naphtholic and phenolic substrates demonstrated, extension of the methodology to the heavier homologues was attempted. In the first instance thiophenols were tested in order to establish their potential in the developed system.

Under standard reaction conditions no arylation products could be observed in the ^{19}F NMR spectrum of the crude material, other than the transmetallation product **21f**. This observation proved surprising as *m*CPBA typically oxidises the transmetallation product completely. Therefore a closer look into the processes in hand had to be undertaken.



Scheme 3.42: Attempted arylation of aromatic thiols using the previously established bismuth-mediated arylation methodology.

In order to elucidate the role of the *m*CPBA, a sequential addition of the oxidant prior to the addition of the thiol substrate was performed. Here, the full oxidation of **21f** was confirmed *via* ^{19}F NMR spectroscopy. Upon addition of the thiophenol a full reduction of the thabismine(V) reagent back to **21f** was observed, indicating oxidation of the thiols to the disulfide motif (confirmed by mass spectrometry). This is in line with previous reports indicating that disulfides are formed from thiophenols with Ar_3BiCl_2 as well as Ar_3BiCO_3 .^{139,218}

3.7 Mechanistic Investigation

3.7.1 Investigation of Oxidation/Arylation

As the methodology has proven to be applicable to an library of both boronic acids and hydroxyaryl motifs, a closer investigation into the mechanism was conducted. It was anticipated that this would aid fundamental understanding of the reaction mechanism in hand as well as allowing the development of a predictive tool for application to unknown substrate

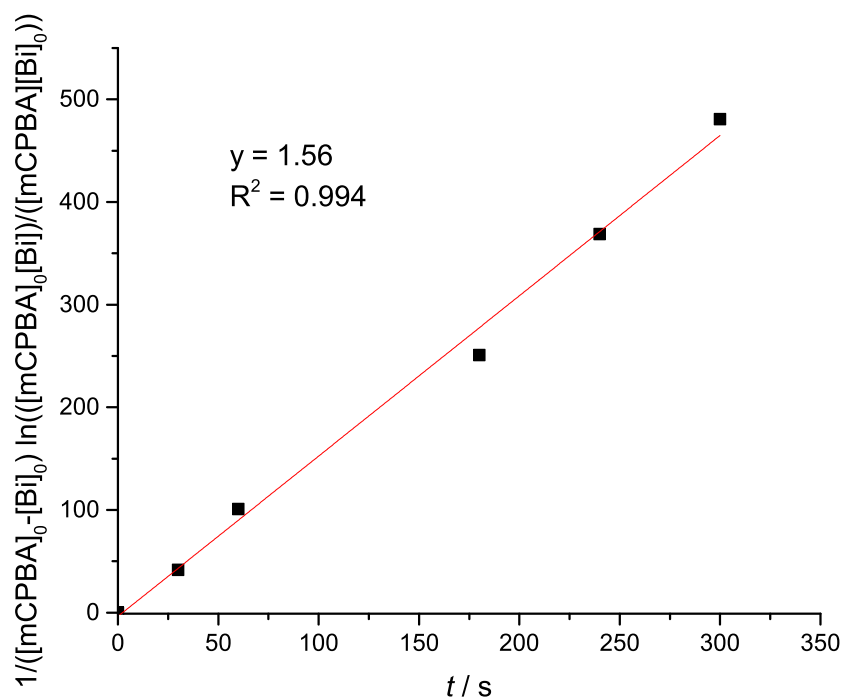
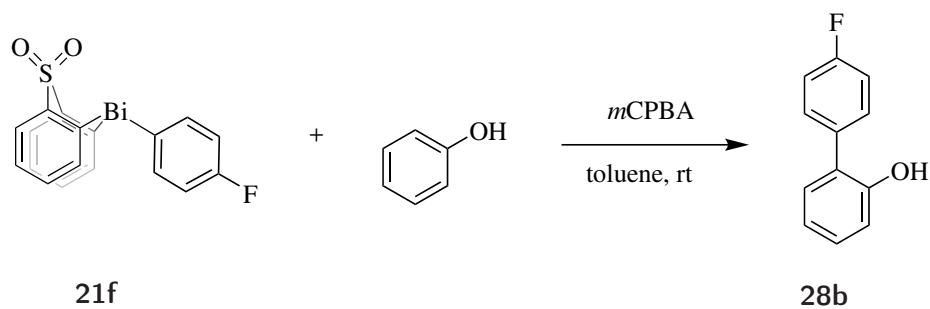
combinations.

The ligand exchange from thiabismine dioxide tosylate **22c** to thiabismine dioxide hydroxide and its dimer **24** has been identified as the rate determining step of the transmetallation process for most boronic acids. For convenience an investigation into the combined oxidation/arylation mechanism was performed *via* a direct oxidation of pre-prepared **21f** in the presence of phenol.

While a reaction time of 5 min has been used throughout the entire substrate scope, the reaction actually completes within seconds under standard conditions. Therefore reaction monitoring using ^{19}F NMR spectroscopy could not be utilised. In order to elongate the reaction time for optimal reaction monitoring, cooling has been dismissed due to the low solubility of the Bi reagent. As all reagents are required in an almost equimolar ratio, a reduction of the concentration of one of the reagents was also not possible. Therefore, dilution of the entire reaction mixture was considered. With concentrations too low for ^{19}F NMR spectroscopy, manual sampling at room temperature with quenching in methanol was used to determine the reaction progression.

It was observed that quenched aliquots contained no Bi(V) reagents nor their decomposition products, but only starting material as well as arylation product. With a full account for the mass balance, this indicates that the oxidation of **21f** is the rate limiting, with the subsequent arylation occurring faster.

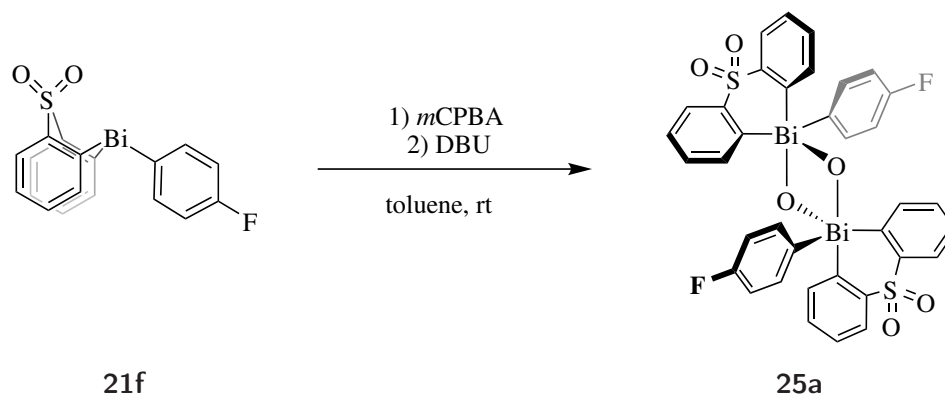
The consumption of **21f** proceeds in a 2^{nd} order fashion, exhibiting a first order dependence on both **21f** and *m*CPBA (see Scheme 3.43). This was expected for a bimolecular reaction and is consistent with the absence of Bi(V)- or Bi(V)-derived (side)products.



Scheme 3.43: 2nd order plot for the oxidation of **21f** and *m*CPBA; $k_{obs} = 1.56 \text{ M}^{-1} \text{ s}^{-1}$, $[\mathbf{21f}]_0 = 3.62 \text{ mM}$, $[m\text{CPBA}]_0 = 2.13 \text{ mM}$ in toluene at room temperature

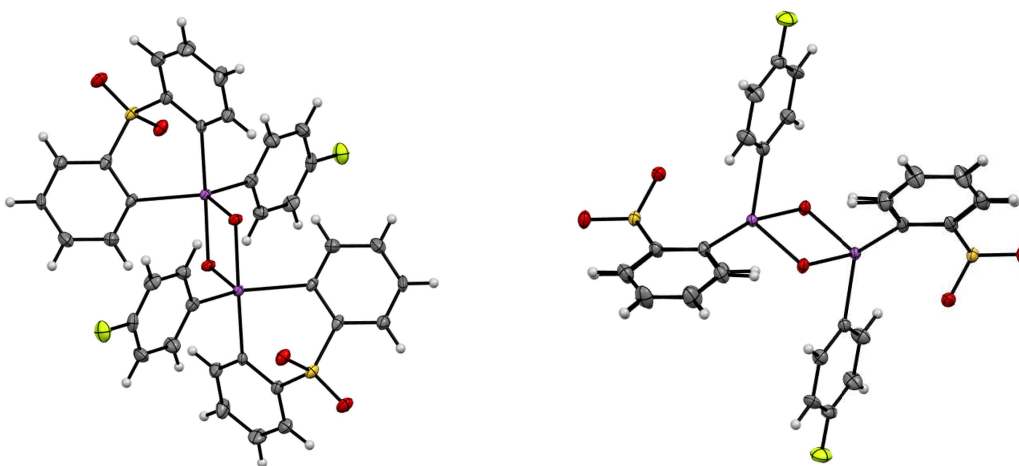
3.7.2 Identification of Aryl Thiabismine(V) Dioxide Reagents

In order to fully understand the reaction mechanism, the identity of the aryl thiabismine(V) dioxide species had to be determined. While the di-*m*CBA-substituted derivative has been reported before,¹⁹¹ the used commercial grade *m*CPBA does not contain enough of this counter ion to produce this species exclusively. As this has not been observed, uncertainty about active species had to be addressed. Upon the addition of DBU, and following an aqueous wash, an oxidation product could be isolated (Scheme 3.44).

Scheme 3.44: Isolation of **25a** from the oxidation of **21f**

A dimeric Bi(V) species with the two Bi centres connected through two μ -oxo bridges was identified as the isolation product of the oxidation upon basic conditions. It can be assumed that under basic aqueous conditions a competition between $m\text{CBA}^-$ and OH^- has been established and the aqueous wash is capable of removing the $m\text{CBA}^-$, favouring the creation of Bi-OH bonds. The Bi μ -oxo motif has shown tendencies to undergo condensation to form dimers for Bi(III) species before (*vide supra*) and has been reported for $(\text{Ar}_3\text{BiO})_n$.^{219,220} In this case, two condensations can be observed to form a dioxadibismetane core for this dimeric isolation product.

The single crystal diffraction allowed for a closer insight into the nature of **25a** (Figure 3.7.1). The distorted trigonal bipyramidal geometry in the solid state includes a diphenylsulfone dioxide scaffold that spans an apical and an equatorial position. Equally the Bi-O bonds orientate in a apical and an equatorial position with different bond lengths of 2.03 Å *vs* 2.20 Å, respectively.

Figure 3.7.1: Crystal structure of **25a** in different orientations. Thermal ellipsoids with 50% probability

The isolated dimeric species shows a different shift in the ^{19}F NMR spectrum than the reaction product of direct oxidation of **21f**. Therefore a titration of **25a** with *m*CBA was conducted to identify possible species. The reaction progress was monitored *via* ^{19}F NMR spectroscopy.

Upon addition of *m*CBA to **25a** a decrease in intensity was observed for the peak at -108.1 ppm with a new peak arising around -105.5 ppm. This trend persists until no **25a**-peak remained with the addition of 1 equivalent of *m*CBA per bismuth. This indicates that the μ -oxo bridges have been broken to form a thiabismine(V) dioxide (OH)(*m*CBA) intermediate **25b**. The loss of observable H–F coupling during the titration suggests that the individual species exist in an equilibrium.

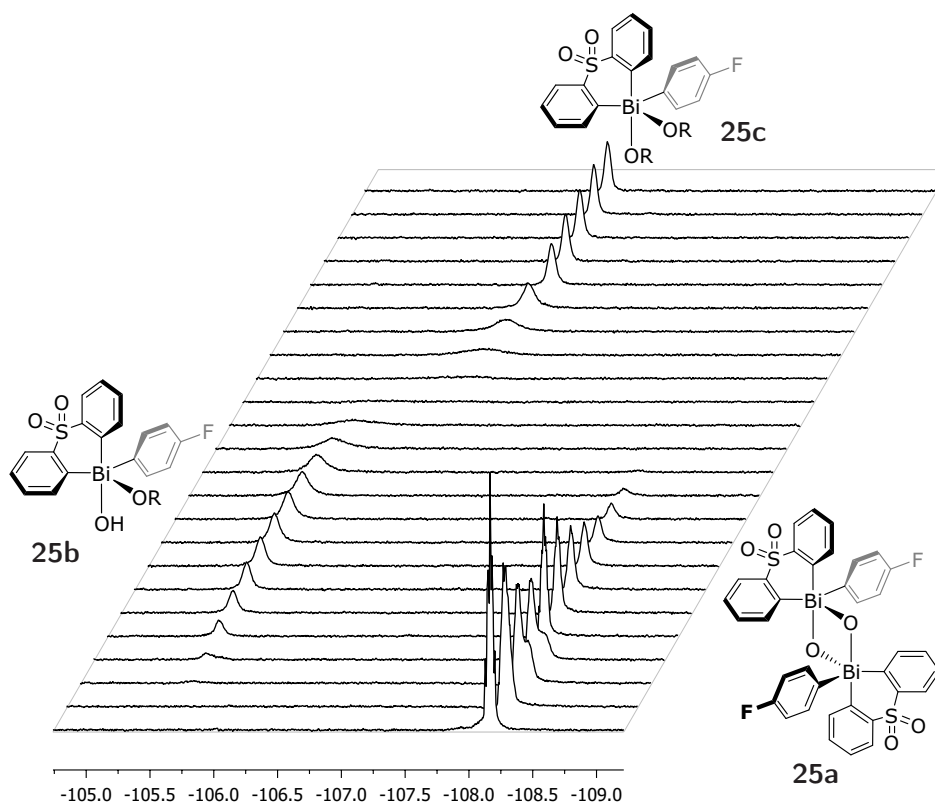


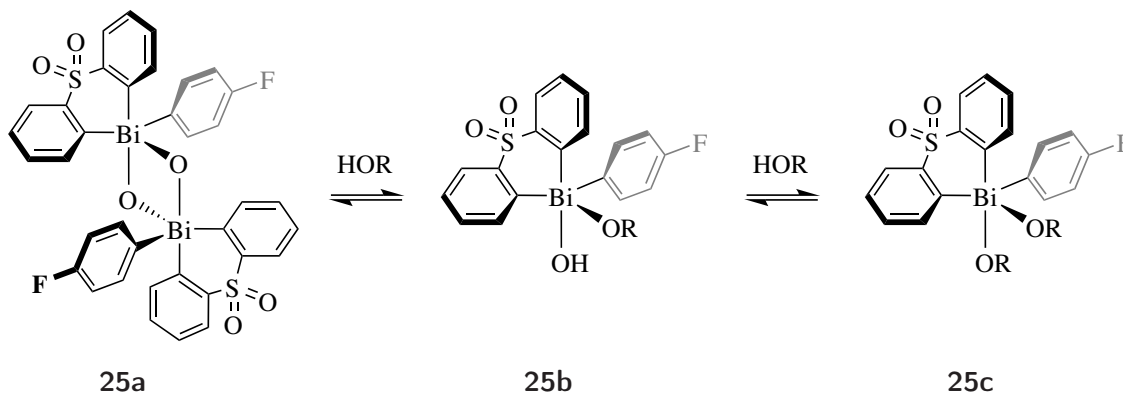
Figure 3.7.2: Stacked ^{19}F NMR spectra for the titration of **25a** with *m*CBA. Each spectrum represents the addition of 0.1 equivalents of *m*CBA, $[\mathbf{25a}]_0 = 9.2 \text{ mM}$ in CDCl_3

Upon step wise addition of another equivalent of *m*CBA, the newly established peak showed a distinct loss of intensity as well as increased peak broadening, resulting in complete disappearance of signal around 60% of the second equivalent. With further titration with *m*CBA, a new peak around -106.6 ppm could be observed with increasing intensity and sharpness, towards a full account of the mass balance. This indicates that a third species is present of type aryl thiabismine(V) dioxide (*m*CBA) $_2$ **25c**. The loss of signal in combination with the decreasing sharpness of the signal assumes another equilibrium between the mono- and disubstituted aryl thiabismine(V) dioxides.

The nature of the newly established peaks in the titration have been confirmed by oxi-

dation of **21f** with either purified *m*CPBA containing no residual acid, or an equimolar amount, resulting in the same peaks observed in the titration.

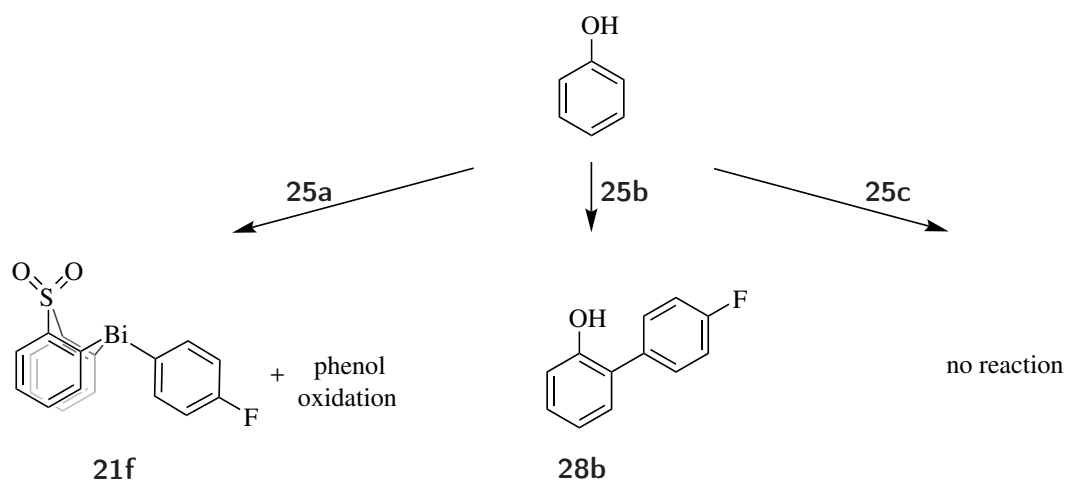
With the general possibility of all species existing in equilibrium (see Scheme 3.45), a closer consideration of the kinetically competent species had to be made.



Scheme 3.45: Different aryl thiabismine(V) dioxide species observed during the titration of **25a**, with OR = *m*CBA

In order to identify the kinetically competent species, each species has been prepared individually by titration and reacted with phenol.

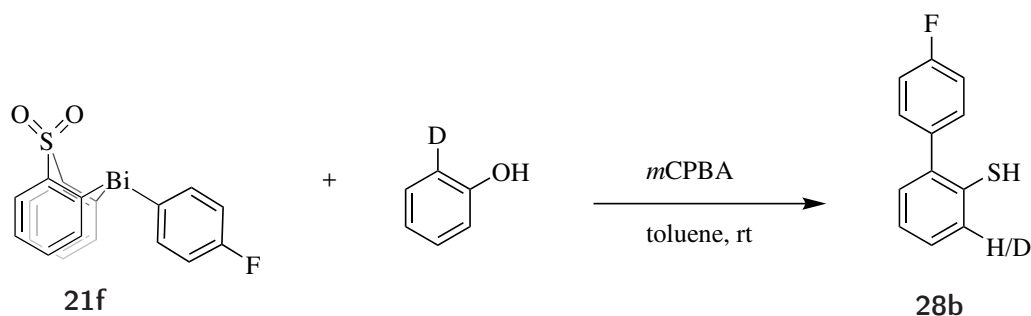
As depicted in Scheme 3.46, the reaction of **25a** with phenol resulted in the reduction back to **21f** with oxidative polymerisation of the phenol substrate. The use of **25b** in combination with phenol rapidly results in the desired arylation product. In contrast, while no reaction has been observed within 2 days when using **25c** as an arylation reagent. This concludes that **25b**, the aryl thiabismine(V) dioxide reagent carrying both an *m*CBA as well as a hydroxyl-group, is as the kinetically competent reagent for the arylation of hydroxyarenes.



Scheme 3.46: Testing the kinetic competency of different Bi(V) species

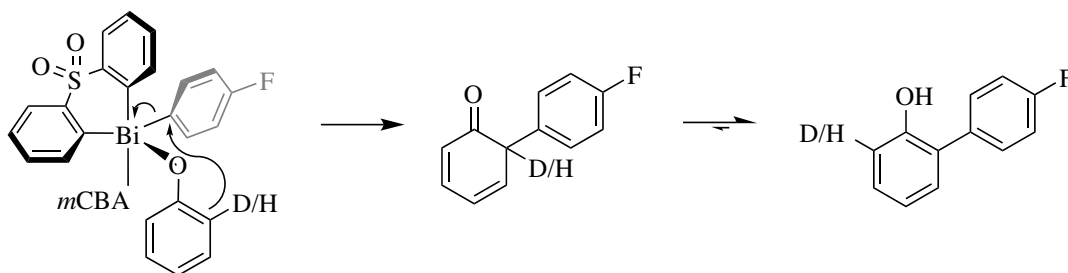
This observation acts in line with previous observations, where the Bi(III)–OH bond is

implicated in facilitating rapid transmetallation with boronic acids. In the arylation reaction, the previously rate limiting nucleophilic attack is probably replaced by a condensation mechanism that is significantly faster. Comparing studies using Ar_3Bi in combination with *m*CPBA and 2-naphthol reveal a significant increase in reactivity, supporting this thesis. With the kinetically competent species identified in **25b** a closer inspection into the arylation mechanism has been performed. For this a direct observation of the the individual rates using ^{19}F NMR spectroscopy was intended. Upon initial examination the reaction has been identified to finish in less than 1 min. Even reduction of the equivalents of phenol and the overall concentration the reagents could not slow down the reaction to a convenient observation time while still maintaining a reasonable signal-to-noise in the ^{19}F NMR spectrum. Therefore a direct observation of the arylation process could not be achieved. In order to still gain information about the arylation process a competitive approach has been chosen. In the first instance 2-deutero-phenol has been used to probe KIEs *via* an intramolecular competition (Scheme 3.47).



Scheme 3.47: Intramolecular competition between C–H and C–D in 2-deutero-phenol, [**21f**] = 62.0 mM, [2-deutero-phenol] = 314.0 mM, [*m*CPBA] = 94.8 mM in toluene

It was observed that the D/H-product ratio yielded $\text{Product}_H/\text{Product}_D = 1.21$, which corresponds to a KIE of $k_H/k_D = 0.83$. This secondary kinetic isotope effect is consistent with the conversion of an sp^2 carbon centre to a sp^3 hybridisation state. This is achieved during electrophilic attack of the aryl group on the bismuth centre on the bound phenol resulting in a [1,1'-biphenyl]-2(*H*)-one intermediate. The subsequent keto-enol-tautomerism results the aryl phenol reaction product (Scheme 3.48).

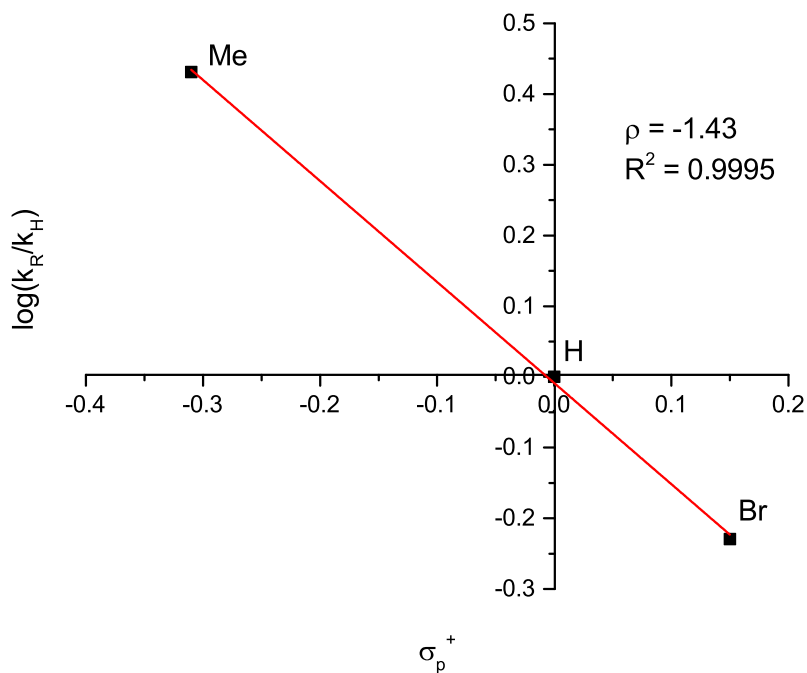
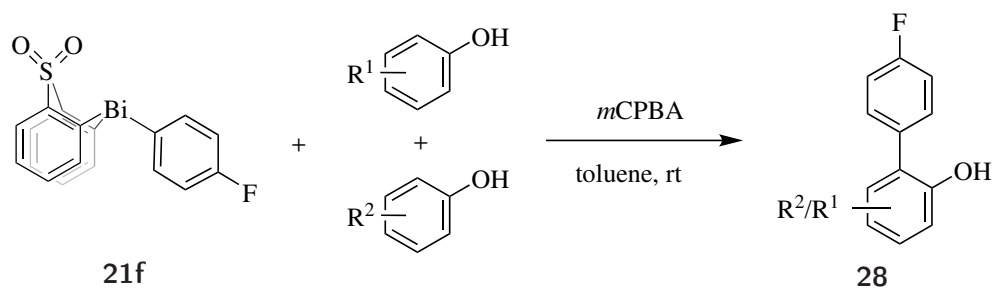


Scheme 3.48: Intramolecular competition between C–H and C–D in 2-deutero-phenol

Further insight was sought from an intermolecular competition of phenols. While mass spectrometry proved a sufficient tool for the differentiation and identification of the mono- and non-deuterated reaction product, a similar approach for the intermolecular competition between d_5 -phenol and d_0 -phenol and their respective products proved insufficient due to the significantly different ionisation potentials of both starting materials and products. Therefore, ^{19}F NMR spectroscopy has been used as an analytical tool. However, the chemical shifts of the deuterated and non-deuterated product are identical. Therefore a competition between 4-bromophenol and either the d_0 - or d_5 -phenol was used. The desired KIE (k_H/k_D) was then calculated from k_H/k_{Br} and k_D/k_{Br} .

No kinetic isotope effect could be observed under these conditions. Assuming no change in the nucleophilicity caused by isotopic effects, it can be assumed that the overall selectivity is determined by the formation of the Bi(V)-OAr species with a subsequent - much faster - oxidative arylation.

As previously mentioned, an electronic dependency was observed. Within this study a brief investigation has been conducted. Here, a Hammett-type plot of relative rate of arylation of electronically different phenols correlates well against the σ^+ -values of their substituents (See Scheme 3.49). While more thorough investigations have to be conducted, excellent first insight into the selectivity determining step of intermolecular competition has been achieved.



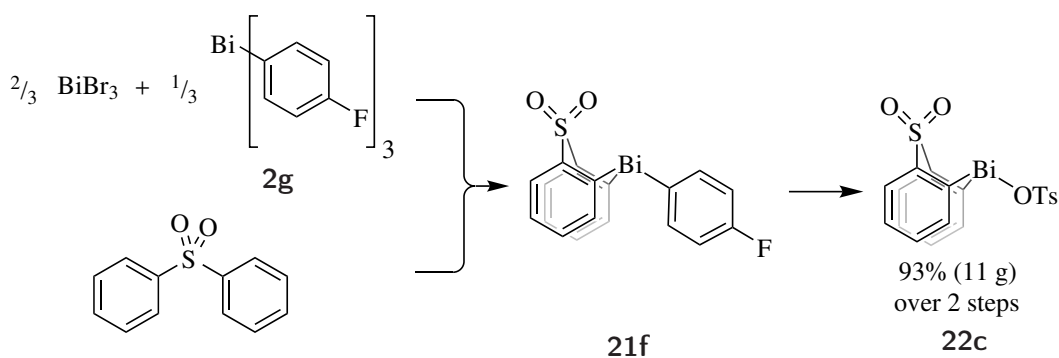
Scheme 3.49: Intermolecular competition of phenols in the arylation reaction, determining the selectivity determining step of the arylation of phenols using an *in situ*-generated aryl thiabismine(V) dioxide reagent

3.8 Large Scale Access to Thiabismine Dioxide Tosylate Precursor

The development of a functioning mechanism does not grant widespread uptake of methodology by the scientific community. Easy access to the starting materials, convenient reaction times and conditions, as well as atom economy have to be addressed. In order to accomplish this an efficient method to access the precursor **22c** needed to be developed. Exploiting different reaction conditions from previous studies a potent telescoping method has been employed.

While the generation of the aryl thiabismine dioxide intermediate **21f** has already been achieved in excellent yields, previously a purification had to be performed prior to the synthesis thiabismine dioxide (*pseudo*)halide species **22**. Through the use of Et₂O as a

reaction solvent a telescoped protocol has been achieved, allowing the synthesis of **22c**, without the use of column chromatography for purification.



Scheme 3.50: Large scale telescoped protocol for the synthesis of **22c** without the use of column chromatography

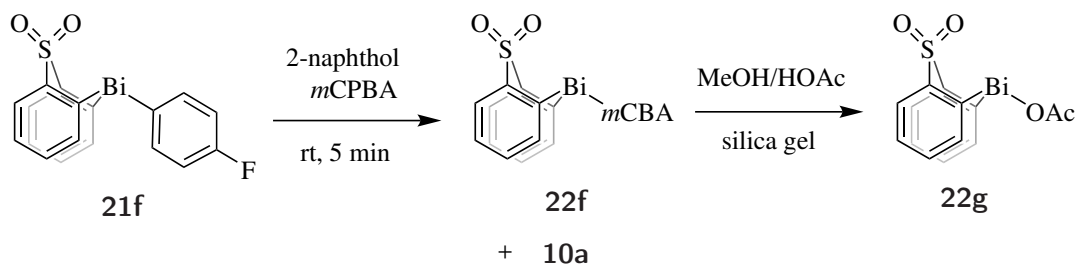
The specific use of Et_2O as a solvent and tosic acid as the protodebismuthation reagent for the second part of the synthesis proved positive as all reagents are soluble, while the reaction product **22c** is insoluble. With reaction progression the product precipitates and can be isolated *via* simple filtration.

This protocol allows for a large scale access of the precursor with excellent yields (93% on an 11 g scale) from commercially available starting materials. In order to further increase accessibility we commercialised **22c** through Key Organics under cat. No. NS-00138, making the developed methodology easily applicable on a lab scale.

3.9 Recovery and Recycling of Thiabismine Dioxide Co-product

Having developed a convenient and scalable route to thiabismine dioxide **22c**, we sought to address atom economy of the reaction, to facilitate a widespread adoption of the methodology. Specifically, a closer look at the thiabismine dioxide co-product of the arylation reaction has to be provided.

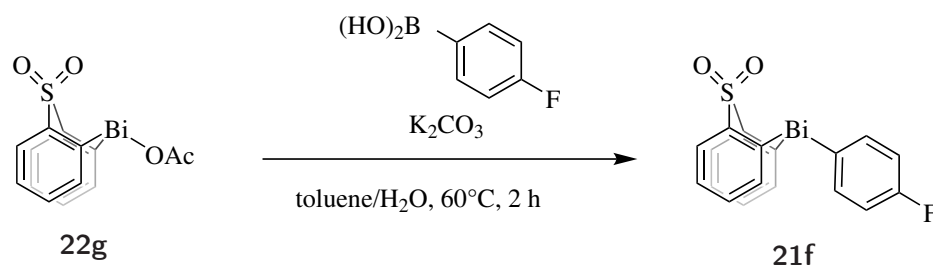
The resulting thiabismine dioxide co-product of phenol arylation was identified as thiabismine dioxide 3-chlorobenzoate **22f**. However, during standard purification procedure using column chromatography on silica gel no bismuth containing material was recovered, rendering **22f** incompatible with standard column chromatography conditions. This was expected given the previously observed affinity towards condensation with various hydroxyl-groups. Using an eluent mixture consisting of MeOH/HOAc (98/2), however afforded in thiabismine dioxide acetate **22g** as the sole product in almost quantitative yield.



Scheme 3.51: Post arylation recovery of the thiabismine dioxide co-product as the thiabismine dioxide acetate **22g**

The obtained **22g** was exposed to the previously established transmetallation conditions to verify its ability for recycling. Here, a full transmetallation has been observed resulting in **21f**.

This demonstrated that the thiabismine dioxide backbone is easily recoverable, rendering it viable for a large scale application with simple recovery and reuse of the bismacyclic reagent.



Scheme 3.52: Transmetallation of the recovered **22g**

3.10 Conclusion

Formal combination of two of the aryl rings of the previously used Ar_3Bi species affords the class of bismacycles, whose properties are determined largely by the nature of the tether. The bismacyclic backbone therefore allows the reactivity and stability of the aryl bismacycle to be controlled. Aryl bismoles, azabismocines and thiabismine dioxides have been prepared in order to investigate their capability to perform the individual reactions necessary (transmetallation, oxidation, arylation) to create a step-wise protocol for the arylation of hydroxyarenes.

While bismoles showed good results in oxidation and arylation, the necessary, stable bismole (*pseudo*)halide species could not be obtained. The instability of this crucial precursor rendered bismole reagents unsuitable for the proposed methodology.

Azabismocine reagents showed general compatibility towards transmetallation, oxidation and arylation but the involvement of the lone pair on the nitrogen of the amine backbone rendered the rates of transmetallation and arylation impractical.

The thiabismine dioxide scaffold showed great activity towards all individual transforma-

tions, prompting an in-depth investigation that led to a one-pot protocol for the arylation of hydroxyarenes. The individual segments of this approach were investigated separately to gain understanding of its mechanism and limitations.

A variety of thiabismine dioxide (*pseudo*)halides were prepared through a protodebismuthation of aryl thiabismine dioxides, from which thiabismine dioxide tosylate **22c** has been identified as an ideal precursor, as it offered excellent transmetallation capabilities and could be prepared easily and on scale through a two-step protocol that did not require column chromatography.

The developed transmetallation protocol proved reliable and proficient in B-to-Bi aryl transfer for a wide range of electronically and sterically substituted aryl groups. Mechanistic investigation identified the exchange of the tosyl group on **22c** with OH⁻ as the rate determining step of this transformation. The equilibrium between the OH-substituted monomer and the dimeric condensation product was observed to allow, in most cases, rapid transmetallation using boronic acids.

Most of the resulting aryl thiabismine dioxides proved stable to moisture, light and air as well as column chromatography. While a variety of aryl thiabismine dioxides were isolated, the proposed one-pot protocol rendered isolation unnecessary.

A scope of oxidants, involving halogenating reagents and peroxides, were tested to perform the oxidation to the active Bi(V). *m*CPBA was identified as a suitable oxidant to perform oxidation, as well as enabling arylation in the absence of base.

Mechanistic investigations identified the oxidation of the bismuth reagent as the rate determining transformation with the arylation proceeding significantly faster. Intermolecular KIE studies gave insight into the selectivity determining creation of the Bi-O-Ar species. A secondary KIE has been observed for intramolecular competitions. The insight gained in these investigations has offered unprecedented insight into the (so far) only proposed mechanisms reported by Barton *et al.*, allowing for an *a priori* prediction of untested substrate combinations and conditions in the future.

The scope of the developed one-pot protocol proved to be extensive. Electron-poor to electron-rich aryl and heteroaryl groups have been transferred onto 2-naphthol in good to excellent yields, with the exception of very electron-rich heterocycles, that suffer from sensitivity and instability of the bismacycle. Sterically-demanding groups were transferred in good yields as well. Substituted naphthols, phenols with an extended π -system, showed excellent yields and regioselectivities. Phenols showed good yields, although a higher relative amount of phenols was required to avoid the ever present issue of overarylation.

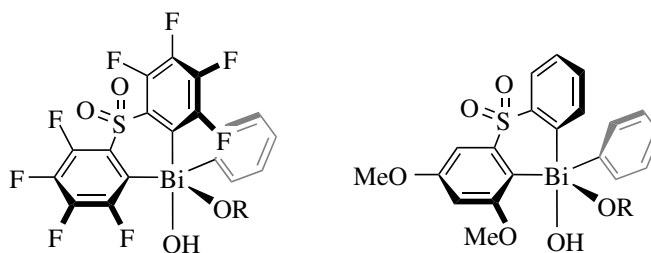
Overall a modular, highly efficient and easy to follow one-pot protocol was developed for the bismuth-mediated arylation of hydroxyarenes, with an easy access through a commercialised, bench-stable precursor.

4 | Future Projects

The work presented in Chapter 3 has shown good results, but contains even greater potential for future investigations. These can be classified into three segments. First the improvement of the properties of the bismuth reagent to increase reactivity, stability and regioselectivity, and introduce enantioselectivity. Second the extension of the substrate scope of this methodology. And third the elevation of this so far stoichiometric protocol to a catalytic application.

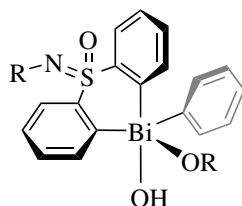
4.1 Tuning the Backbone

While the thiabismine dioxide backbone showed great activity, several drawbacks in stability, reactivity and selectivity have been observed. The presence of the "fixed" backbone on the bismuth centre allows for the tuning of the backbone depending on the specific needs. The so far unsubstituted aromatic ring of the thiabismine dioxide backbone can be functionalised changing electronic and steric properties of the bismuth reagent (Scheme 4.1). Substitution with electron-withdrawing groups increases the electrophilicity of the bismuth centre, hence increasing the rate of formation of the Bi-OAr species, as well as the product forming reductive elimination. The substitution of cumbersome groups at the *ortho*-position to bismuth centre could further increase reductive elimination to relief steric congestion, while also influencing the formation of the Bi-OAr species. The substitution with different sterically demanding groups can allow for a better discrimination between different C_{ortho} positions on a hydroxyarene, increasing regioselectivity and may also promote an enantioselective arylation for prochiral substrates (see 4.2).



Scheme 4.1: Examples of potential aryl thiabismine(V) reagents; Left: electron withdrawing substituents for electronic effects, right: methoxy-groups in a single ring of the backbone for steric effects

Another method to introduce chiral information is the substitution of the sulfone group of the backbone for a sulfoximine motif. This structural motif can be prepared enantioselectively,²²¹ allowing for a transfer of chiral information onto the substrate. Hereby, the increased steric bulk of the imine motif could influence orientation of the backbone in the bismacyle(V) reagent, preventing a change in conformation allowing discrimination of positions of the different groups on the bismuth(V) centre. Equally, the R group attached to the amine can incorporate a chiral motif enabling enantioselective synthesis.

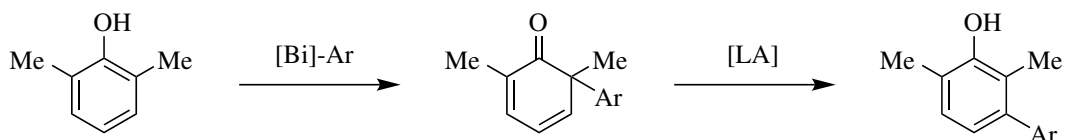


Scheme 4.2: Example of a potential aryl thiabisimine with the sulfone exchanged for a chiral sulfoximines

4.2 Extension Scope

The current protocol has been applied to numerous phenolic substrates. Preliminary results show that di-*ortho*-substituted substrates undergo dearomatising arylation to result in [1,1'-biphenyl]-2(1*H*)-ones (Scheme 4.3). These reagents can be synthetically interesting, highly functionalised starting materials for drug development, especially when produced enantioselectively.

Upon addition of a Lewis acid to these dearomatised compounds, re-aromatisation with aryl migration to the *meta*-position has been observed. While *meta* arylation of phenols have been reported before,^{8,222-224} they often require complicated directing groups or atom inefficient procedures. The proposed protocol offers easy access to *meta*-arylated hydroxyarenes.

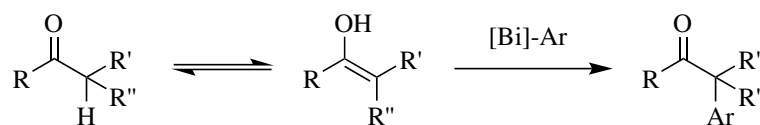


Scheme 4.3: *Meta* arylation of di-*ortho* substituted phenols; with [Bi]-Ar = aryl thiabisimine(V) reagent, LA = Lewis acid

The hidden enol motif of phenols could also be exploited in a non-aromatic surrounding. Classically, aliphatic ketones have been investigated for bismuth-mediated oxidative arylation due to the enol form they tautomerise with.^{76,125}

The developed methodology can be applied to this class of substrates. Arylated cyclic ketones show a tendency to undergo rapid enolisation, allowing for an interchange of configuration in the *per se* chiral carbon centre. For ketones that do not undergo keto-enol-

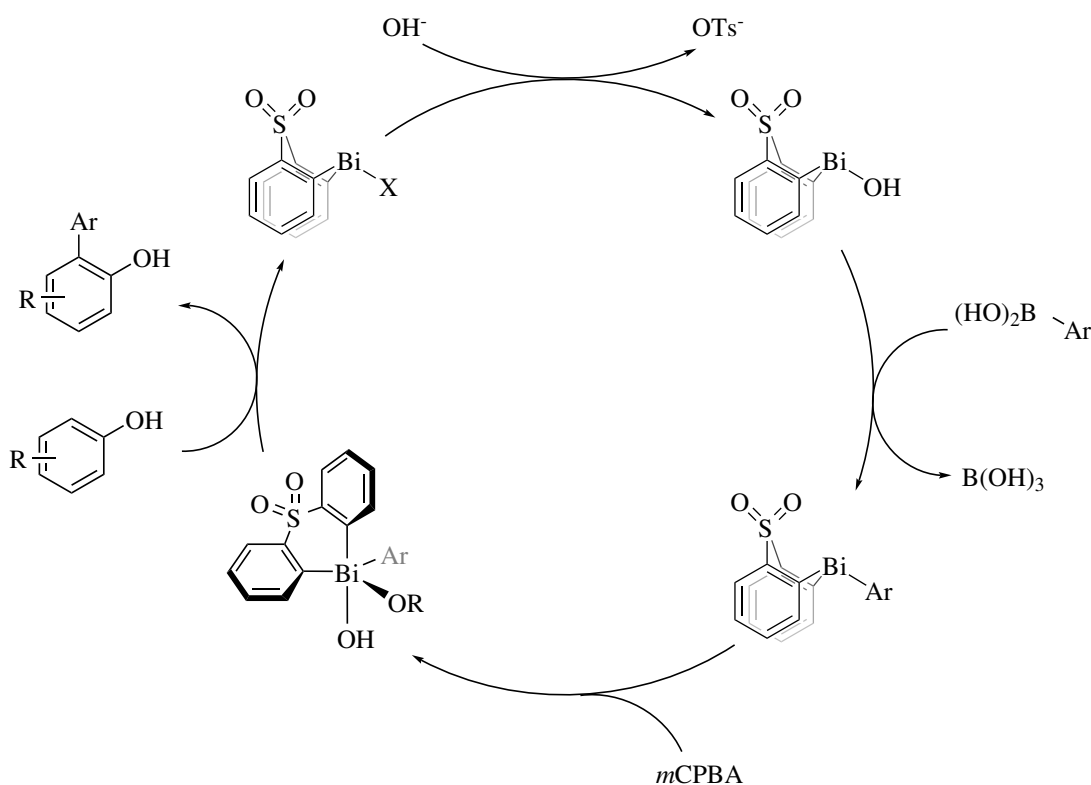
tautomerism quickly an enantiospecific arylation could be attempted using enantioselective bismuth reagents as proposed above.



Scheme 4.4: α -Arylation of ketones; with [Bi]-Ar = aryl thiabismine(V) reagent

4.3 Elevation to a Catalytic Regime

The developed protocol showed good results in a stoichiometric regime. In combination with the excellent recovery and recyclability of the bismuth reagent, one could consider this protocol a stepwise catalytic use of the bismuth reagent through recycling (Scheme 4.5).



Scheme 4.5: "Catalytic" cycle of bismuth-mediated arylation of hydroxyarenes using a thiabismine dioxide reagent

Currently the incompatibility of boronic acid and *m*CPBA prohibits a catalytic application of the developed protocol in a single pot with all reagents present at the same time. Solving the inherent incompatibility of oxidant and transmetalation reagent (chapter 2.8), would allow a catalytic use of the bismuth reagent making this protocol more time- and atom efficient, thus more economic and would massively increase the impact and application of this unique reactivity.

Declaration of Academic Honesty

I hereby confirm that the present thesis on „Bismuth-mediated Oxidative Arylation“ is solely my own work and that if any text passages or diagrams from books, papers, the Web or other sources have been copied or in any other way used, all references have been acknowledged and fully cited.



Mark Jurrat, August 18, 2019

Experimental

General Methods and Materials

Procedures employing oxygen- and/or moisture-sensitive materials were performed with anhydrous solvents (*vide infra*) using standard inert-atmosphere techniques (atmosphere of anhydrous dinitrogen). Analytical thin-layer chromatography was performed on precoated aluminium-backed plates (Silica Gel 60 F254; Merck), and visualized using a combination of UV light (254 and 366 nm) and acidic ethanolic vanillin, aqueous basic potassium permanganate or iodine stains. Preparative TLC was performed on precoated aluminium-backed analytical plates (Silica Gel 60 F254; Merck) or precoated glass-backed preparative plates (Silica Gel 15 F254; Analtech). Column chromatography was performed using Scharlab 60 silica gel (35-70 mesh).

NMR spectra were recorded at 25 °C on a Bruker DPX 300, Bruker DPX 400, Bruker AV400, Bruker AV(III)400, Bruker AV(III)400HD, Bruker AV500 spectrometer (^1H , 500 / 400 / 300 MHz; ^{11}B , 160 / 128 MHz, $^{13}\text{C}\{^1\text{H}\}$, 123 / 101 / 75.4 MHz; ^{19}F NMR, 471 / 376 MHz). Chemical shifts are reported in ppm; coupling constants, J , are reported in Hz and are uncorrected for digitization. The following abbreviations (and their combinations) are used to label the multiplicities: s (singlet), d (doublet), t (triplet), q (quartet), quint (quintet), sept (septet), m (multiplet) and br (broad). ^1H and $^{13}\text{C}\{^1\text{H}\}$ chemical shifts are reported relative to tetramethylsilane, and are referenced to the appropriate residual solvent peaks:

- CDCl_3 : $\delta_{\text{H}} = 7.26$ ppm, $\delta_{\text{C}} = 77.16$ ppm
- $\text{DMSO}-d_6$: $\delta_{\text{H}} = 2.50$ ppm, $\delta_{\text{C}} = 39.52$ ppm
- CD_3OD : $\delta_{\text{H}} = 3.31$ ppm, $\delta_{\text{C}} = 49.00$ ppm

^{11}B and ^{19}F chemical shifts are reported relative to a $\text{BF}_3 \cdot \text{Et}_2\text{O}$.

Infrared spectra of neat compounds were recorded over the range 4000-600 cm^{-1} using either a PerkinElmerSpectrum 1000 Series FTIR spectrometer with an ATR diamond cell, or a Bruker Alpha FTIR spectrometer fitted with a Bruker Platinum ATR QuicksnapTM diamond cell. Melting points were measured using Stuart SMP3 or Gallenkamp melting point apparatus in open capillaries.

Vis/UV-Vis light has been generated by a mercury vapor lamp. UV exclusion has been achieved *via* a below 350 nm filter. High resolution electrospray ionization mass spectra (HRMS) were recorded using a Micromass LCT Premier XE instrument (Waters). MALDI MS was measured using Bruker Ultraflex III.

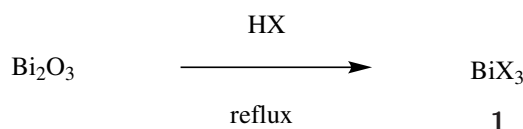
X-ray measurements were made on crystals coated in vacuum grease and mounted on a glass needle using $\text{Mo-K}\alpha$ ($\lambda = 0.71073 \text{ \AA}$) or $\text{Cu-K}\alpha$ ($\lambda = 1.54184 \text{ \AA}$) radiation on SuperNova Atlas or XtaLAB PRO MM007 PILATUS3 R 200K diffractometers at 120(2) K. Structures were solved with Olex2 software, and refined with ShelXL software using Least Squares minimisation.

Reagent grade solvents (Fisher Technical) were employed. Hexane, CH_2Cl_2 , Et_2O , MeCN

and THF were dried using an Inert PureSolv Grubbs-type system (alumina columns, argon atmosphere). Unless stated otherwise, all reagents were obtained from commercial sources and were used as received.

DFT calculations were performed using Gaussian09 and a LANL2DZdp ECP basis set.

Synthesis of Inorganic Bismuth(III) Salts



Bismuth(III) chloride **1a**

Bismuth oxide (20.0 g, 42.9 mmol) was suspended in water (10 mL). To the suspension 4 mL of conc. HCl (11.65 M, 46.6 mmol) were added until the precipitate was fully dissolved. The reaction mixture was then evaporated *in vacuo* at 100 °C to give **1a** as a colourless solid (26.9 g, 99%). mp/°C: 225-227. HRMS calcd. for BiCl_2^+ : 278.9186 [M-Cl]⁺; found (ESI⁺): 278.9168.

Bismuth(III) acetate **1b**

Bismuth oxide (5.00 g, 10.7 mmol) was added to a mixture of acetic acid (40.0 mL, 34.9 mmol) and acetic anhydride (20 mL, 18.1 mmol). The suspension was stirred under reflux until the precipitate was fully dissolved. The solution was allowed to cool, resulting in fine colourless crystals. The solvent was filtered off and the crystals washed with Et₂O. Yield: 7.93 g, 96%. mp/°C: 238-240 (dec.). MS calcd. for $\text{C}_4\text{H}_6\text{BiO}_4$: 327.01 [M-OAc]⁺; found (MALDI⁺): 327.01.

Bismuth(III) tosylate **1c**

Bismuth oxide (5.00 g, 10.7 mmol) was suspended in toluene (100 mL). To the suspension HOTs · H₂O (14.3 g, 75.1 mmol) was added and the reaction mixture stirred under Dean-Stark conditions for 4 h resulting in a heavy white suspension. The precipitate was filtered off resulting in the desired product **1c** as a colourless solid (15.3 g, 99%). mp/°C: >250. ¹H NMR (400 MHz, DMSO-d₆) δ_H 7.5 – 7.4 (m, 2H), 7.1 (d, *J* = 7.9 Hz, 2H), 2.3 (s, 3H). ¹³C{¹H} NMR (126 MHz, DMSO-d₆) δ_C 145.6, 137.8, 128.1, 125.5, 20.8. IR (ATR): $\tilde{\nu}$ = 1597, 1496, 1384, 1187, 1096, 1029, 996, 814, 669, 564, 531 cm⁻¹. HRMS calcd. for $\text{C}_{14}\text{H}_{14}\text{BiO}_6\text{S}_2^-$: 551.0041 [M-OTs]⁺; found (ESI⁺): 551.0041. Colourless crystals. Yield: 15.3 g, 99%.

Bismuth(III) bromide **1d**¹

Bismuth oxide (10.0 g, 21.46 mmol) was added to a stirring solution of hydrobromic acid (100 mL, 48 w/w) at 70 °C until the solids were no longer dissolving. A small quantity of hydrobromic acid was added to dissolve the remaining bismuth oxide. The solution was allowed to cool and hydrogen bromide was distilled off to give **1d** as a yellow solid (9.05 g, 94%); mp/°C: 208–210.

¹This work has been performed by Ellen Nichols under my supervision

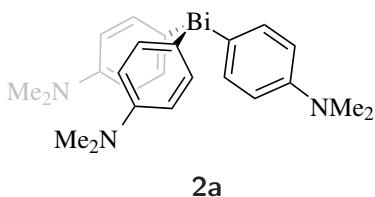
Bismuth(III) trifluoroacetate **1e** ^{II}

Bismuth oxide (504 mg, 1.08 mmol) was suspended in TFA (7.5 mL) and TFAA (1.50 mL, 10.7 mmol) and stirred at room temperature for 2 days. The reaction mixture was then evaporated *in vacuo* to give **1e** as a colourless solid in quantitative yield. mp/°C: >300. Elemental analysis: Found: C, 13.2; H, 0.2; N, 0% Bi(O₂CCF₃)₃ required C, 13.1; H, 0; N, 0%. IR (ATR): $\tilde{\nu}$ = 1620, 1436, 1143, 852, 793, 505. HRMS calcd. for C₄BiF₆O₄⁺: 434.9505 [M-OTf]⁺; found (ESI⁺): 434.96.

Synthesis of Organobismuth(III) Compounds

Protocol A: 4-Bromo-N,N-dimethylaniline (6.2 g, 31 mmol) was dissolved in THF (20 mL) and cooled down in an acetone/dry ice bath. n-BuLi (1.2 mL, 32 mmol, 2.5 M in THF) was added to the solution drop wise over the course of 5 min, resulting in a yellow solution. After 1h a solution of Bi(neo)₃ (10 mmol) in dry THF (10 mL) was slowly added. The resulting solution was allowed to stir for 1h, warmed up to room temperature and then quenched with water. Et₂O was added to the solution and combined phases are filtered and the organic phase separated. The organic phase was washed with water, dried with MgSO₄, filtered and the solvent removed *in vacuo* resulting in desired product (colourless crystals).

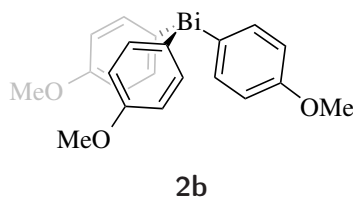
Tri(4-N,N-dimethylaniline) bismuth **2a**



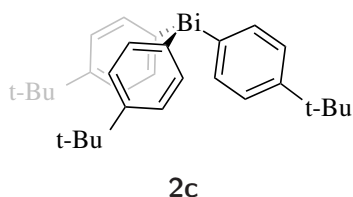
mp/°C: 177-180. ¹H NMR (400 MHz, CDCl₃) δ_H 7.64 – 7.47 (m, 6H), 6.85 – 6.61 (m, 6H), 2.92 (s, 18H). ¹³C{¹H} NMR (126 MHz, CDCl₃) δ_C 150.1, 140.2, 138.6, 114.9, 40.5. IR (ATR): $\tilde{\nu}$ = 2789, 1579, 1493, 1343, 1195, 1165, 1060, 943, 796, 516 cm⁻¹. HRMS calcd. for C₁₆H₂₀BiN₂⁺: 449.1430 [M-C₈H₁₀N]⁺; found (ESI⁺): 449.1435. Colourless crystals. Yield: 4.10 g, 72%. In accordance with literature values.²²⁵

Protocol B: Magnesium (888 mg, 37.0 mmol) was added into a three neck flask with a few crystals of iodine and heated gently. Dry THF (20 mL) was added followed by the dropwise addition of X-1-bromobenzene (31 mmol) (X = 4-OMe, 4-^tBu, 4-Me, 2-Me, H, 4-F, 3-OMe, 4-Cl, 4-CF₃). The resulting Grignard reagent was being transferred to a solution of Bi(neo)₃(10 mmol) in 10 mL dry THF. The reaction mixture was to stirred for 1 h and subsequently quenched with water. Et₂O was added to the solution and the combined phases were filtered through filter paper and the organic phase was separated. The organic phase was washed with water and concentrated *in vacuo*. The resulting product was recrystallised from ethanol.

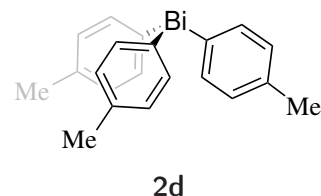
^{II}This work has been performed by Jamie Cadge under my supervision

Tri(4-methoxyphenyl)bismuth 2b

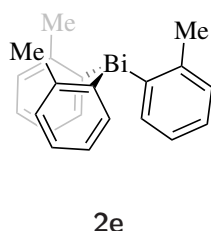
mp/°C: 195-196. $^1\text{H NMR}$ (400 MHz, CDCl_3) δ_{H} 7.64 – 7.52 (m, 6H), 6.95 – 6.87 (m, 6H), 3.79 (s, 9H). $^{13}\text{C}\{^1\text{H}\}$ NMR (101 MHz, CDCl_3) δ_{C} 159.3, 145.1, 138.7, 116.3, 55.0. IR (ATR): $\tilde{\nu}$ = 1698, 1573, 1484, 1435, 1276, 1231, 1174, 1054, 1038, 1023, 815, 783, 576, 516, 466 cm^{-1} . HRMS calcd. for $\text{C}_{14}\text{H}_{14}\text{BiO}_2^+$: 423.0798 $[\text{M}-\text{C}_7\text{H}_7\text{O}]^+$; found (ESI $^+$): 423.0787. Colourless crystals. Yield: 4.03 g, 76%. In accordance with literature values.²²⁶

Tri(4-(*tert*-butyl)phenyl)bismuth 2c

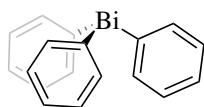
mp/°C 137-139. $^1\text{H NMR}$ (400 MHz, CDCl_3) δ_{H} 7.75 – 7.64 (m, 6H), 7.50 – 7.39 (m, 6H), 1.33 (d, J = 0.6 Hz, 27H). $^{13}\text{C}\{^1\text{H}\}$ NMR (101 MHz, CDCl_3) δ_{C} 157.5, 153.9, 133.6, 128.3, 35.1, 31.3. IR (ATR): $\tilde{\nu}$ = 1483, 1393, 1114, 1052, 1003, 815, 756, 723, 547, 429 cm^{-1} . HRMS calcd. for $\text{C}_{20}\text{H}_{26}\text{Bi}^+$: 475.1838 $[\text{M}-\text{C}_{10}\text{H}_{13}]^+$; found (ESI $^+$): 475.1834. Colourless crystals. Yield: 4.26 g, 70%.

Tri(*p*-tolyl)bismuth 2d

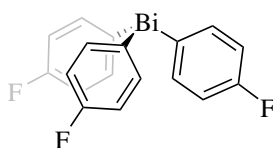
mp/°C: 118-120. $^1\text{H NMR}$ (400 MHz, CDCl_3) δ_{H} 7.63 (dd, J = 7.8, 2.4 Hz, 6H), 7.19 (dd, J = 7.8, 2.2 Hz, 6H), 2.32 (d, J = 2.3 Hz, 9H). $^{13}\text{C}\{^1\text{H}\}$ NMR (101 MHz, CDCl_3) δ_{C} 151.5, 137.6, 137.4, 131.4, 21.6. IR (ATR): $\tilde{\nu}$ = 1574, 1485, 1275, 1172, 1023, 814, 576, 515 cm^{-1} . HRMS calcd. for $\text{C}_{14}\text{H}_{14}\text{Bi}^+$: 391.0899 $[\text{M}-\text{C}_7\text{H}_7]^+$; found (ESI $^+$): 391.0884. Colourless crystals. Yield: 3.42 g, 71%. In accordance with literature values.²²⁵

Tri(*o*-tolyl)bismuth 2e

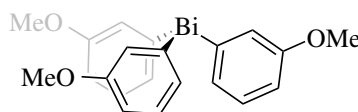
mp/°C: 129-131. $^1\text{H NMR}$ (400 MHz, CDCl_3) δ_{H} 7.55 (dd, J = 7.4, 1.4 Hz, 3H), 7.37 – 7.33 (m, 3H), 7.29 (dd, J = 7.4, 1.4 Hz, 3H), 7.07 (ddd, J = 7.4, 1.5, 0.7 Hz, 3H), 2.44 (s, 9H). $^{13}\text{C}\{^1\text{H}\}$ NMR (101 MHz, CDCl_3) δ_{C} 154.5, 143.8, 138.8, 130.0, 128.8, 128.3, 26.5. IR (ATR): $\tilde{\nu}$ = 1576, 1443, 1265, 1199, 1155, 1112, 1014, 791, 746, 733, 535, 487, 431 cm^{-1} . HRMS calcd. for $\text{C}_{14}\text{H}_{14}\text{BiO}_2^+$: 391.0899 $[\text{M}-\text{C}_7\text{H}_7\text{O}]^+$; found (ESI $^+$): 391.0884. Colourless crystals. Yield: 4.05 g, 84%. In accordance with literature values.²²⁷

Triphenylbismuth 2f**2f**

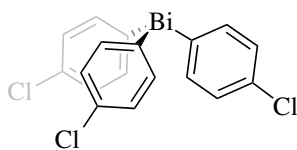
mp/°C: 78-80. $^1\text{H NMR}$ (400 MHz, CDCl_3) δ_{H} 7.77 – 7.72 (m, 6H), 7.42 – 7.35 (m, 6H), 7.35 – 7.28 (m, 3H). $^{13}\text{C}\{^1\text{H}\}$ NMR (101 MHz, CDCl_3) δ_{C} 155.4, 137.7, 130.6, 127.9. IR (ATR): $\tilde{\nu}$ = 1681, 1556, 1469, 1375, 1260, 1180, 1083, 1042, 1003, 833, 800, 712, 476 cm^{-1} . HRMS calcd. for $\text{C}_{12}\text{H}_{10}\text{Bi}^+$: 363.0586 $[\text{M}-\text{C}_6\text{H}_5]^+$; found (ESI $^+$): 363.0579. Colourless crystals. Yield: 4.27 g, 97%. In accordance with literature values.²²⁶

Tri(4-fluorophenyl)bismuth 2g**2g**

mp/°C: 88-90. $^1\text{H NMR}$ (400 MHz, CDCl_3) δ_{H} 7.68 – 7.60 (m, 6H), 7.08 (dd, J = 9.4, 8.5 Hz, 6H). $^{13}\text{C}\{^1\text{H}\}$ NMR (101 MHz, CDCl_3) δ_{C} 162.9 (d, J = 247.5 Hz), 149.6, 139.3 (d, J = 7.1 Hz), 118.1 (d, J = 19.8 Hz). $^{19}\text{F NMR}$ (377 MHz, CDCl_3) δ_{F} -112.76 (tt, J = 9.3, 6.1 Hz). IR (ATR): $\tilde{\nu}$ = 1560, 1480, 1250, 1200, 780, 500 cm^{-1} . HRMS calcd. for $\text{C}_{12}\text{H}_8\text{BiF}_2^+$: 399.0398 $[\text{M}-\text{C}_6\text{H}_4\text{F}]^+$; found (ESI $^+$): 399.0398. Colourless crystals. Yield: 3.95 g, 80%. In accordance with literature values.²²⁷

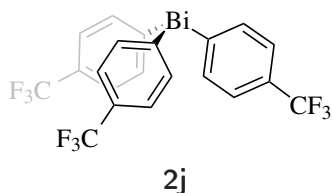
Tri(3-methoxyphenyl)bismuth 2h**2h**

mp/°C: 191-193. $^1\text{H NMR}$ (400 MHz, CDCl_3) δ_{H} 7.38 – 7.29 (m, 9H), 6.84 (ddd, J = 7.0, 2.5, 2.4 Hz, 3H), 3.72 (s, 9H). $^{13}\text{C}\{^1\text{H}\}$ NMR (101 MHz, CDCl_3) δ_{C} 161.6, 156.6, 131.4, 129.8, 123.0, 113.6, 55.2. IR (ATR): $\tilde{\nu}$ = 1560, 1480, 1250, 1200, 780, 500 cm^{-1} . HRMS calcd. for $\text{C}_{14}\text{H}_{14}\text{BiO}_2^+$: 423.0798 $[\text{M}-\text{C}_7\text{H}_7\text{O}]^+$; found (ESI $^+$): 423.0792. Colourless crystals. Yield: 4.56 g, 86%. In accordance with literature values.²²⁸

Tri(4-chlorophenyl)bismuth 2i**2i**

mp/°C: 114-115. $^1\text{H NMR}$ (400 MHz, CDCl_3) δ_{H} 7.64 – 7.57 (m, 6H), 7.37 – 7.33 (m, 6H). $^{13}\text{C}\{^1\text{H}\}$ NMR (101 MHz, CDCl_3) δ_{C} 152.9, 138.9, 134.6, 131.0. IR (ATR): $\tilde{\nu}$ = 3049, 1576, 1443, 1199, 1112, 1014, 791, 746, 734, 535, 432 cm^{-1} . HRMS calcd. for $\text{C}_{12}\text{H}_8\text{BiCl}_2^+$: 430.9807 $[\text{M}-\text{C}_6\text{H}_4\text{Cl}]^+$; found (ESI $^+$): 430.9808. Colourless crystals. Yield: 5.38 g, 99%. In accordance with literature values.⁹⁶

Tris(4-(trifluoromethyl)phenyl)bismuth **2j**



mp/°C: 145-146. $^1\text{H NMR}$ (400 MHz, CDCl_3) δ_{H} 7.84 (d, $J = 8.3$ Hz, 6H), 7.65 (d, $J = 7.8$ Hz, 6H). $^{13}\text{C}\{^1\text{H}\}$ NMR (101 MHz, CDCl_3) δ_{C} 160.0, 137.9, 130.6 (q, $J = 32.4$ Hz), 127.47 (q, $J = 3.7$ Hz), 124.26 (q, $J = 272.4$ Hz). $^{19}\text{F NMR}$ (377 MHz, CDCl_3) δ_{F} -62.88. IR (ATR): $\tilde{\nu} = 1681, 1556, 1469, 1375, 1260, 1180, 1083, 1042, 1003, 833, 800, 712, 476\text{ cm}^{-1}$. HRMS calcd. for $\text{C}_{14}\text{H}_8\text{BiF}_6^+$: 499.0334 [$\text{M}-\text{C}_7\text{H}_4\text{F}_3$] $^+$; found (ESI $^+$): 499.0335. Orange crystals. Yield: 6.12 g, 95%. In accordance with literature values.⁹⁶

Cyclic voltammetric investigation of Bi(III) compounds

General Protocol: A blank solution of NBu_4PF_6 (100 mM) in dry MeCN was prepared. The electrodes (platinum disc working electrode, a platinum counter electrode and a silver wire *pseudo*-reference electrode) were added and the solution degassed by bubbling argon through the solution for 10 minutes. The measurement was started after removal of the argon supply for three scans at sweeps of 100 mV/s in the range of -0.5 and 2.5 V, providing the reference voltammogram.

The sample solution consisting of Ar_3Bi (20.0 mg) and NBu_4PF_6 (5.00 mL, 100 mM in MeCN) was treated equally, with only a single sweep, resulting in a spectrum for the Ar_3Bi species.

The reference spectrum was obtained using a sample solution consisting of Ar_3Bi (20.0 mg) and ferrocene (5.00 mg, 26.9 μmol), in a solution of NBu_4PF_6 (5.00 mL, 100 mM in MeCN) which was treated equally resulting in a spectrum for the Ar_3Bi and ferrocene species.

The peak potential of the bismuth species was compared to ferrocene.

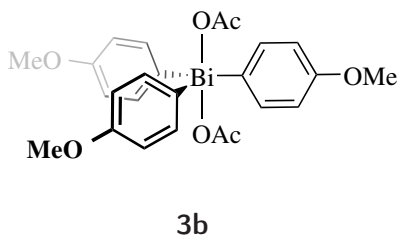
Randles–Sevcik equation

$$I_p^{irrev} = \pm 0.496 \sqrt{\alpha n'} n F A C \sqrt{\frac{FD\nu}{RT}} \quad (4.3.1)$$

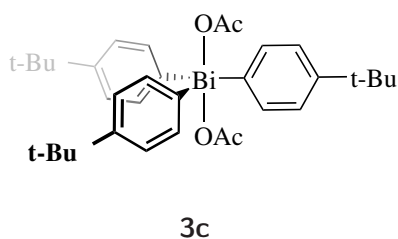
with α = transfer coefficient, n = total number of electrons transferred per molecule in the electrochemical process, n' = number of electrons transferred per mole before the rate determining step, A = geometric area of the electrode, C = concentration of the solution.

Synthesis of Organobismuth(V) Compounds

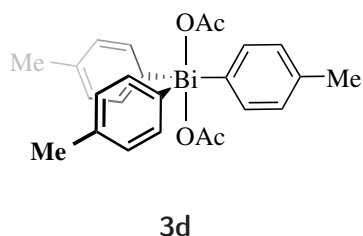
Protocol A: The organobismuth(III) species (4.00 mmol) and sodium perborate $\cdot 4\text{H}_2\text{O}$, (3.06 g, 20.0 mmol) were added to a solution of acetic acid (20 mL) and stirred for 2h. The reaction was quenched with water and extracted with CH_2Cl_2 . The organic phase was dried with MgSO_4 and removed *in vacuo* resulting in the desired product.

Tri(4-methoxyphenyl)bismuth diacetate 3b

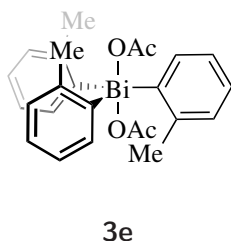
mp/°C 185-186. $^1\text{H NMR}$ (400 MHz, CDCl_3) δ_{H} 8.06 (d, $J = 8.9$ Hz, 6H), 7.07 (d, $J = 8.9$ Hz, 6H), 3.84 (s, 9H), 2.09 (s, 6H). $^{13}\text{C}\{^1\text{H}\}$ NMR (126 MHz, CDCl_3) δ_{C} 177.8, 161.1, 151.9, 135.4, 116.3, 55.5, 22.2. IR (ATR): $\tilde{\nu} = 1567, 1473, 1444, 1418, 1376, 1324, 1284, 1229, 1026, 982, 933, 781, 756, 689, 673, 664, 620, 561, 436\text{ cm}^{-1}$. HRMS calcd. for $\text{C}_{25}\text{H}_{27}\text{BiO}_7\text{Na}^+$: 671.1458 $[\text{M}+\text{Na}]^+$; found (ESI $^+$): 671.1445. Colourless crystals. Yield: 2.26 g, 87%.

Tris(4-(tert-butyl)phenyl)bismuth diacetate 3c

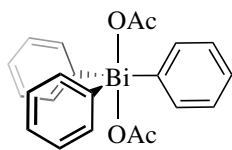
mp/°C 198-200. $^1\text{H NMR}$ (400 MHz, CDCl_3) δ_{H} 8.13 – 7.94 (m, 6H), 7.65 – 7.51 (m, 6H), 1.83 (s, 6H), 1.33 (s, 27H). $^{13}\text{C}\{^1\text{H}\}$ NMR (101 MHz, CDCl_3) δ_{C} 178.3, 157.5, 153.8, 133.6, 128.3, 35.0, 31.3, 22.1. IR (ATR): $\tilde{\nu} = 1711, 1600, 1376, 1266, 993, 825, 687, 622, 541\text{ cm}^{-1}$. HRMS calcd. for $\text{C}_{32}\text{H}_{42}\text{BiO}_2^+$: 667,2989 $[\text{M}-\text{OAc}]^+$; found (ESI $^+$): 667.2966. Colourless crystals. Yield: 2.85 g, 98%.

Tri(4-tolyl)bismuth diacetate 3d

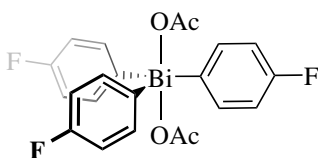
mp/°C 197-199. $^1\text{H NMR}$ (400 MHz, CDCl_3) δ_{H} 8.02 (d, $J = 8.3$ Hz, 4H), 7.38 (d, $J = 8.1$ Hz, 5H), 2.39 (s, 9H), 1.81 (s, 6H). $^{13}\text{C}\{^1\text{H}\}$ NMR (101 MHz, CDCl_3) δ_{C} 207.2, 178.0, 157.6, 140.9, 133.8, 131.7, 31.0, 22.2, 21.5. IR (ATR): $\tilde{\nu} = 1584, 1486, 1377, 1326, 1185, 999, 832, 803, 792, 664, 620, 472\text{ cm}^{-1}$. HRMS calcd. for $\text{C}_{25}\text{H}_{27}\text{BiO}_4\text{Na}^+$: 623.1611 $[\text{M}+\text{Na}]^+$; found (ESI $^+$): 623.1606. Colourless crystals. Yield: 2.18 g, 91%. In accordance with literature values.⁸⁰

Tri(2-tolyl)bismuth diacetate 3e

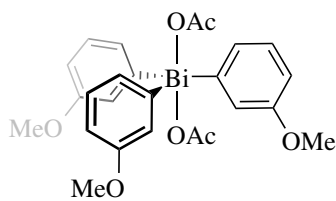
mp/°C 140-142. $^1\text{H NMR}$ (400 MHz, CDCl_3) δ_{H} 8.29 (dd, $J = 7.9, 1.3$ Hz, 3H), 7.55 – 7.33 (m, 9H), 2.61 (s, 9H), 1.74 (s, 6H). $^{13}\text{C}\{^1\text{H}\}$ NMR (101 MHz, CDCl_3) δ_{C} 176.3, 163.2, 141.9, 134.4, 133.3, 130.8, 128.4, 23.7, 22.9. IR (ATR): $\tilde{\nu} = 1556, 1366, 1317, 1291, 995, 749, 658, 613, 431\text{ cm}^{-1}$. HRMS calcd. for $\text{C}_{25}\text{H}_{27}\text{BiO}_4\text{Na}^+$: 623.1611 $[\text{M}+\text{Na}]^+$; found (ESI $^+$): 623.1616. Colourless crystals. Yield: 2.11 g, 91%.

Triphenylbismuth diacetate 3f**3f**

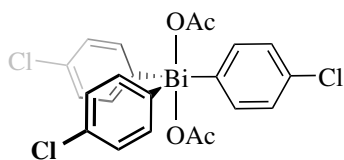
mp/°C 176-178. $^1\text{H NMR}$ (400 MHz, CDCl_3) δ_{H} 8.22 – 8.13 (m, 6H), 7.68 – 7.57 (m, 6H), 7.56 – 7.44 (m, 3H), 1.85 (s, 6H). $^{13}\text{C}\{^1\text{H}\}$ NMR (126 MHz, CDCl_3) δ_{C} 161.1, 134.1, 131.7, 131.3, 130.8, 22.1. IR (ATR): $\tilde{\nu}$ = 1681, 1556, 1469, 1375, 1260, 1180, 1083, 1042, 1003, 833, 800, 712, 476 cm^{-1} . HRMS calcd. for $\text{C}_{22}\text{H}_{21}\text{BiO}_4\text{Na}^+$: 581.1244 $[\text{M}+\text{Na}]^+$; found (ESI $^+$): 581.1170. Colourless crystals. Yield: 1.63 g, 73%. In accordance with literature values.⁸⁰

Tri(4-fluorophenyl)bismuth diacetate 3g**3g**

mp/°C 194-195. $^1\text{H NMR}$ (400 MHz, CDCl_3) δ_{H} 8.21 – 8.12 (m, 6H), 7.34 – 7.27 (m, 6H), 1.85 (s, 6H). $^{13}\text{C}\{^1\text{H}\}$ NMR (101 MHz, CDCl_3) δ_{C} 178.4, 163.9 (d, J = 252.0 Hz), 155.8, 136.0 (d, J = 8.2 Hz), 118.3 (d, J = 21.4 Hz), 21.8. $^{19}\text{F NMR}$ (377 MHz, CDCl_3) δ_{F} -107.79 (tt, J = 8.6, 5.3 Hz). IR (ATR): $\tilde{\nu}$ = 1530, 1460, 1230, 1180, 800, 700, 500 cm^{-1} . HRMS calcd. for $\text{C}_{22}\text{H}_{118}\text{BiF}_3\text{O}_4\text{Na}^+$: 635.0839 $[\text{M}+\text{Na}]^+$; found (ESI $^+$): 635.0837. Colourless crystals. Yield: 2.13 g, 87%.

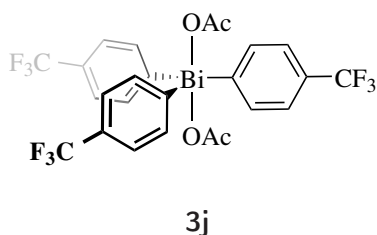
Tri(3-methoxyphenyl)bismuth diacetate 3h**3h**

mp/°C 155-156. $^1\text{H NMR}$ (400 MHz, CDCl_3) δ_{H} 7.85 (dd, J = 2.6, 1.4 Hz, 3H), 7.70 (ddd, J = 7.9, 1.4, 1.1 Hz, 3H), 7.61 – 7.46 (m, 3H), 7.02 (ddd, J = 8.2, 2.5, 0.9 Hz, 3H), 3.86 (s, 9H), 1.87 (s, 6H). $^{13}\text{C}\{^1\text{H}\}$ NMR (101 MHz, CDCl_3) δ_{C} 161.6, 161.5, 131.3, 125.6, 119.1, 117.3, 116.8, 55.6, 22.0. IR (ATR): $\tilde{\nu}$ = 1567, 1473, 1444, 1418, 1376, 1324, 1284, 1229, 1026, 982, 933, 781, 756, 689, 673, 664, 620, 561, 436 cm^{-1} . HRMS calcd. for $\text{C}_{25}\text{H}_{27}\text{BiO}_7\text{Na}^+$: 671.1458 $[\text{M}+\text{Na}]^+$; found (ESI $^+$): 671.1445. Colourless crystals. Yield: 2.44 g, 94%.

Tri(4-chlorophenyl)bismuth diacetate 3i**3i**

mp/°C 162-164. $^1\text{H NMR}$ (400 MHz, CDCl_3) δ_{H} 8.11 – 7.96 (m, 6H), 7.60 – 7.51 (m, 6H), 1.81 (s, 6H). $^{13}\text{C}\{^1\text{H}\}$ NMR (101 MHz, CDCl_3) δ_{C} 159.3, 137.4, 135.1, 131.7, 131.3, 21.8. IR (ATR): $\tilde{\nu}$ = 1681, 1556, 1469, 1375, 1260, 1180, 1083, 1042, 1003, 833, 800, 712, 476 cm^{-1} . HRMS calcd. for $\text{C}_{22}\text{H}_{18}\text{BiCl}_3\text{O}_4\text{Na}^+$: 682.9972 $[\text{M}+\text{Na}]^+$; found (ESI $^+$): 682.9964. Colourless crystals. Yield: 1.61 g, 61%.

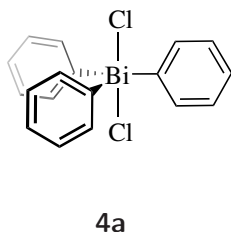
Tris(4-(trifluoromethyl)phenyl)bismuth diacetate **3j**



mp/°C 173-176. $^1\text{H NMR}$ (400 MHz, CDCl_3) δ_{H} 8.33 – 8.14 (m, 6H), 7.86 (d, $J = 8.0$ Hz, 6H), 1.84 (s, 6H). $^{13}\text{C}\{^1\text{H}\}$ NMR (126 MHz, CDCl_3) δ_{C} 179.2, 165.0, 134.3, 133.2 (q, $J = 32.8$ Hz), 128.2 (q, $J = 3.8$ Hz), 123.6 (q, $J = 272.9$ Hz), 21.7. $^{19}\text{F NMR}$ (377 MHz, CDCl_3) δ_{F} -63.01. IR (ATR): $\tilde{\nu} = 1681, 1556, 1469, 1375, 1260, 1180, 1083, 1042, 1003, 833, 800, 712, 476\text{ cm}^{-1}$. HRMS calcd. for $\text{C}_{25}\text{H}_{18}\text{BiF}_9\text{O}_4\text{Na}^+$: 785.0763 $[\text{M}+\text{Na}]^+$; found (ESI $^+$): 785.0767. Colourless crystals. Yield: 1.50 g, 52%.

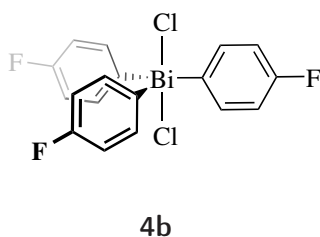
Protocol B: Freshly distilled sulfuryl chloride (92.0 μL , 0.90 mmol) was added to a solution of a organobismuth(III) compounds (0.81 mmol) in anhydrous CH_2Cl_2 (10 mL) and allowed to stir for 10 min. The solvent was removed *in vacuo*, resulting in colourless crystals.

Triphenylbismuth dichloride **4a**



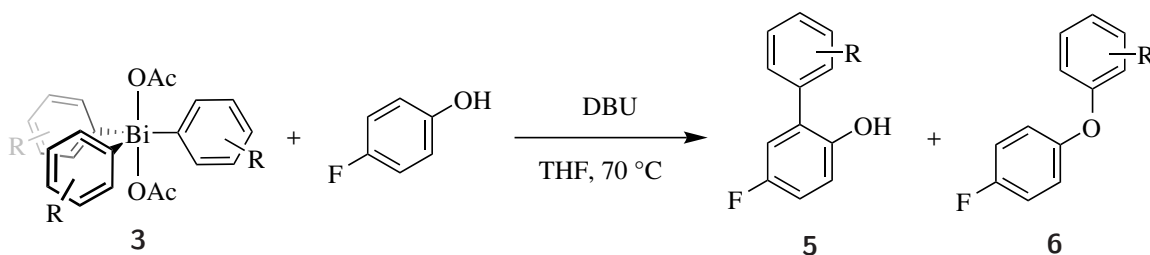
mp/°C 157-159. $^1\text{H NMR}$ (400 MHz, CDCl_3) δ_{H} 8.57 – 8.49 (m, 6H), 7.71 – 7.63 (m, 6H), 7.59 – 7.50 (m, 3H). $^{13}\text{C}\{^1\text{H}\}$ NMR (101 MHz, CDCl_3) δ_{C} 156.1, 134.6, 131.9, 131.6. IR (ATR): $\tilde{\nu} = 1555, 1465, 1434, 981, 725, 674, 640, 434\text{ cm}^{-1}$. HRMS calcd. for $\text{C}_{18}\text{H}_{15}\text{BiCl}^+$: 475.0666 $[\text{M}-\text{Cl}]^+$; found (ESI $^+$): 475.0677. Colourless crystals. Yield: 405.6 mg, 98%. In accordance with literature values.⁹⁶

Tri(4-fluorophenyl)bismuth dichloride **4b**



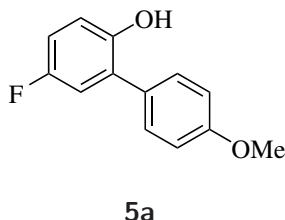
mp/°C 136-137. $^1\text{H NMR}$ (400 MHz, CDCl_3) δ_{H} 8.58 – 8.51 (m, 1H), 7.39 – 7.29 (m, 1H). $^{13}\text{C}\{^1\text{H}\}$ NMR (101 MHz, CDCl_3) δ_{C} 164.4 (d, $J = 254.5$ Hz), 149.7, 136.6 (d, $J = 8.5$ Hz), 118.8 (d, $J = 22.2$ Hz). $^{19}\text{F NMR}$ (377 MHz, CDCl_3) δ_{F} -106.36 (tt, $J = 8.3, 5.1$ Hz). IR (ATR): $\tilde{\nu} = 1681, 1556, 1469, 1375, 1260, 1180, 1083, 1042, 1003, 833, 800, 712, 476\text{ cm}^{-1}$. HRMS calcd. for $\text{C}_{18}\text{H}_{12}\text{BiClF}_3^+$: 529.0383 $[\text{M}-\text{Cl}]^+$; found (ESI $^+$): 529.0418. Colourless crystals. Yield: 444.0 mg, 97%. In accordance with literature values.⁷⁷

Arylation of 4-fluorophenol



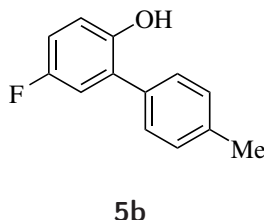
4-Fluorophenol (10.0 mg, 89.0 μmol) as well as the individual organobismuth(V) compound (89 μmol) were added to a vacuum/back-filled J. Young's NMR tube. Dry THF (0.7 mL) and DBU (33.0 μL , 222.5 μmol) were added and the NMR tube, closed and shook vigorously until all solid material was dissolved. The reaction mixture was allowed to stand at 70 $^\circ\text{C}$ for 20 h. After the reaction the mixture was analysed *via* ^{19}F NMR spectroscopy. The products were subsequently separated by preparative TLC on silica on an aluminium plate in toluene. While the *O*-arylated species showed a high sensitivity towards the added group the *C*_{ortho}-arylated products maintained rather similar shifts.

5-Fluoro-4'-methoxy-[1,1'-biphenyl]-2-ol 5a

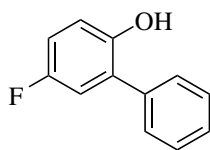


^1H NMR (400 MHz, CDCl_3) δ_{H} 7.41 (m, 2H), 7.01 (m, 2H), 6.99 (m, 1H), 6.95 (m, 1H), 6.89 (m, 1H), 5.45 (m, 1H), 3.85 (s, 3H). $^{13}\text{C}\{^1\text{H}\}$ NMR (101 MHz, CDCl_3) δ_{C} 159.2, 156.9 (d, $J = 236.8$ Hz), 148.4 (d, $J = 2.2$ Hz), 130.0, 128.8 (d, $J = 7.6$ Hz), 128.4, 116.5 (d, $J = 8.4$ Hz), 116.2 (d, $J = 23.1$ Hz), 114.6 (d, $J = 22.7$ Hz), 114.5, 55.1. ^{19}F NMR (377 MHz, CDCl_3) δ_{F} -124.27 (m). HRMS calcd. for $\text{C}_{13}\text{H}_{10}\text{FO}_2^-$ (M-H) 217.0670, found 217.0673. In accordance with literature values.²²⁹

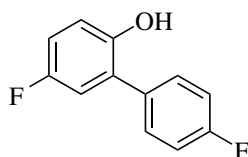
5-Fluoro-4'-methyl-[1,1'-biphenyl]-2-ol 5b



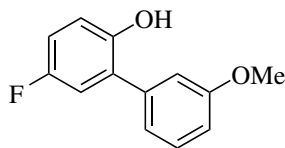
^1H NMR (400 MHz, CDCl_3) δ_{H} 7.38 – 7.27 (m, 4H), 6.98 – 6.86 (m, 3H), 5.02 (s, 1H), 2.42 (s, 3H). ^{19}F NMR (377 MHz, CDCl_3) δ_{F} -124.28 (m). HRMS calcd. for $\text{C}_{13}\text{H}_{10}\text{FO}^-$ (M-H) 201.0721, found 201.0564. In accordance with literature values.²³⁰

5-Fluoro-[1,1'-biphenyl]-2-ol 5c**5c**

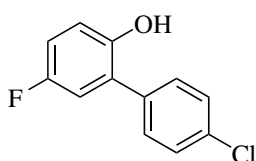
$^1\text{H NMR}$ (400 MHz, CDCl_3) δ_{H} 7.56 – 7.38 (m, 5H), 7.00 – 6.87 (m, 3H), 5.00 (s, 1H). $^{13}\text{C}\{^1\text{H}\}$ NMR (101 MHz, CDCl_3) δ_{C} 157.2 (d, $J = 237.1$ Hz), 148.5 (d, $J = 2.1$ Hz), 136.1, 129.4, 129.0 (d, $J = 7.6$ Hz), 128.9, 128.3, 116.7 (d, $J = 7.9$ Hz), 116.4 (d, $J = 23.0$ Hz), 115.4 (d, $J = 23.1$ Hz); $^{19}\text{F NMR}$ (377 MHz, CDCl_3) δ_{F} -124.15 (m). HRMS calcd. for $\text{C}_{12}\text{H}_8\text{FO}^-$ (M-H) 187.0565, found 187.0566. In accordance with literature values.²³¹

4',5-Difluoro-[1,1'-biphenyl]-2-ol 5d**5d**

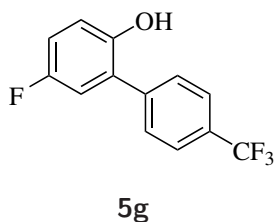
$^1\text{H NMR}$ (400 MHz, CDCl_3) δ_{H} 7.49 – 7.40 (m, 2H), 7.24 – 7.14 (m, 2H), 7.09 – 6.86 (m, 3H). $^{19}\text{F NMR}$ (377 MHz, CDCl_3) δ_{F} -113.32 (tt, $J = 8.3, 5.4$ Hz), -123.86 (td, $J = 8.4, 5.0$ Hz). HRMS calcd. for $\text{C}_{12}\text{H}_7\text{F}_2\text{O}^-$ (M-H) 205.0470, found 205.0479. MS (ESI $^-$): m/z : 205.0479 (M-H). In accordance with literature values.²³²

5-Fluoro-3'-methoxy-[1,1'-biphenyl]-2-ol 5e**5e**

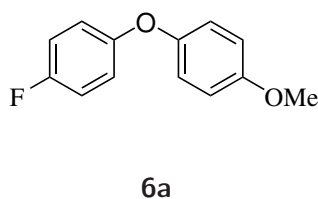
$^1\text{H NMR}$ (400 MHz, CDCl_3) δ_{H} 7.52 – 7.41 (m, 4H), 7.08 – 6.90 (4, 3H), 3.82 (s, 3H). $^{13}\text{C}\{^1\text{H}\}$ NMR (101 MHz, CDCl_3) δ_{C} 159.9, 156.8 (d, $J = 237.2$ Hz), 148.4 (d, $J = 2.2$ Hz), 137.6 (d, $J = 1.5$ Hz), 130.2, 128.8 (d, $J = 7.6$ Hz), 121.0, 116.7 (d, $J = 7.9$ Hz), 116.2 (d, $J = 23.6$ Hz), 115.2 (d, $J = 22.8$ Hz), 114.4, 113.6, 55.1. $^{19}\text{F NMR}$ (377 MHz, CDCl_3) δ_{F} -124.20 (m). HRMS calcd. for $\text{C}_{13}\text{H}_{10}\text{FO}_2^-$ (M-H) 217.0670, found 217.0676. In accordance with literature values.²²⁹

4'-Chloro-5-fluoro-[1,1'-biphenyl]-2-ol 5f**5f**

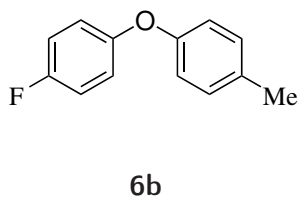
$^1\text{H NMR}$ (400 MHz, CDCl_3) δ_{H} 7.49 – 7.38 (m, 4H), 7.00 – 6.87 (m, 3H), 4.85 (s, 1H). $^{13}\text{C}\{^1\text{H}\}$ NMR (101 MHz, CDCl_3) δ_{C} 115.4 (d, $J = 8.2$ Hz), 116.5 (d, $J = 3.0$ Hz), 116.9 (d, $J = 25.0$ Hz), 128.0 (d, $J = 7.7$ Hz), 129.3, 130.3, 134.3, 134.7, 148.3, 156.0 (d, $J = 239.2$ Hz). $^{19}\text{F NMR}$ (377 MHz, CDCl_3) δ_{F} -123.68 (m). HRMS calcd. for $\text{C}_{12}\text{H}_7\text{ClFO}^-$ (M-H) 221.0175, found 221.0170. In accordance with literature values.^{6,233}

5-Fluoro-4'-(trifluoromethyl)-[1,1'-biphenyl]-2-ol 5g

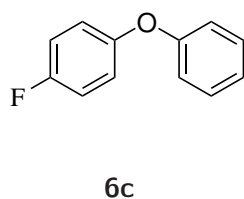
$^1\text{H NMR}$ (400 MHz, CDCl_3) δ_{H} 7.78 – 7.72 (m, 2H), 7.65 – 7.59 (m, 2H), 7.03 – 6.95 (m, 2H), 6.94 – 6.88 (m, 1H). $^{19}\text{F NMR}$ (377 MHz, CDCl_3) δ_{F} -62.67, -123.36 (m). HRMS calcd. for $\text{C}_{13}\text{H}_7\text{F}_4\text{O}^-$ (M-H) 255.0439, found 255.0436.

1-Fluoro-4-(4-methoxyphenoxy)benzene 6a

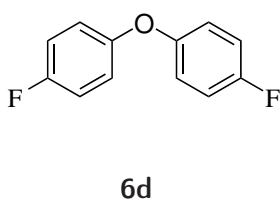
$^1\text{H NMR}$ (400 MHz, CDCl_3) δ_{H} 6.96 (m, 2H), 6.93 (m, 2H), 6.90 (m, 2H), 6.86 (m, 2H). $^{13}\text{C}\{^1\text{H}\}$ NMR (101 MHz, CDCl_3) δ_{C} 158.4 (d, $J=240.4$ Hz), 155.9, 154.3, 150.7, 120.3, 119.2 (d, $J=8.2$ Hz), 116.2 (d, $J=23.3$ Hz), 115.0, 55.6. $^{19}\text{F NMR}$ (377 MHz, CDCl_3) δ_{F} -120.79 (m). HRMS calcd. for $\text{C}_{13}\text{H}_{11}\text{FNaO}_2^+$: 241.0641 $[\text{M}+\text{Na}]^+$; found (ESI $^+$): 241.2166. In accordance with with literature values.²³⁴

1-Fluoro-4-(p-tolyloxy)benzene 6b

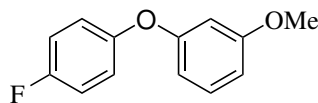
$^1\text{H NMR}$ (400 MHz, CDCl_3) δ_{H} 7.14 (d, 2H, $J=8.1$ Hz), 7.07-6.92 (m, 4H), 6.89 (d, 2H, $J=8.2$ Hz), 2.35 (s, 3H). $^{13}\text{C}\{^1\text{H}\}$ NMR (101 MHz, CDCl_3) δ_{C} 158.6 (d, $J=241.0$ Hz), 155.3, 153.5, 132.9, 130.3, 120.0 (d, $J=8.2$ Hz), 118.6, 116.2 (d, $J=23.3$ Hz), 20.7. $^{19}\text{F NMR}$ (377 MHz, CDCl_3) δ_{F} -120.79 (m). HRMS calcd. for $\text{C}_{13}\text{H}_{10}\text{FO}^-$: 201.0721 $[\text{M}-\text{H}]^+$; found (ESI $^+$): 201.0714. In accordance with with literature values.²³⁵

1-Fluoro-4-phenoxybenzene 6c

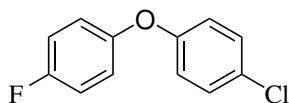
$^1\text{H NMR}$ (400 MHz, CDCl_3) δ_{H} 7.34–7.31 (m, 2H), 7.09 (m, 1H), 7.05–7.01 (m, 2H), 7.00–6.97 (m, 4H). $^{13}\text{C}\{^1\text{H}\}$ NMR (101 MHz, CDCl_3) δ_{C} 158.9 (d, $J=242.3$ Hz), 157.7, 152.9, 129.7, 123.1, 120.6 (d, $J=8.4$ Hz), 118.2, 116.3 (d, $J=22.8$ Hz). $^{19}\text{F NMR}$ (377 MHz, CDCl_3) δ_{F} -120.56 (m). HRMS calcd. for $\text{C}_{12}\text{H}_9\text{FNaO}^+$: 211.0530 $[\text{M}+\text{Na}]^+$; found (ESI $^+$): 211.0552. In accordance with with literature values.²³⁶

4,4'-Oxybis(fluorobenzene) 6d

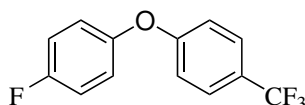
$^1\text{H NMR}$ (400 MHz, CDCl_3) δ_{H} 7.03 – 6.99 (m, 4H), 6.97 – 6.92 (m, 4H). $^{13}\text{C}\{^1\text{H}\}$ NMR (101 MHz, CDCl_3) δ_{C} 158.7 (d, $J=241.5$ Hz), 153.5 (d, $J=2.4$ Hz), 119.8 (d, $J=8.2$ Hz), 116.3 (d, $J=23.3$ Hz). $^{19}\text{F NMR}$ (377 MHz, CDCl_3) δ_{F} -120.24 (m). HRMS calcd. for $\text{C}_{12}\text{H}_8\text{F}_2\text{ONa}^+$: 229.0441 $[\text{M}+\text{Na}]^+$; found (ESI $^+$): 229.0435. In accordance with with literature values.²³⁷

1-Fluoro-4-(3-methoxyphenoxy)benzene 6e**6e**

^1H NMR (400 MHz, CDCl_3) δ_{H} 7.18–7.22 (m, 1H), 6.90–7.10 (m, 4H), 6.62–6.65 (m, 1H), 6.52–6.54 (m, 1H), 3.76 (s, 3H). $^{13}\text{C}\{^1\text{H}\}$ NMR (101 MHz, CDCl_3) δ_{C} 161.0, 158.9, 158.9 (d, $J = 241.8$ Hz), 152.6 (d, $J = 2.6$ Hz), 130.1, 120.7 (d, $J = 8.3$ Hz), 116.3 (d, $J = 23.3$ Hz), 110.3, 108.7, 104.3, 55.3. ^{19}F NMR (377 MHz, CDCl_3) δ_{F} -120.24 (m). HRMS calcd. for $\text{C}_{13}\text{H}_{11}\text{FNaO}_2^+$: 241.0641 $[\text{M}+\text{Na}]^+$; found (ESI $^+$): 241.0621. In accordance with with literature values.²³⁸

1-Chloro-4-(4-fluorophenoxy)benzene 6f**6f**

^1H NMR (400 MHz, CDCl_3) δ_{H} 6.97 (m, 2H), 7.20 (m, 2H), 7.26 (m, 2H), 7.43 (m, 2H). $^{13}\text{C}\{^1\text{H}\}$ NMR (101 MHz, CDCl_3) δ_{C} 159.2 ($J = 241.4$ Hz), 156.6, 152.7 ($J = 2.5$ Hz), 129.9, 128.3, 120.8 ($J = 8$ Hz), 119.6, 116.7 ($J = 23.1$ Hz). ^{19}F NMR (377 MHz, CDCl_3) δ_{F} -119.47 (m). HRMS calcd. for $\text{C}_{12}\text{H}_8\text{ClFONa}^+$: 245.0145 $[\text{M}+\text{Na}]^+$; found (ESI $^+$): 245.0124. In accordance with with literature values.²³⁹

1-Fluoro-4-(4-(trifluoromethyl)phenoxy)benzene 6g**6g**

^1H NMR (400 MHz, CDCl_3) δ_{H} 7.50 (m, 4H), 6.90 (m, 4H). ^{19}F NMR (377 MHz, CDCl_3) δ_{F} -61.84 (s, 3F), 118.25 (m, 1F). HRMS calcd. for $\text{C}_{13}\text{H}_7\text{F}_4\text{O}^-$: 255.0439 $[\text{M}-\text{H}]^-$; found (ESI $^-$): 255.0433. In accordance with with literature values.²⁴⁰

Time Resolved Observation

4-Fluorophenol (1.2 mg, 10.9 μmol) and **3g** (10 mg 16 μmol) were added to a vacuum/backfilled Young's NMR tube. Dry THF (0.7 mL), DBU (4.0 μL , 27 μmol) and one drop of benzene- d_6 were added and the NMR tube was closed and shaken vigorously until all material is dissolved. The reaction mixture was allowed to stand at 70 $^\circ\text{C}$. The sample was analysed by ^{19}F NMR spectroscopy at 1, 2, 3, 4, 5, 15, 21, 34 h. An internal standard of 1-bromo-4-(trifluoromethyl)benzene has been used for quantification.

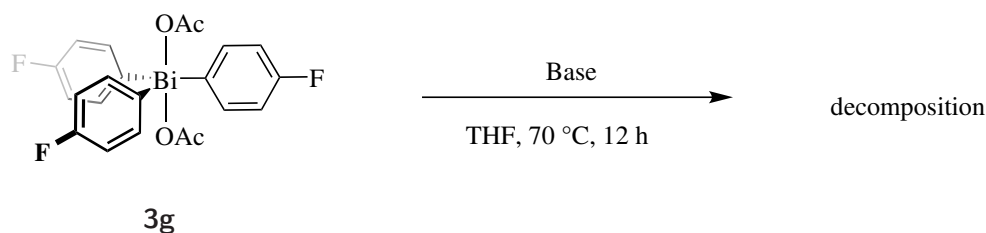
Component Effects

Three NMR samples were prepared: 4-Fluorophenol (1.20 mg, 10.9 μmol) and **3g** (10 mg 16 μmol) were added to the first NMR tube. **3g** (10 mg 16 μmol) and DBU (4.0 μL , 27 μmol) were added to the second NMR tube. 4-Fluorophenol (1.2 mg, 10.9 μmol) and DBU (4 μL , 27 μmol) were added to the third NMR tube. 0.7 mL of dry THF, and one drop of benzene- d_6 was added to each sample. Subsequently the NMR tube was closed and shaken vigorously until all material was dissolved. The reaction mixtures were allowed to stand at 70 $^\circ\text{C}$ for 12 h and were analysed by ^{19}F NMR spectroscopy. An internal standard of 1-bromo-4-(trifluoromethyl)benzene has been used for quantification.

Kinetic Investigation of the Decomposition of **3g** with DBU

3g (35.9 mg, 58.8 μmol) was added to a solution of DBU (8.0 μL , 54 μmol) in THF (0.7 mL) with one drop of benzene- d_6 in an NMR tube and allowed to stand at 25 $^\circ\text{C}$ for 300 h. The sample was analysed at various time points using ^{19}F NMR spectroscopy. An internal standard of 1-bromo-4-(trifluoromethyl)benzene was used for quantification.

Decomposition of **3g** using Different Bases



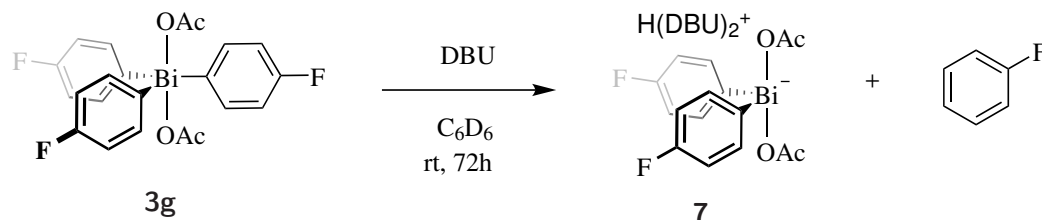
Scheme 4.6: Decomposition of **3g** after 12 h at 70 $^\circ\text{C}$. Conditions: [**3g**], [Base] = 27.2 μM , with base = pyridine, 2.4.6-collidine, pempiridine, DABCO, quinuclidine, Hünig's base, sodium valproate

Tri(4-fluorophenyl)bismuth diacetate **3g** (10.0 mg, 16.3 μmol) has been added to 0.6 mL of THF and one drop of benzene- d_6 . To this 1.0 equiv. of base has been added and the solution allowed to stand at 70 $^\circ\text{C}$ for 12 h before being analysed by ^{19}F NMR spectroscopy. An internal standard of 1-bromo-4-(trifluoromethyl)benzene was used for quantification.

Pre-deprotonation of 4-Fluorophenol

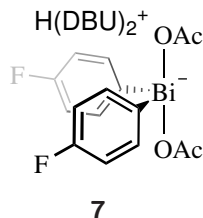
Tri(4-fluorophenyl)bismuth diacetate **3g** (10.0 mg, 16.3 μmol) was added to 0.6 mL of THF and one drop of benzene- d_6 . To this, sodium 4-fluorophenolate (2.2 mg, 16 μmol) was added and the solution was allowed to stand at 70 $^\circ\text{C}$ for 12 h before being analysed by ^{19}F NMR spectroscopy. An internal standard of 1-bromo-4-(trifluoromethyl)benzene was used for quantification.

Isolation of the Diarylbismuth Species **7**



3g (20 mg, 32 μmol) and DBU (20.0 μL , 134 μmol) were added to benzene- d_6 (0.6 mL). The reaction was allowed to stand at room temperature until consumption of **3g** was observed (72 h). Reaction progress was monitored by ^1H NMR spectroscopy. Upon complete conversion of **3g** the reaction mixture was dried *in vacuo* and triturated with Et_2O , resulting

in a yellow oil.



^1H NMR (400 MHz, Benzene- d_6) δ_H 8.84 – 8.70 (m, 2H), 7.16 (d, $J = 1.8$ Hz, 2H), 4.96 (s, 1H), 2.45 (dd, $J = 11.6, 5.9$ Hz, 4H), 2.39 (d, $J = 5.1$ Hz, 2H), 2.24 – 2.23 (m, 3H), 1.34 – 1.28 (m, 3H), 1.19 (d, $J = 6.2$ Hz, 2H), 1.10 (q, $J = 5.7$ Hz, 2H), 0.92 (p, $J = 5.5, 4.7$ Hz, 3H). $^{13}\text{C}\{^1\text{H}\}$ NMR (126 MHz, Benzene- d_6) δ_C 178.01, 164.45, 162.82 (d, $J = 244.9$ Hz), 139.59 (d, $J = 6.5$ Hz), 118.01 (d, $J = 19.1$ Hz), 61.20, 53.22, 48.01, 39.67, 33.36, 29.20, 27.11, 25.01, 24.55, 20.29. ^{14}N NMR (41 MHz, Benzene- d_6) δ_N -197.7, -270.6. ^{19}F NMR (376 MHz, Benzene- d_6) δ_F -114.79 (tt, $J = 9.6, 6.5$ Hz) IR (ATR): $\tilde{\nu} = 3249, 2927, 2857, 1641, 1572, 1483, 1444, 1383, 1323, 1212, 1160, 1108, 1013, 817, 650, 507, 411. \text{cm}^{-1}$. calcd. for $\text{C}_{16}\text{H}_{14}\text{BiF}_2\text{O}_4^-$: 517.0664 [M-HDBU $_2$] $^-$; found (ESI $^-$): 517.0679., calcd. for $\text{C}_9\text{H}_{17}\text{N}_2^+$: 153.1386 [HDBU] $^+$; found (ESI $^+$): 153.1396.

NOT In accordance with with literature values.¹⁰⁹

Trapping of the Potential Aryne Intermediate

Tri(4-fluorophenyl)bismuth diacetate **3g** (35.9 mg, 58.8 μmol) and furan (39.0 μL , 540 μmol) were added a solution of DBU (8.0 μL , 54 μmol) in THF (0.7 mL) with one drop of benzene- d_6 in an NMR tube and allowed to stand at 70 $^\circ\text{C}$ for 5 h. The sample was analysed using ^{19}F NMR spectroscopy and mass spectrometry.

Influence of Base Equivalents

From stock solutions tri(4-fluorophenyl)bismuth diacetate **3g** (16.1 mg, 26.3 μmol), 1-bromo-4-(tri-fluoromethyl)benzene (5.9 mg, 26 μmol), 4-fluorophenol (3.0 mg, 26.3 μmol) and DBU (0.9-25.0 equivalents) have been added to make up 0.7 mL of THF with one drop of benzene- d_6 . The reaction mixtures were allowed to stand at 70 $^\circ\text{C}$ for 20 h and subsequently analysed by ^{19}F NMR spectroscopy.

Solvent Scope

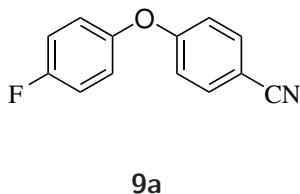
Tri(4-fluorophenyl)bismuth diacetate **3g** (10.0 mg, 16.3 μmol), DBU (4.0 μL , 27.0 μmol) and 4-fluorophenol (1.2 mg, 10.8 μmol) were added to an NMR tube of 0.6 mL of solvent (THF (dry), toluene, CDCl_3 , DMF, MeCN, THF (wet), DMPU, 2-MeTHF, DMSO) and one drop of benzene- d_6 . To this sodium 4-fluorophenolate (2.2 mg, 16.3 μmol) has been added and the solution was allowed to stand at 70 $^\circ\text{C}$ for 12 h. The samples were dried *in vacuo* before being redissolved in CDCl_3 and analysed by ^{19}F NMR spectroscopy. An internal standard of 1-bromo-4-(trifluoromethyl)benzene has been used for quantification.

Substrate Scope

Tri(4-fluorophenyl)bismuth diacetate **3g** (20.0 mg, 32.6 μmol), DBU (8.0 μL , 54 μmol) and the corresponding phenol (32.6 μmol) were added to 0.6 mL of THF and allowed to stand

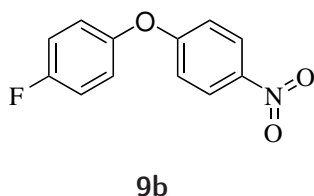
for 20 h at 70 °C. For substrates that did not show full conversion after 20 h the set up was repeated at 100 °C for the same time.

4-(4-Fluorophenoxy)benzonitrile **9a**



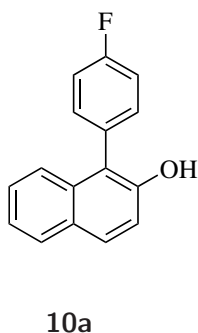
mp/°C: 66-67. $^1\text{H NMR}$ (400 MHz, CDCl_3) δ_{H} 7.64 – 7.56 (d, $J = 7.6$ Hz), 7.16 – 7.06 (m, 2H), 7.09 – 7.00 (m, 2H), 7.02 – 6.93 (d, $J = 7.5$ Hz). $^{13}\text{C}\{^1\text{H}\}$ NMR (126 MHz, CDCl_3) δ_{C} : 161.8, 159.8 (d, $J = 242.8$ Hz), 150.5, 134.2, 122.0 (d, $J = 8.4$ Hz), 118.7, 117.5, 116.8 (d, $J = 23.4$ Hz), 105.9. $^{19}\text{F NMR}$ (377 MHz, CDCl_3) δ_{F} -117.26 (tt, $J = 8.1, 4.5$ Hz). HRMS calcd. for $\text{C}_{13}\text{H}_7\text{FNO}^+$: 212.0506 $[\text{M}-\text{H}]^+$; found (ESI $^+$): 212.0517. $^1\text{H NMR}$ In accordance with with literature values. $^{13}\text{C}\{^1\text{H}\}$ NMR spectra of all literature presence contradict each other and do not match the spectrum reported in this thesis.²⁴¹⁻²⁴³

1-Fluoro-4-(4-nitrophenoxy)benzene **9b**



mp/°C: 58-59. $^1\text{H NMR}$ (400 MHz, CDCl_3) δ_{H} 8.23 – 8.18 (m, 2H), 7.16 – 7.10 (m, 2H), 7.09 – 7.04 (m, 2H), 7.01 – 6.96 (m, 2H). $^{13}\text{C}\{^1\text{H}\}$ NMR (126 MHz, CDCl_3) δ_{C} : 163.7, 161.4 (t, $J = 236.6$ Hz), 150.5 (d, $J = 126$ Hz), 143.3, 126.2, 122.4 (d, $J = 36$ Hz), 117.5, 117.1. $^{19}\text{F NMR}$ (377 MHz, CDCl_3) δ_{F} -116.85 (tt, $J = 8.3, 4.5$ Hz). IR (ATR): $\tilde{\nu} = 1585, 1502, 1488, 1341, 1254, 1214, 1111, 842, 747$. HRMS calcd. for $\text{C}_{12}\text{H}_8\text{FNO}_3^+$: 233.0483 $[\text{M}]^+$; found (ESI $^+$): 233.0432. In accordance with with literature values.^{244,245}

1-(4-Fluorophenyl)naphthalen-2-ol **10a**



mp/°C: 110-111. $^1\text{H NMR}$ (400 MHz, CDCl_3) δ_{H} 7.85 – 7.79 (m, 2H), 7.44 – 7.37 (m, 2H), 7.38 – 7.22 (m, 6H), 5.00 (s, 1H). $^{13}\text{C}\{^1\text{H}\}$ NMR (126 MHz, CDCl_3) δ_{C} : 163.0 (d, $J = 248.1$ Hz), 150.4, 133.5, 133.2 (d, $J = 8.1$ Hz), 131.7 (d, $J = 8.1$ Hz), 130.1 (d, $J = 3.5$ Hz), 129.9, 129.1, 128.2, 126.8, 124.5, 123.6, 120.1, 116.9 (d, $J = 21.4$ Hz). $^{19}\text{F NMR}$ (377 MHz, CDCl_3) δ_{F} -113.07 (tt, $J = 9.5, 5.4$ Hz). IR (ATR): $\tilde{\nu} = 1696, 1574, 1416, 1304, 1262, 898, 748, 720, 668, 568, 549$. cm^{-1} . HRMS calcd. for $\text{C}_{16}\text{H}_{10}\text{FO}^+$: 237.0721 $[\text{M}-\text{H}]^-$; found (ESI $^-$): 237.0720. In accordance with with literature values.¹³⁸

Influence of Light

From stock solutions of **3g** (20.0 mg, 32.6 μmol), 4-fluoro-phenol (3.4 mg, 31 μmol), 1-bromo-4-(trifluoromethyl)benzene (6.9 mg, 31 μmol) and DBU (11.1 μL , 75.5 μmol) were added to make up 0.7 mL of THF with one drop of benzene- d_6 in NMR tubes. The reaction mixtures were exposed to UV-VIS/VIS/no light for 20 h at 25 or 70 °C and analysed by $^{19}\text{F NMR}$ spectroscopy.

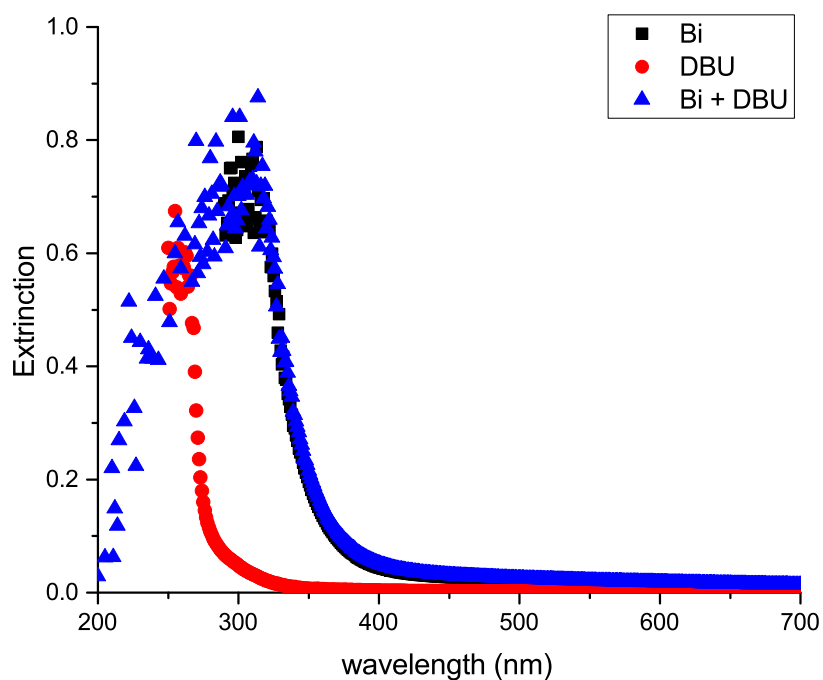


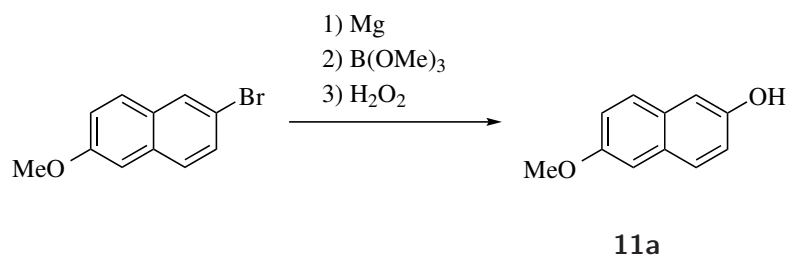
Figure 4.3.1: UV spectrum of **3g**, DBU and a mixture of both

Kinetic Investigation of the Arylation of 6-Fluoro-2-naphthol

From stock solutions 6-fluoro-2-naphthol (3.0 mg, 19 μmol) and $\text{Ar}_3\text{Bi}(\text{OAc})_2$ (20.4 μmol) were added to an NMR tube and the combined solutions filled up to 0.7 mL of THF/ C_6D_6 (99/1). The NMR tube was inserted into the NMR machine and allowed equilibrate at 50 $^\circ\text{C}$ for 5 min. An ^1H NMR spectrum was collected to correctly identify the ratio of the individual reagents. Subsequently, the NMR tube was removed from the machine, DBU (5.5 μL , 37 μmol) was added, the NMR tube shaken vigorously and added back to the NMR machine. The kinetic measurement was started directly after addition resulting in the kinetic array of ^{19}F NMR spectra.

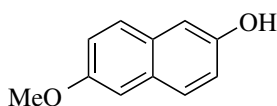
Synthesis of 6-substituted Naphthols^{III}

6-Methoxy-2-naphthol **11a**



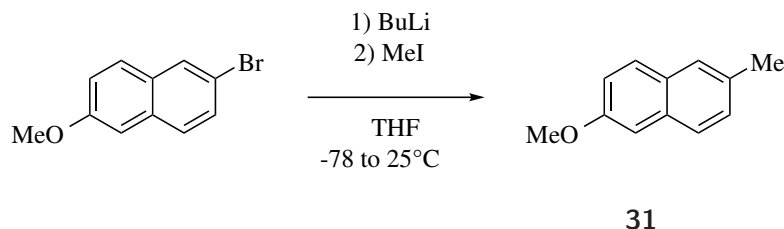
^{III}This work has been performed by James Gillespie under my supervision

Under an atmosphere of nitrogen, magnesium turnings (118 mg, 4.85 mmol) and a few iodine crystals were heated gently until the evolution of purple vapour. Dry THF (3.0 mL) was then added followed by the dropwise addition of a solution of 2-bromo-6-methoxynaphthalene (809 mg, 3.41 mmol) in dry THF (2.0 mL). The resulting brown solution was stirred for 1 h, then added to a solution of trimethylborate (0.51 mL, 4.57 mmol) in dry THF (3.0 mL) at 0 °C. The resulting cloudy solution was stirred for 18 h, then glacial acetic acid (0.30 mL), hydrogen peroxide (30% aqueous solution, 1.2 mL) and water (0.35 mL) were added at 0 °C. The solution was then stirred for 4 h, filtered and the organics extracted with Et₂O (3 × 10 mL). The combined organic fractions were washed with aqueous sodium thiosulfate (2 × 25 mL) and brine (3 × 10 mL), then dried with MgSO₄, filtered and the solvent removed *in vacuo*. The resulting orange residue was purified by silica gel column chromatography to give the title compound as a yellow crystalline solid (366 mg, 2.10 mmol, 62%).

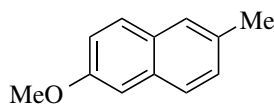
**11a**

mp/°C 149-151. ¹H NMR (500 MHz, CDCl₃) δ_H 8.54 (d, *J* = 1.7 Hz, 1H), 8.01 (d, *J* = 8.6, 1.7 Hz, 2H), 7.87 (d, *J* = 8.6 Hz, 1H), 7.71 (d, *J* = 8.7 Hz, 1H), 7.21-7.09 (m, 2H), 5.16 (s, 1H), 3.97 (s, 1H). ¹³C{¹H} NMR (126 MHz, CDCl₃) δ_C 167.4, 155.4, 131.5, 131.0, 127.9, 126.5, 126.0, 125.3, 118.6, 109.5, 52.1. IR (ATR): $\tilde{\nu}$ = 3413, 2951, 1681, 1627, 1572, 1509, 1482, 1434, 1351, 1302, 1278, 1241, 1202, 1154, 1129, 1100, 973, 956, 917, 879, 852, 810, 772, 755, 653, 605, 544, 522, 492, 478. HRMS calcd. for C₁₁H₉O₂⁻: 173.0608 [M-H]⁻; found (ESI⁻): 173.0609. R_f: (cyclohexane:Et₂O, 7:3) 0.36. Yield: 366 mg (62%). In accordance with literature values.²⁴⁶

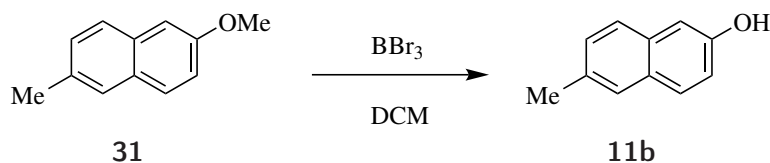
6-Methyl-2-naphthol 11b

**31**

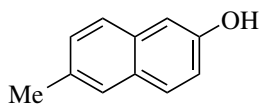
Under an atmosphere of nitrogen, nBuLi (0.85 mL, 2.13 mmol, 2.5 M) was added dropwise, over the course of 10 min, to solution of 2-bromo-6-methoxynaphthalene (501 mg, 2.11 mmol) in dry THF (10 mL) at -78 °C. The bright yellow solution was vigorously stirred for 45 min. Iodomethane (0.14 mL, 2.24 mmol) was then added and the resulting colourless solution was stirred for 18 h and allowed to warm to room temperature. The solution was then poured into HCl/ice (pH < 1) and the organics extracted with dichloromethane (3 × 15 mL). The combined organic fractions were then washed with water (3 × 15 mL), dried with MgSO₄, filtered and the solvent removed *in vacuo* to give 2-methoxy-6-methylnaphthalene as a pale yellow solid (326 mg, 1.89 mmol, 90%).

**31**

mp/°C 57-58. $^1\text{H NMR}$ (500 MHz, CDCl_3) δ_{H} 7.69-7.60 (m, 2H), 7.54 (m, 1H), 7.28 (dd, $J = 8.4, 1.8$ Hz), 7.14-7.09 (m, 2H), 3.91 (s, 3H), 2.48 (s, 3H). $^{13}\text{C}\{^1\text{H}\}$ NMR (126 MHz, CDCl_3) δ_{C} 157.0, 133.0, 132.6, 129.1, 128.7, 128.6, 126.7, 126.6, 118.6, 105.6, 55.3, 21.4. IR (ATR): $\tilde{\nu} = 3053, 3003, 2961, 1630, 1603, 1502, 1481, 1463, 1450, 1437, 1388, 1337, 1263, 1226, 1194, 1173, 1157, 1117, 1032, 956, 924, 894, 853, 816, 802, 752, 668, 653, 582, 551, 524, 473$. HRMS calcd. for $\text{C}_{12}\text{H}_{13}\text{O}^+$: 173.0961 $[\text{M}+\text{H}]^+$; found (ESI $^-$): 173.0609. Yield: 326 mg (90%). In accordance with with literature values.²⁴⁷

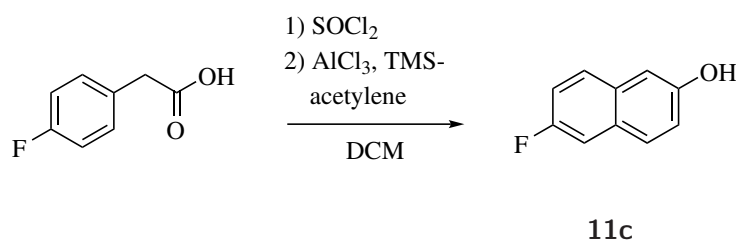
**31****11b**

Under an atmosphere of nitrogen, boron tribromide (0.10 mL, 1.04 mmol) was added to a solution of 2-methoxy-6-methylnaphthalene (150 mg, 0.871 mmol) in dry dichloromethane (3 mL) at 0 °C. The resulting orange solution was vigorously stirred for 18 h and allowed to warm to room temperature. Aqueous sodium hydroxide (3 mL, 2.5 M) was then added and the resulting aqueous phase was separated from the organics. The aqueous phase was then acidified with concentrated hydrochloric acid (3 mL) and then extracted with dichloromethane (3 × 10 mL). The combined organic fractions were washed with water (3 × 10 mL) and saturated aqueous sodium bicarbonate (3 × 10 mL), then filtered, dried with MgSO_4 and the solvent removed *in vacuo* to yield the title compound as an off-white solid (113 mg, 0.714 mmol, 82%).

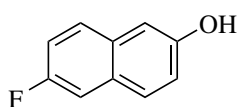
**11b**

mp/°C 105-106. $^1\text{H NMR}$ (500 MHz, CDCl_3) δ_{H} 7.77 (d, $J = 8.7$ Hz, 1H), 7.71 (d, $J = 8.4$ Hz, 1H), 7.62 (s, 1H), 7.43 (d, $J = 2.5$ Hz, 1H), 7.36 (dd, $J = 8.4, 1.7$ Hz), 7.16 (dd, $J = 8.9, 2.4$ Hz), 2.51 (s, 3H). $^{13}\text{C}\{^1\text{H}\}$ NMR (126 MHz, CDCl_3) δ_{C} 152.8, 133.0, 132.7, 131.0, 129.1, 128.9, 126.8, 126.2, 117.8, 109.4, 21.5. IR (ATR): $\tilde{\nu} = 3272, 2980, 1604, 1481, 1390, 1351, 1270, 1250, 1208, 1172, 1146, 1126, 963, 929, 861, 822, 812, 649, 583, 529, 478, 434, 421, 408$. HRMS calcd. for $\text{C}_{11}\text{H}_9\text{O}^-$: 157.0659 $[\text{M}-\text{H}]^-$; found (ESI $^-$): 157.0661. Yield: 113 mg (82%). In accordance with with literature values.²⁴⁸

6-Fluoro-2-naphthol 11c

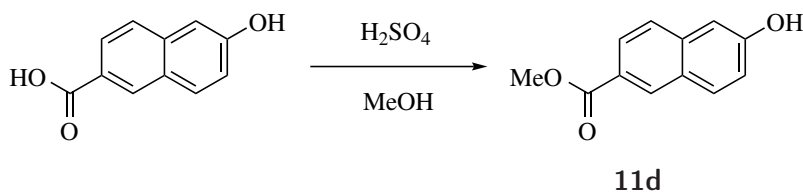
**11c**

Under an atmosphere of nitrogen, thionyl chloride (4.00 mL, 54.8 mmol) and a single drop of DMF were added to 4-fluorophenylacetic acid (4.97 g, 32.2 mmol). The reaction mixture was stirred at 50 °C for 1 h, then excess thionyl chloride was removed *in vacuo*. The resulting acid chloride was then added to a stirred suspension of aluminium chloride (6.18 g, 46.3 mmol) in dry dichloromethane (25 mL) at 0 °C. Ethynyltrimethylsilane (5.20 mL, 37.5 mmol) was then added dropwise to the resulting red solution over the course of 45 min. The resulting black solution was stirred at room temperature for 1 h. The reaction mixture was then poured onto ice and the organics were extracted with dichloromethane (3 × 80 mL). The combined organic fractions were then extracted with aqueous sodium hydroxide (2.5 M, 3 × 150 mL). The aqueous fractions were combined, acidified with concentrated hydrochloric acid (pH <1) and then extracted with dichloromethane (3 × 150 mL). The combined organic fractions were then dried with MgSO₄, filtered and the solvent was removed *in vacuo*. The resulting crude residue was purified by silica gel column chromatography (eluent: petroleum Et₂O: Et₂O, 3:1) to yield the title compound as an orange solid (823 mg, 4.92 mmol, 15%).

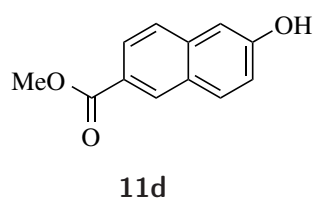
**11c**

mp/°C 114-115. ¹H NMR (500 MHz, CDCl₃) δ_H 7.68 (d, *J* = 8.7 Hz, 1H), 7.64 (m, 1H), 7.39 (dd, *J* = 9.8, 2.6 Hz, 1H), 7.22 (td, *J* = 8.8, 2.6 Hz, 1H), 7.18-7.10 (m, 2H), 5.17 (s, 1H). ¹³C{¹H} NMR (126 MHz, CDCl₃) δ_C 159.3 (d, *J* = 242.9 Hz), 152.8 (d, *J* = 2.6 Hz), 131.4, 129.2 (d, *J* = 8.8 Hz), 129.0 (d, *J* = 5.4 Hz), 128.4 (d, *J* = 8.6 Hz), 118.8, 116.8 (d, *J* = 25.3 Hz), 110.8 (d, *J* = 20.5 Hz), 109.7. ¹⁹F NMR (377 MHz, CDCl₃) δ_F -118.32 (ddd, *J* = 9.1, 8.9, 5.4 Hz). IR (ATR): $\tilde{\nu}$ = 3241, 1602, 1511, 1453, 1394, 1378, 1360, 1278, 1224, 1140, 1107, 958, 940, 870, 806, 680, 652, 578, 525, 481, 471, 425 HRMS calcd. for C₁₀H₆FO⁻: 161.0408 [M-H]⁻; found (ESI⁻): 161.0410. Yield: 823 mg (15%).

Methyl 6-hydroxy-2-naphthoate 11d

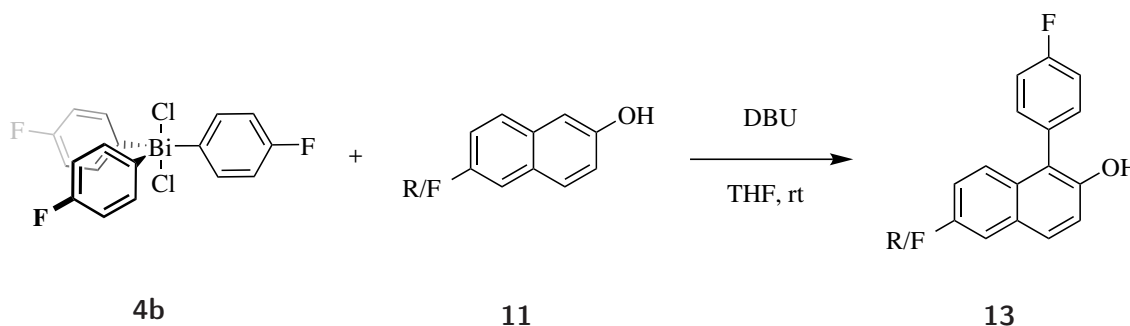


Concentrated sulfuric acid (0.10 mL) was added to a solution of 6-hydroxy-2-naphthoic acid (189 mg, 1.00 mmol) in methanol (2.0 mL). The solution was then heated under reflux for 24 h, allowed to cool to room temperature and then filtered by suction. The crude residue was then recrystallised from hot methanol to give the title compound as a white solid (152 mg, 0.75 mmol, 75%).



mp/°C 150-151. ^1H NMR (500 MHz, CDCl_3) δ_{H} 8.54 (d, $J = 1.7$ Hz, 1H), 8.01 (d, $J = 8.6$, 1.7 Hz 2H), 7.87 (d, $J = 8.6$ Hz, 1H), 7.71 (d, $J = 8.7$ Hz, 1H), 7.21-7.09 (m, 2H), 5.16 (s, 1H), 3.97 (s, 1H). $^{13}\text{C}\{^1\text{H}\}$ NMR (126 MHz, CDCl_3) δ_{C} 167.4, 155.4, 131.5, 131.0, 127.9, 126.5, 126.0, 125.3, 118.6, 109.5, 52.1. IR (ATR): $\tilde{\nu} = 3413$, 2951, 1681, 1627, 1572, 1509, 1482, 1434, 1351, 1302, 1278, 1241, 1202, 1154, 1129, 1100, 973, 956, 917, 879, 852, 810, 772, 755, 653, 605, 544, 522, 492, 478. HRMS calcd. for $\text{C}_{12}\text{H}_9\text{O}_3^-$: 201.0557 $[\text{M}-\text{H}]^-$; found (ESI $^-$): 201.0559. Yield: 823 mg (15%). In accordance with literature values.²⁴⁹

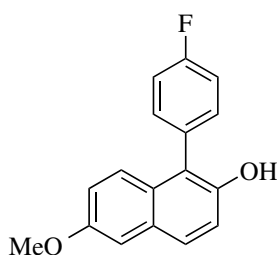
Synthesis of 1-(4-Fluorophenyl)-2-naphthol Derivatives



General Procedure: 6-substituted 2-naphthol (1 equiv.) and tri(4-fluorophenyl)bismuth dichloride **4b** (1.1 equiv.) were added to 0.6 mL of CDCl_3 , followed by DBU (2.5 equiv.). The yellow reaction mixture was allowed to stand at room temperature overnight and glacial acetic acid (1.0 mL) was added. The acetic acid and solvent were then removed *in vacuo*. The resulting crude residue was then purified by preparative TLC.

1-(4-Fluorophenyl)-6-methoxy-2-naphthol **13a**

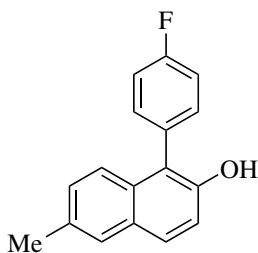
Following the general procedure, 6-methoxynaphthalen-2-ol (9.80 mg, 56.3 μmol), tri(4-fluorophenyl)bismuth dichloride (37.6 mg, 66.5 μmol) and DBU (25 μL) were reacted together in deuterated chloroform. The crude residue was purified by preparative TLC (eluent: toluene) to give the title compound as white solid (9.40 mg, 35.8 μmol , 64%).

**13a**

mp/°C 136-137. $^1\text{H NMR}$ (500 MHz, CDCl_3) δ_{H} 7.75-7.70 (m, 2H), 7.58-7.53 (m, 1H), 7.45-7.38 (m, 2H), 7.34-7.28 (m, 2H), 7.22 (d, $J = 8.9$ Hz, 1H), 7.14 (d, $J = 2.6$ Hz, 1H), 7.03 (dd, $J = 8.9$ Hz, 2.6 Hz, 1H), 3.91 (s, 3H). $^{13}\text{C}\{^1\text{H}\}$ NMR (126 MHz, CDCl_3) δ_{C} 155.9, 148.7, 132.9 (d, $J = 8.2$ Hz), 132.5, 130.9, 129.8, 128.8, 128.6, 128.3, 125.9, 119.1, 117.7, 116.6 (d, $J = 21.4$ Hz), 106.4, 55.4. $^{19}\text{F NMR}$ (377 MHz, CDCl_3) δ_{F} -113.18 (tt, $J = 8.6, 5.4$ Hz). IR (ATR): $\tilde{\nu} = 3531, 2956, 2927, 2857, 1724, 1601, 1507, 1460, 1427, 1375, 1347, 1272, 1239, 1215, 1181, 1157, 1121, 1092, 1072, 1035, 1016, 992, 953, 914, 859, 851, 839, 820, 777, 741, 705, 678, 651, 632, 591, 544, 525, 512, 469, 438, 408$. HRMS calcd. for $\text{C}_{17}\text{H}_{12}\text{FO}_2$: 267.0827 $[\text{M}-\text{H}]^-$; found (ESI $^-$): 267.0830. Yield: 9.40 mg (64%).

1-(4-Fluorophenyl)-6-methyl-2-naphthol 13b

Following GP-1, 6-methyl-2-naphthol (10.3 mg, 65.1 μmol), DBU (25 μL) and **4b** (48.8 mg, 86.3 μmol) were reacted together in deuterated chloroform (600 μL). The crude residue was purified by preparative TLC (eluent: cyclohexane:ethyl acetate, 3:2) to give the title compound as an orange solid (7.60 mg, 30.1 μmol , 46%).

**13b**

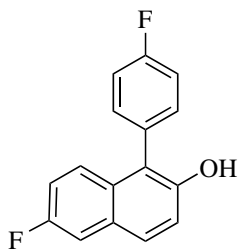
mp/°C 111-112. $^1\text{H NMR}$ (500 MHz, CDCl_3) δ_{H} 7.73 (d, $J = 8.9$ Hz, 1H), 7.63 (d, $J = 1.7$ Hz), 7.43-7.35 (m, 2H), 7.32-7.26 (m, 3H), 7.22 (dd, $J = 8.8, 1.9$ Hz, 1H), 7.20 (d, $J = 8.9$ Hz, 1H), 6.63 (s, 1H), 2.45 (s, 3H). $^{13}\text{C}\{^1\text{H}\}$ NMR (126 MHz, CDCl_3) δ_{C} 162.3 (d, $J = 243.5$ Hz), 150.6, 133.0 (d, $J = 8.1$ Hz), 132.6, 132.1 (d, $J = 3.3$ Hz), 131.9, 129.0, 128.7, 128.6, 126.9, 124.1, 120.4, 118.0, 115.4 (d, $J = 21.6$ Hz), 20.3. $^{19}\text{F NMR}$ (377 MHz, CDCl_3) δ_{F} -117.00 (m). IR (ATR): $\tilde{\nu} = 3411, 2924, 2855, 1669, 1601, 1505, 1476, 1378, 1344, 1307, 1276, 1221, 1158, 1145, 1091, 1057, 1015, 992, 951, 881, 833, 819, 776, 722, 677, 631, 580, 539, 526, 496, 473, 437, 407$. HRMS calcd. for $\text{C}_{17}\text{H}_{12}\text{FO}$: 251.0878 $[\text{M}-\text{H}]^-$; found (ESI $^-$): 251.0879. Yield: 7.6 mg (46%).

1-(4-Fluorophenyl)-2-naphthol 10a

Following GP-1, 2-naphthol (10.0 mg, 69.4 μmol), DBU (27 μL) and **4b** (45.0 mg, 79.6 μmol) were reacted together in deuterated chloroform (0.60 mL). The crude residue was purified by preparative TLC (eluent: toluene) to give the title compound as a white solid (14.0 mg, 58.8 μmol , 85%).

6-Fluoro-1-(4-fluorophenyl)-2-naphthol 13c

Following GP-1, 6-fluoro-2-naphthol (10.4 mg, 64.1 μmol), DBU (23 μL) and **4b** (39.1 mg, 69.2 μmol) were reacted together in deuterated chloroform (600 μL). The crude residue was purified by preparative TLC (eluent: cyclohexane:ethyl acetate, 9:1) to give the title compound as a yellow oil (10.2 mg, 39.8 μmol , 62%).

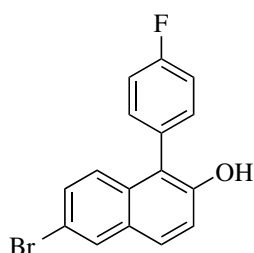


13c

mp/°C 136-137. ^1H NMR (500 MHz, CDCl_3) δ_{H} 7.73 (d, $J = 8.9$ Hz, 1H), 7.46 (dd, $J = 9.9, 2.7$ Hz, 1H), 7.39 (m, 1H), 7.37-7.32 (m, 2H), 7.26-7.22 (m, 3H), 7.12 (ddd, $J = 9.3, 8.4, 2.7$ Hz, 1H). $^{13}\text{C}\{^1\text{H}\}$ NMR (126 MHz, CDCl_3) δ_{C} 163.0 (d, $J = 248.1$ Hz), 150.4, 133.5, 133.2 (d, $J = 8.1$ Hz), 131.7 (d, $J = 8.1$ Hz), 130.1 (d, $J = 3.5$ Hz), 129.9, 129.1, 128.2, 126.8, 124.5, 123.6, 120.1, 116.9 (d, $J = 21.4$ Hz). ^{19}F NMR (471 MHz, CDCl_3) δ_{F} -113.15 (tt, $J = 8.5, 5.6$ Hz), -118.87 (td, $J = 8.9, 5.4$ Hz). IR (ATR): $\tilde{\nu} = 3544, 2924, 1608, 1520, 1507, 1375, 1230, 1169, 1106, 961, 867, 836, 816, 631, 580, 498$. HRMS calcd. for $\text{C}_{16}\text{H}_9\text{F}_2\text{O}^-$: 255.0627 [M-H] $^-$; found (ESI $^-$): 255.0638.

6-Bromo-1-(4-fluorophenyl)-2-naphthol 13d

Following GP-1, 6-bromo-2-naphthol (27.0 mg, 121 μmol), DBU (51 μL) and **4b** (83.6 mg, 148 μmol) were reacted in deuterated chloroform (600 μL). The crude residue was purified by preparative TLC (eluent: cyclohexane:ethyl acetate, 9:1) to give the title compound as a yellow solid (33.8 mg, 107 μmol , 88%).

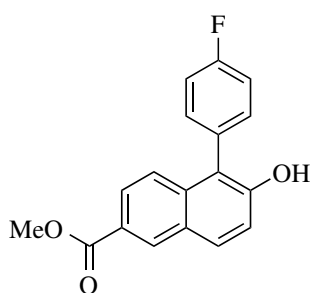


13d

mp/°C 141-142. ^1H NMR (500 MHz, CDCl_3) δ_{H} 7.74 (d, $J = 2.1$ Hz, 1H), 7.29 (dd, $J = 9.0, 2.1$ Hz, 1H), 7.22 (d, $J = 8.9$ Hz, 1H), 7.07 (d, $J = 8.9$ Hz, 1H), 6.79-6.68 (m, 4H), 4.65 (s, 1H). $^{13}\text{C}\{^1\text{H}\}$ NMR (126 MHz, CDCl_3) δ_{C} 163.4 (d, $J = 247.7$ Hz), 151.5, 133.3 (d, $J = 8.1$ Hz), 132.8, 130.9, 130.8, 130.5, 130.0 (d, $J = 3.3$ Hz), 129.5, 126.9, 120.8, 119.1, 117.9, 117.1 (d, $J = 21.6$ Hz). ^{19}F NMR (471 MHz, CDCl_3) δ_{F} -113.02 (m). IR (ATR): $\tilde{\nu} = 2920, 1586, 1509, 1462, 1378, 1308, 1270, 1222, 1144, 1092, 948, 934, 874, 859, 838, 809, 667, 549, 528, 504, 425$. HRMS calcd. for $\text{C}_{16}\text{H}_9\text{FBrO}^-$: 314.9826 [M-H] $^-$; found (ESI $^-$): 314.9832. Yield: 33.6 mg (88%).

Methyl 5-(4-fluorophenyl)-6-hydroxy-2-naphthoate 13e

Following GP-1, methyl 6-hydroxy-2-naphthoate (12.7 mg, 62.8 μmol), tri(4-fluorophenyl)-bismuth dichloride (43.8 mg, 77.5 μmol) and DBU (26 μL) were reacted in deuterated MeCN (600 μL). The crude residue was purified by preparative TLC (eluent: cyclohexane:ethyl acetate, 3:2) to give the title compound as a pale orange solid (9.9 mg, 33.4 μmol , 53%).

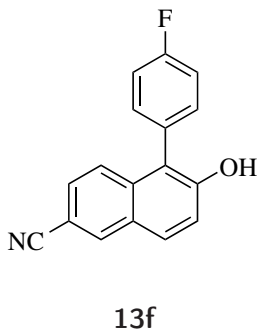


13e

mp/°C 146-147. ^1H NMR (500 MHz, CDCl_3) δ_{H} 8.59 (d, $J = 1.8$ Hz, 1H), 7.96-7.93 (m, 2H), 7.45-7.37 (m, 3H), 7.36-7.31 (m, 3H), 5.24 (s, 1H), 3.99 (s, 3H). $^{13}\text{C}\{^1\text{H}\}$ NMR (126 MHz, CDCl_3) δ_{C} 167.3, 163.0 (d, $J = 249$ Hz), 152.4, 135.8, 133.0 (d, $J = 8$ Hz), 131.34, 131.32, 129.3 (d, $J = 4$ Hz), 128.0, 126.1, 125.1, 124.6, 120.1, 118.3, 117.0 (d, $J = 21$ Hz), 52.2. ^{19}F NMR (471 MHz, CDCl_3) δ_{F} -112.43 (m). IR (ATR): $\tilde{\nu} = 3314, 2921, 1683, 1622, 1484, 1440, 1322, 1284, 1214, 1158, 1103, 983, 828, 815, 801, 758, 746, 554, 533, 510$. HRMS calcd. for $\text{C}_{18}\text{H}_{12}\text{FO}_3^-$: 295.0776 [M-H] $^-$; found (ESI $^-$): 295.0788. Yield: 9.9 mg (53%).

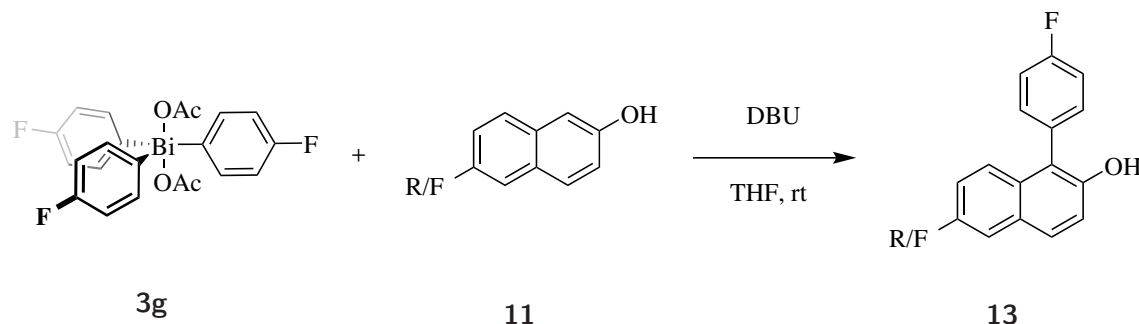
1-(4-Fluorophenyl)-6-hydroxy-2-naphthonitrile **13f**

Following GP-1, 6-hydroxy-2-naphthonitrile (9.70 mg, 57.3 μmol), tri(4-fluorophenyl)bismuth dichloride (36.8 mg, 65.1 μmol) and DBU (26 μL) were reacted in deuterated MeCN (600 μL). The crude residue was purified by preparative TLC (eluent: cyclohexane:ethyl acetate, 3:2) to yield the title compound as a white solid (12.0 mg, 45.6 μmol , 80%).



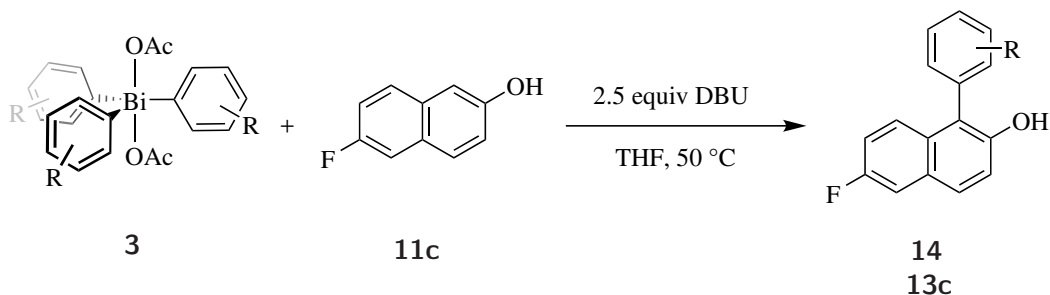
mp/ $^{\circ}\text{C}$ 185-186. ^1H NMR (500 MHz, CDCl_3) δ_{H} 8.32 (d, $J = 1.7$ Hz, 1H), 7.93 (d, $J = 8.7$ Hz, 1H), 7.52 (dd, $J = 8.9, 1.7$ Hz, 1H), 7.46 (d, $J = 8.8$ Hz, 1H), 7.40-7.35 (m, 3H), 7.35-7.28 (m, 2H), 7.23 (s, 1H). $^{13}\text{C}\{^1\text{H}\}$ NMR (126 MHz, CDCl_3) δ_{C} 162.5 (d, $J = 244$ Hz), 154.2, 135.5, 134.4, 133.0 (d, $J = 8$ Hz), 130.8 (d, $J = 3$ Hz), 130.1, 127.5, 127.0, 125.5, 121.0, 119.8, 119.4, 115.7 (d, $J = 22$ Hz), 106.0. ^{19}F NMR (471 MHz, CDCl_3) δ_{F} -116.23 (m). IR (ATR): $\tilde{\nu} = 3404, 2921, 2851, 2226, 1616, 1508, 1468, 1384, 1278, 1218, 1158, 1137, 1091, 898, 831, 814, 680, 545, 517, 486, 432, 406$. HRMS calcd. for $\text{C}_{17}\text{H}_9\text{FNO}^-$: 262.0674 $[\text{M}-\text{H}]^-$; found (ESI $^-$): 262.0681. Yield: 12.0 mg (80%).

Competitive Hammett Studies



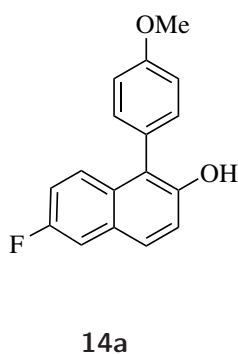
6-Fluoro-2-naphthol (**11c**) (13.2 mg, 81.7 μmol) and a 6-substituted 2-naphthol (81.7 μmol) were added to an NMR tube and dissolved in CDCl_3 (0.7 mL). A time-zero ^1H NMR spectrum was taken to determine the initial ratio of the two substrates. Tri(4-fluorophenyl)bismuth diacetate **3g** (10.0 mg, 16.3 μmol) was then added, followed by DBU (61.1 μL , 408 μmol). The orange reaction mixture shaken, then allowed to stand for 24 h at room temperature. The reaction was then quenched with glacial acetic acid (1.0 mL) and concentrated under reduced pressure. The product ratio was established using ^{19}F NMR spectroscopy. The integration ratio of the two different aryl-fluorine peaks corresponds to the ratio of the two different arylated products. The initial time-zero ^1H NMR was then used to back calculate any differences between the initial 6-substituted-2-naphthol concentrations.

Variation of Aryl Groups on Bi-centre



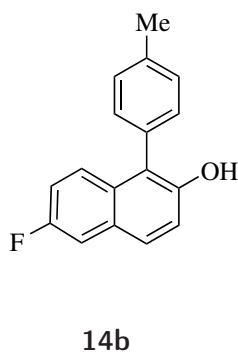
$\text{Ar}_3\text{BiOAc}_2$ (20.4 μmol) and 6-fluoro-2-naphthol (3.0 mg, 19 μmol) were added to an NMR tube with 0.6 mL of a solution of THF/ C_6D_6 (9/1). A ^1H NMR spectrum was collected, to acquire the initial ratios that are necessary for the kinetic calculations. The solution was heated to 50 °C in the NMR machine and allowed to equilibrate for 5 min. DBU (5.5 μL , 37 μmol) have been added to the solution and the kinetic acquisition was started. The data collection has been stopped upon full conversion of the $\text{Ar}_3\text{BiOAc}_2$.

6-Fluoro-1-(4-methoxyphenyl)naphthalen-2-ol 14a

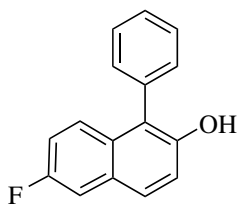


^1H NMR (400 MHz, CDCl_3) δ_{H} 7.72 (d, $J = 8.9$ Hz, 1H), 7.45 – 7.36 (m, 2H), 7.35 – 7.30 (m, 2H), 7.28 (dd, $J = 9.0, 0.8$ Hz, 1H), 7.15 – 7.10 (m, 3H), 5.10 (d, $J = 0.5$ Hz, 1H), 3.91 (s, 3H). $^{13}\text{C}\{^1\text{H}\}$ NMR (126 MHz, CDCl_3) δ_{C} 160.0, 159.3 (d, $J = 243.3$ Hz), 150.0 (d, $J = 2.6$ Hz), 132.4, 130.7, 129.5 (d, $J = 8.7$ Hz), 128.5 (d, $J = 5.1$ Hz), 127.2 (d, $J = 8.6$ Hz), 125.6, 121.1, 118.6, 116.6 (d, $J = 24.9$ Hz), 115.3, 111.1 (d, $J = 20.4$ Hz), 55.6. ^{19}F NMR (377 MHz, CDCl_3) δ_{F} -119.45 (ddd, $J = 8.9, 8.9, 5.5$ Hz). IR (ATR): $\tilde{\nu} = 3533, 1608, 1521, 1376, 1287, 1246, 1176, 1107, 1032, 961, 867, 832, 584$. HRMS calcd. for $\text{C}_{16}\text{H}_9\text{F}_2\text{O}^-$: 267.0827 [M-H] $^-$; found (ESI $^-$): 267.0830.

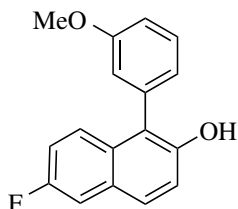
6-Fluoro-1-(p-tolyl)naphthalen-2-ol 14b



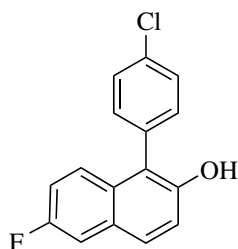
^1H NMR (400 MHz, CDCl_3) δ_{H} 7.74 – 7.70 (m, 1H), 7.45 – 7.37 (m, 4H), 7.32 – 7.27 (m, 3H), 7.11 (ddd, $J = 9.3, 8.3, 2.7$ Hz, 1H), 5.10 (d, $J = 0.5$ Hz, 1H), 2.48 (s, 3H). $^{13}\text{C}\{^1\text{H}\}$ NMR (126 MHz, CDCl_3) δ_{C} 159.3 (d, $J = 243.2$ Hz), 149.8 (d, $J = 2.6$ Hz), 138.7, 131.0, 130.7, 130.6, 130.5, 129.5 (d, $J = 8.9$ Hz), 128.5 (d, $J = 5.0$ Hz), 127.2 (d, $J = 8.6$ Hz), 121.4, 118.6, 116.5 (d, $J = 24.8$ Hz), 111.1 (d, $J = 20.4$ Hz), 21.5. ^{19}F NMR (377 MHz, CDCl_3) δ_{F} -119.43 (ddd, $J = 9.0, 9.0, 5.6$ Hz). IR (ATR): $\tilde{\nu} = 3533, 1608, 1521, 1376, 1287, 1246, 1176, 1107, 1032, 961, 867, 832, 584$. HRMS calcd. for $\text{C}_{17}\text{H}_{12}\text{FO}^-$: 251.0878 [M-H] $^-$; found (ESI $^-$): 251.0876.

6-Fluoro-1-phenylnaphthalen-2-ol 14c**14c**

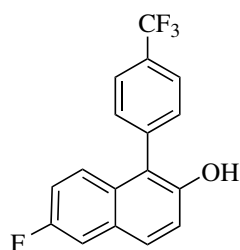
^1H NMR (400 MHz, CDCl_3) δ_H 7.74 (d, $J = 8.9$ Hz, 1H), 7.65 – 7.56 (m, 2H), 7.56 – 7.49 (m, 1H), 7.45 – 7.36 (m, 4H), 7.29 (dd, $J = 8.9, 0.8$ Hz, 1H), 7.12 (ddd, $J = 9.3, 8.3, 2.7$ Hz, 1H), 5.07 (s, 1H). $^{13}\text{C}\{^1\text{H}\}$ NMR (126 MHz, CDCl_3) δ_C 159.3 (d, $J = 243.1$ Hz), 149.7 (d, $J = 2.6$ Hz), 134.0, 131.2, 130.4, 129.9, 129.5 (d, $J = 8.9$ Hz), 128.8, 128.7 (d, $J = 5.2$ Hz), 127.1 (d, $J = 8.6$ Hz), 121.4, 118.7, 116.6 (d, $J = 24.7$ Hz), 111.2 (d, $J = 20.5$ Hz). ^{19}F NMR (377 MHz, CDCl_3) δ_F -119.27 (ddd, $J = 8.9, 8.9, 5.5$ Hz). IR (ATR): $\tilde{\nu} = 1608, 1588, 1519, 1377, 1233, 1171, 1142, 1108, 960, 867, 821, 810, 758, 703, 667, 592$. HRMS calcd. for $\text{C}_{16}\text{H}_{10}\text{FO}^-$: 237.0721 [M-H] $^-$; found (ESI $^-$): 237.0750.

6-Fluoro-1-(3-methoxyphenyl)naphthalen-2-ol 14d**14d**

^1H NMR (400 MHz, CDCl_3) δ_H 7.78 – 7.74 (m, 1H), 7.53 (ddd, $J = 8.4, 7.4, 0.4$ Hz, 1H), 7.48 – 7.42 (m, 2H), 7.31 (dd, $J = 9.0, 0.8$ Hz, 1H), 7.15 (ddd, $J = 9.3, 8.3, 2.7$ Hz, 1H), 7.08 (ddd, $J = 8.4, 2.6, 1.0$ Hz, 1H), 7.01 (ddd, $J = 7.4, 1.5, 1.0$ Hz, 1H), 6.96 (dd, $J = 2.7, 1.5$ Hz, 1H), 5.17 (s, 1H), 3.88 (s, 3H). $^{13}\text{C}\{^1\text{H}\}$ NMR (126 MHz, CDCl_3) δ_C 160.7, 159.3 (d, $J = 243.4$ Hz), 149.6 (d, $J = 2.5$ Hz), 135.3, 131.0, 130.2, 129.5 (d, $J = 8.7$ Hz), 128.7 (d, $J = 5.1$ Hz), 127.2 (d, $J = 8.4$ Hz), 123.2, 121.3, 118.6, 116.7 (d, $J = 24.9$ Hz), 116.3, 114.6, 111.2 (d, $J = 20.4$ Hz), 55.5. ^{19}F NMR (377 MHz, CDCl_3) δ_F -119.24 (ddd, $J = 8.9, 8.9, 5.5$ Hz). IR (ATR): $\tilde{\nu} = 3521, 1607, 1587, 1519, 1486, 1430, 1378, 1345, 1316, 1284, 1228, 1206, 1183, 1160, 1107, 1045, 961, 867, 787, 706, 664, 585, 508, 472, 441, 426, 414$. HRMS calcd. for $\text{C}_{17}\text{H}_{12}\text{FO}_2^-$: 267.0827 [M-H] $^-$; found (ESI $^-$): 267.0827.

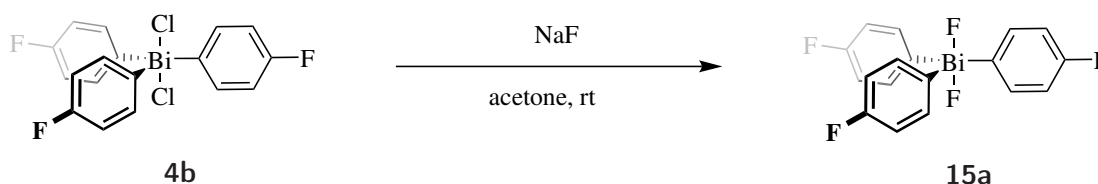
1-(4-Chlorophenyl)-6-fluoronaphthalen-2-ol 14e**14e**

^1H NMR (400 MHz, CDCl_3) δ_H 7.74 (d, $J = 8.9$ Hz, 1H), 7.61 – 7.56 (m, 2H), 7.44 (dd, $J = 9.6, 2.7$ Hz, 1H), 7.38 – 7.28 (m, 4H), 7.13 (ddd, $J = 9.3, 8.3, 2.7$ Hz, 1H), 4.94 (d, $J = 0.5$ Hz, 1H). $^{13}\text{C}\{^1\text{H}\}$ NMR (126 MHz, CDCl_3) δ_C 159.2 (d, $J = 243.7$ Hz), 149.6 (d, $J = 2.6$ Hz), 134.8, 132.5, 132.4, 130.1, 130.0, 129.4 (d, $J = 8.9$ Hz), 129.0 (d, $J = 5.2$ Hz), 126.7 (d, $J = 8.4$ Hz), 120.1, 118.6, 116.8 (d, $J = 24.8$ Hz), 111.2 (d, $J = 20.5$ Hz). ^{19}F NMR (377 MHz, CDCl_3) δ_F -118.91 (ddd, $J = 8.8, 8.8, 5.4$ Hz). IR (ATR): $\tilde{\nu} = 3536, 1676, 1607, 1489, 1376, 1343, 1262, 1233, 1166, 1142, 1089, 1016, 961, 867, 826, 691, 671, 605, 471, 424$. HRMS calcd. for $\text{C}_{16}\text{H}_9\text{ClFO}^-$: 271.0331 [M-H] $^-$; found (ESI $^-$): 271.0333.

6-Fluoro-1-(4-(trifluoromethyl)phenyl)naphthalen-2-ol **14f****14f**

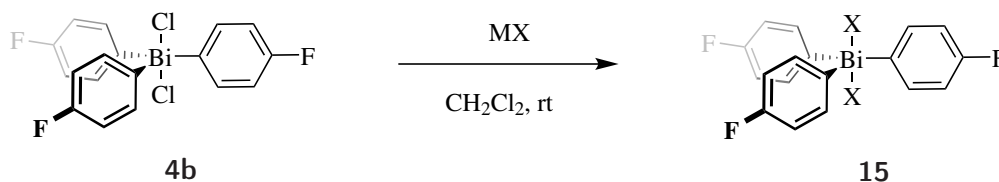
^1H NMR (400 MHz, CDCl_3) δ_{H} 7.89 – 7.84 (m, 2H), 7.77 (d, $J = 8.9$ Hz, 1H), 7.59 – 7.54 (m, 2H), 7.45 (dd, $J = 9.5$, 2.7 Hz, 1H), 7.34 – 7.27 (m, 2H), 7.14 (ddd, $J = 9.3$, 8.2, 2.7 Hz, 1H), 4.89 (s, 1H). $^{13}\text{C}\{^1\text{H}\}$ NMR (126 MHz, CDCl_3) δ_{C} 159.4 (d, $J = 244.2$ Hz), 149.6 (d, $J = 2.5$ Hz), 138.4, 131.8, 131.0 (q, $J = 32.7$ Hz), 130.0, 129.6 (d, $J = 8.8$ Hz), 129.4 (d, $J = 5.0$ Hz), 126.7 (q, $J = 6.2$, 2.5 Hz), 124.1 (q, $J = 272.4$ Hz), 120.1, 118.9, 117.1 (d, $J = 24.9$ Hz), 111.4 (d, $J = 20.5$ Hz). ^{19}F NMR (377 MHz, CDCl_3) δ_{F} -62.68 (s, 3F), -118.62 (ddd, $J = 8.8$, 8.8, 5.3 Hz, 1F). IR (ATR): $\tilde{\nu} = 1608$, 1523, 1380, 1324, 1234, 1167, 1126, 1106, 1066, 1019, 963, 841, 676, 613. HRMS calcd. for $\text{C}_{17}\text{H}_9\text{F}_4\text{O}^-$: 305.0595 $[\text{M}-\text{H}]^-$; found (ESI $^-$): 305.0599.

Synthesis of Tri(4-fluorophenyl)bismuth(V) Species



In a 50 mL round-bottom flask tri(4-fluorophenyl)bismuth dichloride **4b** (1.13 g, 2.00 mmol) was dissolved in acetone (15 mL). In another 50 mL flask NaF (420 mg, 10.0 mmol, 5.00 equiv.) was dissolved in 15 mL of water and this solution was added to the previous flask. The resulting mixture was allowed to stir for 1 h, then acetone was removed *in vacuo*. CH_2Cl_2 was added and the mixture was extracted with water (3×20 mL). The organic phase removed *in vacuo* and the resulting solid recrystallised from cyclohexane to yield the desired product (1.02 g, 1.92 mmol, 96%) as a white solid. mp/ $^\circ\text{C}$ 111-112. ^1H NMR (500 MHz, CDCl_3) δ_{H} 8.22 (dd, $J = 9.1$, 5.4 Hz, 6H), 7.36 (dd, $J = 8.7$, 5.5 Hz, 6H). $^{13}\text{C}\{^1\text{H}\}$ NMR (126 MHz, CDCl_3) δ_{C} 165.1 (d, $J = 253.4$ Hz), 147.7 (td, $J = 10.3$, 2.9 Hz), 136.3 (dt, $J = 8.1$, 4.0 Hz), 118.7 (d, $J = 21.8$ Hz). ^{19}F NMR (471 MHz, CDCl_3) δ_{F} -106.13– -106.34 (m, 3F), -157.81 (s, 2F). IR (ATR): $\tilde{\nu} = 1573$, 1476, 1392, 1216, 1155, 1010, 828, 802, 572, 500. HRMS calcd. for $\text{C}_{18}\text{H}_{12}\text{BiF}_4^+$: 513.0673 $[\text{M}-\text{F}]^+$; found (ESI $^+$): 513.0662.

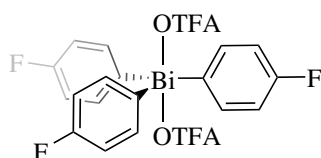
Salt Metathesis of Tri(4-fluorophenyl)bismuth Dichloride



X:	F	OTFA	NO_3	OTf	BF_4	ClO_4	OTs
	15a	15b	15c	15d	15e	15f	15g
	96%	99%	99%	99%	99%	99%	99%

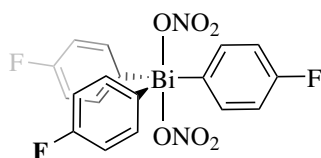
General Protocol: Tri(4-fluorophenyl)bismuth dichloride **4b** (250 mg, 0.440 mmol) was added to CH₂Cl₂ (5.0 mL). To the solution the corresponding silver salt was added (2.5 equiv.) and the suspension was allowed to stir under the exclusion of light for 1 h. The reaction mixture was filtered and the solvent removed *in vacuo*, resulting in a white to off-white solid as the desired product.

Tri(4-fluorophenyl)bismuth bis(2,2,2-trifluoroacetate) **15b**

**15b**

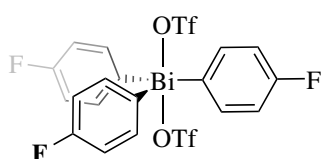
mp/°C 138-140. ¹H NMR (500 MHz, CDCl₃) δ_H 8.19 – 8.00 (m, 1H), 7.50 – 7.35 (m, 1H). ¹³C{¹H} NMR (126 MHz, CDCl₃) δ_C 164.8 (d, *J* = 256.0 Hz), 162.0 (d, *J* = 39.1 Hz), 149.7, 136.5 (d, *J* = 8.3 Hz), 119.8 (d, *J* = 22.6 Hz), 115.5 (q, *J* = 288.9 Hz). ¹⁹F NMR (471 MHz, CDCl₃) δ_F -74.86 (s, 6F), -103.80 (m, 3F). IR (ATR): $\tilde{\nu}$ = 1677, 1571, 1480, 1424, 1234, 1203, 1170, 1159, 997, 823, 729, 502. HRMS calcd. for C₂₀H₁₂BiF₆O₂⁺: 607.0540 [M-OTFA]⁺; found (ESI⁺): 607.0519.

Tri(4-fluorophenyl)bismuth dinitrate **15c**

**15c**

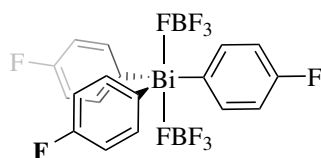
mp/°C 156-157. ¹H NMR (500 MHz, CDCl₃) δ_H 8.22 – 7.91 (m, 1H), 7.68 – 7.35 (m, 1H). ¹³C{¹H} NMR (126 MHz, CDCl₃) δ_C 165.0 (d, *J* = 257.0 Hz), 151.9 (d, *J* = 3.0 Hz), 136.4 (d, *J* = 8.4 Hz), 120.2 (d, *J* = 22.5 Hz). ¹⁹F NMR (471 MHz, CDCl₃) δ_F -102.90 (tt, *J* = 8.2, 4.2 Hz). IR (ATR): $\tilde{\nu}$ = 1573, 1508, 1480, 1394, 1266, 1233, 1161, 995, 822, 570, 501. HRMS calcd. for C₁₈H₁₂BiF₃NO₃⁺: 556.0568 [M-NO₃]⁺; found (ESI⁺): 556.0537.

Tri(4-fluorophenyl)bismuth bis(2,2,2-trifluoroacetate) **15d**

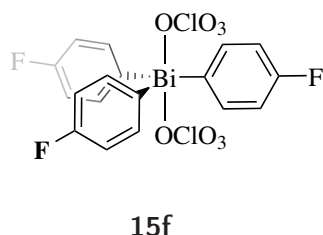
**15d**

mp/°C 188-190. ¹H NMR (500 MHz, CDCl₃) δ_H 8.37 – 7.93 (m, 1H), 7.77 – 7.43 (m, 1H). ¹³C{¹H} NMR (126 MHz, CDCl₃) δ_C 165.6 (d, *J* = 258.8 Hz), 158.6 (q, *J* = 58.7 Hz), 149.5, 137.0 (d, *J* = 8.8 Hz), 120.9 (d, *J* = 22.7 Hz), 118.6 (q, *J* = 318.1 Hz). ¹⁹F NMR (471 MHz, CDCl₃) δ_F -77.42 (s, 6F), -100.13 (m, 3F). IR (ATR): $\tilde{\nu}$ = 2364, 1574, 1483, 1396, 1284, 1235, 1161, 1027, 1002, 824, 635, 572, 500. HRMS calcd. for C₁₉H₁₂BiF₆O₃S⁺: 643.0210 [M-OTf]⁺; found (ESI⁺): 643.0177.

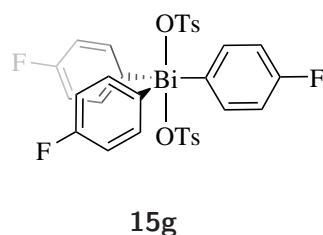
Tri(4-fluorophenyl)bismuth bis(tetrafluoroborate) **15e**

**15e**

mp/°C 220-221. ¹H NMR (500 MHz, CDCl₃) δ_H 8.19 – 7.99 (m, 1H), 7.51 (dd, *J* = 8.6, 8.5 Hz, 1H). ¹³C{¹H} NMR (126 MHz, CDCl₃) δ_C 165.5 (d, *J* = 256.9 Hz), 148.1 (d, *J* = 2.8 Hz), 136.1 (d, *J* = 9.0 Hz), 120.3 (d, *J* = 22.6 Hz). ¹⁹F NMR (471 MHz, CDCl₃) δ_F -102.37 (m, 3F), -146.19/-146.25 (d, *J* = 25.3 Hz, 2F). IR (ATR): $\tilde{\nu}$ = 2358, 1575, 1481, 1395, 1232, 1161, 1062, 1006, 827, 573, 501. HRMS calcd. for C₁₈H₁₂BBiF₇⁺: 581.0724 [M-OTf]⁺; found (ESI⁺): 581.0742.

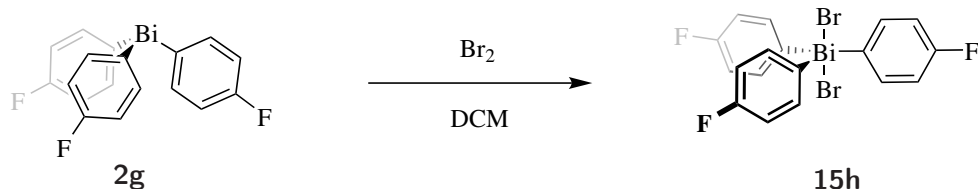
Tri(4-fluorophenyl)bismuth bis(perchlorate) **15f**

mp/°C 220-221. $^1\text{H NMR}$ (500 MHz, CDCl_3) δ_{H} 8.22 – 8.05 (m, 1H), 7.67 – 7.53 (m, 1H). $^{13}\text{C}\{^1\text{H}\}$ NMR (126 MHz, CDCl_3) δ_{C} 165.6 (q, $J = 258.2$ Hz), 149.3, 137.1 (d, $J = 9.1$ Hz), 121.0 (d, $J = 23.1$ Hz). $^{19}\text{F NMR}$ (471 MHz, CDCl_3) δ_{F} -100.22 (m). IR (ATR): $\tilde{\nu} = 2358, 1573, 1482, 1396, 1236, 1163, 1099, 1002, 824, 624, 501$. HRMS calcd. for $\text{C}_{18}\text{H}_{12}\text{BiClF}_3\text{O}_4^+$: 593.0175 $[\text{M}-\text{ClO}_4]^+$; found (ESI $^+$): 593.0163.

Tri(4-fluorophenyl)bismuth bis(4-methylbenzenesulfonate) **15g**

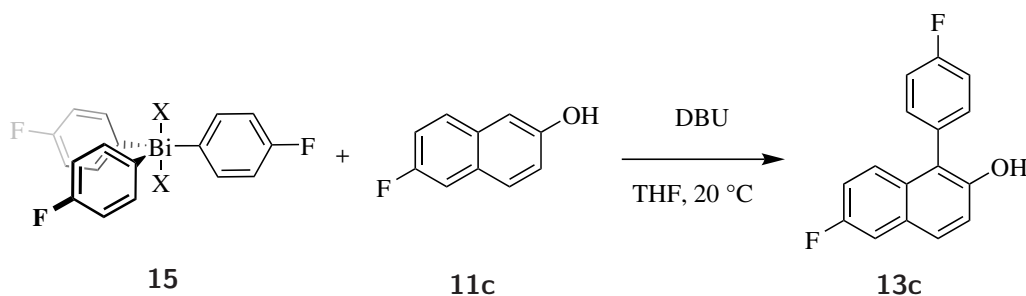
mp/°C 199-200. $^1\text{H NMR}$ (500 MHz, CDCl_3) δ_{H} 8.39 – 8.27 (m, 6H), 7.64 – 7.52 (m, 6H), 7.42 (d, $J = 8.0$ Hz, 4H), 7.23 (d, $J = 8.0$ Hz, 4H), 2.50 (s, 6H). $^{13}\text{C}\{^1\text{H}\}$ NMR (126 MHz, CDCl_3) δ_{C} 164.9 (d, $J = 256.1$ Hz), 151.0, 142.2, 139.0, 137.2 (d, $J = 9.0$ Hz), 129.2, 126.1, 119.7 (d, $J = 22.0$ Hz), 21.5. $^{19}\text{F NMR}$ (471 MHz, CDCl_3) δ_{F} -103.26 (tt, $J = 8.2, 5.0$ Hz). IR (ATR): $\tilde{\nu} = 2361, 2340, 1572, 1482, 1379, 1281, 1232, 1161, 1095, 938, 814, 679, 568, 503$. HRMS calcd. for $\text{C}_{25}\text{H}_{19}\text{BiF}_3\text{O}_3\text{S}^+$: 665.0805 $[\text{M}-\text{ClO}_4]^+$; found (ESI $^+$): 665.4624.

Oxidation of Tri(4-fluorophenyl) bismuth with Bromine



Tri(4-fluorophenyl) bismuth **2g** (250 mg, 505 μmol) was dissolved in 20.0 mL of CH_2Cl_2 . At 0 °C bromine (26 μL , 51 μmol) was added dropwise. The reaction mixture was washed with $\text{KHCO}_3(\text{aq})$. The organic layer dried with MgSO_4 and the solvent removed *in vacuo* to yield the title compound as a white solid (304 mg, 465 μmol , 92%). mp/°C 112-114. $^1\text{H NMR}$ (500 MHz, CDCl_3) δ_{H} 8.55 – 8.48 (m, 1H), 7.36 – 7.29 (m, 1H). $^{13}\text{C}\{^1\text{H}\}$ NMR (126 MHz, CDCl_3) δ_{C} 164.4 (d, $J = 254.4$ Hz), 149.5 (d, $J = 2.7$ Hz), 136.8 (d, $J = 8.3$ Hz), 118.8 (d, $J = 22.3$ Hz). $^{19}\text{F NMR}$ (471 MHz, CDCl_3) δ_{F} -106.34 (tt, $J = 8.6, 5.2$ Hz). IR (ATR): $\tilde{\nu} = 3083, 2359, 1571, 1477, 1389, 1230, 1158, 1002, 818, 564, 497$. HRMS calcd. for $\text{C}_{18}\text{H}_{12}\text{BiBrF}_3^+$: 572.9873 $[\text{M}-\text{ClO}_4]^+$; found (ESI $^+$): 572.9798.

Kinetic Investigation of the Influence of Counter Ions



Ar_3BiX_2 (20.4 μmol) and 6-fluoro-2-naphthol **11c** (3.0 mg, 19 μmol) were added to an NMR tube with 0.6 mL of a solution of THF/ C_6D_6 (9/1). This solution has been used in a ^1H NMR spectroscopy for a back calculation of the actual amounts used for the kinetic calculations. The solution was allowed to reach temperature (20 $^\circ\text{C}$) in the NMR machine and allowed to acclimatise for 5 min. DBU (5.5 μL , 37 μmol) was added to the solution, the reaction mixture was shaken thoroughly and the kinetic acquisition was started. The data collection was stopped upon full conversion of the 6-fluoro-2-naphthol.

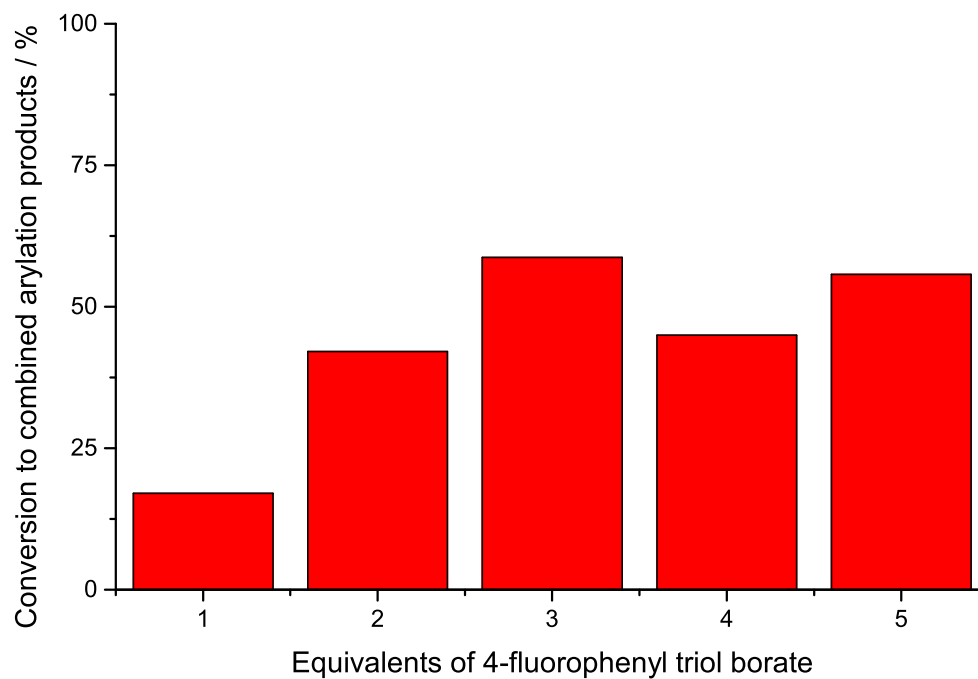
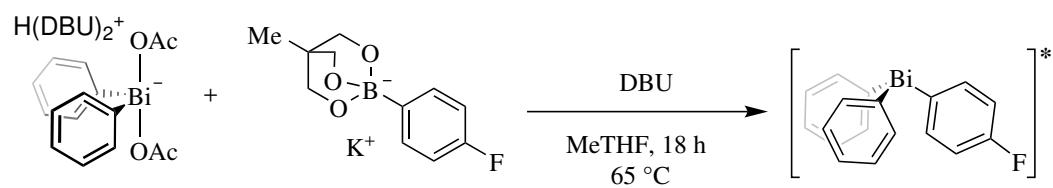
Re-arylation of $[\text{Ph}_2\text{BiOAc}_2]^-$

The aryl boron reagents used in this investigation have been prepared according the known procedures.^{169,250–253,253–257}

$\text{Ph}_3\text{Bi}(\text{OAc})_2$ **3f** (11.4 mg, 20.4 μmmol), 6-fluoro-2-naphthol (3.3 mg, 20.4 μmmol), DBU (5.5 μL , 37 μmmol) and 4-fluorophenyl-boron species (40.8 μmmol) have been added to THF (2.0 mL) and allowed to stir for 18 h at 65 $^\circ\text{C}$. In the following an aliquot (0.5 mL) was taken and added to CDCl_3 (0.5 mL) was added and analysed by ^{19}F NMR spectroscopy.

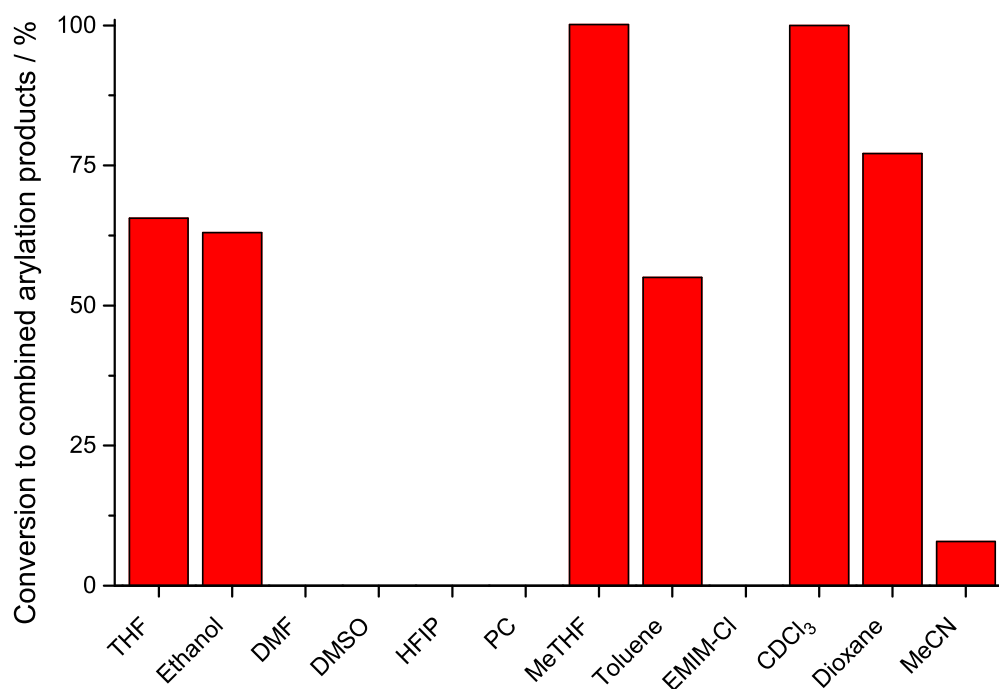
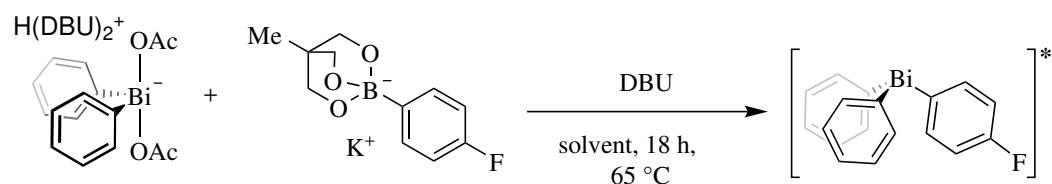
Variation of Equivalent of 4-Fluorophenyl Triol Borate

$\text{Ph}_3\text{Bi}(\text{OAc})_2$ **3f** (11.4 mg, 20.4 μmmol), 6-fluoro-2-naphthol (3.3 mg, 20 μmmol), DBU (5.5 μL , 37 μmmol) and 1-(4-fluorophenyl)-triol borate (varying equivalents) were added to THF (2.0 mL) and allowed to stir for 18 h at 65 $^\circ\text{C}$. In the following an aliquot (0.5 mL) was taken and added to CDCl_3 (0.5 mL) and analysed by ^{19}F NMR spectroscopy.



Scope of Solvents

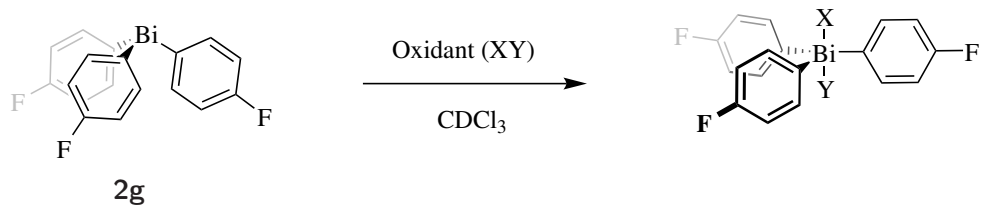
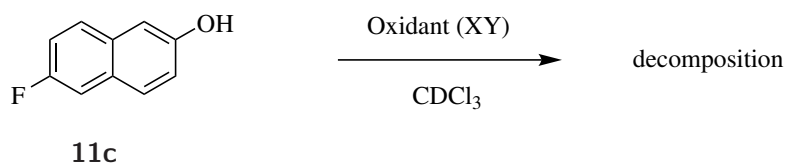
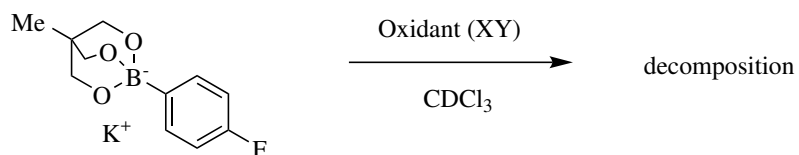
$\text{Ph}_3\text{Bi(OAc)}_2$ **3f** (11.4 mg, $20.4\ \mu\text{mmol}$), 6-fluoro-2-naphthol (3.3 mg, $20\ \mu\text{mmol}$), DBU ($5.5\ \mu\text{L}$, $37\ \mu\text{mmol}$) and potassium 4-fluorophenyl triol borate (16.0 mg, $61.2\ \mu\text{mmol}$) have been added to 2.0 mL of different solvents and allowed to stir for 18 h at 65°C . In the following an aliquot (0.5 mL) was taken, added to CDCl_3 (0.5 mL), and analysed by ^{19}F NMR spectroscopy.



Oxidation of tri(4-fluorophenyl)bismuth **3g**

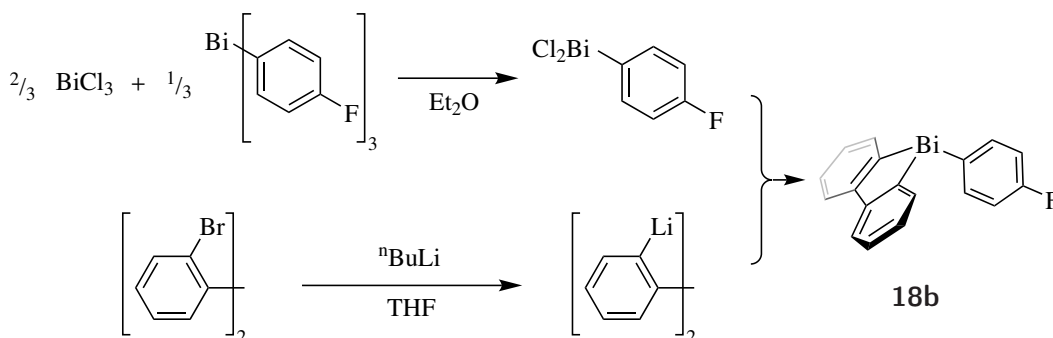
The oxidant screen was separated into three sections: Oxidation of tri(4-fluorophenyl) bismuth **3g**, decomposition of 6-fluoro-2-naphthol **11c**, and oxidation of 4-fluorophenyl triol borate.

In the first part, tri(4-fluorophenyl)bismuth (10.0 mg, 19.0 μmol) was dissolved in CDCl_3 (0.6 mL) in an NMR tube. Subsequently the oxidant (1.0 equiv.) was added and the sample analysed by ^{19}F NMR spectroscopy. A signal between -105 - -109 ppm indicates oxidation products as this range has been determined previously. If the addition of oxidant did not result in consumption of the signal of 6-fluoro-2-naphthol **11c**, 1-(4-fluorophenyl)-tiol borate was suspended in CDCl_3 (0.6 mL) in an NMR tube. Subsequently the oxidant (1.0 equiv.) was added, the NMR tube was shaken, and the sample analysed by ^{19}F NMR spectroscopy.

a) Oxidation of tri(4-fluorophenyl)bismuth**b) Decomposition of 6-fluoro-2-naphthol****c) Decomposition of organoboron reagent**

	Oxidant	Oxidation	2-naphthol	Boronate
F ⁺	XeF ₂	✓	✗	
	NFSI	✓	✗	
	Selectfluor	✓	✗	
	1-Fluoro-2,4,6-trimethylpyridinium BF ₄	✓	✓	✗
Cl ⁺	Chloramine T	✓	✗	
	Sulfuryl chloride	✓	✗	
	Hexachloroacetone	✗		
	Cl ₃ C–CCl ₃	✗		
	^t BuOCl	✓	✗	
	NaClO	✓	✗	
	N-chloro-morpholine	✗		
	N-chloro-2,2,6,6-tetramethylpiperidine	✗		
	N-chloro benzotriazol	✓	✗	
	Br ⁺	Br ₂	✓	✗
Cl ₂ BrC–CBrCl ₂		✗		
Bromamine T		✓	✗	✗
N-Bromobenzamide		✓	✗	
4,4-dibromo-2,6-di- <i>tert</i> -butylcyclohexa-2,5-dien-1-one		✓	✗	
ROOH		Peracetic acid	✓	✓
	<i>m</i> CPBA	✓	✓	✗
	<i>tert</i> -butyl hydroperoxide	✓	✓	✗
	H ₂ O ₂	✗		
	Benzimidoperoxoic acid	✗		
	<i>tert</i> -butyl hydroperoxide	✓	✓	✗
ROOR	<i>tert</i> -butyl perbezoate	✓	✗	
	Benzoyl peroxide	✓	✗	
	Lauroyl peroxide	✓	✓	✗
	Morpholino benzoate	✗		
Quinone	DDQ	✗		
	2-methyl quinone	✗		
	2-methyl Naphtaquinone	✗		
	2-methyl Antraquinone	✗		
	3,4,5,6-tetrachloro-1,2-benzoquinone	✗		
others	Sodium percarboante	✓	✓	✗
	Oxone	✗		
	(NBu ₄) ₂ Oxone	✓	✗	
	Sodium perborate	✗		
	NOBF ₄	✗		
	DMP	✗		
	IBX	✗		
	[Bis(trifluoroacetoxy)iodo]benzene	✗		
	Diphenyl iodonium chloride	✓	✓	✗
	Amyl nitrite	✗		
	(NH ₄) ₂ Ce(NO ₃) ₆	✓	✗	✗
	N-cyano benzotriazol	✗		
	TEMPO	✗		
	(+)-(8,8-Dichlorocamphorylsulfonyl)-oxaziridine	✗		

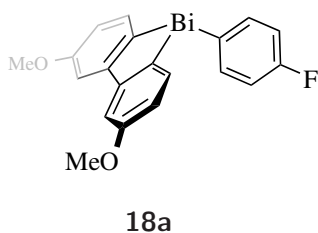
Synthesis of Bismole(III) compounds



Scheme 4.7: Synthesis of Bismoles

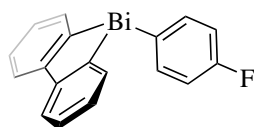
Anhydrous Et₂O (20 mL) was added to BiCl₃ (1.14 g, 3.60 mmol) and tri(4-fluorophenyl)bismuth **2g** (889 mg, 1.80 mmol) in a two neck flask and allowed to pre-mix under N₂ to form 4-fluorophenylbismuth dichloride. In a Schlenk flask n-BuLi (4.5 mL, 11 mmol, 2.5 M in hexane) was added drop wise to a solution of the 2,2'-dibromo-1,1'-biphenyl species (5.4 mmol) in 20 mL of anhydrous THF at -78 °C. After complete addition the solution was allowed to stir for 1 h at -78 °C before the prepared Cl₂BiPhF solution was added drop wise, resulting in a red solution. After allowing the reaction mixture to stir for 1 h, it was quenched with water and Et₂O 10 mL was added. The organic layer was separated and washed three times with water, dried (MgSO₄) and the solvent removed *in vacuo*, resulting in a colourless crystalline product.

5-(4-Fluorophenyl)-5,5'-dimethoxy-5H-dibenzo[b,d]bismole **18a**

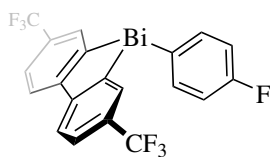
**18a**

mp/°C 156-157. ¹H NMR (400 MHz, CDCl₃) δ_H 7.69 – 7.54 (m, 4H), 7.42 (d, *J* = 2.5 Hz, 2H), 6.98 – 6.82 (m, 4H), 3.88 (d, *J* = 1.0 Hz, 6H). ¹³C{¹H} NMR (101 MHz, CDCl₃) δ_C 162.7 (d, *J* = 246.0 Hz), 160.1, 140.5, 139.0 (d, *J* = 6.9 Hz), 138.5, 117.5 (d, *J* = 19.9 Hz), 114.8, 113.2, 55.4. Peaks *ipso* to bismuth centre could not be observed. ¹⁹F NMR (377 MHz, CDCl₃) δ_F -113.85 (tt, *J* = 9.7, 6.2 Hz). IR (ATR): $\tilde{\nu}$ = 1575, 1457, 1396, 1311, 1281, 1206, 1182, 1158, 1041, 1012, 842, 881, 557, 501, 420. HRMS calcd. for C₂₀H₁₆BiFNaO₂⁺: 539.0830 [M+Na]⁺; found (ESI⁻): 539.0824. Colourless crystals. Yield: 1.06 g, 38%.

5-(4-Fluorophenyl)-5H-dibenzo[b,d]bismole **18b**

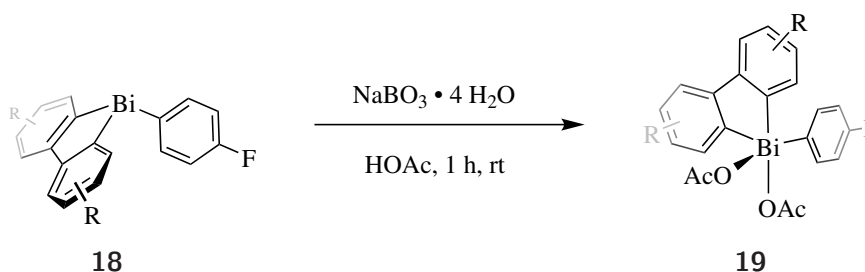
**18b**

mp/°C 150-152. ¹H NMR (400 MHz, CDCl₃) δ_H 7.94 (dd, *J* = 7.8, 1.3 Hz, 2H), 7.76 (dd, *J* = 7.1, 1.5 Hz, 2H), 7.69 – 7.58 (m, 2H), 7.53 – 7.35 (m, 4H), 6.92 – 6.83 (m, 2H). ¹³C{¹H} NMR (101 MHz, CDCl₃) δ_C 163.9, 162.6 (d, *J* = 246.2 Hz), 158.1, 146.4, 139.0 (d, *J* = 6.9 Hz), 137.4, 128.7, 128.1, 126.7, 117.6 (d, *J* = 19.8 Hz). ¹⁹F NMR (377 MHz, CDCl₃) δ_F -113.67 (tt, *J* = 9.5, 6.2 Hz). IR (ATR): $\tilde{\nu}$ = 1570, 1481, 1429, 1215, 1158, 1013, 813, 741, 614, 499, 408. HRMS calcd. for C₁₈H₁₃BiF⁺: 457.0800 [M+H]⁺; found (ESI⁻): 457.0817. Colourless crystals. Yield: 2.12 g, 86%.

5-(4-Fluorophenyl)-4,4'-bis(trifluoromethyl)-5H-dibenzo[b,d]bismole **18c****18c**

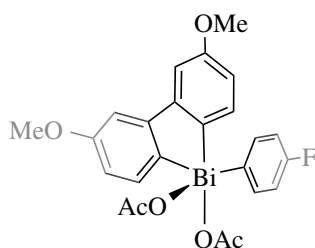
mp/°C 224-225. $^1\text{H NMR}$ (400 MHz, CDCl_3) δ_H 8.08 (d, $J = 8.2$ Hz, 1H), 8.06 – 8.04 (m, 1H), 7.75 (dd, $J = 8.4, 1.8$ Hz, 1H), 7.64 – 7.57 (m, 1H), 6.98 – 6.89 (m, 1H). $^{13}\text{C}\{^1\text{H}\}$ NMR (101 MHz, CDCl_3) δ_C 165.4, 162.9 (d, $J = 247.6$ Hz), 160.1, 147.8, 139.1 (d, $J = 7.1$ Hz), 134.4 (d, $J = 3.9$ Hz), 131.2 (q, $J = 32.2$ Hz), 127.4, 125.6 (q, $J = 272.8$ Hz), 125.6 (q, $J = 3.7$ Hz), 118.3 (d, $J = 20.2$ Hz). $^{19}\text{F NMR}$ (377 MHz, CDCl_3) δ_F -62.34 (s, 6F), -112.21 (tt, $J = 9.3, 6.0$ Hz, 1F). IR (ATR): $\tilde{\nu}$ 1598, 1572, 1484, 1384, 1316, 1108, 1074, 1045, 896, 678, 499, 423. HRMS calcd. for $\text{C}_{20}\text{H}_{10}\text{BiF}_7^+$: 592.0469 $[\text{M}^+]^+$; found (ESI $^+$): 592.0432. Colourless crystals. Yield: 0.927 g, 29%.

Oxidation of Bismoles

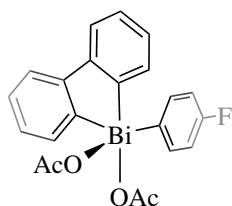


Scheme 4.8: Oxidation of bismoles

5-(4-Fluorophenyl)-5H-dibenzo[b,d]bismole (1.0 g, 2.2 mmol) and sodium perborate tetrahydrate (1.68 g, 11.0 mmol) were added to 20 mL of acetic acid and allowed to stir for 30 min. The reaction was quenched with water and extracted with 20 mL of CH_2Cl_2 . The organic phase was washed with water (3×20 mL) and dried with MgSO_4 . The organic phase was evaporated, resulting in a white solid. The crude was recrystallised in cyclohexane.

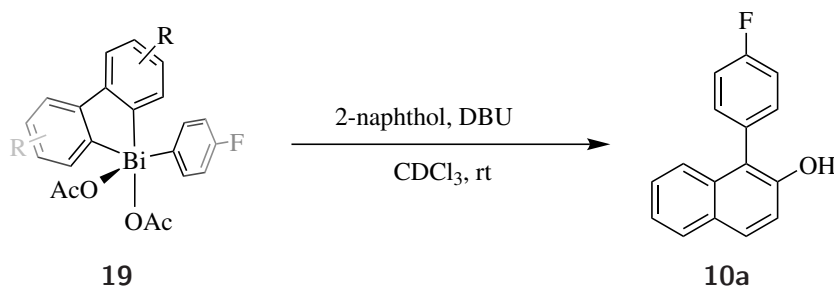
5-(4-Fluorophenyl)-5,5'-dimethoxy-5H-dibenzo[b,d]bismole diacetate **19a****19a**

mp/°C 184-186. $^1\text{H NMR}$ (400 MHz, CDCl_3) δ_H 8.29 (dd, $J = 8.7, 5.1$ Hz, 2H), 8.25 (dd, $J = 7.8, 1.3$ Hz, 2H), 8.13 (dd, $J = 7.4, 1.3$ Hz, 2H), 7.69 (td, $J = 7.4, 1.3$ Hz, 2H), 7.62 (dd, $J = 7.5, 1.3$ Hz, 2H), 7.42 (m, 2H), 1.85 (s, 6H). $^{13}\text{C}\{^1\text{H}\}$ NMR (126 MHz, CDCl_3) δ_C 165.0, 163.0, 155.6, 137.4, 133.5, 133.4, 132.7, 131.5, 131.3, 125.2, 119.2, 119.0, 21.0. $^{19}\text{F NMR}$ (377 MHz, CDCl_3) δ_F -106.79 (m). IR (ATR): $\tilde{\nu} = 1560, 1474, 1406, 1386, 1310, 1219, 1161, 1043, 815, 667, 504$. HRMS calcd. for $\text{C}_{24}\text{H}_{22}\text{BiFO}_6\text{Na}^+$: 657.0112 $[\text{M}+\text{Na}]^+$; found (ESI $^-$): 657.0123. Colourless crystals. Yield: 1.32 g, 64%.

5-(4-Fluorophenyl)-5H-dibenzo[b,d]bismole diacetate **19b****19b**

mp/°C 194-196. $^1\text{H NMR}$ (400 MHz, CDCl_3) δ_{H} 8.29 (dd, $J = 8.7, 5.1$ Hz, 2H), 8.25 (dd, $J = 7.8, 1.3$ Hz, 2H), 8.13 (dd, $J = 7.4, 1.3$ Hz, 2H), 7.69 (dd, $J = 7.4, 1.3$ Hz, 2H), 7.62 (dd, $J = 7.5, 1.3$ Hz, 2H), 7.42 (dd, $J = 8.7$ Hz, 8.7 Hz, 2H), 1.85 (s, 6H). $^{13}\text{C}\{^1\text{H}\}$ NMR (126 MHz, CDCl_3) δ_{C} 180.1, 164.0 (d, $J = 253.0$ Hz), 155.6, 137.4, 133.5 (d, $J = 8.5$ Hz), 132.8, 132.21 (d, $J = 4.1$ Hz), 131.6, 131.4, 125.2, 119.2 (d, $J = 22.2$ Hz), 21.1. $^{19}\text{F NMR}$ (377 MHz, CDCl_3) δ_{F} -106.79 (m). IR (ATR): $\tilde{\nu} = 1570, 1480, 1428, 1214, 1428, 1214, 1158, 808, 741, 499, 408$. HRMS calcd. for $\text{C}_{22}\text{H}_{18}\text{BiFO}_4\text{Na}^+$: 597.0885 $[\text{M}+\text{Na}]^+$; found (ESI $^-$): 597.0847. Colourless crystals. Yield: 1.53 g, 84%.

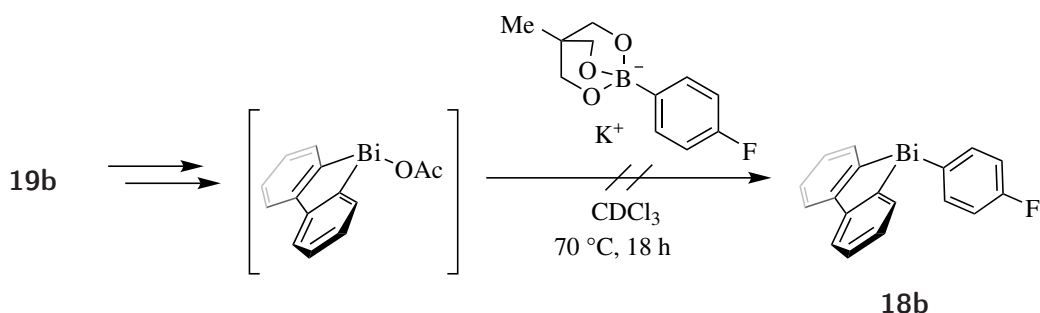
Arylation of 2-naphthol using 5-(4-fluorophenyl)-5H-dibenzo[b,d]bismole diacetate



Scheme 4.9: Arylation of 2-naphthol using bismole(V) reagents

Anhydrous CDCl_3 (0.6 mL) was added to 5-(4-fluorophenyl)-5H-dibenzo[b,d]bismole diacetate (11.7 mg, 20.4 μmol), 2-naphthol (3.0 mg, 19 μmol) and DBU (5.5 μL , 37 μmol) in an NMR tube. The reaction mixture was shaken vigorously and subsequently analysed by $^{19}\text{F NMR}$ spectroscopy, which indicated >99% conversion to the desired 1-(4-fluorophenyl)naphthalen-2-ol in less than 1 minute.

Transmetallation using 19b

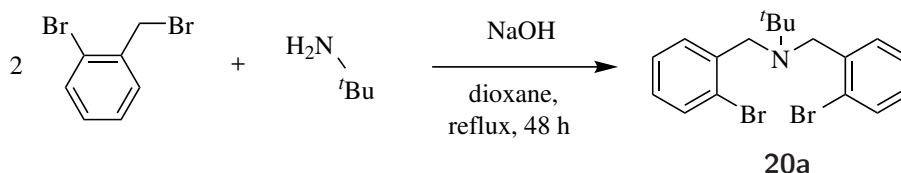


Scheme 4.10: Approach for the transmetallation of bismole-OAc-type species created from the arylation of 2-naphthol using **19b**

Anhydrous CDCl_3 (0.6 mL) was added to 5-(4-fluorophenyl)-5H-dibenzo[b,d]bismole diacetate (11.7 mg, 20.4 μmol), 2-naphthol (3.0 mg, 19 μmol) and DBU (5.5 μL , 37 μmol) in an NMR tube. The reaction mixture was shaken vigorously, and full conversion was confirmed by ^{19}F NMR spectroscopic analysis. The reaction mixture was added to potassium 4-fluorophenyl triol borate (16.0 mg, 61.0 μmol) in a microwave tube. The resulting reaction mixture was stirred at 70 $^\circ\text{C}$ for 18 h. No transmetallation product was observed.

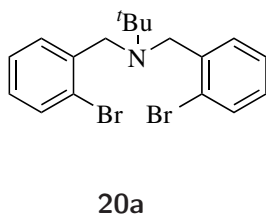
Synthesis of Azabismocine

Synthesis of *N,N*-di(2-bromobenzyl)-2-methylpropan-2-amine



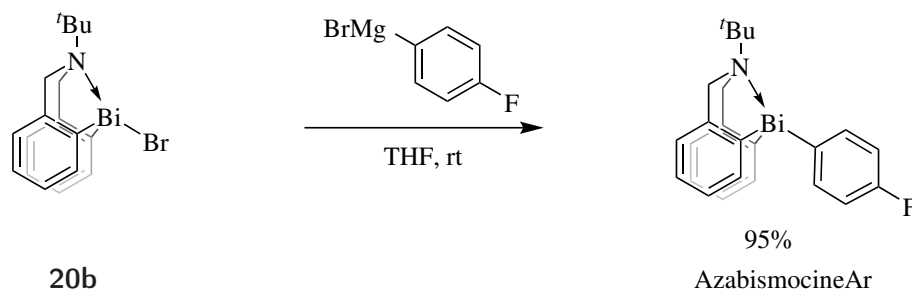
tert-Butyl amine (1.30 mL, 12.2 mmol) and bromobenzyl bromide (6.70 g, 26.8 mmol) were added to a mixture of dioxane (50 mL) and NaOH (40 mL, 1.0 M in H_2O) and allowed to reflux for 48 h. The reaction mixture was cooled to room temperature and extracted with CH_2Cl_2 . The combined organic fraction were dried (MgSO_4) and the solvent removed *in vacuo* and purified by column chromatography (conditions see below).

N,N-di(2-bromobenzyl)-2-methylpropan-2-amine **20a**



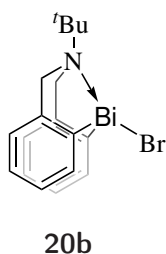
mp/ $^\circ\text{C}$ 99-100. ^1H NMR (400 MHz, CDCl_3) δ_{H} 7.57 (dd, $J = 7.6, 1.7$ Hz, 2H), 7.33 (dd, $J = 8.0, 1.3$ Hz, 2H), 7.10 (ddd, $J = 7.6, 7.5, 1.3$ Hz, 2H), 6.90 (ddd, $J = 7.6, 7.5, 1.8$ Hz, 2H), 3.85 (s, 4H), 1.21 (s, 9H). $^{13}\text{C}\{^1\text{H}\}$ NMR (126 MHz, CDCl_3) δ_{C} 140.6, 132.2, 132.2, 131.3, 127.8, 126.8, 123.6, 56.3, 54.1, 27.2. IR (ATR): $\tilde{\nu} = 2967, 2865, 1565, 1466, 1438, 1391, 1352, 1242, 1198, 1130, 1042, 1024, 957, 931, 751$ cm^{-1} . HRMS calcd. for $\text{C}_{18}\text{H}_{22}\text{Br}_2\text{N}^+$: 412.0093 $[\text{M}+\text{H}]^+$; found (ESI $^+$): 412.0091. Rf: (petrol) 0.62. Colourless crystals. Yield: 4.8 g (96%).

Synthesis of 12-Bromo-6-(*tert*-butyl)-5,6,7,12-tetrahydrodibenzo[*c,f*][1,5]azabismocine



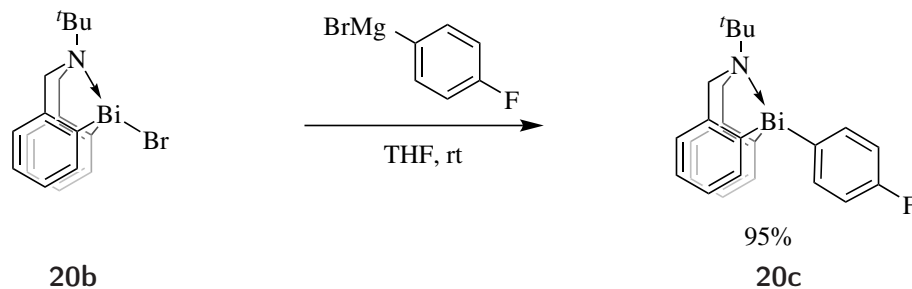
Anhydrous THF (10 mL) was added to *N,N*-di(2-bromobenzyl)-2-methylpropan-2-amine (761 mg, 1.86 mmol) and the reaction mixture cooled to -78°C . BuLi (1.55 mL, 2.4 M in hexane) was added and the solution allowed to stir for 30 min at -78°C . A solution of BiBr₃ (834 mg, 1.86 mmol) in THF (10 mL) was added dropwise at -78°C and the mixture allowed to warm to room temperature over the course of 30 min and subsequently quenched with brine. The mixture was extracted with CH₂Cl₂ and the organic phase was dried (MgSO₄) and evaporated *in vacuo* to result in the desired product as a colourless solid (575 mg, 57%).

12-Bromo-6-(*tert*-butyl)-5,6,7,12-tetrahydrodibenzo[*c,f*][1,5]azabismocine 20b



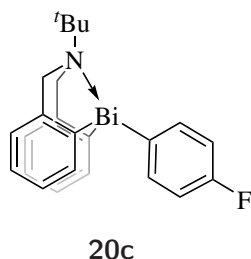
mp/ $^\circ\text{C}$ 245-246. ¹H NMR (500 MHz, CDCl₃) δ_H (dd, $J = 7.5$, 1.3 Hz, 2H), 7.46 (ddd, $J = 7.4$, 7.4, 1.4 Hz, 2H), 7.40 (dd, $J = 7.6$, 1.3 Hz, 2H), 7.34 (ddd, $J = 7.4$, 7.4, 1.3 Hz, 2H), 4.50 (d, $J = 15.4$ Hz, 2H), 4.12 (d, $J = 15.4$ Hz, 2H), 1.33 (s, 9H). ¹³C{¹H} NMR (126 MHz, CDCl₃) δ_C 167.4, 151.1, 140.2, 131.1, 128.4, 127.3, 60.27, 60.25, 27.9. IR (ATR): $\tilde{\nu} = 3047$, 2972, 1579, 1462, 1434, 1401, 1376, 1267, 1233, 1188, 1089, 1015, 967, 943, 922, 847, 824, 754, 735, 699, 536, 517, 483, 434 cm⁻¹. HRMS calcd. for C₁₈H₂₁BiN⁺: 460.1478 [M-Br]⁺; found (ESI⁺): 460.1473. Colourless crystals. Yield: 575 mg (57%).

Arylation of 12-bromo-6-(*tert*-butyl)-5,6,7,12-tetrahydrodibenzo[*c,f*][1,5]azabismocine



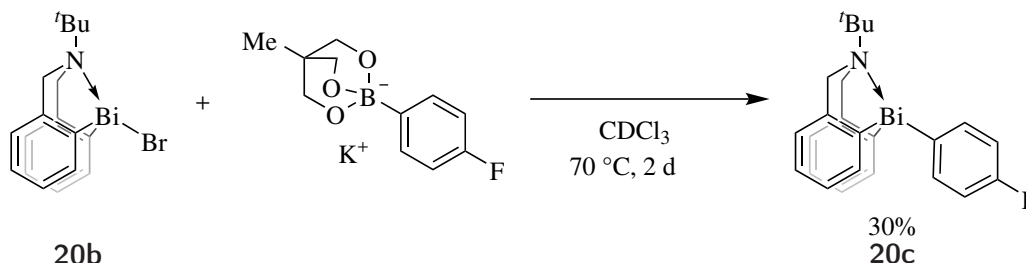
Anhydrous THF (10 mL) was added to 12-bromo-6-(*tert*-butyl)-5,6,7,12-tetrahydrodibenzo[*c,f*][1,5]azabismocine (575 mg, 1.06 mmol). A solution of (4-fluorophenyl) magnesium bromide (550 μ L, 1.94 M in THF) was added and the solution allowed to stir for 1 h. Subsequently the solution was quenched with water and extracted with CH_2Cl_2 . The organic phase was washed with water, dried with MgSO_4 and the solvent evaporated *in vacuo* to result in the desired product as a colourless crystalline solid. (559 mg, 95%)

6-(*tert*-Butyl)-12-(4-fluorophenyl)-5,6,7,12-tetrahydrodibenzo[*c,f*][1,5]azabismocine 20c



mp/ $^{\circ}\text{C}$ 177-178. ^1H NMR (500 MHz, CDCl_3) δ_{H} 7.82 - 7.73 (m, 2H), 7.54 (dd, $J = 7.1, 1.0$ Hz, 2H), 7.22 - 7.16 (m, 4H), 7.10 (dddd, $J = 11.0, 8.4, 6.3, 2.6$ Hz, 4H), 4.19 (d, $J = 15.3$ Hz, 2H), 3.85 (d, $J = 15.4$ Hz, 2H), 1.22 (s, 9H). $^{13}\text{C}\{^1\text{H}\}$ NMR (126 MHz, CDCl_3) δ_{C} 162.8 (d, $J = 245.2$ Hz), 160.6, 152.5, 149.3, 141.4 (d, $J = 6.3$ Hz), 139.0, 129.1, 127.7, 127.5, 117.2 (d, $J = 19.0$ Hz), 57.6, 56.7, 27.5. ^{19}F NMR (377 MHz, CDCl_3) δ_{F} -114.45 (tt, $J = 9.7, 6.5$ Hz). IR (ATR): $\tilde{\nu} = 3050, 2361, 2339, 1573, 1485, 1436, 1302, 1222, 1150, 1088, 1013, 909, 818, 763, 740, 588, 566, 508, 462$ cm^{-1} . HRMS calcd. for $\text{C}_{18}\text{H}_{21}\text{BiN}^+$: 460.1478 [$\text{M}-\text{C}_6\text{H}_4\text{F}$] $^+$; found (ESI $^+$): 460.1469. Colourless crystals. Yield: 559 mg (95%).

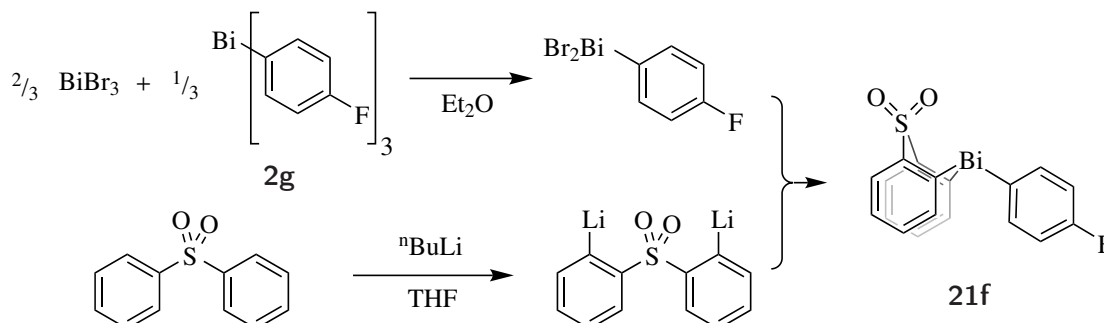
Arylation of 12-bromo-6-(*tert*-butyl)-5,6,7,12-tetrahydrodibenzo[*c,f*][1,5]azabismocine using an organoboron reagent



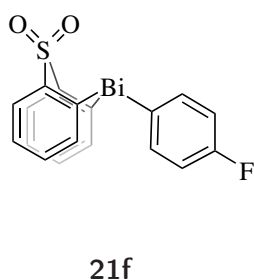
Anhydrous CDCl_3 (0.6 mL) was added to 2-bromo-6-(*tert*-butyl)-5,6,7,12-tetrahydrodibenzo[*c,f*][1,5]azabismocine (11.0 mg, 19.2 μ mol) and potassium 4-fluorophenyl triol boronate (16.0 mg, 61.0 μ mol) in an NMR tube. The mixture was heated at 70 $^{\circ}\text{C}$. Analysis by ^{19}F NMR spectroscopy indicated 30% conversion to the desired 6-(*tert*-Butyl)-12-(4-fluorophenyl)-5,6,7,12-tetrahydrodibenzo[*c,f*][1,5]azabismocine within 2 days.

Stoichiometric approach

Preparation of 10-(4-fluorophenyl)-10H-dibenzo[b,e][1,4]thiabismine 5,5-dioxide

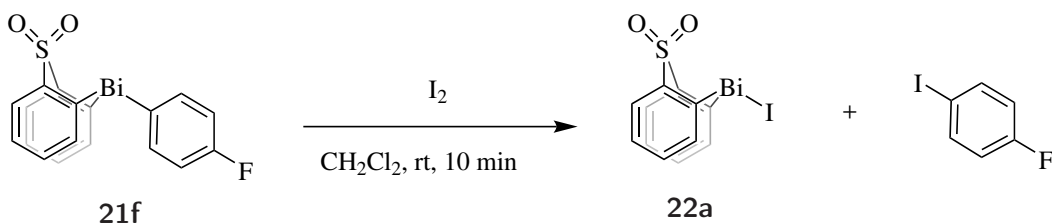


n-Butyllithium (2.5 M in hexanes; 24 mL, 60 mmol) was added dropwise over 20 mins to a solution of diphenylsulfone (6.55 g, 30.0 mmol) in anhydrous THF (120 mL) at -78°C . The resulting solution was stirred for 1 h at -78°C . A solution of tri(4-fluorophenyl)bismuth (4.74 g, 9.60 mmol) in anhydrous Et_2O (50 mL) was added dropwise to a solution of BiBr_3 (8.63 g, 19.2 mmol) in anhydrous Et_2O (50 mL) over 10 min. The resulting heavy yellow suspension was stirred for 3 h, then anhydrous THF (60 mL) was added. The resulting milky solution was then added dropwise to the solution of dilithiodiphenylsulfone (prepared as above) at -78°C over 30 min. The reaction mixture was allowed to warm to room temperature over 18 h before brine was added. The mixture was extracted with EtOAc ($\times 1$) and CH_2Cl_2 ($\times 2$). The organic portions were dried (MgSO_4) and concentrated *in vacuo* to yield the title compound as a colourless crystalline solid (14.6 g, 27.9 mmol, 97%) in 98% purity as determined by ^1H and ^{19}F NMR spectroscopic analysis.



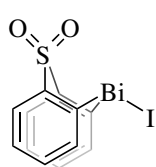
mp/ $^{\circ}\text{C}$ 176-178. ^1H NMR (500 MHz, CDCl_3) δ_{H} 8.38 (dd, $J = 7.7, 1.4$ Hz, 1H), 7.85 (dd, $J = 7.2, 1.3$ Hz, 1H), 7.76 - 7.67 (m, 1H), 7.41 (ddd, $J = 7.6, 7.3, 1.3$ Hz, 1H), 7.36 (ddd, $J = 7.6, 7.3, 1.4$ Hz, 1H), 7.12 - 7.03 (m, 1H). $^{13}\text{C}\{^1\text{H}\}$ NMR (126 MHz, CDCl_3) δ_{C} 163.1 (d, $J = 248.5$ Hz), 141.8, 141.0 (d, $J = 7.1$ Hz), 137.6, 133.6, 128.4, 127.3, 118.4 (d, $J = 19.9$ Hz). ^{19}F NMR (377 MHz, CDCl_3) δ_{F} -111.15 (tt, $J = 9.5, 6.1$ Hz) IR (ATR): $\tilde{\nu} = 3050, 2361, 2339, 1573, 1485, 1436, 1302, 1222, 1150, 1088, 1013, 909, 818, 763, 740, 588, 566, 508, 462$ cm^{-1} . HRMS calcd. for $\text{C}_{18}\text{H}_{13}\text{BiFO}_2\text{S}^+$: 521.0419 $[\text{M}+\text{H}]^+$; found (ESI $^+$): 521.0398. Colourless crystals. Yield: 14.6 g, 27.9 mmol, 97%.

Synthesis of 5,5-Dioxido-10H-dibenzo[b,e][1,4]thiabismine-10-yl iodide **22a**



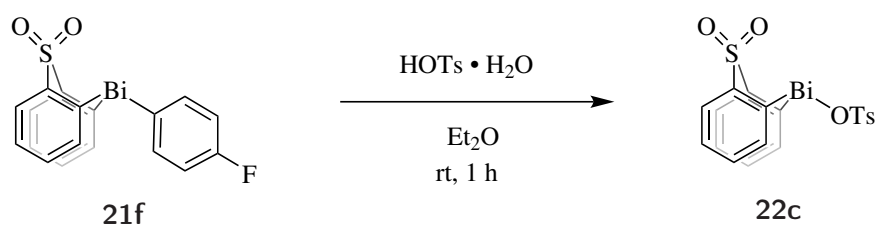
10-(4-Fluorophenyl)-10H-dibenzo[b,e][1,4]thiabismine 5,5-dioxide (50.0 mg, 0.96 mmol) was dissolved in CH_2Cl_2 (5 mL). To the solution iodine (25.4 mg, 1.00 mmol) was added and allowed to stir at room temperature for 10 min. The solvent is removed *in vacuo* and resulted in 5,5-dioxido-10H-dibenzo[b,e][1,4]thiabismine-10-yl iodide (45.5 mg, 86%).

5,5-Dioxido-10H-dibenzo[b,e][1,4]thiabismine-10-yl iodide **22a**

**22a**

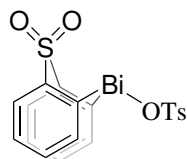
mp/ $^{\circ}\text{C}$ 208-209. $^1\text{H NMR}$ (500 MHz, CDCl_3) δ_{H} 9.22 (dd, $J = 7.4, 1.2$ Hz, 1H), 8.31 (dd, $J = 7.7, 1.4$ Hz, 1H), 7.62 (ddd, $J = 7.6, 7.4, 1.3$ Hz, 1H), 7.49 (ddd, $J = 7.6, 7.4, 1.2$ Hz, 1H). $^{13}\text{C}\{^1\text{H}\}$ NMR (126 MHz, CDCl_3) δ_{C} 163.8, 140.4, 140.2, 136.0, 128.9, 127.7. IR (ATR): $\tilde{\nu} = 2359, 2340, 1436, 1301, 1289, 1251, 1141, 1113, 1086, 1008, 764, 739, 586, 564, 508, 462$. HRMS calcd. for $\text{C}_{12}\text{H}_8\text{BiO}_2\text{S}^+$: 425.0049 $[\text{M}-\text{I}]^+$; found (ESI $^+$): 425.0047. White solid 45.5 mg, 86%.

Preparation of 5,5-dioxido-10H-dibenzo[b,e][1,4]thiabismine-10-yl 4-methylbenzenesulfonate **22c**



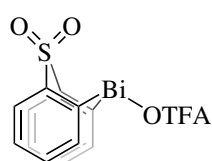
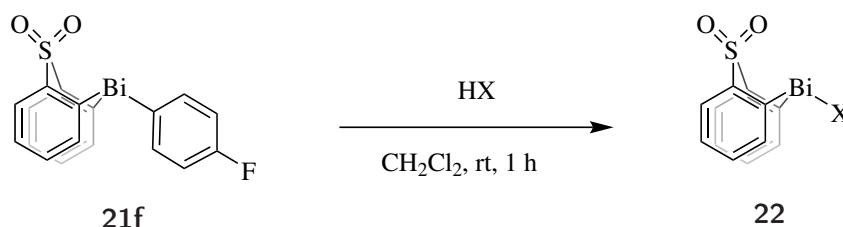
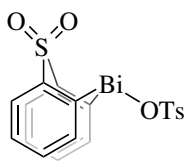
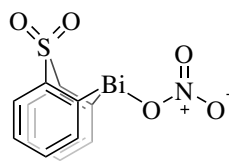
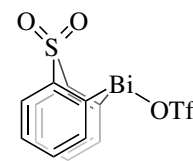
Toluenesulfonic acid monohydrate (4.20 g, 22.0 mmol) was added to a stirred solution of 10-(4-fluorophenyl)-10H-dibenzo[b,e][1,4]thiabismine 5,5-dioxide (10.0 g, 19.3 mmol) in Et_2O (60 mL). The resulting suspension was stirred for 1 h at room temperature, then the precipitate was collected by Büchner filtration, washed with Et_2O and dried under a flow of air to afford the title compound as a white powder (11.0 g, 18.5 mmol, 96%).

5,5-Dioxido-10H-dibenzo[b,e][1,4]thiabismine-10-yl 4-methylbenzenesulfonate **22c**

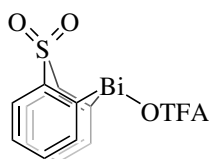
**22c**

mp/°C 191-192. $^1\text{H NMR}$ (500 MHz, CDCl_3) δ_{H} 9.0 - 8.8 (m, 2H), 8.4 (dd, $J = 7.7, 1.2$ Hz, 2H), 7.9 - 7.8 (m, 4H), 7.5 (ddd, $J = 7.6, 7.7, 1.1$ Hz, 2H), 7.3 (s, 2H), 2.4 (s, 3H). $^{13}\text{C}\{^1\text{H}\}$ NMR (126 MHz, CDCl_3) δ_{C} 189.4, 142.6, 139.8, 138.5, 136.4, 135.7, 129.6 (2 C), 129.1, 126.6, 21.7. IR (ATR): $\tilde{\nu} = 2361, 2342, 1304, 1256, 1150, 1137, 1097, 961, 814, 740, 680, 587, 565$ cm^{-1} . HRMS calcd. for $\text{C}_{12}\text{H}_8\text{BiO}_2\text{S}^+$: 425.0049 $[\text{M-OTs}]^+$; found (ESI $^+$): 425.0047.

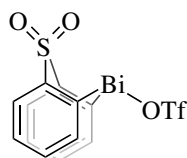
Preparation of 5,5-dioxido-10H-dibenzo[b,e][1,4]thiabismine-10-yl X species

98%
22b96%
22c96%
22d93%
22e

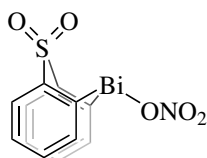
10-(4-Fluorophenyl)-10H-dibenzo[b,e][1,4]thiabismine 5,5-dioxide (50.0 mg, 0.96 mmol) was dissolved in 5 mL of CH_2Cl_2 . HX (1.00 mmol) was added to this solution and the reaction mixture allowed to stir at room temperature for 10 min. The reaction mixture was concentrated *in vacuo* and resulted in 5,5-dioxido-10H-dibenzo[b,e][1,4]thiabismine-10-yl X species.

5,5-Dioxido-10H-dibenzo[b,e][1,4]thiabismine-10-yl 2,2,2-trifluoroacetate 22b**22b**

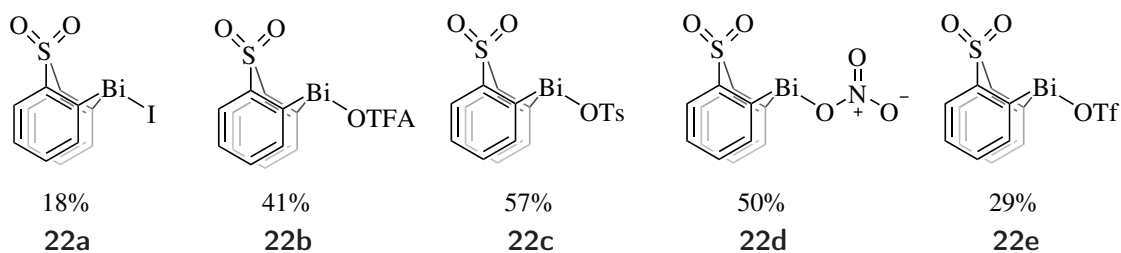
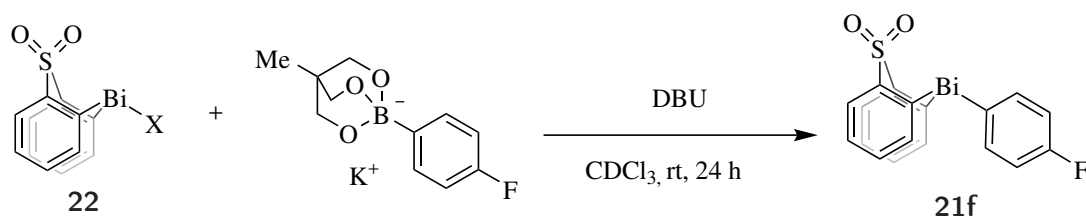
mp/°C 180-181. $^1\text{H NMR}$ (500 MHz, CDCl_3) δ_{H} 8.73 (dd, $J = 7.4, 1.1$ Hz, 1H), 8.41 (dd, $J = 7.7, 1.2$ Hz, 1H), 7.79 (ddd, $J = 7.6, 7.4, 1.2$ Hz, 1H), 7.51 (ddd, $J = 7.6, 7.4, 1.1$ Hz, 1H). $^{13}\text{C}\{^1\text{H}\}$ NMR (126 MHz, CDCl_3) δ_{C} 185.9, 140.3, 137.6, 136.1, 135.6, 129.5, 129.2, 127.9 (d, $J = 141.6$ Hz). $^{19}\text{F NMR}$ (377 MHz, CDCl_3) δ_{F} -73.95. IR (ATR): $\tilde{\nu} = 2924, 2853, 2361, 2338, 1682, 1410, 1289, 1184, 1157, 852, 792, 759, 735, 582, 563\text{ cm}^{-1}$. HRMS calcd. for $\text{C}_{12}\text{H}_8\text{BiO}_2\text{S}^+$: 425.0049 $[\text{M-OTFA}]^+$; found (ESI $^+$): 425.0043. White solid. Yield: 50.4 mg, 98%.

5,5-Dioxido-10H-dibenzo[b,e][1,4]thiabismine-10-yl trifluoromethanesulfonate 22e**22e**

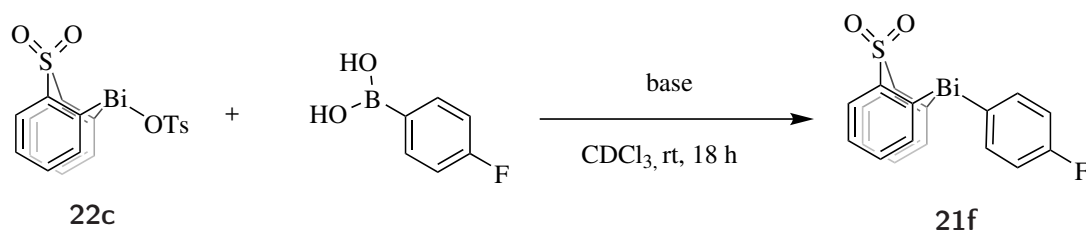
mp/°C 210-212. $^1\text{H NMR}$ (500 MHz, CDCl_3) δ_{H} 9.0 (dd, $J = 7.5, 1.1$ Hz, 1H), 8.5 (dd, $J = 7.6, 1.3$ Hz, 1H), 8.0 (ddd, $J = 7.6, 7.5, 1.3$ Hz, 1H), 7.6 (ddd, $J = 7.6, 7.5, 1.1$ Hz, 1H). $^{13}\text{C}\{^1\text{H}\}$ NMR (126 MHz, CDCl_3) δ_{C} 190.7, 138.8, 137.0, 135.2, 130.1, 129.5, 119.0 (q, $J = 318.3$ Hz). $^{19}\text{F NMR}$ (377 MHz, CDCl_3) δ_{F} -76.9. IR (ATR): $\tilde{\nu} = 2360, 1610, 1443, 1312, 1288, 1230, 1212, 1177, 1164, 1137, 1087, 1030, 1005, 762, 741, 637, 590, 564, 507, 462$. HRMS calcd. for $\text{C}_{12}\text{H}_8\text{BiO}_2\text{S}^+$: 425.0049 $[\text{M-OTf}]^+$; found (ESI $^+$): 425.0050. White solid. Yield: 51.2 mg, 93%.

5,5-Dioxido-10H-dibenzo[b,e][1,4]thiabismine-10-yl nitrate 22d**22d**

mp/°C 200-202. $^1\text{H NMR}$ (500 MHz, CDCl_3) δ_{H} 8.8 (dd, $J = 7.4, 1.1$ Hz, 1H), 8.4 (dd, $J = 7.7, 1.4$ Hz, 1H), 7.8 (ddd, $J = 7.6, 7.4, 1.3$ Hz, 1H), 7.5 (ddd, $J = 7.6, 7.4, 1.1$ Hz, 1H). $^{13}\text{C}\{^1\text{H}\}$ NMR (126 MHz, CDCl_3) δ_{C} 189.1, 140.0, 136.4, 135.4, 129.8, 129.3. IR (ATR): $\tilde{\nu} = 2361, 2342, 1304, 1256, 1150, 1137, 1097, 961, 814, 740, 680, 587, 565$. HRMS calcd. for $\text{C}_{12}\text{H}_8\text{BiO}_2\text{S}^+$: 425.0049 $[\text{M-NO}_3]^+$; found (ESI $^+$): 425.0051. White solid. Yield: 44.8 mg, 96%.

Transmetallation of Differently Substituted Bismacycle X Species **22**

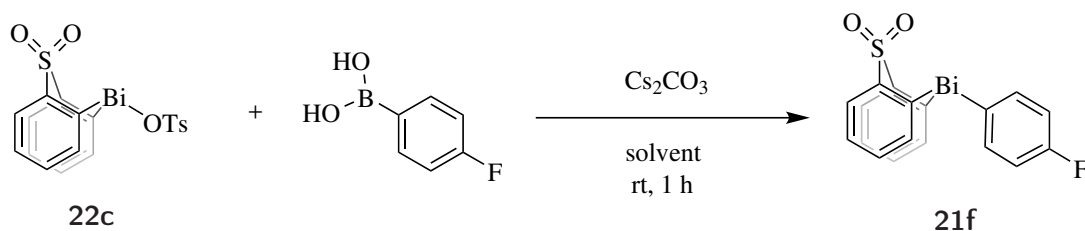
DBU (3.00 μL , 20.2 μmol) was added to bismacycle-X (10.1 μmol) and potassium 4-fluorophenyl triol boronate (5.00 mg, 20.2 μmol) in CDCl_3 (0.6 mL). The reaction was allowed to stir for 24 h at room temperature and then analysed by ^1H NMR spectroscopy.

Transmetallation of **22c** Using Different Bases

CDCl_3 (0.6 mL) was added to **22c** (5.00 mg, 8.40 μmol), base (16.8 μmol), and 4-fluorophenylboronic acid (2.40 mg (16.8 μmol)) in a microwave vial. The reaction mixture was allowed to stir at room temperature for 18 h and was subsequently analysed by ^1H NMR spectroscopy.

Table 4.3.1: Transmetallation of bismacycle OTs with different bases

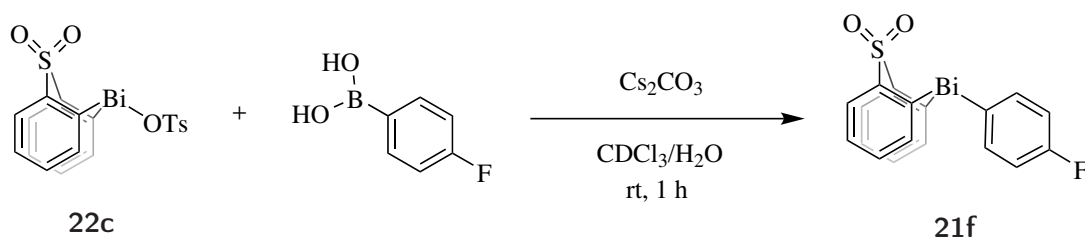
Entry	Base	Conversion [%]
1	K_2CO_3	58
2	NaOH	>99
3	K_3PO_4	86
4	Cs_2CO_3	>99

Transmetallation of **22c** in Different Solvent

The corresponding solvent (0.6 mL) was added to 5,5-dioxido-10H-dibenzo[b,e][1,4]thiabismine-10-yl 4-methylbenzenesulfonate (10.0 mg, 16.8 μmol), Cs_2CO_3 (11.0 mg, 33.6 μmol) and 4-fluorophenylboronic acid (2.40 mg, 16.8 μmol) in a microwave vial. The solution was allowed to stir at room temperature for 1 h and was subsequently analysed by ^1H NMR spectroscopy.

Table 4.3.2: Transmetallation of **22c** in different solvents

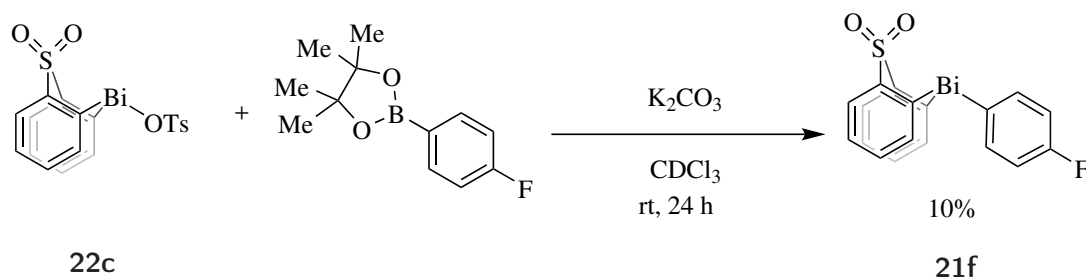
Entry	Solvent	Conversion [%]
1	methanol- d_4	0
2	MeCN	0
3	THF	0
4	acetone	0
5	CDCl_3	20
6	toluene	27
7	$\text{CDCl}_3/\text{H}_2\text{O}$ (9/1)	80
8	$\text{CH}_2\text{Cl}_2/\text{methanol}$ (9/1)	0
9	toluene/methanol (9/1)	0

Transmetallation of **22c** upon Addition of Different Amounts of Water

CDCl_3 (0.6 mL) and water (varying amounts) were added to **22c** (10.0 mg, 16.8 μmol), Cs_2CO_3 (11.0 mg, 33.6 μmol) and 4-fluorophenylboronic acid (2.40 mg, 16.8 μmol) in a microwave vial. The mixture was allowed to stir at room temperature for 1 h and was subsequently analysed by ^1H NMR spectroscopy.

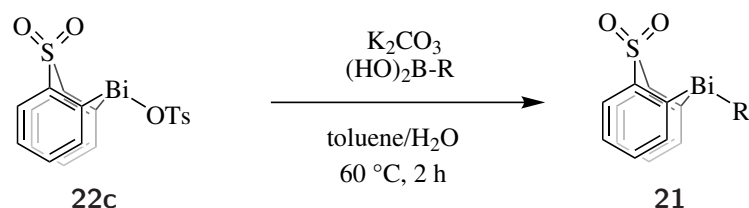
Entry	H ₂ O [Vol%]	Conversion [%]
1	0	20
2	0.1	53
3	0.5	56
4	1	65
5	5	83
6	10	84

Transmetallation of 22c from Aryl-Bpin



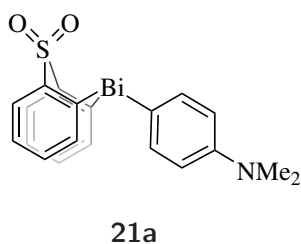
5,5-Dioxido-10H-dibenzo[b,e][1,4]thiabismine-10-yl 4-methylbenzenesulfonate (50 mg, 84 μmol) and 4-fluorophenylboronic acid pinacol ester (22.0 mg, 100 μmol) and K_2CO_3 (15.0 mg, 100 μmol) were stirred in CDCl_3 (5.0 mL) at room temperature for 24 h. Subsequent analysis using ^{19}F NMR spectroscopy indicated 10% conversion towards the desired product.

Transmetallation– Initial Scope



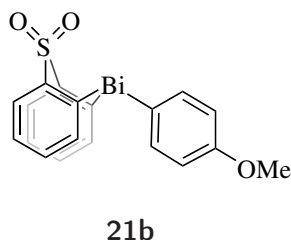
General Protocol Transmetallation: A mixture of toluene (2.00 mL) and water (0.01 mL) was added to 5,5-dioxido-10H-dibenzo[b,e][1,4]thiabismine-10-yl 4-methylbenzenesulfonate (5.0 mg, 8.4 μmol), K_2CO_3 (1.4 mg, 10.1 μmol) and the corresponding boronic acid (9.2 μmol) in a 10 mL microwave vial and allowed to stir at 60 $^\circ\text{C}$ for 2 h. The reaction mixture was analysed by ^1H NMR spectroscopy, then either purified by preparative TLC, crystallisation, or characterised *in situ*.

10-(4-(Dimethylamino)phenyl)-10H-dibenzo[b,e][1,4]thiabismine 5,5-dioxide 21a



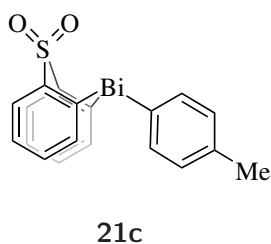
mp/°C 202-203. $^1\text{H NMR}$ (500 MHz, CDCl_3) δ_{H} 8.4 (dd, $J = 7.7, 1.4$ Hz, 1H), 7.9 (dd, $J = 7.2, 1.8$ Hz, 1H), 7.6 (dd, $J = 8.8, 2.2$ Hz, 1H), 7.4 (dd, $J = 7.6, 1.4$ Hz, 1H), 7.3 (dd, $J = 7.3, 1.5$ Hz, 1H), 6.7 (dd, $J = 8.8, 2.1$ Hz, 1H), 3.0 (s, 3H). $^{13}\text{C}\{^1\text{H}\}$ NMR (126 MHz, CDCl_3) δ_{C} 165.7, 158.2, 150.5, 141.9, 140.1, 137.8, 133.3, 128.1, 127.0, 114.8, 40.3. IR (ATR): $\tilde{\nu} = 2361, 2342, 1304, 1256, 1150, 1137, 1097, 961, 814, 740, 680, 587, 565$. HRMS calcd. for $\text{C}_{20}\text{H}_{18}\text{BiNO}_2\text{SNa}^+$: 568.0760 $[\text{M}+\text{Na}]^+$; found (ESI $^+$): 568.0758. (^1H Conversion: >99%, isolated by recrystallisation from $\text{CH}_2\text{Cl}_2/\text{cyclohexane}$)

10-(4-(Methoxy)phenyl)-10H-dibenzo[b,e][1,4]thiabismine 5,5-dioxide 21b

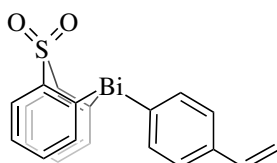


mp/°C 223-224. $^1\text{H NMR}$ (500 MHz, CDCl_3) δ_{H} 8.4 (dd, $J = 7.7, 1.4$ Hz, 1H), 7.9 (dd, $J = 7.2, 1.3$ Hz, 2H), 7.7 – 7.6 (m, 1H), 7.4 (dd, $J = 7.5, 1.3$ Hz, 2H), 7.4 (dd, $J = 7.4, 1.4$ Hz, 2H), 7.0 – 6.9 (m, 2H), 3.8 (s, 3H). $^{13}\text{C}\{^1\text{H}\}$ NMR (126 MHz, CDCl_3) δ_{C} 159.9, 141.7, 140.3, 137.6, 133.3, 128.1, 127.0, 116.8, 55.1. (peaks *ipso* to Bi could not be observed) IR (ATR): $\tilde{\nu} = 2361, 2342, 1304, 1256, 1150, 1137, 1097, 961, 814, 740, 680, 587, 565$. HRMS calcd. for $\text{C}_{19}\text{H}_{15}\text{BiO}_3\text{NaS}^+$: 555.0483 $[\text{M}+\text{Na}]^+$; found (ESI $^+$): 555.0426. Rf: (2/1, petrol/ Et_2O) 0.28. (^1H NMR Conversion: >99%, isolated by preparative TLC)

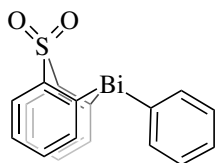
10-(4-(Methyl)phenyl)-10H-dibenzo[b,e][1,4]thiabismine 5,5-dioxide 21c



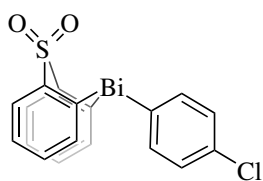
mp/°C 209-210. $^1\text{H NMR}$ (500 MHz, CDCl_3) δ_{H} 8.4 (dd, $J = 7.7, 1.4$ Hz, 2H), 7.9 (dd, $J = 7.2, 1.3$ Hz, 2H), 7.7 (d, $J = 1.5$ Hz, 2H), 7.4 (td, $J = 7.5, 1.3$ Hz, 2H), 7.3 (td, $J = 7.3, 1.4$ Hz, 2H), 7.3 – 7.2 (m, 2H), 2.3 (s, 3H). $^{13}\text{C}\{^1\text{H}\}$ NMR (126 MHz, CDCl_3) δ_{C} 162.4, 158.5, 141.9, 138.9, 138.7, 137.7, 133.5, 131.9, 128.3, 127.2, 21.8. IR (ATR): $\tilde{\nu} = 3049, 2954, 2920, 2861, 2360, 2341, 1562, 1438, 1303, 1286, 1252, 1151, 1088, 1011, 910, 794, 763, 740, 704, 588, 566, 513, 480, 462$. HRMS calcd. for $\text{C}_{19}\text{H}_{15}\text{BiO}_2\text{NaS}^+$: 539.0489 $[\text{M}+\text{Na}]^+$; found (ESI $^+$): 539.0472. Rf: (2/1, petrol/ Et_2O) 0.38. (^1H NMR Conversion: >99%, isolated by preparative TLC)

10-(4-Vinylphenyl)-10H-dibenzo[b,e][1,4]thiabismine 5,5-dioxide 21d**21d**

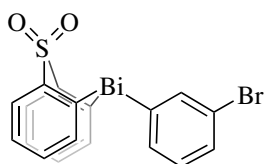
mp/°C 163-164. $^1\text{H NMR}$ (500 MHz, CDCl_3) δ_{H} 8.38 (dd, $J=7.7$, 1.4 Hz, 2H), 7.87 (dd, $J=7.2$, 1.4 Hz, 2H), 7.77 – 7.68 (m, 2H), 7.46 – 7.43 (m, 2H), 7.40 (ddd, $J=7.6$, 7.3, 1.3 Hz, 2H), 7.34 (ddd, $J=7.6$, 7.3, 1.4 Hz, 2H), 6.68 (dd, $J=17.6$, 10.9 Hz, 1H), 5.77 (dd, $J=17.6$, 0.8 Hz, 1H), 5.27 (dd, $J=11.0$, 0.9 Hz, 1H). $^{13}\text{C}\{^1\text{H}\}$ NMR (126 MHz, CDCl_3) δ_{C} 165.6, 157.6, 141.9, 139.2, 137.9, 137.7, 136.9, 133.6, 128.7, 128.4, 127.3, 114.8. IR (ATR): $\tilde{\nu}=1742$, 1718, 1562, 1425, 1385, 1303, 1286, 1151, 1074, 1058, 991, 910, 826, 763, 740, 588, 566, 461. HRMS calcd. for $\text{C}_{20}\text{H}_{15}\text{BiO}_2\text{NaS}^+$: 551.0489 $[\text{M}+\text{Na}]^+$; found (ESI $^+$): 551.0483. Rf: (2/1, petrol/Et $_2$ O) 0.22. ($^1\text{H NMR}$ Conversion: >99%, isolated by preparative TLC)

10-Phenyl-10H-dibenzo[b,e][1,4]thiabismine 5,5-dioxide 21e**21e**

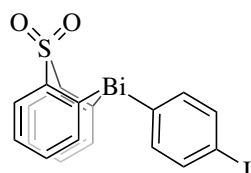
mp/°C 215-216. $^1\text{H NMR}$ (500 MHz, CDCl_3) δ_{H} 8.4 (dd, $J=7.7$, 1.4 Hz, 2H), 7.9 (dd, $J=7.2$, 1.3 Hz, 2H), 7.8 – 7.7 (m, 2H), 7.5 – 7.4 (m, 5H), 7.3 (dd, $J=7.4$, 1.4 Hz, 2H). $^{13}\text{C}\{^1\text{H}\}$ NMR (126 MHz, CDCl_3) δ_{C} 165.9, 158.8, 141.8, 138.8, 137.7, 133.6, 131.0, 128.7, 128.3, 127.3. IR (ATR): $\tilde{\nu}=3049$, 2961, 2920, 2849, 2360, 2341, 1562, 1428, 1302, 1286, 1252, 1150, 1074, 1012, 909, 763, 728, 696, 588, 566, 514, 462. HRMS calcd. for $\text{C}_{18}\text{H}_{13}\text{BiO}_2\text{NaS}^+$: 525.0332 $[\text{M}+\text{Na}]^+$; found (ESI $^+$): 525.0322. Rf: (2/1, petrol/Et $_2$ O) 0.35. ($^1\text{H NMR}$ Conversion: >99%, isolated by preparative TLC)

10-(4-(Chloro)phenyl)-10H-dibenzo[b,e][1,4]thiabismine 5,5-dioxide 21g**21g**

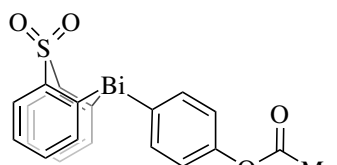
mp/°C 215-216. $^1\text{H NMR}$ (500 MHz, CDCl_3) δ_{H} 8.4 (dd, $J=7.6$, 1.4 Hz, 1H), 7.8 (dd, $J=7.2$, 1.3 Hz, 1H), 7.7 – 7.6 (m, 1H), 7.4 (td, $J=7.6$, 1.3 Hz, 1H), 7.4 – 7.3 (m, 2H). $^{13}\text{C}\{^1\text{H}\}$ NMR (126 MHz, CDCl_3) δ_{C} 163.7, 158.8, 141.8, 140.4, 137.6, 135.1, 133.7, 131.3, 128.5, 127.4. IR (ATR): $\tilde{\nu}=3050$, 2360, 2342, 1561, 1472, 1438, 1426, 1377, 1303, 1286, 1252, 1150, 1123, 1088, 1046, 1006, 909, 805, 763, 740, 715, 588, 566, 513, 483, 462. HRMS calcd. for $\text{C}_{18}\text{H}_{12}\text{BiClO}_2\text{NaS}^+$: 558.9943 $[\text{M}+\text{Na}]^+$; found (ESI $^+$): 558.9925. Rf: (2/1, petrol/Et $_2$ O) 0.30. ($^1\text{H NMR}$ Conversion: >99%, isolated by preparative TLC)

10-(3-Bromophenyl)-10H-dibenzo[b,e][1,4]thiabismine 5,5-dioxide 21h**21h**

$^1\text{H NMR}$ (500 MHz, CDCl_3) δ_{H} 8.40 (dd, $J = 7.5, 1.5$ Hz, 2H), 7.93 (dd, $J = 2.0, 1.0$ Hz, 1H), 7.87 (dd, $J = 7.1, 1.4$ Hz, 2H), 7.65 (dt, $J = 7.2, 1.1$ Hz, 1H), 7.49 (ddd, $J = 8.0, 2.1, 1.1$ Hz, 1H), 7.41 (ddd, $J = 21.2, 7.4, 1.4$ Hz, 4H), 7.30 (t, $J = 7.6$ Hz, 1H). HRMS calcd. for $\text{C}_{18}\text{H}_{12}\text{BiBrO}_2\text{NaS}^+$: 579.9545 $[\text{M}+\text{Na}]^+$; found (ESI $^+$): 579.9555. ($^1\text{H NMR}$ Conversion: >99%, characterised *in situ*)

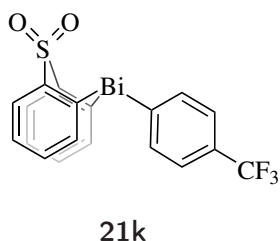
10-(4-Iodophenyl)-10H-dibenzo[b,e][1,4]thiabismine 5,5-dioxide 21i**21i**

mp/ $^{\circ}\text{C}$ 176-177. $^1\text{H NMR}$ (500 MHz, CDCl_3) δ_{H} 8.38 (dd, $J = 7.7, 1.4$ Hz, 1H), 7.85 (dd, $J = 7.1, 1.3$ Hz, 1H), 7.77 – 7.70 (m, 1H), 7.51 – 7.46 (m, 1H), 7.42 (ddd, $J = 7.6, 7.4, 1.3$ Hz, 1H), 7.36 (ddd, $J = 7.6, 7.4, 1.4$ Hz, 1H). $^{13}\text{C}\{^1\text{H}\}$ NMR (126 MHz, CDCl_3) δ_{C} 164.9, 158.8, 141.8, 140.7, 139.9, 137.6, 133.7, 128.5, 127.4, 95.7. IR (ATR): $\tilde{\nu} = 3050, 2363, 2325, 1562, 1545, 1483, 1438, 1369, 1303, 1286, 1150, 1107, 1074, 996, 908, 796, 762, 739, 587, 566, 465$. HRMS calcd. for $\text{C}_{18}\text{H}_{12}\text{BiIO}_2\text{NaS}^+$: 650.9299 $[\text{M}+\text{Na}]^+$; found (ESI $^+$): 650.9282. Rf: (1/1, petrol/ Et_2O) 0.35. ($^1\text{H NMR}$ Conversion: >99%, isolated by preparative TLC)

4-(5,5-Dioxido-10H-dibenzo[b,e][1,4]thiabismine-10-yl)phenyl acetate 21j**21j**

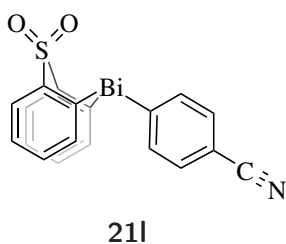
mp/ $^{\circ}\text{C}$ 208-209. $^1\text{H NMR}$ (500 MHz, CDCl_3) δ_{H} 8.40 (dd, $J = 7.7, 1.4$ Hz, 2H), 7.90 (dd, $J = 7.2, 1.3$ Hz, 2H), 7.83 – 7.77 (m, 2H), 7.43 (td, $J = 7.5, 1.3$ Hz, 2H), 7.40 – 7.34 (m, 2H), 7.17 – 7.07 (m, 2H), 2.32 (s, 3H). $^{13}\text{C}\{^1\text{H}\}$ NMR (126 MHz, CDCl_3) δ_{C} 199.2, 169.3, 158.6, 151.0, 141.7, 140.1, 137.6, 133.5, 128.3, 127.2, 124.2, 21.2. IR (ATR): $\tilde{\nu} = 3050, 2957, 2927, 2855, 2360, 2332, 1768, 1747, 1574, 1484, 1368, 1303, 1194, 1166, 1151, 1009, 910, 740, 588, 567$. HRMS calcd. for $\text{C}_{20}\text{H}_{15}\text{BiO}_4\text{NaS}^+$: 583.0387 $[\text{M}+\text{Na}]^+$; found (ESI $^+$): 583.0373. Rf: (2/1, petrol/ Et_2O) 0.22. ($^1\text{H NMR}$ Conversion: >99%, isolated by preparative TLC)

10-(4-(Trifluoromethyl)phenyl)-10H-dibenzo[b,e][1,4]thiabismine 5,5-dioxide 21k



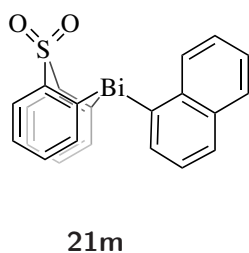
mp/°C 178-179. $^1\text{H NMR}$ (500 MHz, CDCl_3) δ_{H} 8.4 (dd, $J = 7.7, 1.4$ Hz, 1H), 7.9 – 7.9 (m, 1H), 7.8 (dd, $J = 7.2, 1.3$ Hz, 1H), 7.6 – 7.6 (m, 1H), 7.4 (dd, $J = 7.6, 1.3$ Hz, 1H), 7.4 (dd, $J = 7.3, 1.4$ Hz, 1H). $^{13}\text{C}\{^1\text{H}\}$ NMR (126 MHz, CDCl_3) δ_{C} 164.2, 159.0, 141.8, 139.3, 137.6, 133.9, 130.8 (q, $J = 32.6$ Hz), 128.6, 127.4 (q, $J = 3.8$ Hz), 124.3 (q, $J = 272.4$ Hz). $^{19}\text{F NMR}$ (471 MHz, CDCl_3) δ_{F} -62.85. IR (ATR): $\tilde{\nu} = 3050, 2924, 2857, 2360, 2341, 1324, 1151, 1124, 1074, 1041, 1009, 822, 763, 741, 674, 588, 566$. HRMS calcd. for $\text{C}_{19}\text{H}_{12}\text{BiF}_3\text{O}_2\text{NaS}^+$: 593.0206 $[\text{M}+\text{Na}]^+$; found (ESI $^+$): 593.0185. Rf: (2/1, petrol/ Et_2O) 0.25. ($^1\text{H NMR}$ Conversion: 47% (>99% after 6 h), isolated by preparative TLC)

4-(5,5-Dioxido-10H-dibenzo[b,e][1,4]thiabismine-10-yl)benzonitrile 21l

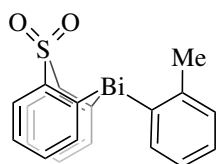


mp/°C 177-178. $^1\text{H NMR}$ (500 MHz, CDCl_3) δ_{H} 8.4 (dd, $J = 7.6, 1.4$ Hz, 1H), 7.9 – 7.9 (m, 1H), 7.8 (dd, $J = 7.2, 1.3$ Hz, 1H), 7.7 – 7.6 (m, 1H), 7.4 (ddd, $J = 7.6, 7.4, 1.3$ Hz, 1H), 7.4 (ddd, $J = 7.6, 7.4, 1.4$ Hz, 1H). $^{13}\text{C}\{^1\text{H}\}$ NMR (126 MHz, CDCl_3) δ_{C} 164.8, 159.3, 141.8, 139.6, 137.5, 134.0, 133.8, 128.8, 127.6, 118.9, 112.4. IR (ATR): $\tilde{\nu} = 3050, 2961, 2916, 2226, 1560, 1303, 1286, 1253, 1150, 1088, 1010, 912, 816, 764, 740, 718, 668, 588, 566$. HRMS calcd. for $\text{C}_{19}\text{H}_{12}\text{BiNO}_2\text{NaS}^+$: 550.0286 $[\text{M}+\text{Na}]^+$; found (ESI $^+$): 550.0277. Rf: (2/1, petrol/ Et_2O) 0.05. ($^1\text{H NMR}$ Conversion: 72% (>99% after 6 h), isolated by preparative TLC)

10-(Naphthalen-1-yl)-10H-dibenzo[b,e][1,4]thiabismine 5,5-dioxide 21m



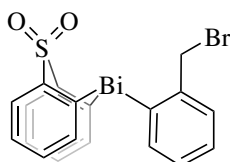
mp/°C 202-203. $^1\text{H NMR}$ (500 MHz, CDCl_3) δ_{H} 8.4 (dd, $J = 7.7, 1.3$ Hz, 2H), 8.1 – 7.9 (m, 4H), 7.8 (dd, $J = 7.4, 1.2$ Hz, 2H), 7.6 – 7.5 (m, 1H), 7.5 – 7.4 (m, 4H), 7.3 (ddd, $J = 7.4, 7.4, 1.3$ Hz, 2H). $^{13}\text{C}\{^1\text{H}\}$ NMR (126 MHz, CDCl_3) δ_{C} 167.6, 157.8, 141.7, 140.2, 139.0, 138.0, 134.8, 133.4, 130.7, 129.6, 129.2, 128.9, 128.3, 127.1, 126.4, 126.0. IR (ATR): $\tilde{\nu} = 3049, 2360, 2341, 1562, 1499, 1437, 1303, 1252, 1151, 1013, 908, 793, 764, 740, 587, 566$. HRMS calcd. for $\text{C}_{22}\text{H}_{15}\text{BiO}_2\text{NaS}^+$: 575.0489 $[\text{M}+\text{Na}]^+$; found (ESI $^+$): 575.0477. Rf: (2/1, petrol/ Et_2O) 0.25. ($^1\text{H NMR}$ Conversion: >99%, isolated by preparative TLC)

10-(*o*-Tolyl)-10H-dibenzo[b,e][1,4]thiabismine 5,5-dioxide 21n

21n

$^1\text{H NMR}$ (500 MHz, CDCl_3) δ_H 8.37 (dd, $J = 7.6, 1.4$ Hz, 2H), 7.87 (dd, $J = 7.2, 1.3$ Hz, 2H), 7.58 (dd, $J = 7.4, 1.4$ Hz, 1H), 7.44 (d, $J = 7.7$ Hz, 1H), 7.40 (ddd, $J = 7.6, 7.3, 1.3$ Hz, 2H), 7.33 (ddd, $J = 7.6, 7.3, 1.4$ Hz, 2H), 7.21 – 7.16 (m, 1H), 7.11 – 7.02 (m, 1H), 2.79 (s, 3H). HRMS calcd. for $\text{C}_{19}\text{H}_{15}\text{BiO}_2\text{NaS}^+$: 539.0489 $[\text{M}+\text{Na}]^+$; found (ESI $^+$): 539.0478.

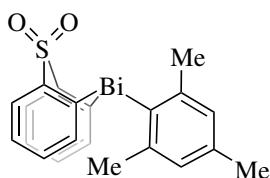
10-(2-(Bromomethyl)phenyl)-10H-dibenzo[b,e][1,4]thiabismine 5,5-dioxide 21o



21o

$^1\text{H NMR}$ (500 MHz, CDCl_3) δ_H 8.38 (dd, $J = 7.7, 1.3$ Hz, 2H), 7.93 (d, $J = 7.3$ Hz, 2H), 7.57 (t, $J = 8.2$ Hz, 2H), 7.41 (ddd, $J = 7.5, 7.4, 1.2$ Hz, 2H), 7.33 (ddd, $J = 7.5, 7.4, 1.4$ Hz, 3H), 7.09 (dd, $J = 8.0, 6.8$ Hz, 1H), 4.86 (s, 2H). HRMS calcd. for $\text{C}_{19}\text{H}_{14}\text{BiBrO}_2\text{NaS}^+$: 616.9594 $[\text{M}+\text{Na}]^+$; found (ESI $^+$): 616.9587. ($^1\text{H NMR}$ Conversion: 87%, characterised *in situ*)

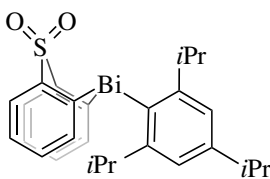
10-Mesityl-10H-dibenzo[b,e][1,4]thiabismine 5,5-dioxide 21p



21p

mp/ $^{\circ}\text{C}$ 163-164. $^1\text{H NMR}$ (500 MHz, CDCl_3) δ_H 8.42 (dd, $J = 7.9, 1.3$ Hz, 2H), 8.04 (dd, $J = 7.3, 1.3$ Hz, 2H), 7.42 (ddd, $J = 7.6, 7.4, 1.3$ Hz, 2H), 7.32 (ddd, $J = 7.6, 7.4, 1.3$ Hz, 2H), 7.04 (s, 2H), 2.27 (s, 6H), 1.43 (s, 3H). $^{13}\text{C}\{^1\text{H}\}$ NMR (126 MHz, CDCl_3) δ_C 165.5, 155.1, 146.5, 141.1, 139.1, 137.8, 133.1, 129.8, 128.4, 127.3, 28.0, 21.2. IR (ATR): $\tilde{\nu} = 1573, 1446, 1300, 1284, 1149, 1121, 1088, 1013, 849, 770, 740, 668, 588, 568$ cm^{-1} . HRMS calcd. for $\text{C}_{21}\text{H}_{19}\text{BiO}_2\text{NaS}^+$: 567.0802 $[\text{M}+\text{Na}]^+$; found (ESI $^+$): 567.0802. (^1H Conversion: 86%, isolated by recrystallisation from $\text{CH}_2\text{Cl}_2/\text{cyclohexane}$)

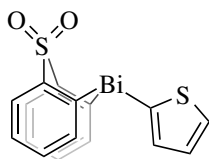
10-(2,4,6-Triisopropylphenyl)-10H-dibenzo[b,e][1,4]thiabismine 5,5-dioxide 21q



21q

$^1\text{H NMR}$ (500 MHz, CDCl_3) δ_H 8.58 (dd, $J = 7.3, 1.2$ Hz, 2H), 8.33 (dd, $J = 7.8, 1.2$ Hz, 2H), 7.63 (ddd, $J = 7.6, 7.4, 1.3$ Hz, 2H), 7.42 (ddd, $J = 7.6, 7.4, 1.2$ Hz, 2H), 7.00 (s, 2H), 3.13 – 3.04 (m, 1H), 2.95 – 2.83 (m, 2H), 1.31 (d, $J = 6.8$ Hz, 12H), 1.28 (d, $J = 6.9$ Hz, 6H). HRMS calcd. for $\text{C}_{12}\text{H}_8\text{BiO}_2\text{S}^+$: 425.0049 $[\text{M}-\text{TiPS}]^+$; found (ESI $^+$): 425.0051. (^1H Conversion: >99%, characterised *in situ*)

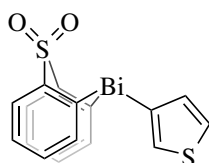
10-(Thiophen-2-yl)-10H-dibenzo[b,e][1,4]thiabismine 5,5-dioxide 21r



21r

^1H NMR (500 MHz, CDCl_3) δ_{H} 8.40 – 8.35 (m, 2H), 8.07 – 8.00 (m, 2H), 7.70 (dd, $J = 4.8, 0.8$ Hz, 1H), 7.52 (dd, $J = 3.3, 0.9$ Hz, 1H), 7.45 – 7.34 (m, 4H), 7.20 (dd, $J = 4.8, 3.3$ Hz, 1H). HRMS calcd. for $\text{C}_{16}\text{H}_{11}\text{BiO}_2\text{NaS}_2^+$: 507.9902 $[\text{M}+\text{Na}]^+$; found (ESI $^+$): 507.9971. (^1H Conversion: >99%, characterised *in situ*)

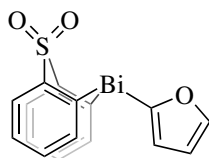
10-(Thiophen-3-yl)-10H-dibenzo[b,e][1,4]thiabismine 5,5-dioxide 21s



21s

mp/ $^{\circ}\text{C}$ 182-183. ^1H NMR (500 MHz, CDCl_3) δ_{H} 8.4 (dd, $J = 7.6, 1.4$ Hz, 2H), 7.9 (dd, $J = 7.1, 1.3$ Hz, 2H), 7.7 (dd, $J = 2.5, 1.0$ Hz, 1H), 7.4 (dd, $J = 4.8, 2.6$ Hz, 1H), 7.4 (td, $J = 7.5, 1.4$ Hz, 2H), 7.4 (td, $J = 7.3, 1.4$ Hz, 2H), 7.0 (dd, $J = 4.8, 1.1$ Hz, 1H). $^{13}\text{C}\{^1\text{H}\}$ NMR (126 MHz, CDCl_3) δ_{C} 157.2, 147.5, 141.8, 137.73, 136.8, 136.0, 133.4, 129.0, 128.4, 127.3. IR (ATR): $\tilde{\nu} = 2359, 2333, 1562, 1437, 1369, 1302, 1286, 1150, 1088, 1073, 1013, 763, 740, 601, 566, 462$. HRMS calcd. for $\text{C}_{16}\text{H}_{11}\text{BiO}_2\text{NaS}_2^+$: 507.9902 $[\text{M}+\text{Na}]^+$; found (ESI $^+$): 507.9972. Rf: (2/1, petrol/ Et_2O) 0.36. (^1H NMR Conversion: >99%, isolated by preparative TLC)

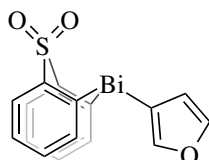
10-(Furan-2-yl)-10H-dibenzo[b,e][1,4]thiabismine 5,5-dioxide 21t



21t

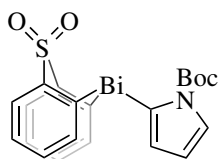
mp/ $^{\circ}\text{C}$ 196-197. ^1H NMR (500 MHz, CDCl_3) δ_{H} 8.43 – 8.35 (m, 2H), 8.22 – 8.09 (m, 2H), 7.70 (d, $J = 1.7$ Hz, 1H), 7.45 – 7.41 (m, 4H), 6.63 (d, $J = 3.1$ Hz, 1H), 6.51 (dd, $J = 3.2, 1.7$ Hz, 1H). $^{13}\text{C}\{^1\text{H}\}$ NMR (126 MHz, CDCl_3) δ_{C} 157.7, 148.9, 144.9, 141.4, 137.7, 133.5, 128.4, 127.5, 124.7, 111.1. IR (ATR): $\tilde{\nu} = 3061, 2364, 2342, 1563, 1435, 1303, 1287, 1150, 1088, 1074, 996, 883, 740, 588, 566$. HRMS calcd. for $\text{C}_{16}\text{H}_{11}\text{BiO}_3\text{NaS}^+$: 515.0125 $[\text{M}+\text{Na}]^+$; found (ESI $^+$): 515.0121. (^1H Conversion: >99%, isolated by recrystallisation from $\text{CH}_2\text{Cl}_2/\text{cyclohexane}$)

10-(Furan-3-yl)-10H-dibenzo[b,e][1,4]thiabismine 5,5-dioxide 21u

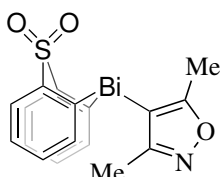


21u

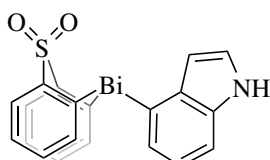
^1H NMR (500 MHz, CDCl_3) δ_{H} 8.39 – 8.32 (m, 2H), 8.02 – 7.93 (m, 2H), 7.57 (t, $J = 1.5$ Hz, 1H), 7.53 (dd, $J = 1.3, 0.8$ Hz, 1H), 7.47 – 7.31 (m, 4H), 6.14 (dd, $J = 1.7, 0.8$ Hz, 1H). HRMS calcd. for $\text{C}_{16}\text{H}_{11}\text{BiO}_3\text{NaS}^+$: 515.0125 $[\text{M}+\text{Na}]^+$; found (ESI $^+$): 515.0118. (^1H Conversion: >99%, characterised *in situ*)

tert-Butyl 2-(5,5-dioxido-10H-dibenzo[b,e][1,4]thiabismine-10-yl)-1H-pyrrole-1-carboxylate 21v**21v**

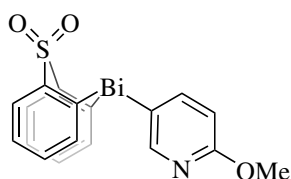
$^1\text{H NMR}$ (500 MHz, CDCl_3) δ_H 8.42 – 8.31 (m, 2H), 8.21 – 8.14 (m, 2H), 7.47 – 7.36 (m, 4H), 6.32 (dd, $J = 3.1, 3.1$ Hz, 1H), 6.26 – 6.21 (m, 2H), 1.73 (s, 9H). HRMS calcd. for $\text{C}_{16}\text{H}_{11}\text{BiNO}_2\text{S}^-$: 490.3014 $[\text{M-Boc}]^+$; found (ESI $^-$): 490.0319. (^1H Conversion: >99%, characterised *in situ*)

10-(3,5-Dimethylisoxazol-4-yl)-10H-dibenzo[b,e][1,4]thiabismine 5,5-dioxide 21w**21w**

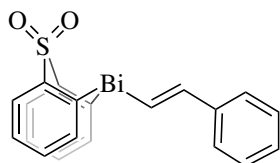
mp/ $^\circ\text{C}$ 282-283. $^1\text{H NMR}$ (500 MHz, CDCl_3) δ_H 8.39 (dd, $J = 7.7, 1.4$ Hz, 2H), 8.01 (dd, $J = 7.2, 1.3$ Hz, 2H), 7.44 (ddd, $J = 7.6, 7.3, 1.3$ Hz, 2H), 7.39 (ddd, $J = 7.6, 7.3, 1.4$ Hz, 2H). Methyl protons were observed as broad singlets between 3.0-1.0 ppm. due to rotameric broadening. $^{13}\text{C}\{^1\text{H}\}$ NMR (126 MHz, CDCl_3) δ_C 166.2, 152.8, 141.66, 137.9, 137.5, 133.5, 129.1, 128.8, 127.4, 13.8, 12.6. IR (ATR): $\tilde{\nu} = 3027, 2971, 2928, 2872, 1492, 1450, 1368, 1314, 1280, 1207, 1149, 1089, 1021, 999, 969, 910, 886, 815, 758, 698, 610, 555, 513, 437$. HRMS calcd. for $\text{C}_{17}\text{H}_{15}\text{BiNO}_3\text{S}^+$: 522.0571 $[\text{M+H}]^+$; found (ESI $^+$): 522.0552. (^1H Conversion: >99%, isolated by recrystallisation from $\text{CH}_2\text{Cl}_2/\text{cyclohexane}$)

10-(1H)-Indol-4-yl)-10H-dibenzo[b,e][1,4]thiabismine 5,5-dioxide 21x**21x**

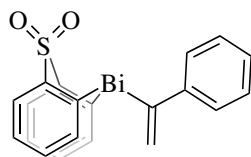
$^1\text{H NMR}$ (500 MHz, CDCl_3) δ_H 8.44 (dt, $J = 7.8, 1.5$ Hz, 2H), 7.88 (dt, $J = 7.3, 1.5$ Hz, 2H), 7.68 (d, $J = 7.8$ Hz, 1H), 7.58 (d, $J = 7.0$ Hz, 1H), 7.49 (dt, $J = 8.1, 1.4$ Hz, 1H), 7.45 – 7.37 (m, 3H), 7.19 – 7.11 (m, 1H), 7.07 (s, 1H), 6.59 (dd, $J = 3.3, 1.6$ Hz, 1H). HRMS calcd. for $\text{C}_{20}\text{H}_{15}\text{BiNO}_2\text{S}^+$: 542.0622 $[\text{M+H}]^+$; found (ESI $^+$): 542.0628. ($^1\text{H NMR}$ Conversion: 84%, characterised *in situ*)

10-(6-Methoxypyridin-3-yl)-10H-dibenzo[b,e][1,4]thiabismine 5,5-dioxide 21y**21y**

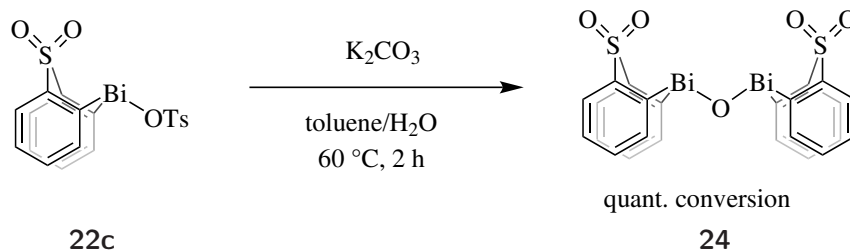
$^1\text{H NMR}$ (500 MHz, CDCl_3) δ_H 8.42 – 8.37 (m, 2H), 8.37 – 8.35 (m, 1H), 7.90 – 7.84 (m, 2H), 7.74 (dd, $J = 8.3, 2.0$ Hz, 1H), 7.39 (ddd, $J = 19.9, 7.4, 1.4$ Hz, 4H), 6.70 (dd, $J = 8.3, 0.8$ Hz, 1H), 3.94 (s, 3H). HRMS calcd. for $\text{C}_{18}\text{H}_{12}\text{BiBrO}_2\text{NaS}^+$: 579.9545 $[\text{M+Na}]^+$; found (ESI $^+$): 579.9555. ($^1\text{H NMR}$ Conversion: >99%, characterised *in situ*)

(E)-10-Styryl-10H-dibenzo[b,e][1,4]thiabismine 5,5-dioxide 23a**23a**

mp/°C 211-212. $^1\text{H NMR}$ (500 MHz, CDCl_3) δ_{H} 9.04 (d, $J = 18.4$ Hz, 1H), 8.40 – 8.34 (m, 2H), 8.20 – 8.10 (m, 2H), 7.66 (d, $J = 18.4$ Hz, 1H), 7.45 – 7.40 (m, 6H), 7.38 – 7.35 (m, 2H), 7.32 – 7.28 (m, 1H). $^{13}\text{C}\{^1\text{H}\}$ NMR (126 MHz, CDCl_3) δ_{C} 155.5, 153.6, 147.7, 141.7, 139.5, 137.1, 133.5, 128.9, 128.8, 128.4, 127.4, 126.6. IR (ATR): $\tilde{\nu} = 1562, 1492, 1442, 1303, 1286, 1151, 1108, 1074, 1013, 975, 909, 763, 740, 726, 588, 566$. HRMS calcd. for $\text{C}_{20}\text{H}_{15}\text{BiO}_2\text{NaS}^+$: 551.0489 $[\text{M}+\text{Na}]^+$; found (ESI $^+$): 551.0477. Rf: (2/1, petrol/ Et_2O) 0.40. ($^1\text{H NMR}$ Conversion: >99%, isolated by preparative TLC)

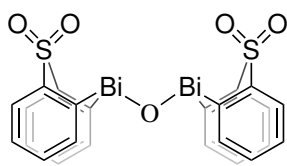
10-(1-Phenylvinyl)-10H-dibenzo[b,e][1,4]thiabismine 5,5-dioxide 23b**23b**

mp/°C 177-178. $^1\text{H NMR}$ (500 MHz, CDCl_3) δ_{H} 8.4 (dd, $J = 7.5, 1.4$ Hz, 2H), 8.0 (dd, $J = 7.1, 1.3$ Hz, 2H), 7.6 (s, 1H), 7.4 (ddd, $J = 7.5, 7.3, 1.3$ Hz, 2H), 7.3 (ddd, $J = 7.5, 7.3, 1.5$ Hz, 2H), 7.2 – 7.1 (m, 2H), 7.1 – 7.1 (m, 1H), 7.0 – 6.9 (m, 2H), 6.0 (s, 1H). $^{13}\text{C}\{^1\text{H}\}$ NMR (126 MHz, CDCl_3) δ_{C} 159.9, 145.6, 141.5, 137.5, 133.4, 130.0, 128.8, 128.4, 128.4, 127.8, 127.5, 127.4. IR (ATR): $\tilde{\nu} = 3051, 2926, 2851, 2363, 2341, 1681, 1598, 1563, 1439, 1303, 1252, 1149, 762, 740, 716, 588, 566$. HRMS calcd. for $\text{C}_{20}\text{H}_{15}\text{BiO}_2\text{NaS}^+$: 551.0489 $[\text{M}+\text{Na}]^+$; found (ESI $^+$): 551.0481. Rf: (2/1, petrol/ Et_2O) 0.42. ($^1\text{H NMR}$ Conversion: >99%, isolated by preparative TLC)

Transmetalation– Identification of Intermediate

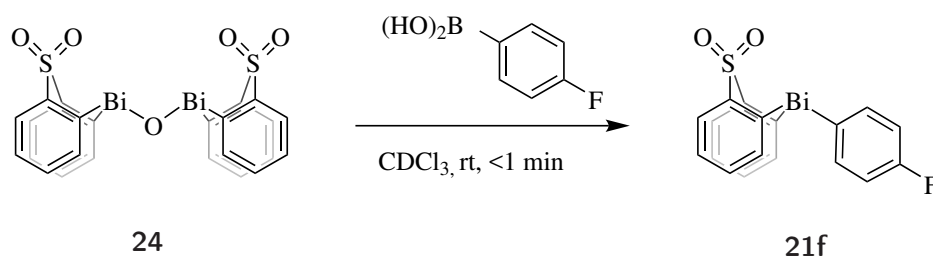
5,5-Dioxido-10H-dibenzo[b,e][1,4]thiabismine-10-yl 4-methylbenzenesulfonate (5.0 mg, 8.4 μmol) and K_2CO_3 (1.4 mg, 10 μmol) were added to a mixture of toluene (2.0 mL) and water (0.01 mL) and allowed to stir at 50 °C for 2 h. The reaction mixture was washed with water and the organic phase was concentrated *in vacuo* to yield in the desired product as a white solid.

Bis(5,5-dioxido-10H-dibenzo[b,e][1,4]thiabismine-10-yl) oxide **24**

**24**

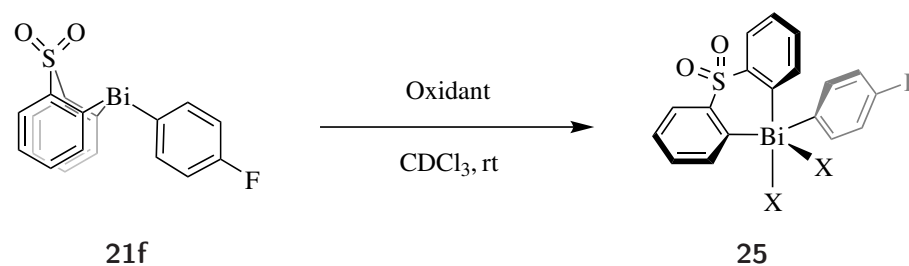
mp/°C 230-231. $^1\text{H NMR}$ (500 MHz, CDCl_3) δ_{H} 8.45 (d, $J = 7.3$ Hz, 1H), 8.37 (d, $J = 7.7$ Hz, 1H), 7.74 – 7.60 (m, 1H), 7.45 (dd, $J = 7.6$ Hz, 7.6 Hz, 1H). $^{13}\text{C}\{^1\text{H}\}$ NMR (126 MHz, CDCl_3) δ_{C} 182.6, 141.5, 134.4, 134.0, 128.6, 128.3. IR (ATR): $\tilde{\nu} = 1562, 1438, 1302, 1287, 1146, 1086, 1070, 1012, 911$. HRMS calcd. for $\text{C}_{24}\text{H}_{17}\text{Bi}_2\text{O}_5\text{S}_2^+$: 867.0120 $[\text{M}+\text{H}]^+$; found (ESI $^+$): 867.0136. White solid 3.5 mg, 96%.

Transmetalation– Utilisation of Intermediate

**24****21f**

CDCl_3 (0.6 mL) was added to bis(5,5-dioxido-10H-dibenzo[b,e][1,4]thiabismine-10-yl) oxide (5.0 mg, 5.8 μmol) and 4-fluorophenyl boronic acid (0.8 mg, 5.8 μmol). The reaction mixture was shaken vigorously for 8 s and analysed by ^1H and ^{19}F NMR spectroscopy to result in **21f** as the sole product within less than 5 min.

Oxidation of **21f**

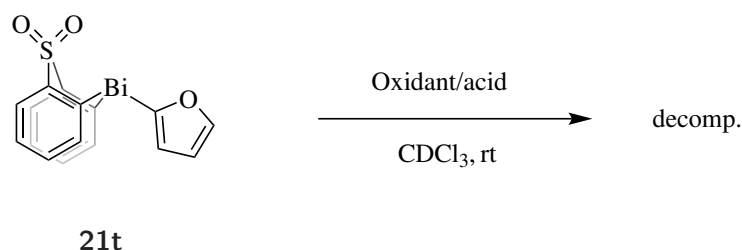
**21f****25**

CDCl_3 (0.6 mL) was added to 10-(4-fluorophenyl)-10H-dibenzo[b,e][1,4]thiabismine 5,5-dioxide (3.0 mg, 5.7 μmol) in a NMR tube. Subsequently the oxidant (11.4 μmol) was added, the tube shaken vigorously and analysed by ^{19}F NMR spectroscopy.

Table 4.3.3: Scope of possible oxidants for the oxidation of **21f**

Solvent	Oxidation [%]	Decomposition-product
<i>m</i> CPBA	100	
TBHP	0	
Lauryl peroxide	0	
NBu ₄ OXONE	7	
Selectfluor	0	
NFSI	88	
1-Fluoro-2,4,6-trimethylpyridinium BF ₄	0	
Chloramine T	0	
Iodine	100 (dec)	1-fluoro-4-iodobenzene
Bromine	100 (dec)	1-bromo-4-fluorobenzene
1-chloro-benzotriazol	29 (dec)	1-chloro-4-fluorobenzene
XeF ₂	100	
SO ₂ Cl ₂	100	
NCS	0	
Trichloroisocyanurate	100 (dec)	1-chloro-4-fluorobenzene
NBS	100 (dec)	1-bromo-4-fluorobenzene
PhI(OAc) ₂	2	

Oxidation of Furan

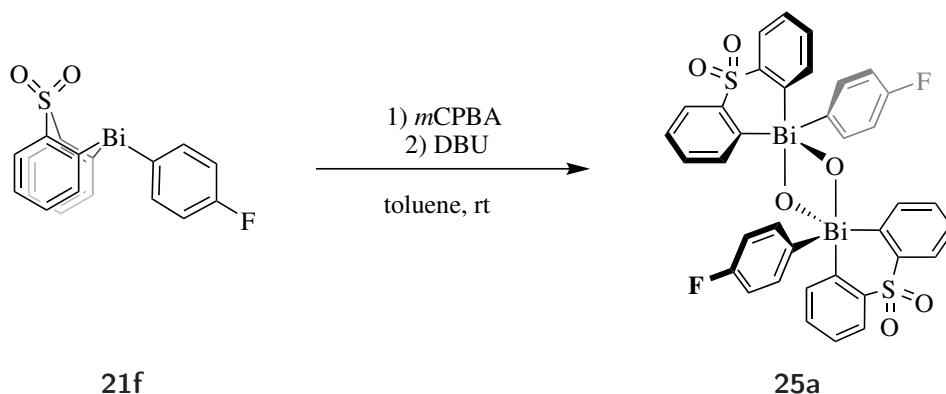


CDCl₃ (0.6 mL was added to 10-(furan-2-yl)-10H-dibenzo[b,e][1,4]thiabismine 5,5-dioxide (3.0 mg, 5.7 μmol) in a NMR tube. Subsequently the oxidant/acid (11.4 μmol) was added, the tube shaken vigorously and analysed by ¹⁹F NMR spectroscopy.

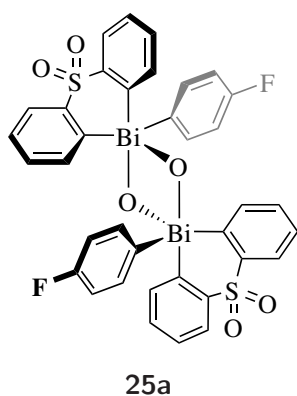
Table 4.3.4: Oxidants for the oxidation of **21t**

Entry	Reagent	Oxidation [%]	Decomposition-product
1	<i>m</i> CPBA (pure)	100 (dec)	N.D.
2	<i>m</i> CBA	100 (dec)	Furan
3	1-chloro-benzotriazol	72 (dec)	N.D.
4	TBHP	40 (dec)	Furan
5	NFSI	80 (dec)	Furan
6	SO ₂ Cl ₂	100 (dec)	N.D.
7	4,4-dibromo-2,6-di- <i>tert</i> -butylcyclohexa-2,5-dien-1-one	18 (dec)	Furan

Isolation of Aryl Thiabismine Dioxide Dimer 25a

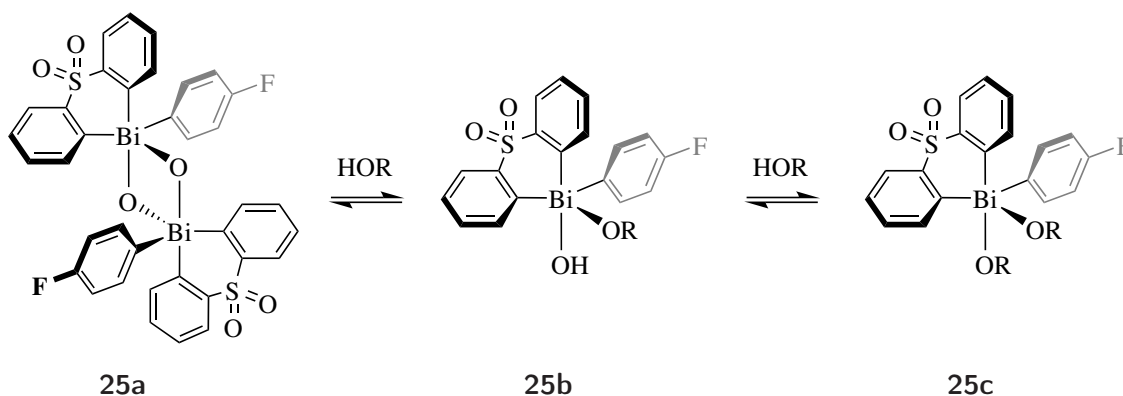


10-(4-Fluorophenyl)-10H-dibenzo[b,e][1,4]thiabismine 5,5-dioxide (50.0 mg, 0.96 mmol) has been added to 30 mL of CH_2Cl_2 . *m*CPBA (20.0 mg, 1.15 mmol) has been added to the solution and allowed to stir at room temperature for 5 min. DBU (716 μL , 4.80 mmol) is added and organic phase extracted with H_2O . The organic phase has been dried to result in the desired product (49.4 mg, 96%)

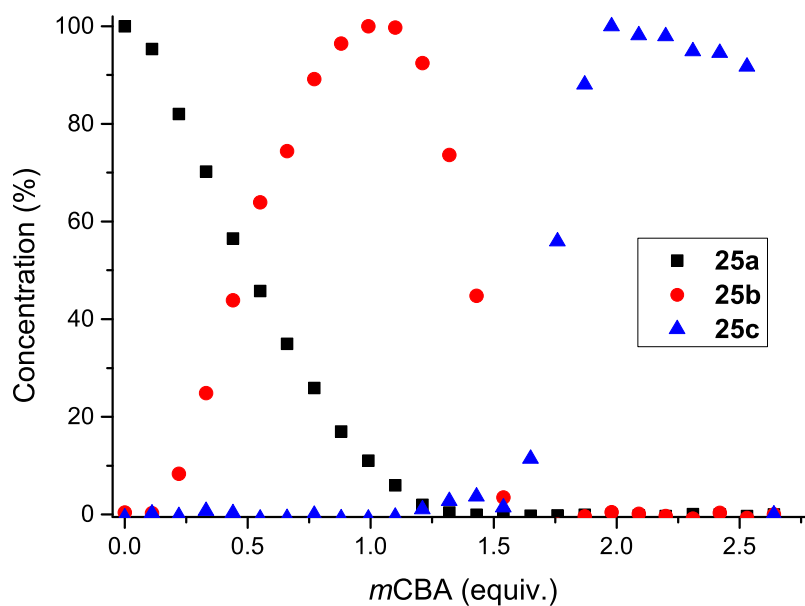
Di- μ -oxo dimer 25a

mp/ $^{\circ}\text{C}$ 164-165. ^1H NMR (500 MHz, CDCl_3) δ_{H} 8.63 (d, $J = 7.4$ Hz, 1H), 8.25 (dd, $J = 7.6, 1.3$ Hz, 1H), 8.16 (dd, $J = 8.5, 5.4$ Hz, 1H), 7.59 (ddd, $J = 7.5, 7.4, 1.3$ Hz, 1H), 7.55 – 7.48 (m, 1H), 7.08 (dd, $J = 8.6$ Hz, 1H). $^{13}\text{C}\{^1\text{H}\}$ NMR (126 MHz, CDCl_3) δ_{C} 164.9, 164.2 (d, $J = 190.2$ Hz), 151.1, 147.6, 136.6 (d, $J = 8.2$ Hz), 136.6, 134.0, 130.1, 127.5, 117.6 (d, $J = 21.6$ Hz). ^{19}F NMR (471 MHz, CDCl_3) δ_{F} -108.20 (td, $J = 8.8, 4.5$ Hz). IR (ATR): $\tilde{\nu} = 1574, 1479, 1433, 1316, 1289, 1227, 1155, 1131, 1088, 1023, 1008, 909, 825, 763, 740, 713, 587, 564, 498, 461, 441$. HRMS calcd. for $\text{C}_{36}\text{H}_{26}\text{Bi}_2\text{F}_2\text{O}_6\text{S}_2^{2+}$: 537.0368 $[\text{M}+2\text{H}]^{2+}$; found (ESI $^+$): 537.0352.

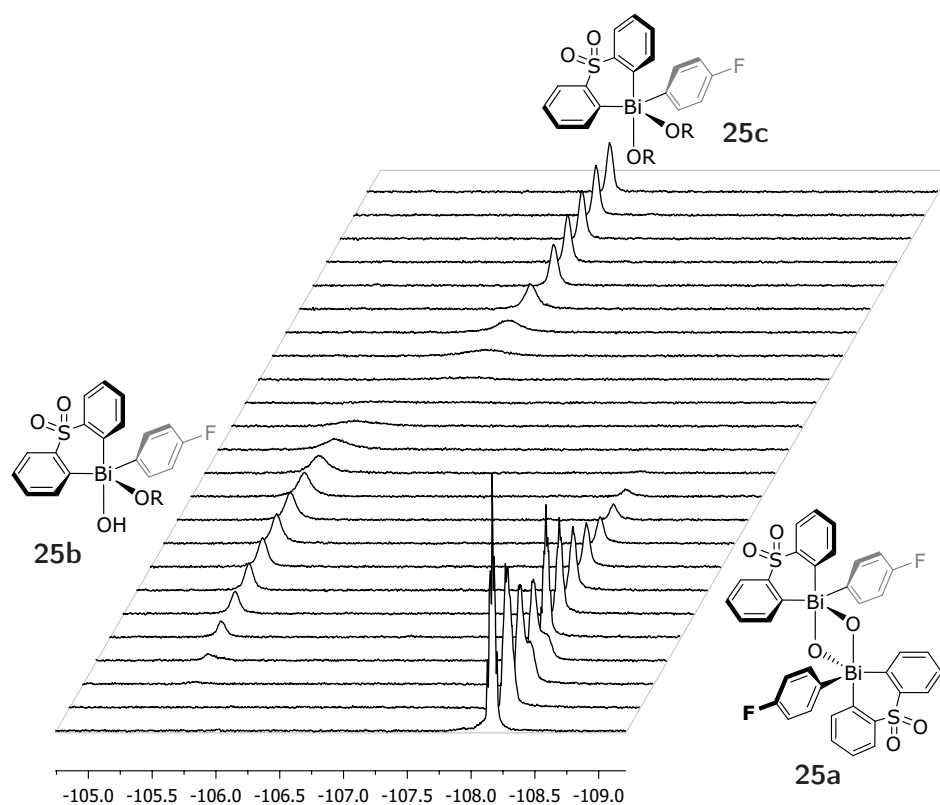
Identification of the kinetically competent Bi(V) species by titration of **25**



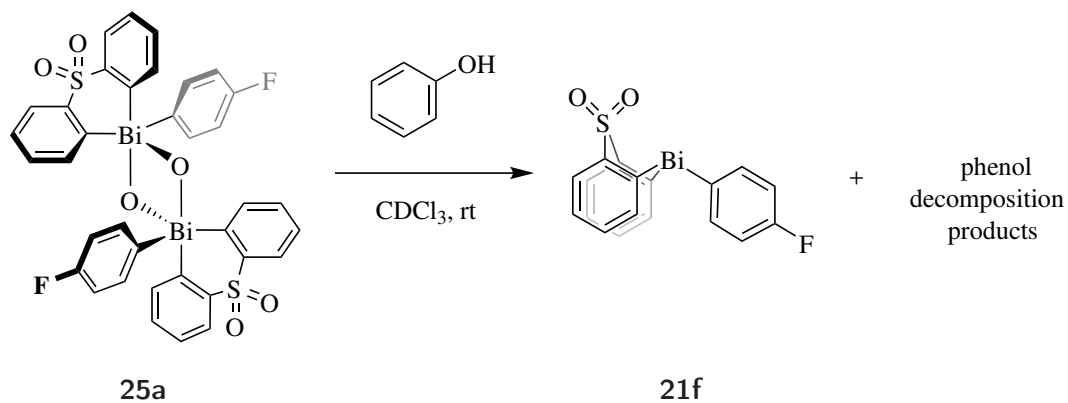
μ -O-Dimer **25a** (5.0 mg, 4.6 μ mmol) was added to CDCl_3 (0.5 mL). *m*CBA (3.6 mg, 23 μ mmol) were dissolved in 1.5 mL of CDCl_3 . The *m*CBA solution was added in segments of 0.05 mL with the recording of a ^{19}F NMR spectrum after each addition.



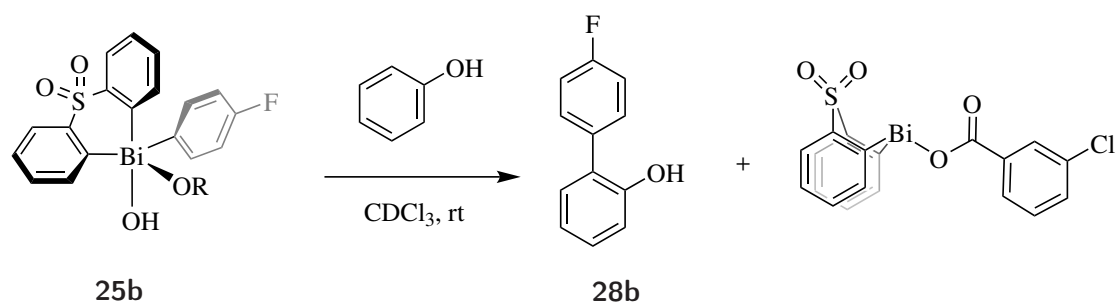
The mass balance could not be fully accounted for between 1.2 and 1.9 equivalents of *m*CBA due to peak broadening into the baseline in the ^{19}F NMR spectrum due to equilibrium on the timescale of the NMR acquisition.



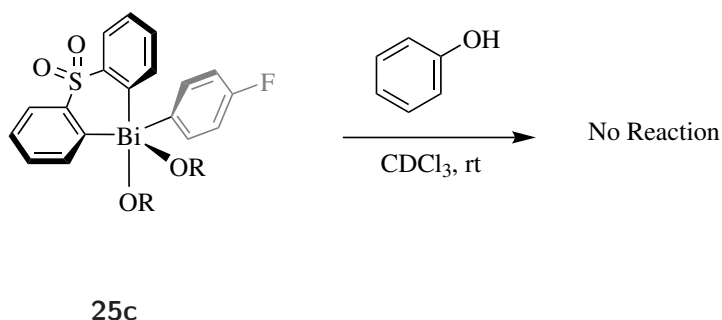
Arylation using 25a



Phenol (8.0 mg, 85 μmol) was added to a solution of μ -O-dimer (5.0 mg, 4.6 μmol) in CDCl_3 (0.6 mL) in an NMR tube and the reaction mixture was shaken vigorously. A ^{19}F NMR spectrum was recorded after 5 min revealing the corresponding Bi(III) species **21f** in quantitative conversion and a variety of oxidation products of phenol.

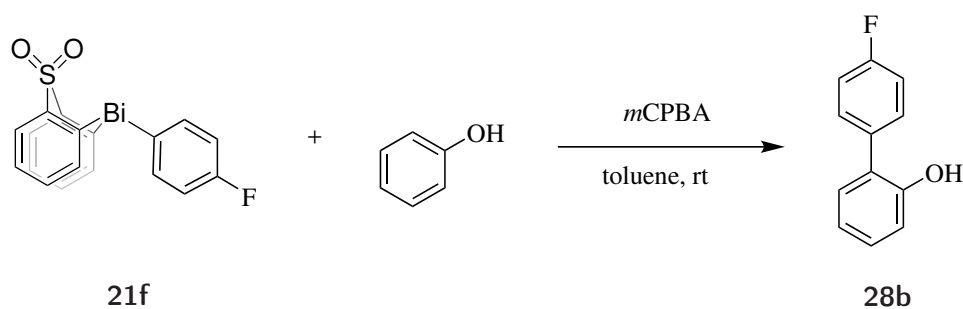
Arylation using **25b**

CDCl₃ (0.3 mL) was added to the μ -O-Dimer **25a** (6.7 mg, 6.3 μ mmol) in an NMR tube and the tube was shaken vigorously. A ¹⁹F NMR spectrum was taken before *m*CBA (1.97 mg, 12.6 μ mmol) was added as a solution in 0.2 mL CDCl₃ and the formation of intermediate **25b** was confirmed by a subsequent ¹⁹F NMR spectrum. Phenol (1.19 mg, 12.6 μ mmol) was added as a solution of 0.2 mL in CDCl₃. A kinetic array was started immediately, and the first spectrum was acquired 58 s after addition of phenol. In this first spectrum full conversion was observed. ([**25b**]₀ = 18 mM, [phenol]₀ = 18 mM)

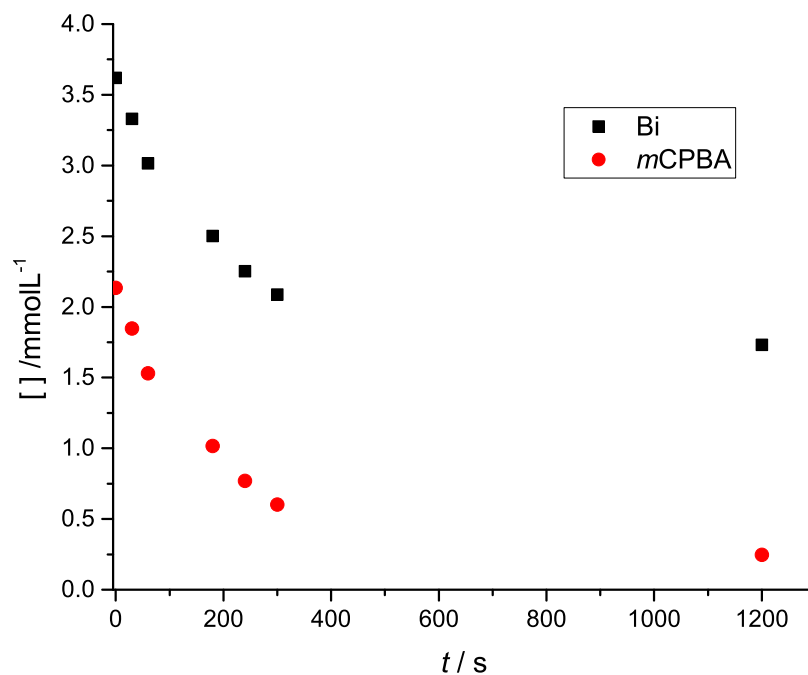
Arylation using **25c**

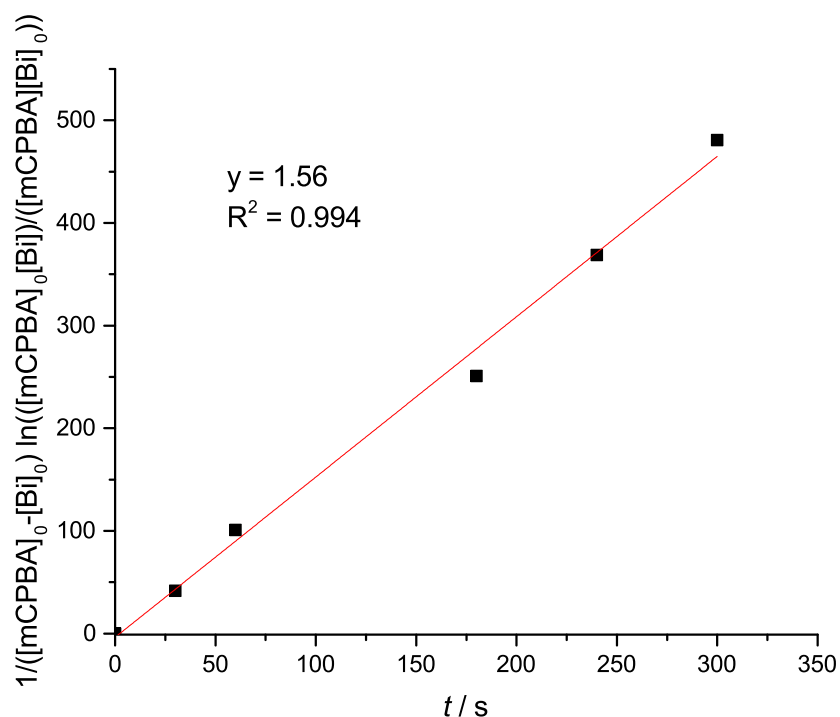
CDCl₃ (0.3 mL) was added to the μ -O-Dimer **25a** (5.0 mg, 4.6 μ mmol) and *m*CBA (15 mg, 98 μ mmol) in a NMR tube and the tube was shaken vigorously. In the following a ¹⁹F NMR spectrum was taken confirming the formation of **25c**. The subsequent addition of phenol (8 mg, 85 μ mmol) did not result in the formation of any arylation product within 2 days.

Determination of the Rate Determining Step of the Oxidation/Arylation Step

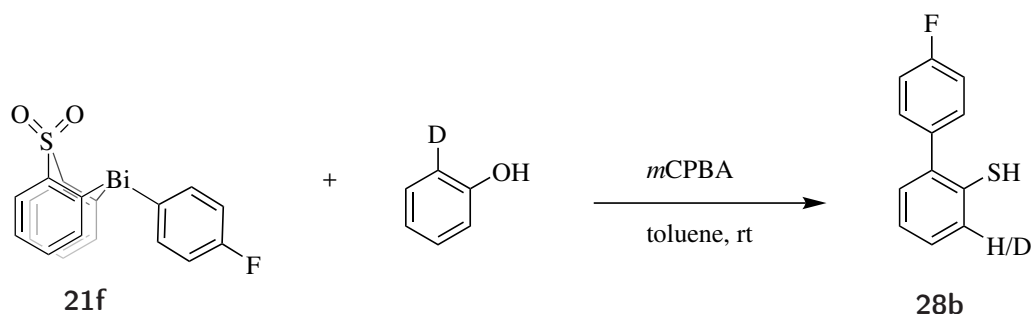


Toluene (10.0 mL) was added to 10-(4-fluorophenyl)-10H-dibenzo[b,e][1,4]thiabismine 5,5-dioxide (20.0 mg, 38.0 μmol), phenol (36.0 mg, 380 μmol) and 4,4'-bis(trifluoromethyl)-1,1'-biphenyl (1.86 mg, 6.41 μmol) in a microwave vial. A solution of *m*CPBA (8.0 mg) in toluene (0.5 mL) was added to the solution. The reaction was stirred at room temperature and samples were taken at various time points, quenched in methanol and analysed *via* ^{19}F NMR spectroscopy. $k_{\text{obs}} = 1.56 \text{ Lmol}^{-1}\text{s}^{-1}$



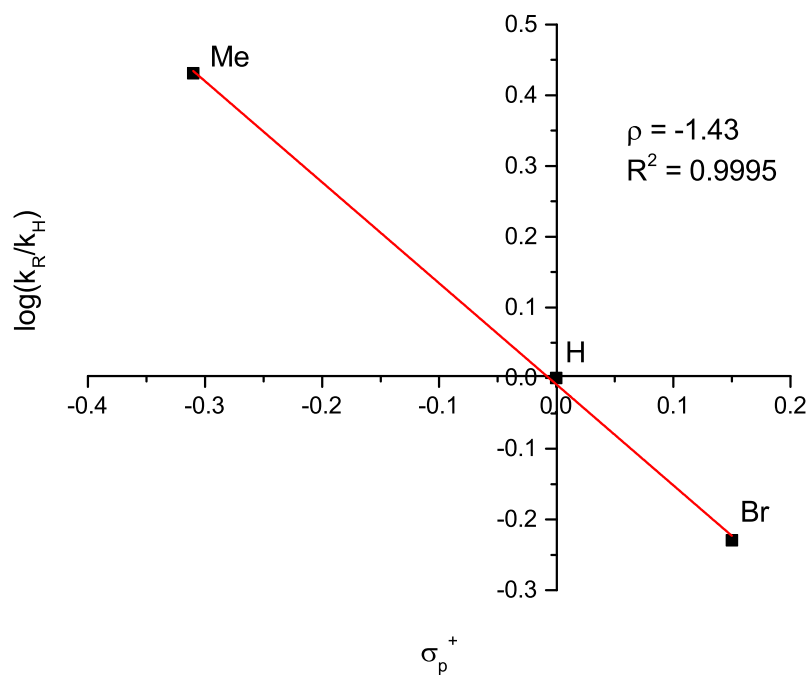
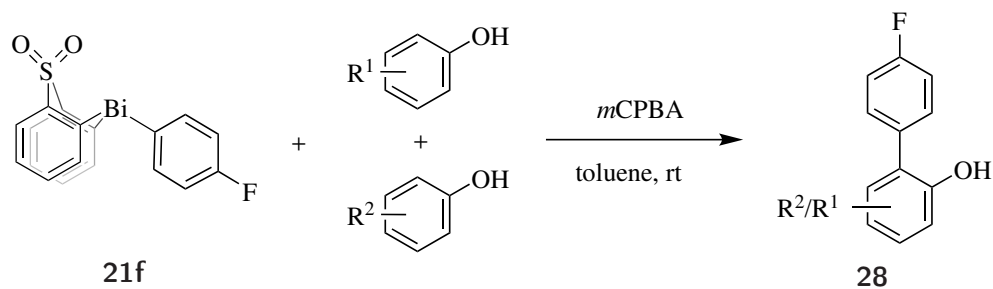


Intramolecular isotopic competition experiments



Toluene (5.0 mL) was added to 10-(4-fluorophenyl)-10H-dibenzo[b,e][1,4]thiabismine 5,5-dioxide (163 mg, 310 μmol) and 2-deutero-phenol (150 mg, 1.57 mmol, 99%-d₁). *mCPBA* (81 mg, 474 μmol) was added and the reaction allowed to stir for 5 min at room temperature. The reaction was quenched with MeOH (2 mL) and Et₂O (20 mL) was added and the organic phase was washed with saturated KHCO₃ solution. The organic phase was dried (MgSO₄) and the solvent reduced *in vacuo*. The resulting crude was purified using column chromatography (Rf: (toluene) 0.33). The isotopic ratio was analysed by high-resolution mass spectrometry. (Product_H/Product_D = 1.21, k_H/k_D = 0.83)

Intermolecular Isotopic Competition Experiments



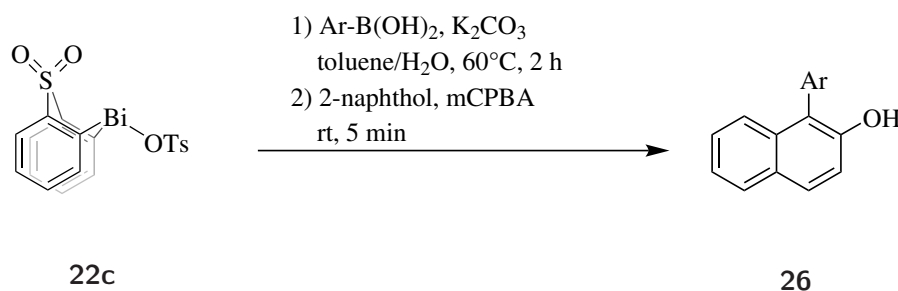
	Competing phenols		
	H/4-Me	H/4-Br	2-D/4-Br
initial ratio	1 : 0.91	1 : 0.93	1 : 0.93
product ratio	1 : 2.46	1 : 0.55	1 : 0.57
k_R/k_H	2.7	0.59	0.61
σ_p^+	0.15	-0.31	0.15

CDCl_3 (0.6 mL) was added to 10-(4-fluorophenyl)-10H-dibenzo[b,e][1,4]thiabismine 5,5-dioxide (16.0 mg, 30.7 μmol) and 2 phenols (77.5 μmol each) in an NMR tube. The initial ratio of phenols was determined by ^1H NMR spectroscopy. Subsequently *m*CPBA (10 mg, 58.4 μmol) were added, the NMR tube was shake vigorously and the resulting mixture analysed by ^{19}F NMR spectroscopy.

$$\frac{k_{Br}}{k_H} \cong \frac{k_{Br}}{k_D}$$

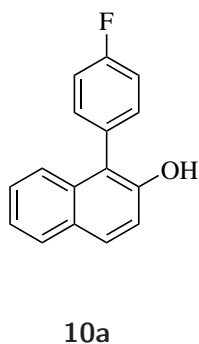
$$\frac{k_H}{k_D} \cong 1$$

Arylation of 2-Naphthol



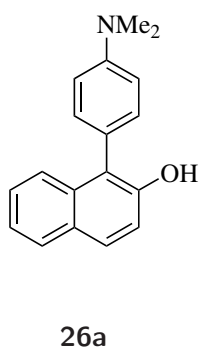
General Protocol A: 5,5-Dioxido-10H-dibenzo[b,e][1,4]thiabismine-10-yl 4-methylbenzenesulfonate (137 mg, 229 μmol), K₂CO₃ (40.0 mg, 290 μmol) and boronic acid (270 μmol) were added to a mixture of toluene (5.00 mL) and water (0.01 mL) and allowed to stir at 60 °C for 2 h. 2-Naphthol (30.3 mg, 210 μmol) and *m*CPBA (72.5 mg, 420 μmol) were added sequentially and the reaction mixture was stirred for 5 min. The reaction was quenched with MeOH (2.0 mL) and Et₂O (20.0 mL) were added. The organic phase was separated and washed with saturated KHCO₃ solution. The organics were dried (MgSO₄) and concentrated *in vacuo*. The reaction product was purified by column chromatography.

1-(4-Fluorophenyl)naphthalen-2-ol 10a

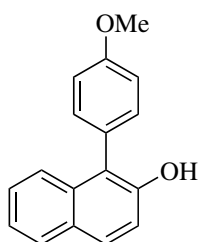


mp/°C 110-111. ¹H NMR (500 MHz, CDCl₃) δ_H 7.85 – 7.79 (m, 2H), 7.44 – 7.37 (m, 2H), 7.38 – 7.22 (m, 6H), 5.00 (s, 1H). ¹³C{¹H} NMR (126 MHz, CDCl₃) δ_C 162.9 (d, *J* = 248.1 Hz), 150.4, 133.5, 133.2 (d, *J* = 8.1 Hz), 131.7, 130.1 (d, *J* = 3.5 Hz), 129.9, 129.1, 128.2, 126.8, 124.5, 123.6, 120.1, 116.9 (d, *J* = 21.4 Hz). ¹⁹F NMR (471 MHz, CDCl₃) δ_F -113.07 (tt, *J* = 9.5, 5.4 Hz). IR (ATR): $\tilde{\nu}$ = 1574, 1479, 1433, 1316, 1289, 1227, 1155, 1131, 1088, 1023, 1008, 909, 825, 763, 740, 713, 587, 564, 498, 461, 441. HRMS calcd. for C₁₆H₁₀FO⁻: 237.0721 [M-H]⁻; found (ESI⁻): 237.0720. Rf: (5/2, petrol/Et₂O) 0.55. Yield: 48.2 mg (96%).

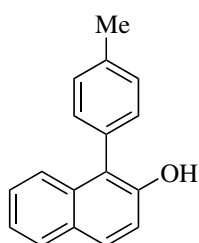
1-(4-Dimethylaminophenyl)naphthalen-2-ol 26a



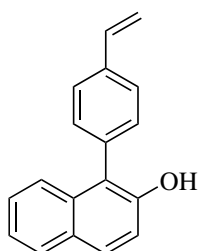
mp/°C 120-121. ¹H NMR (500 MHz, CDCl₃) δ_H 7.82 (dd, *J* = 7.4, 2.0 Hz, 1H), 7.79 (d, *J* = 8.9 Hz, 1H), 7.55 – 7.49 (m, 1H), 7.39 – 7.32 (m, 2H), 7.31 (d, *J* = 8.7 Hz, 2H), 7.28 (d, *J* = 8.9 Hz, 1H), 6.97 – 6.92 (m, 2H), 5.33 (s, 1H), 3.08 (s, 6H). ¹³C{¹H} NMR (126 MHz, CDCl₃) δ_C 150.6, 150.43, 133.9, 131.9, 128.9, 128.9, 127.9, 126.2, 124.9, 123.1, 121.2, 120.7, 117.1, 113.2, 40.5. IR (ATR): $\tilde{\nu}$ = 3520, 2360, 2340, 1734, 1612, 1523, 1387, 1351, 1224, 1173, 1145, 816, 749. HRMS calcd. for C₁₈H₁₆NO⁻: 262.1237 [M-H]⁻; found (ESI⁻): 237.0720. Rf: (5/1.5, petrol/Et₂O) 0.32. Yield: 48.2 mg (87%).

1-(4-Methoxyphenyl)naphthalen-2-ol **26b****26b**

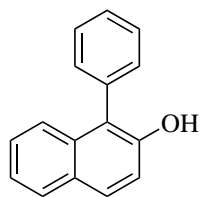
mp/°C 98-99. $^1\text{H NMR}$ (500 MHz, CDCl_3) δ_{H} 7.83 (dd, $J = 9.1$, 7.0 Hz, 2H), 7.47 – 7.42 (m, 1H), 7.41 – 7.32 (m, 4H), 7.29 (d, $J = 8.9$ Hz, 1H), 7.15 (d, $J = 8.5$ Hz, 2H), 5.15 (s, 1H), 3.94 (s, 3H). $^{13}\text{C}\{^1\text{H}\}$ NMR (126 MHz, CDCl_3) δ_{C} 159.8, 150.4, 133.6, 132.4, 129.3, 128.9, 128.0, 126.4, 125.8, 124.7, 123.2, 120.6, 117.2, 115.1, 55.4. IR (ATR): $\tilde{\nu} = 3059, 2956, 2933, 2835, 1618, 1608, 1597, 1509, 1464, 1387, 1286, 1245, 1176, 1145, 1032, 816, 749$. HRMS calcd. for $\text{C}_{17}\text{H}_{13}\text{O}_2^-$: 249.0921 $[\text{M-H}]^-$; found (ESI $^-$): 249.0924. Rf: (5/1.5, petrol/ Et_2O) 0.26. Yield: 49.9 mg (95%).

1-(4-Tolyl)naphthalen-2-ol **26c****26c**

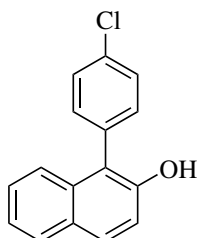
mp/°C 73-74. $^1\text{H NMR}$ (500 MHz, CDCl_3) δ_{H} 7.84 – 7.77 (m, 2H), 7.41 (dd, $J = 11.0, 8.7$ Hz, 3H), 7.37 – 7.29 (m, 4H), 7.26 (d, $J = 8.9$ Hz, 1H), 5.15 (s, 1H), 2.48 (s, 3H). $^{13}\text{C}\{^1\text{H}\}$ NMR (126 MHz, CDCl_3) δ_{C} 150.4, 138.5, 133.5, 131.2, 131.0, 130.5, 129.5, 129.1, 128.2, 126.5, 124.8, 123.4, 121.1, 117.4, 21.5. IR (ATR): $\tilde{\nu} = 3059, 2956, 2933, 2835, 1618, 1608, 1597, 1509, 1464, 1387, 1286, 1245, 1176, 1145, 1032, 816, 749$. HRMS calcd. for $\text{C}_{17}\text{H}_{13}\text{O}^-$: 233.0972 $[\text{M-H}]^-$; found (ESI $^-$): 233.0974. Rf: (5/1.5, petrol/ Et_2O) 0.20. Yield: 46.8 mg (95%).

1-(4-Vinylphenyl)naphthalen-2-ol **26d****26d**

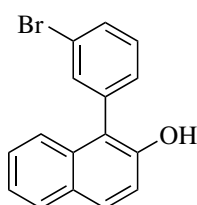
$^1\text{H NMR}$ (500 MHz, CDCl_3) δ_{H} 7.85 – 7.75 (m, 2H), 7.68 – 7.58 (m, 2H), 7.47 – 7.39 (m, 3H), 7.34 (m, 2H), 7.26 (d, $J = 8.9$ Hz, 1H), 6.83 (dd, $J = 17.6, 10.9$ Hz, 1H), 5.88 (d, $J = 17.6$ Hz, 1H), 5.37 (d, $J = 10.9$ Hz, 1H), 5.12 (s, 1H). $^{13}\text{C}\{^1\text{H}\}$ NMR (126 MHz, CDCl_3) δ_{C} 150.3, 137.9, 136.4, 133.7, 133.4, 131.5, 129.7, 129.1, 128.2, 127.6, 126.7, 124.7, 123.5, 120.8, 117.5, 115.0. IR (ATR): $\tilde{\nu} = 1620, 1596, 1517, 1464, 1389, 1345, 1309, 1271, 1222, 1171, 1146, 989, 912, 845, 816, 748, 661, 467, 435$. HRMS calcd. for $\text{C}_{18}\text{H}_{13}\text{O}^-$: 245.0972 $[\text{M-H}]^-$; found (ESI $^-$): 245.0973. Rf: (5/1.5, petrol/ Et_2O) 0.38. Yield: 45.9 mg (89%).

1-Phenyl-naphthalen-2-ol **26e****26e**

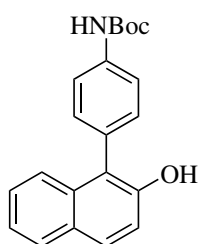
mp/°C 91-92. $^1\text{H NMR}$ (500 MHz, CDCl_3) δ_{H} 7.86 – 7.78 (m, 2H), 7.60 (dd, $J = 8.1, 6.9$ Hz, 2H), 7.55 – 7.48 (m, 1H), 7.47 – 7.38 (m, 3H), 7.37 – 7.30 (m, 2H), 5.12 (s, 1H). $^{13}\text{C}\{^1\text{H}\}$ NMR (126 MHz, CDCl_3) δ_{C} 150.1, 134.1, 133.3, 131.2, 129.7, 129.5, 128.9, 128.5, 128.0, 126.5, 124.6, 123.3, 121.0, 117.4. IR (ATR): $\tilde{\nu} = 3059, 2956, 2933, 2835, 1618, 1608, 1597, 1509, 1464, 1387, 1286, 1245, 1176, 1145, 1032, 816, 749$. HRMS calcd. for $\text{C}_{16}\text{H}_{11}\text{O}^-$: 219.0815 $[\text{M-H}]^-$; found (ESI $^-$): 219.0813. Rf: (5/1.5, petrol/Et $_2$ O) 0.34. Yield: 41.1 mg (89%).

1-(4-Chlorophenyl)-naphthalen-2-ol **26f****26f**

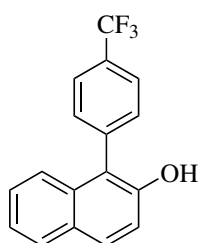
mp/°C 83-84. $^1\text{H NMR}$ (500 MHz, CDCl_3) δ_{H} 7.87 – 7.77 (m, 2H), 7.61 – 7.54 (m, 2H), 7.41 – 7.31 (m, 5H), 7.25 (d, $J = 8.4$ Hz, 1H), 4.98 (s, 1H). $^{13}\text{C}\{^1\text{H}\}$ NMR (126 MHz, CDCl_3) δ_{C} 150.1, 134.6, 133.1, 132.7, 132.6, 129.9, 129.9, 128.9, 128.1, 126.7, 124.3, 123.5, 119.8, 117.4. IR (ATR): $\tilde{\nu} = 3532, 1619, 1597, 1490, 1464, 1390, 1345, 1345, 1308, 1268, 1221, 1170, 1145, 1088, 1016, 816, 748, 645, 564, 497, 453, 431$. HRMS calcd. for $\text{C}_{16}\text{H}_{10}\text{ClO}^-$: 253.0426 $[\text{M-H}]^-$; found (ESI $^-$): 253.0425. Rf: (5/1.5, petrol/Et $_2$ O) 0.31. Yield: 48.2 mg (90%).

1-(3-Bromophenyl)-naphthalen-2-ol **26g****26g**

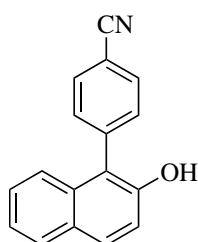
$^1\text{H NMR}$ (500 MHz, CDCl_3) δ_{H} 7.88 – 7.79 (m, 2H), 7.68 (ddd, $J = 8.0, 2.0, 1.1$ Hz, 1H), 7.63 (dd, $J = 1.8, 1.6$ Hz, 1H), 7.49 (dd, $J = 7.8, 7.8$ Hz, 1H), 7.40 (m, 4H), 7.27 (d, $J = 9.0$ Hz, 1H), 5.03 (s, 1H). $^{13}\text{C}\{^1\text{H}\}$ NMR (126 MHz, CDCl_3) δ_{C} 150.1, 136.6, 134.2, 133.0, 131.7, 131.1, 130.0, 129.9, 128.9, 128.1, 126.8, 124.3, 123.6, 123.5, 119.6, 117.4. IR (ATR): $\tilde{\nu} = 1620, 1593, 1557, 1509, 1461, 1387, 1344, 1308, 1267, 1218, 1173, 1146, 1116, 1090, 989, 949, 814, 790, 747, 697, 676, 563, 432$. HRMS calcd. for $\text{C}_{16}\text{H}_{10}\text{BrO}^-$: 296.9921 $[\text{M-H}]^-$; found (ESI $^-$): 296.9930. Rf: (5/1.5, petrol/Et $_2$ O) 0.26. Yield: 54.3 mg (87%).

***tert*-Butyl (4-(2-hydroxynaphthalen-1-yl)phenyl)carbamate 26i****26i**

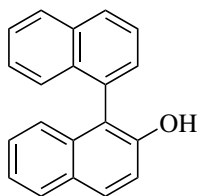
^1H NMR (500 MHz, CDCl_3) δ_{H} 7.79 (d, $J = 8.4$ Hz, 2H), 7.59 (d, $J = 8.0$ Hz, 2H), 7.41 (d, $J = 7.8$ Hz, 1H), 7.36 (d, $J = 7.9$ Hz, 2H), 7.35 – 7.29 (m, 2H), 7.24 (s, 1H), 6.62 (s, 1H), 5.13 (s, 1H), 1.56 (s, 9H). $^{13}\text{C}\{^1\text{H}\}$ NMR (126 MHz, CDCl_3) δ_{C} 152.9, 150.5, 138.8, 133.6, 132.0, 129.6, 129.1, 128.5, 128.2, 126.6, 124.8, 123.4, 120.6, 119.7, 117.4, 81.1, 28.5. IR (ATR): $\tilde{\nu} = 1620, 1596, 1517, 1464, 1389, 1345, 1309, 1271, 1222, 1171, 1146, 989, 912, 845, 816, 748, 661, 467, 435$. HRMS calcd. for $\text{C}_{21}\text{H}_{20}\text{NO}_3^-$: 334.1449 [M-H] $^-$; found (ESI $^-$): 334.1452. Rf: (toluene) 0.12. Yield: 119 mg (94%).

1-(4-(Trifluoromethyl)phenyl)naphthalen-2-ol 26j**26j**

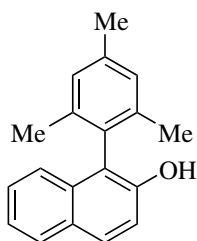
mp/ $^{\circ}\text{C}$ 102-103. ^1H NMR (500 MHz, CDCl_3) δ_{H} 7.85 (m, 4H), 7.58 (d, $J = 7.9$ Hz, 2H), 7.36 (ddd, $J = 10.0, 6.1, 2.7$ Hz, 3H), 7.26 (d, $J = 8.8$ Hz, 1H), 4.92 (s, 1H). $^{13}\text{C}\{^1\text{H}\}$ NMR (126 MHz, CDCl_3) δ_{C} 150.05, 138.52, 132.92, 131.75, 130.67 (q, $J = 32.8$ Hz), 130.19, 128.96, 128.19, 126.91, 126.48 (q, $J = 3.8$ Hz), 124.21, 124.07 (q, $J = 272.0$ Hz), 123.65, 119.70, 117.54. ^{19}F NMR (471 MHz, CDCl_3) δ_{F} -62.63. IR (ATR): $\tilde{\nu} = 3551, 1739, 1617, 1617, 1507, 1465, 1390, 1323, 1167, 1125, 1066, 1020, 845, 814, 748$. HRMS calcd. for $\text{C}_{17}\text{H}_{11}\text{F}_3\text{O}^-$: 287.0689 [M-H] $^-$; found (ESI $^-$): 287.0692. Rf: (5/1.5, petrol/ Et_2O) 0.32. Yield: 57.9 mg (96%).

4-(2-Hydroxynaphthalen-1-yl)benzotrile 26k**26k**

mp/ $^{\circ}\text{C}$ 190-191. ^1H NMR (500 MHz, CDCl_3) δ_{H} 7.91 – 7.86 (m, 2H), 7.86 – 7.81 (m, 2H), 7.60 – 7.56 (m, 2H), 7.39 – 7.35 (m, 2H), 7.34 – 7.28 (m, 1H), 7.24 (d, $J = 8.9$ Hz, 1H), 4.94 (s, 1H). $^{13}\text{C}\{^1\text{H}\}$ NMR (126 MHz, CDCl_3) δ_{C} 150.0, 140.2, 133.2, 132.8, 132.3, 130.6, 129.1, 128.4, 127.2, 124.1, 123.9, 119.6, 118.7, 117.8, 112.4. IR (ATR): $\tilde{\nu} = 2231, 1620, 1585, 1512, 1502, 1466, 1435, 1371, 1345, 1305, 1271, 1223, 1171, 1146, 984, 943, 842, 814, 748, 584$. HRMS calcd. for $\text{C}_{17}\text{H}_{10}\text{NO}^-$: 244.0768 [M-H] $^-$; found (ESI $^-$): 244.0771. Rf: (5/1.5, petrol/ Et_2O) 0.10. Yield: 46.9 mg (91%).

[1,1'-Binaphthalen]-2-ol 26l**26l**

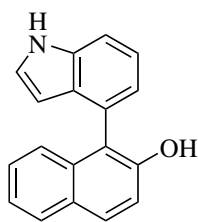
mp/°C 111-112. $^1\text{H NMR}$ (500 MHz, CDCl_3) δ_{H} 8.04 (d, $J = 8.3$ Hz, 1H), 7.99 (d, $J = 8.2$ Hz, 1H), 7.91 (d, $J = 8.9$ Hz, 1H), 7.87 (dd, $J = 8.2, 1.2$ Hz, 1H), 7.67 (dd, $J = 8.3, 6.9$ Hz, 1H), 7.54 (ddd, $J = 14.8, 7.5, 1.4$ Hz, 2H), 7.42 – 7.30 (m, 4H), 7.26 – 7.22 (m, 1H), 7.10 (d, $J = 8.4$ Hz, 1H), 4.90 (s, 1H). $^{13}\text{C}\{^1\text{H}\}$ NMR (126 MHz, CDCl_3) δ_{C} 151.1, 134.4, 134.0, 133.0, 131.5, 130.0, 130.0, 129.8, 129.4, 129.1, 128.6, 128.2, 127.0, 126.71, 126.69, 126.2, 125.9, 125.1, 123.5, 118.9, 117.6. IR (ATR): $\tilde{\nu} = 3511, 3430, 3057, 1619, 1594, 1515, 1505, 1459, 1384, 1193, 1167, 1146, 1127, 969, 817, 804, 780, 749, 574, 439$. HRMS calcd. for $\text{C}_{20}\text{H}_{13}\text{O}^-$: 269.0972 $[\text{M-H}]^-$; found (ESI $^-$): 270.1054. Rf: (5/1.5, petrol/ Et_2O) 0.42. Yield: 48.1 mg (85%).

1-(Mesityl)naphthalen-2-ol 26n**26n**

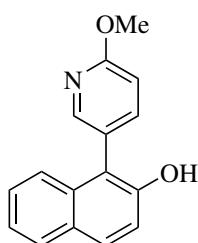
mp/°C 94-95. $^1\text{H NMR}$ (500 MHz, CDCl_3) δ_{H} 7.86 – 7.75 (m, 2H), 7.36 – 7.27 (m, 2H), 7.17 – 7.10 (m, 1H), 7.08 (s, 2H), 4.83 (s, 1H), 2.40 (s, 3H), 1.90 (s, 6H). $^{13}\text{C}\{^1\text{H}\}$ NMR (126 MHz, CDCl_3) δ_{C} 150.0, 139.0, 138.6, 132.8, 129.3, 129.3, 129.2, 129.0, 128.3, 126.7, 124.1, 123.4, 119.2, 117.2, 21.3, 20.0. IR (ATR): $\tilde{\nu} = 1619, 1597, 1517, 1463, 1385, 1345, 1309, 1268, 1219, 1180, 1142, 853, 816, 749, 645$. HRMS calcd. for $\text{C}_{19}\text{H}_{17}\text{O}^-$: 261.1285 $[\text{M-H}]^-$; found (ESI $^-$): 261.1287. Rf: (5/1.5, petrol/ Et_2O) 0.56. Yield: 48.6 mg (89%).

1-(Thiophen-3-yl)naphthalen-2-ol 26r**26r**

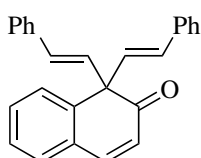
$^1\text{H NMR}$ (500 MHz, CDCl_3) δ_{H} 7.81 (dd, $J = 8.5, 4.0$ Hz, 2H), 7.64 (dd, $J = 4.8, 3.0$ Hz, 1H), 7.51 (d, $J = 8.2$ Hz, 1H), 7.45 (d, $J = 2.9$ Hz, 1H), 7.41 – 7.31 (m, 2H), 7.26 (d, $J = 8.9$ Hz, 1H), 7.20 (d, $J = 4.9$ Hz, 1H), 5.36 (s, 1H). $^{13}\text{C}\{^1\text{H}\}$ NMR (126 MHz, CDCl_3) δ_{C} 151.0, 134.3, 133.7, 130.1, 129.9, 129.0, 128.2, 127.8, 126.8, 125.7, 124.6, 123.5, 117.3, 115.8. IR (ATR): $\tilde{\nu} = 3507, 3097, 3060, 1620, 1595, 1509, 1465, 1381, 1343, 1270, 1221, 1195, 1166, 1145, 955, 858, 816, 778, 749, 656, 429$. HRMS calcd. for $\text{C}_{14}\text{H}_9\text{SO}^-$: 225.0380 $[\text{M-H}]^-$; found (ESI $^-$): 225.0380. Rf: (5/1.5, petrol/ Et_2O) 0.34. Yield: 28.5 mg (61%).

1-(1H-Indol-4-yl)naphthalen-2-ol **26w****26w**

mp/°C 151-152. $^1\text{H NMR}$ (500 MHz, CDCl_3) δ_{H} 8.35 (s, 1H), 7.89 – 7.81 (m, 2H), 7.61 – 7.51 (m, 1H), 7.44 – 7.37 (m, 2H), 7.36 – 7.27 (m, 3H), 7.24 – 7.17 (m, 2H), 6.14 (ddd, $J = 3.2, 2.1, 1.0$ Hz, 1H), 5.29 (s, 1H). $^{13}\text{C}\{^1\text{H}\}$ NMR (126 MHz, CDCl_3) δ_{C} 150.7, 136.5, 133.5, 129.5, 129.1, 128.3, 128.1, 126.4, 126.0, 125.4, 125.0, 123.3, 123.0, 122.8, 119.6, 117.5, 111.6, 102.6. IR (ATR): $\tilde{\nu} = 1619, 1595, 1516, 1506, 1464, 1392, 1347, 1266, 1227, 1187, 1148, 962, 895, 817, 756$. HRMS calcd. for $\text{C}_{18}\text{H}_{13}\text{NO}^-$: 258.0924 $[\text{M-H}]^-$; found (ESI $^-$): 258.0929. Rf: (5/1.5, petrol/ Et_2O) 0.05. Yield: 24.5 mg (45%).

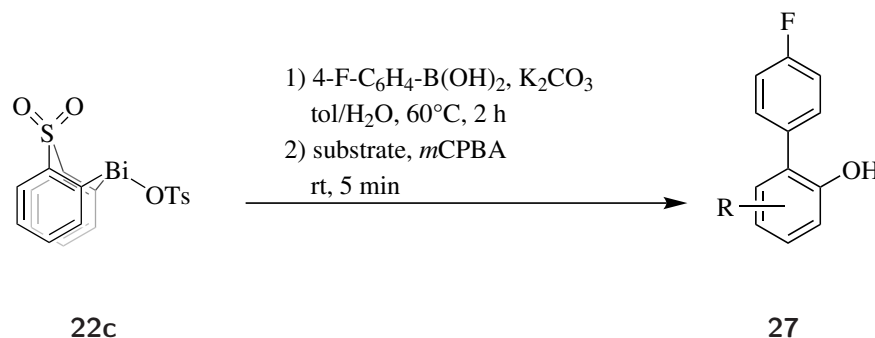
1-(6-Methoxypyridin-3-yl)naphthalen-2-ol **26x****26x**

mp/°C 175-176. $^1\text{H NMR}$ (500 MHz, CDCl_3) δ_{H} 8.21 (d, $J = 2.4$ Hz, 1H), 7.95 – 7.72 (m, 2H), 7.64 (dd, $J = 8.4, 2.5$ Hz, 1H), 7.43 – 7.29 (m, 3H), 7.26 (d, $J = 8.9$ Hz, 1H), 6.96 (d, $J = 8.4$ Hz, 1H), 5.53 (s, 1H), 4.02 (s, 3H). $^{13}\text{C}\{^1\text{H}\}$ NMR (126 MHz, CDCl_3) δ_{C} 164.3, 151.2, 149.0, 142.0, 133.9, 130.2, 129.1, 128.3, 126.9, 124.4, 123.6, 123.0, 117.8, 117.3, 111.9, 53.9. IR (ATR): $\tilde{\nu} = 1607, 1562, 1493, 1466, 1435, 1367, 1342, 1286, 1248, 1174, 1145, 1029, 983, 908, 817, 750, 731$. HRMS calcd. for $\text{C}_{16}\text{H}_{12}\text{NO}_2^-$: 250.0874 $[\text{M-H}]^-$; found (ESI $^-$): 250.0874. Rf: (5/1.5, petrol/ Et_2O) 0.12. Yield: 45.3 mg (86%).

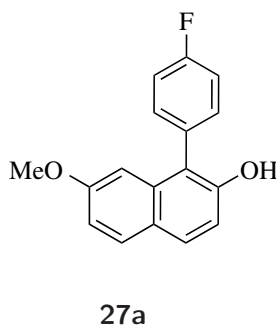
1,1-Di((E)-styryl)naphthalen-2(1H)-one **26y****26y**

mp/°C 162-163. $^1\text{H NMR}$ (500 MHz, CDCl_3) δ_{H} 7.46 – 7.41 (m, 5H), 7.37 (d, $J = 7.3$ Hz, 4H), 7.30 (t, $J = 7.5$ Hz, 4H), 7.24 (t, $J = 7.3$ Hz, 2H), 6.45 (d, $J = 16.1$ Hz, 2H), 6.33 (d, $J = 16.1$ Hz, 2H), 6.20 (d, $J = 9.9$ Hz, 1H). $^{13}\text{C}\{^1\text{H}\}$ NMR (126 MHz, CDCl_3) δ_{C} 200.0, 144.9, 141.5, 136.7, 132.9, 131.2, 130.5, 130.3, 130.1, 130.0, 128.7, 128.0, 128.0, 126.8, 124.8, 62.2. IR (ATR): $\tilde{\nu} = 3027, 1662, 1620, 1563, 1494, 1447, 1395, 1235, 1204, 967, 827, 744, 692$. HRMS calcd. for $\text{C}_{26}\text{H}_{21}\text{O}^+$: 349.1587 $[\text{M+H}]^+$; found (ESI $^+$): 349.1584. Rf: (5/1.5, petrol/ Et_2O) 0.39. Yield: 36.4 mg (90%).

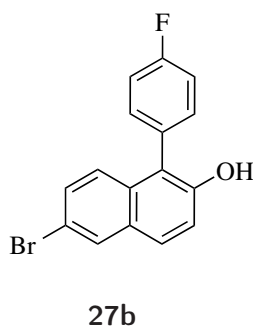
Arylation of Phenolic Substrates



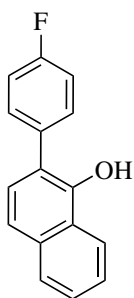
General Protocol A: 5,5-Dioxido-10H-dibenzo[b,e][1,4]thiabismine-10-yl 4-methylbenzenesulfonate (1.0 equiv.), K_2CO_3 (1.5 equiv.) and 4-Fluorophenyl boronic acid (1.1 equiv.) were added to a mixture of toluene (5.00 mL) and water (0.01 mL) and allowed to stir at 60°C for 2 h. The phenol (50 mg, 1.0 equiv.) and *m*CPBA (1.5 equiv.) were added sequentially and the reaction mixture was stirred for 5 min. The reaction was quenched with MeOH (2.0 mL) and Et_2O (20.0 mL) were added. The organic phase was separated and washed with saturated KHCO_3 solution. The organics were dried (MgSO_4) and concentrated *in vacuo*. The reaction product was purified by column chromatography.

1-(4-Fluorophenyl)-7-methoxynaphthalen-2-ol **27a**

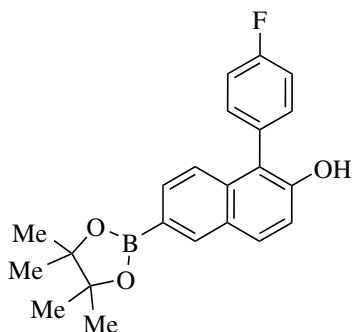
$^1\text{H NMR}$ (500 MHz, CDCl_3) δ_{H} 7.73 (d, $J = 8.8$ Hz, 1H), 7.71 (d, $J = 8.9$ Hz, 1H), 7.45 – 7.38 (m, 2H), 7.33 – 7.26 (m, 2H), 7.10 (d, $J = 8.8$ Hz, 1H), 7.00 (dd, $J = 8.9, 2.5$ Hz, 1H), 6.64 (d, $J = 2.5$ Hz, 1H), 4.97 (s, 1H), 3.71 (s, 3H). $^{13}\text{C}\{^1\text{H}\}$ NMR (126 MHz, CDCl_3) δ_{C} 162.9 (d, $J = 248.0$ Hz), 158.6, 151.1, 134.9, 133.1 (d, $J = 8.1$ Hz), 130.3 (d, $J = 3.5$ Hz), 129.8, 129.6, 124.5, 119.3, 116.9 (d, $J = 21.4$ Hz), 115.6, 114.9, 103.7, 55.3. $^{19}\text{F NMR}$ (471 MHz, CDCl_3) δ_{F} -113.06 (tt, $J = 8.7, 5.5$ Hz). IR (ATR): $\tilde{\nu} = 1621, 1510, 1466, 1450, 1430, 1380, 1333, 1309, 1270, 1228, 1164, 1035, 832, 807, 796$. HRMS calcd. for $\text{C}_{17}\text{H}_{12}\text{FO}_2^-$: 267.0827 [M-H] $^-$; found (ESI $^-$): 267.0827. Rf: (petrol/ Et_2O) 0.43. Yield: 71.7 mg (92%).

6-Bromo-1-(4-fluorophenyl)naphthalen-2-ol **27b**

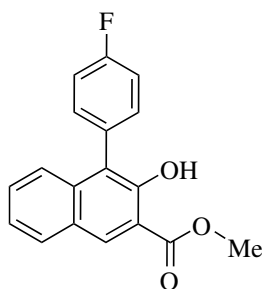
mp/ $^\circ\text{C}$ 191-192. $^1\text{H NMR}$ (500 MHz, CDCl_3) δ_{H} 7.96 (d, $J = 2.1$ Hz, 1H), 7.72 (d, $J = 8.9$ Hz, 1H), 7.43 – 7.34 (m, 3H), 7.31 – 7.26 (m, 3H), 7.22 (d, $J = 9.0$ Hz, 1H), 5.04 (s, 1H). $^{13}\text{C}\{^1\text{H}\}$ NMR (126 MHz, CDCl_3) δ_{C} 163.1 (d, $J = 248.8$ Hz), 150.8, 133.1 (d, $J = 8.2$ Hz), 132.1, 130.2, 130.1, 130.0, 129.5 (d, $J = 3.6$ Hz), 128.9, 126.4, 120.3, 118.7, 117.4, 117.0 (d, $J = 21.4$ Hz). $^{19}\text{F NMR}$ (471 MHz, CDCl_3) δ_{F} -112.52 (tt, $J = 8.6, 5.3$ Hz). IR (ATR): $\tilde{\nu} = 3523, 1603, 1509, 1380, 1338, 1223, 1168, 1147, 948, 933, 878, 860, 837, 810, 674, 527, 503$. HRMS calcd. for $\text{C}_{16}\text{H}_9\text{BrFO}^-$: 314.9826 [M-H] $^-$; found (ESI $^-$): 314.9849. Rf: (toluene) 0.5. Yield: 61.0 mg (86%).

2-(4-Fluorophenyl)naphthalen-1-ol 27c**27c**

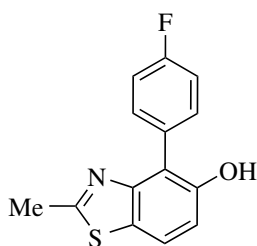
mp/°C 189-191. $^1\text{H NMR}$ (500 MHz, CDCl_3) δ_H 8.33 – 8.23 (m, 1H), 7.87 – 7.80 (m, 1H), 7.57 – 7.46 (m, 5H), 7.32 (dd, $J = 8.5$, 1.5 Hz, 1H), 7.28 – 7.20 (m, 2H), 5.66 (d, $J = 1.7$ Hz, 1H). $^{13}\text{C}\{^1\text{H}\}$ NMR (126 MHz, CDCl_3) δ_C 162.6 (d, $J = 247.9$ Hz), 147.9, 134.4, 133.4 (d, $J = 3.3$ Hz), 131.3 (d, $J = 8.0$ Hz), 127.7 (2C), 126.7, 125.8, 124.4, 122.5, 120.5, 120.5, 116.71 (d, $J = 21.5$ Hz). $^{19}\text{F NMR}$ (471 MHz, CDCl_3) δ_F -113.84 (tt, $J = 8.6$, 5.3 Hz). IR (ATR): $\tilde{\nu} = 3286$, 1614, 1567, 1508, 1465, 1361, 1343, 1320, 1295, 1274, 1222, 1190, 1157, 1092, 1046, 1013, 882, 836, 811, 745, 725, 669, 593, 575, 543, 516, 423. HRMS calcd. for $\text{C}_{16}\text{H}_{10}\text{FO}^-$: 237.0721 [M-H] $^-$; found (ESI $^-$): 237.0719. Rf: (petrol/ Et_2O , 5/1) 0.56. Yield: 77.3 mg (86%).

1-(4-Fluorophenyl)-6-(4,4,5,5-tetramethyl-1,3,2-dioxaborolan-2-yl)naphthalen-2-ol 27d**27d**

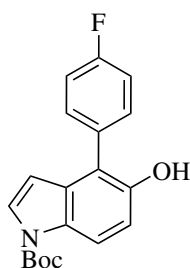
For isolation purposes the crude (5-(4-fluorophenyl)-6-hydroxynaphthalen-2-yl)boronic acid has been treated with pinacol in Et_2O for 5 min. $^1\text{H NMR}$ (500 MHz, CDCl_3) δ_H 8.33 (s, 1H), 7.85 (d, $J = 8.9$ Hz, 1H), 7.70 (d, $J = 8.5$ Hz, 1H), 7.39 (dd, $J = 8.3$, 5.4 Hz, 2H), 7.34 – 7.20 (m, 4H), 5.09 (s, 1H), 1.38 (s, 12H). $^{11}\text{B NMR}$ (128 MHz, CDCl_3) δ_B 31.12. $^{13}\text{C}\{^1\text{H}\}$ NMR (126 MHz, CDCl_3) δ_C 162.9 (d, $J = 248.3$ Hz), 151.5, 136.6, 135.2, 133.2 (d, $J = 8.1$ Hz), 131.5, 130.8, 129.9, 128.5, 123.6, 120.0, 117.4, 116.9 (d, $J = 21.3$ Hz), 84.0, 29.9, 25.0. $^{19}\text{F NMR}$ (471 MHz, CDCl_3) δ_F -113.01 (tt, $J = 8.8$, 4.6 Hz). IR (ATR): $\tilde{\nu} = 2920$, 2850, 1620, 1510, 1499, 1477, 1436, 1374, 1353, 1328, 1296, 1274, 1220, 1143, 1083, 964, 908, 834, 729, 700, 528. HRMS calcd. for $\text{C}_{22}\text{H}_{21}\text{BFO}_3^-$: 363.1573 [M-H] $^-$; found (ESI $^-$): 363.1590. Rf: (toluene) 0.15. Yield: 63.0 mg (64%).

Methyl 4-(4-Fluorophenyl)-3-hydroxy-2-naphthoate 27e**27e**

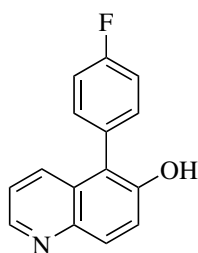
mp/°C 168-169. $^1\text{H NMR}$ (500 MHz, CDCl_3) δ_H 10.72 (s, 1H), 8.57 (d, $J = 0.6$ Hz, 1H), 7.92 – 7.78 (m, 1H), 7.47 – 7.32 (m, 5H), 7.25 – 7.19 (m, 2H), 4.05 (s, 3H). $^{13}\text{C}\{^1\text{H}\}$ NMR (126 MHz, CDCl_3) δ_C 170.7, 162.4 (d, $J = 246.1$ Hz), 153.3, 137.0, 132.7 (d, $J = 8.1$ Hz), 132.4, 131.4 (d, $J = 3.6$ Hz), 129.8, 129.4, 127.1, 124.9, 124.8, 124.0, 115.6 (d, $J = 21.3$ Hz), 114.0, 52.9. $^{19}\text{F NMR}$ (471 MHz, CDCl_3) δ_F -115.02 (tt, $J = 8.8$, 5.5 Hz). IR (ATR): $\tilde{\nu} = 3210$, 1679, 1625, 1599, 1577, 1512, 1441, 1338, 1318, 1212, 1156, 1074, 988, 950, 834, 797, 751, 552. HRMS calcd. for $\text{C}_{18}\text{H}_{12}\text{FO}_3^-$: 295.0776 [M-H] $^-$; found (ESI $^-$): 295.0774. Rf: (petrol/ Et_2O) 0.38. Yield: 63.2 mg (85%).

4-(4-Fluorophenyl)-2-methylbenzo[d]thiazol-5-ol **27f****27f**

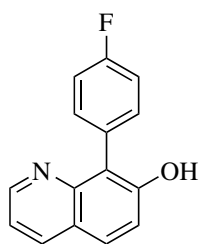
mp/°C 191-192. $^1\text{H NMR}$ (500 MHz, CDCl_3) δ_{H} 7.66 (d, $J = 8.6$ Hz, 1H), 7.58 – 7.48 (m, 2H), 7.23 (dd, $J = 8.7$, 8.7 Hz, 2H), 7.05 (d, $J = 8.6$ Hz, 1H), 5.29 (s, 1H), 2.75 (s, 3H). $^{13}\text{C}\{^1\text{H}\}$ NMR (126 MHz, CDCl_3) δ_{C} 168.3, 162.8 (d, $J = 247.9$ Hz), 152.8, 151.4, 132.6 (d, $J = 8.0$ Hz), 129.5 (d, $J = 3.4$ Hz), 128.0, 121.3, 120.2, 116.4 (d, $J = 21.4$ Hz), 114.4. $^{19}\text{F NMR}$ (471 MHz, CDCl_3) δ_{F} -113.32 (tt, $J = 8.7$, 5.4 Hz). IR (ATR): $\tilde{\nu} = 1592$, 1511, 1463, 1386, 1366, 1329, 1299, 1269, 1213, 1161, 1111, 1086, 955, 941, 841, 825, 803, 771, 738, 668, 495. HRMS calcd. for $\text{C}_{14}\text{H}_{11}\text{FNOS}^+$: 260.0540 $[\text{M}+\text{H}]^+$; found (ESI $^+$): 260.0551. Rf: (toluene) 0.1. Yield: 70.8 mg (90%).

tert-Butyl 4-(4-fluorophenyl)-5-hydroxy-1H-indole-1-carboxylate **27g****27g**

mp/°C 190-191. $^1\text{H NMR}$ (500 MHz, CDCl_3) δ_{H} 8.05 (d, $J = 8.2$ Hz, 1H), 7.57 (d, $J = 3.7$ Hz, 1H), 7.55 – 7.43 (m, 2H), 7.26 (dd, $J = 8.7$, 8.7 Hz, 2H), 7.01 (d, $J = 8.9$ Hz, 1H), 6.30 (d, $J = 3.7$ Hz, 1H), 4.87 (s, 1H), 1.70 (s, 9H). $^{13}\text{C}\{^1\text{H}\}$ NMR (126 MHz, CDCl_3) δ_{C} 162.49 (d, $J = 247.7$ Hz), 149.70, 147.9, 131.9 (d, $J = 8.1$ Hz), 130.7, 130.7, 130.6 (d, $J = 3.3$ Hz), 126.9, 117.9, 116.4 (d, $J = 21.7$ Hz), 115.6, 113.2, 105.9, 83.7, 28.2. $^{19}\text{F NMR}$ (471 MHz, CDCl_3) δ_{F} -113.69 (m). IR (ATR): $\tilde{\nu} = 3433$, 2979, 2365, 1732, 1600, 1513, 1491, 1475, 1427, 1398, 1369, 1355, 1335, 1293, 1265, 1225, 1152, 1133, 1024, 885, 836, 811, 732. HRMS calcd. for $\text{C}_{19}\text{H}_{17}\text{FNO}_3^-$: 326.1198 $[\text{M}-\text{H}]^-$; found (ESI $^-$): 326.1198. Rf: (toluene) 0.2. Yield: 60.1 mg (86%).

5-(4-Fluorophenyl)quinolin-6-ol **27i****27i**

mp/°C 246-247. $^1\text{H NMR}$ (500 MHz, CDCl_3) δ_{H} 8.80 – 8.70 (m, 1H), 8.09 (d, $J = 9.2$ Hz, 1H), 7.79 – 7.71 (m, 1H), 7.49 (d, $J = 9.1$ Hz, 1H), 7.44 – 7.38 (m, 2H), 7.30 (m, 3H), 5.48 (s, 1H). $^{13}\text{C}\{^1\text{H}\}$ NMR (126 MHz, CDCl_3) δ_{C} 163.1 (d, $J = 249.0$ Hz), 150.8, 147.6, 143.9, 133.1 (d, $J = 8.2$ Hz), 133.0, 130.9, 129.02 (d, $J = 3.4$ Hz), 128.6, 121.6, 121.3, 119.8, 117.0 (d, $J = 21.6$ Hz). $^{19}\text{F NMR}$ (471 MHz, CDCl_3) δ_{F} -112.36 (tt, $J = 8.6$, 5.5 Hz). IR (ATR): $\tilde{\nu} = 1592$, 1511, 1463, 1386, 1366, 1329, 1299, 1269, 1213, 1161, 1111, 1086, 955, 941, 841, 825, 803, 771, 738, 668, 495. HRMS calcd. for $\text{C}_{15}\text{H}_{11}\text{FNO}^+$: 240.0819 $[\text{M}+\text{H}]^+$; found (ESI $^+$): 240.0827. Rf: (5/2, petrol/ Et_2O) 0.2. Yield: 69.2 mg (84%).

8-(4-Fluorophenyl)quinolin-7-ol **27j****27j**

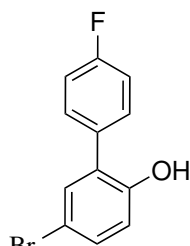
mp/°C 187-189. $^1\text{H NMR}$ (500 MHz, CDCl_3) δ_{H} 8.82 (dd, $J = 4.3, 1.8$ Hz, 1H), 8.12 (dd, $J = 8.2, 1.8$ Hz, 1H), 7.95 (dd, $J = 7.2, 1.8$ Hz, 1H), 7.78 (d, $J = 8.9$ Hz, 1H), 7.49 (ddd, $J = 14.2, 8.2, 5.9$ Hz, 3H), 7.34 (d, $J = 8.9$ Hz, 1H), 7.32 – 7.24 (m, 1H), 5.45 (s, 1H). $^{13}\text{C}\{^1\text{H}\}$ NMR (126 MHz, CDCl_3) δ_{C} 162.9 (d, $J = 247.8$ Hz), 153.7, 150.9, 147.8, 136.2, 133.1 (d, $J = 8.1$ Hz), 129.3 (d, $J = 3.4$ Hz), 129.2, 127.8, 123.2, 121.6, 118.4, 116.7 (d, $J = 21.4$ Hz). $^{19}\text{F NMR}$ (471 MHz, CDCl_3) δ_{F} -113.38 (tt, $J = 8.7, 5.4$ Hz). IR (ATR): $\tilde{\nu} = 1618, 1596, 1580, 1511, 1498, 1430, 1319, 1286, 1216, 1156, 1106, 832, 802, 731, 687, 564, 589$. HRMS calcd. for $\text{C}_{15}\text{H}_9\text{FNO}^-$: 238.0674 [M-H] $^-$; found (ESI $^-$): 238.0678. Rf: (toluene/ Et_2O , 10/1) 0.12. Yield: 76.0 mg (93%).

6,6-Bis(4-fluorophenyl)isoquinolin-5(6H)-one **27l****27l**

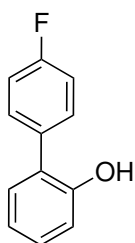
$^1\text{H NMR}$ (500 MHz, CDCl_3) δ_{H} 8.73 – 8.64 (m, 2H), 7.78 (d, $J = 5.0$ Hz, 1H), 7.22 – 7.12 (m, 4H), 7.04 – 6.95 (m, 4H), 6.85 (d, $J = 9.8$ Hz, 1H), 6.57 (d, $J = 9.8$ Hz, 1H). $^{13}\text{C}\{^1\text{H}\}$ NMR (126 MHz, CDCl_3) δ_{C} 199.6, 162.5 (d, $J = 247.8$ Hz), 150.8, 149.4, 140.3, 136.9 (d, $J = 3.3$ Hz), 133.7, 131.1, 130.5 (d, $J = 8.2$ Hz), 120.7, 119.7, 115.8 (d, $J = 21.7$ Hz), 62.4. $^{19}\text{F NMR}$ (471 MHz, CDCl_3) δ_{F} -114.07 (tt, $J = 8.4, 5.2$ Hz). IR (ATR): $\tilde{\nu} = 1691, 1602, 1505, 1420, 1385, 1299, 1232, 1161, 1106, 1029, 1015, 878, 830, 812, 727, 593, 560, 541, 527$. HRMS calcd. for $\text{C}_{21}\text{H}_{14}\text{F}_2\text{NO}^+$: 334.1038 [M+H] $^+$; found (ESI $^-$): 334.1034. Rf: (petrol/ Et_2O , 5/2) 0.21. Yield: 42.0 mg (71%).

General Protocol B: 5,5-Dioxido-10H-dibenzo[b,e][1,4]thiabismine-10-yl 4-methylbenzenesulfonate (1.0 equiv.), K_2CO_3 (1.5 equiv.) and 4-Fluorophenyl boronic acid (1.1 equiv.)^{IV} were added to a mixture of toluene (5.00 mL) and water (0.01 mL) and allowed to stir at 60 °C for 2 h. The phenol (150 mg, 3.0 equiv.) and *m*CPBA (1.5 equiv.) were added sequentially and the reaction mixture was stirred for 5 min. The reaction was quenched with MeOH (2.0 mL) and Et_2O (20.0 mL) were added. The organic phase was separated and washed with saturated KHCO_3 solution. The organics were dried (MgSO_4) and concentrated *in vacuo*. The reaction product was purified by column chromatography.

^{IV} **28j** was prepared following the same protocol but using 4-(N-Boc-amino)phenylboronic acid

5-Bromo-4'-fluoro-[1,1'-biphenyl]-2-ol 28a**28a**

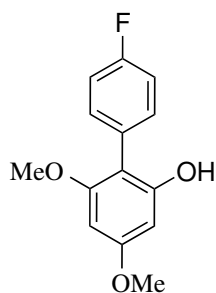
^1H NMR (500 MHz, CDCl_3) δ_{H} 7.46 – 7.40 (m, 2H), 7.36 – 7.33 (m, 2H), 7.22 – 7.16 (m, 2H), 6.88 – 6.83 (m, 1H), 5.05 (s, 1H). $^{13}\text{C}\{^1\text{H}\}$ NMR (126 MHz, CDCl_3) δ_{C} 162.9 (d, $J = 248.4$ Hz), 151.7, 132.9, 132.0, 131.9 (d, $J = 3.5$ Hz), 130.9 (d, $J = 8.3$ Hz), 129.3, 117.88, 116.5 (d, $J = 21.7$ Hz), 113.0. ^{19}F NMR (471 MHz, CDCl_3) δ_{F} -113.10 (tt, $J = 8.6, 5.3$ Hz). IR (ATR): $\tilde{\nu} = 3560, 2960, 2925, 2870, 1621, 1603, 1570, 1514, 1488, 1455, 1427, 1306, 1223, 1173, 1156, 1033, 838, 799, 517, 509$. HRMS calcd. for $\text{C}_{12}\text{H}_7\text{BrFO}^-$: 264.9670 $[\text{M}-\text{H}]^-$; found (ESI $^-$): 264.9668. Rf: (petrol/Et $_2$ O, 5/1) 0.41. Yield: 45.5 mg (59%).

4'-Fluoro-[1,1'-biphenyl]-2-ol 28b**28b**

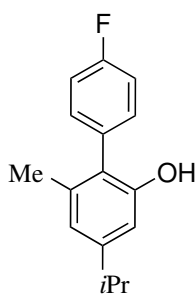
^1H NMR (500 MHz, CDCl_3) δ_{H} 7.49 – 7.42 (m, 2H), 7.30 – 7.24 (m, 1H), 7.22 (dd, $J = 7.6, 1.7$ Hz, 1H), 7.20 – 7.14 (m, 2H), 7.03 – 6.94 (m, 2H), 5.00 (s, 1H). $^{13}\text{C}\{^1\text{H}\}$ NMR (126 MHz, CDCl_3) δ_{C} 162.5 (d, $J = 247.5$ Hz), 152.4, 133.1 (d, $J = 3.3$ Hz), 130.9 (d, $J = 8.2$ Hz), 130.4, 129.3, 127.2, 121.0, 116.1 (d, $J = 21.5$ Hz), 115.9. ^{19}F NMR (471 MHz, CDCl_3) δ_{F} -114.20 (tt, $J = 8.7, 5.4$ Hz). IR (ATR): $\tilde{\nu} = 3545, 3408, 1604, 1514, 1493, 1482, 1452, 1402, 1332, 1286, 1267, 1224, 1182, 1158, 1106, 1094, 1009, 833, 809, 754$. HRMS calcd. for $\text{C}_{12}\text{H}_8\text{FO}^-$: 187.0565 $[\text{M}-\text{H}]^-$; found (ESI $^-$): 187.0567. Rf: (toluene) 0.33. Yield: 69.0 mg (69%).

4,4',6-Trifluoro-[1,1'-biphenyl]-2-ol 28c**28c**

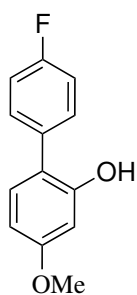
mp/ $^{\circ}\text{C}$ 103-104. ^1H NMR (500 MHz, CDCl_3) δ_{H} 7.39 – 7.31 (m, 2H), 7.24 – 7.18 (m, 2H), 6.55 (dt, $J = 9.8, 2.1$ Hz, 1H), 6.51 (td, $J = 9.2, 2.5$ Hz, 1H), 5.24 (s, 1H). $^{13}\text{C}\{^1\text{H}\}$ NMR (126 MHz, CDCl_3) δ_{C} 163.1 (d, $J = 249.0$ Hz), 162.9 (dd, $J = 246.6, 15.8$ Hz), 160.4 (dd, $J = 246.4, 15.1$ Hz), 154.9 (dd, $J = 14.6, 7.8$ Hz), 132.5 (d, $J = 8.2$ Hz), 125.2 (d, $J = 3.6$ Hz), 116.7 (d, $J = 21.6$ Hz), 112.1 (dd, $J = 19.4, 4.0$ Hz), 99.5 (dd, $J = 25.0, 3.7$ Hz), 96.7 (dd, $J = 27.2, 25.9$ Hz). ^{19}F NMR (471 MHz, CDCl_3) δ_{F} -109.81 (td, $J = 9.4, 6.8$ Hz), -112.22 (ddt, $J = 8.6, 6.2, 3.2$ Hz), -109.81 (d, $J = 6.9$ Hz), -112.22, -112.23 (d, $J = 7.1$ Hz). IR (ATR): $\tilde{\nu} = 3518, 2940, 2840, 2359, 2339, 1623, 1599, 1583, 1494, 1466, 1207, 1153, 1102, 1090, 1061, 838, 816$. HRMS calcd. for $\text{C}_{12}\text{H}_6\text{F}_3\text{O}^-$: 223.0376 $[\text{M}-\text{H}]^-$; found (ESI $^-$): 223.0385. Rf: (toluene) 0.38. Yield: 50.0 mg (58%).

4'-Fluoro-4,6-dimethoxy-[1,1'-biphenyl]-2-ol **28d****28d**

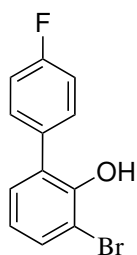
mp/°C 109-110. $^1\text{H NMR}$ (500 MHz, CDCl_3) δ_{H} 7.36 – 7.28 (m, 2H), 7.22 – 7.10 (m, 2H), 6.22 (d, $J = 2.3$ Hz, 1H), 6.16 (d, $J = 2.4$ Hz, 1H), 4.93 (s, 1H), 3.82 (s, 3H), 3.70 (s, 3H). $^{13}\text{C}\{^1\text{H}\}$ NMR (126 MHz, CDCl_3) δ_{C} 162.4 (d, $J = 247.1$ Hz), 160.9, 158.2, 154.3, 132.9 (d, $J = 8.1$ Hz), 128.2 (d, $J = 3.5$ Hz), 116.2 (d, $J = 21.4$ Hz), 108.9, 92.8, 91.6, 55.8, 55.5. $^{19}\text{F NMR}$ (471 MHz, CDCl_3) δ_{F} -114.10 (tt, $J = 8.7, 5.5$ Hz). IR (ATR): $\tilde{\nu} = 3518, 2940, 2840, 2359, 2339, 1623, 1599, 1583, 1494, 1466, 1207, 1153, 1102, 1090, 1061, 838, 816$. HRMS calcd. for $\text{C}_{14}\text{H}_{13}\text{FO}_3^-$: 247.0776 $[\text{M}-\text{H}]^-$; found (ESI $^-$): 247.0779. Rf: (toluene) 0.32. Yield: 62.0 mg (77%).

4'-Fluoro-4-isopropyl-6-methyl-[1,1'-biphenyl]-2-ol **28f****28f**

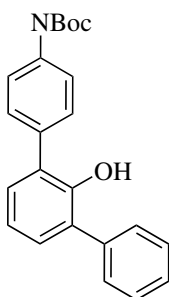
$^1\text{H NMR}$ (500 MHz, CDCl_3) δ_{H} 7.31 – 7.22 (m, 2H), 7.22 – 7.15 (m, 2H), 6.82 – 6.53 (m, 2H), 4.59 (s, 1H), 2.86 (hept, $J = 6.9$ Hz, 1H), 2.05 (d, $J = 0.7$ Hz, 3H), 1.27 (d, $J = 6.9$ Hz, 6H). $^{13}\text{C}\{^1\text{H}\}$ NMR (126 MHz, CDCl_3) δ_{C} 162.6 (d, $J = 247.5$ Hz), 152.9, 150.1, 137.2, 132.4 (d, $J = 8.1$ Hz), 131.5 (d, $J = 3.6$ Hz), 124.6, 120.6, 116.5 (d, $J = 21.3$ Hz), 110.8, 34.1, 24.0, 20.6. $^{19}\text{F NMR}$ (471 MHz, CDCl_3) δ_{F} -113.93 (tt, $J = 8.7, 5.5$ Hz). IR (ATR): $\tilde{\nu} = 3560, 2960, 2925, 2870, 1621, 1603, 1570, 1514, 1488, 1455, 1427, 1306, 1223, 1173, 1156, 1033, 838, 799, 517, 509$. HRMS calcd. for $\text{C}_{16}\text{H}_{17}\text{FO}^-$: 243.1191 $[\text{M}-\text{H}]^-$; found (ESI $^-$): 243.1194. Rf: (toluene/petrol, 1/1) 0.26. Yield: 57.9 mg (72%).

4'-Fluoro-4-methoxy-[1,1'-biphenyl]-2-ol **28h****28h**

$^1\text{H NMR}$ (500 MHz, CDCl_3) δ_{H} 7.47 – 7.36 (m, 2H), 7.19 – 7.13 (m, 2H), 7.12 (d, $J = 8.5$ Hz, 1H), 6.57 (dd, $J = 8.3, 2.5$ Hz, 1H), 6.55 (d, $J = 2.4$ Hz, 1H), 5.09 (s, 1H), 3.82 (s, 3H). $^{13}\text{C}\{^1\text{H}\}$ NMR (126 MHz, CDCl_3) δ_{C} 162.4 (d, $J = 247.0$ Hz), 160.7, 153.5, 133.1 (d, $J = 3.5$ Hz), 131.0, 130.9 (d, $J = 8.0$ Hz), 120.1, 116.3 (d, $J = 21.4$ Hz), 107.1, 101.6, 55.6. $^{19}\text{F NMR}$ (471 MHz, CDCl_3) δ_{F} -114.70 (tt, $J = 8.6, 5.4$ Hz). IR (ATR): $\tilde{\nu} = 3560, 2960, 2925, 2870, 1621, 1603, 1570, 1514, 1488, 1455, 1427, 1306, 1223, 1173, 1156, 1033, 838, 799, 517, 509$. HRMS calcd. for $\text{C}_{13}\text{H}_{10}\text{FO}_2^-$: 217.0670 $[\text{M}-\text{H}]^-$; found (ESI $^-$): 217.0692. Rf: (toluene) 0.56. Yield: 38.1 mg (69%).

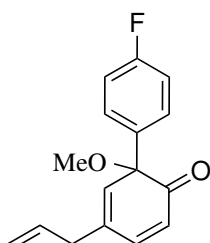
3-Bromo-4'-fluoro-[1,1'-biphenyl]-2-ol 28i**28i**

$^1\text{H NMR}$ (500 MHz, CDCl_3) δ_{H} 7.53 – 7.49 (m, 2H), 7.47 (dd, $J = 8.0, 1.6$ Hz, 1H), 7.23 (ddd, $J = 7.7, 1.6, 0.5$ Hz, 1H), 7.13 (dd, $J = 8.7, 8.0$ Hz, 2H), 6.92 – 6.84 (m, 1H), 5.66 (d, $J = 0.5$ Hz, 1H). $^{13}\text{C}\{^1\text{H}\}$ NMR (126 MHz, CDCl_3) δ_{C} 162.5 (d, $J = 247.1$ Hz), 149.3, 133.4 (d, $J = 3.5$ Hz), 131.6, 131.04 (d, $J = 8.1$ Hz), 130.3, 128.8, 121.9, 115.5 (d, $J = 21.5$ Hz), 111.4. $^{19}\text{F NMR}$ (471 MHz, CDCl_3) δ_{F} -114.50 (tt, $J = 8.7, 5.4$ Hz). IR (ATR): $\tilde{\nu} = 3560, 2960, 2925, 2870, 1621, 1603, 1570, 1514, 1488, 1455, 1427, 1306, 1223, 1173, 1156, 1033, 838, 799, 517, 509$. HRMS calcd. for $\text{C}_{12}\text{H}_7\text{BrFO}^-$: 264.9670 $[\text{M-H}]^-$; found (ESI $^-$): 264.9670. Rf: (petrol/ Et_2O , 5/1) 0.56. Yield: 42.4 mg (55%).

tert-Butyl (2'-hydroxy-[1,1':3',1''-terphenyl]-4-yl)carbamate 28j**28j**

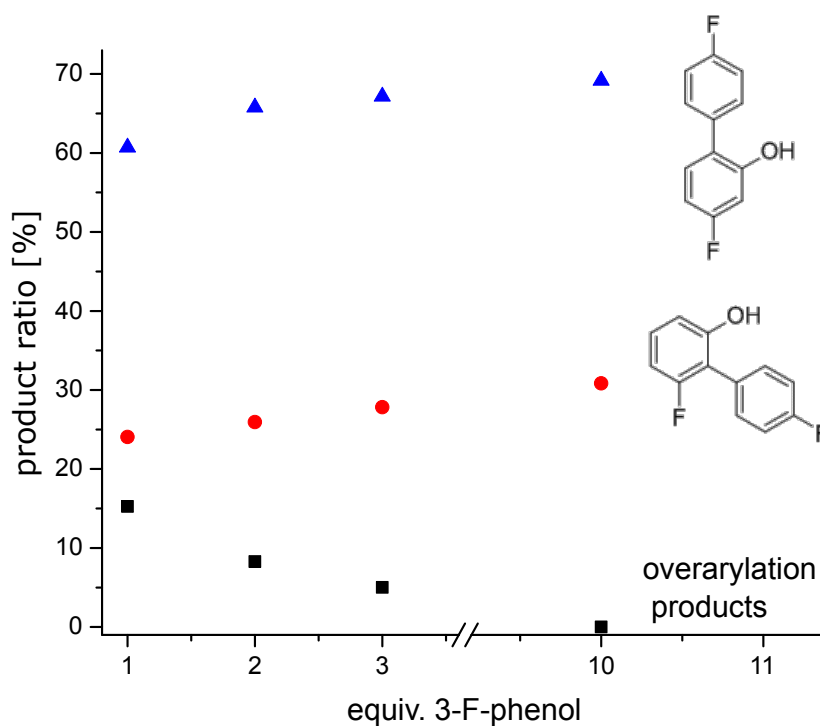
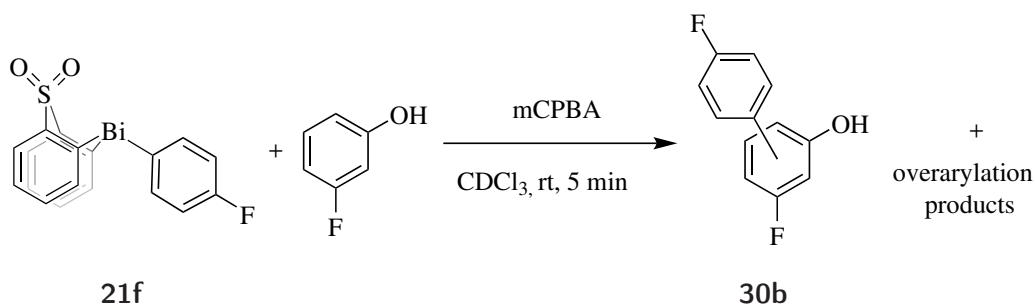
$^1\text{H NMR}$ (500 MHz, CDCl_3) δ_{H} 7.58 – 7.52 (m, 2H), 7.52 – 7.42 (m, 6H), 7.42 – 7.34 (m, 1H), 7.29 – 7.22 (m, 2H), 7.04 (dd, $J = 7.9, 7.3$ Hz, 1H), 6.53 (s, 1H), 5.37 (s, 1H), 1.54 (s, 9H). $^{13}\text{C}\{^1\text{H}\}$ NMR (126 MHz, CDCl_3) δ_{C} 152.9, 149.5, 138.0, 137.8, 132.3, 130.1, 130.0, 129.9, 129.5, 128.9, 128.9, 128.4, 127.8, 120.8, 118.9, 80.9, 28.5. IR (ATR): $\tilde{\nu} = 1726, 1706, 1612, 1589, 1523, 1505, 1454, 1432, 1399, 1367, 1316, 1226, 1158, 1099, 1054, 1018, 842, 829, 796, 759, 701$. HRMS calcd. for $\text{C}_{23}\text{H}_{22}\text{NO}_3^-$: 360.1605 $[\text{M-H}]^-$; found (ESI $^-$): 360.1610. Rf: (toluene) 0.10. Yield: 71.0 mg (68%).

The arylation products of 3-fluorophenol and 3-bromophenol have been isolated as mixtures of regioisomers in yields of 60% (55.0 mg) and 57% (49.9 mg), respectively. Authentic samples of the regioisomers of (4-fluorophenyl)-3-fluorophenol have been prepared individually (*vide infra*).

5-Allyl-4'-fluoro-1-methoxy-[1,1'-biphenyl]-2(1H)-one 28k**28k**

$^1\text{H NMR}$ (500 MHz, CDCl_3) δ_{H} 7.51 – 7.38 (m, 2H), 7.02 – 6.95 (m, 2H), 6.93 (dd, $J = 10.0, 2.3$ Hz, 1H), 6.15 (ddd, $J = 2.2, 1.5, 0.7$ Hz, 1H), 6.06 (dd, $J = 10.0, 0.7$ Hz, 1H), 5.89 (dddd, $J = 17.0, 10.5, 10.5, 6.6$ Hz, 1H), 5.23 – 5.21 (m, 1H), 5.18 (dddd, $J = 9.2, 1.4, 1.4, 1.4$ Hz, 2H), 3.31 (s, 3H), 3.11 (dddd, $J = 6.6, 1.5, 1.5, 1.5$ Hz, 2H). $^{13}\text{C}\{^1\text{H}\}$ NMR (126 MHz, CDCl_3) δ_{C} 201.0, 162.9 (d, $J = 247.2$ Hz), 144.4, 138.0, 135.9, 134.4, 133.6 (d, $J = 3.0$ Hz), 127.6 (d, $J = 8.3$ Hz), 126.6, 118.3, 115.7 (d, $J = 21.6$ Hz), 82.9, 54.0, 39.5. $^{19}\text{F NMR}$ (471 MHz, CDCl_3) δ_{F} -113.68 (tt, $J = 8.5, 5.3$ Hz). IR (ATR): $\tilde{\nu} = 2931, 2827, 1679, 1652, 1601, 1504, 1402, 1227, 1158, 1128, 1080, 1014, 921, 841, 819, 593, 560, 533$. HRMS calcd. for $\text{C}_{16}\text{H}_{16}\text{FO}_2^+$: 259.1129 $[\text{M+H}]^+$; found (ESI $^+$): 259.0696. (petrol/ Et_2O , 5/1) 0.21. Yield: 68.7 mg (87%).

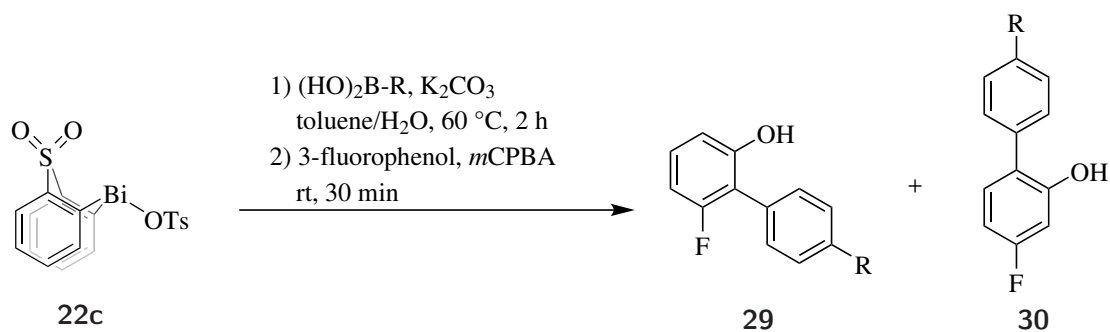
Preventing Overarylation



Variation of the relative amount of 3-fluorophenol and its dependency on the degree of overarylation

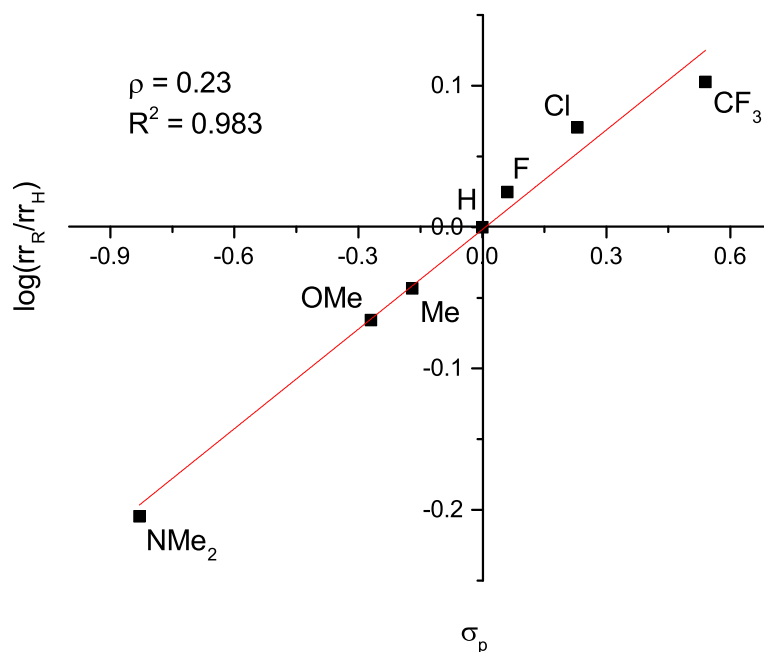
CDCl₃ was added to 10-(4-fluorophenyl)-10H-dibenzo[b,e][1,4]thiabismine 5,5-dioxide (10.0 mg, 19.3 μmol) and 3-fluorophenol (varying equivalents) in an NMR tube. *m*CPBA (6.67 mg, 38.6 μmol) was added and the solution and the NMR tube was shaken vigorously before being analysed by ¹⁹F NMR spectroscopy. 95% of monoarylated products observed with 3.0 equiv. of substrate.

Investigation on the Electronic Dependency of the Transferred Aryl Group on the Selectivity on 3-fluorophenol



Entry	R	σ_P	rr_R	$\log(rr_R/rr_H)$
1	CF_3	0.54	2.8	0.102
2	Cl	0.23	2.6	0.070
3	F	0.06	2.34	0.024
4	H	0	2.21	0
5	Me	-0.17	2	-0.043
6	OMe	-0.27	1.9	-0.065
7	NMe_2	-0.83	1.38	-0.204

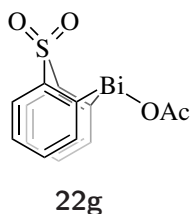
K_2CO_3 (15.2 mg, 109.9 μmol), 5,5-dioxido-10H-dibenzo[b,e][1,4]thiabismin-10-yl 4-methylbenzene-sulfonate (50.0 mg, 84.5 μmol) and aryl boronic acid (92.9 μmol) were added to a mixture of toluene (5.00 mL) and water (0.01 mL) and allowed to stir at $60\text{ }^\circ\text{C}$ for 2 h. Subsequently 3-fluorophenol (94.7 mg, 845 μmol) and *m*CPBA (29.2 mg, 169 μmol) were added sequentially and the reaction mixture was stirred for 5 min. The reaction was quenched with HOAc (0.5 mL) and MeOH (2.0 mL) and an aliquot (0.4 mL) was taken and diluted with CDCl_3 (0.2 mL). The reaction mixture was analysed by ^{19}F NMR spectroscopy.



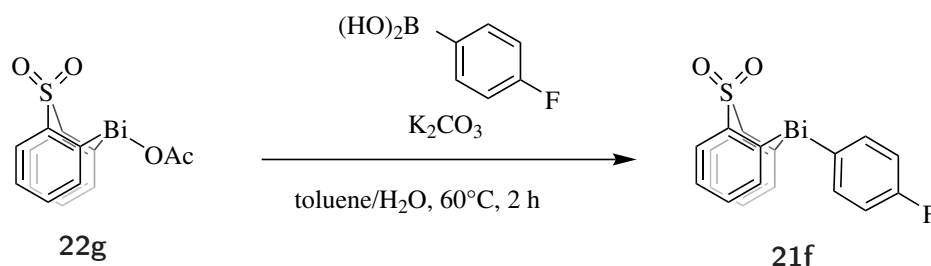
Selectivity of the arylation of 3-fluorophenol in dependency of the electronic properties of the transferred aryl group

10-(4-Fluorophenyl)-10H-dibenzo[b,e][1,4]thiabismine 5,5-dioxide (50.0 mg, 96.0 μmol) and 2-naphthol (13.9 mg, 96.0 μmol) were dissolved in toluene (5 mL). *m*CPBA (20 mg, 115 μmol) was added and the resulting solution was stirred at room temperature for 5 min. The reaction was quenched with MeOH (2.0 mL). Et₂O (20 mL) was added and the organic phase washed with saturated KHCO₃ solution, dried (MgSO₄) and concentrated *in vacuo*. Once the arylation product eluted with Et₂O, the silica was flushed with (MeOH/HOAc, 98/2) resulting in the desired product as a white solid.

5,5-Dioxido-10H-dibenzo[b,e][1,4]thiabismine-10-yl acetate **22g**

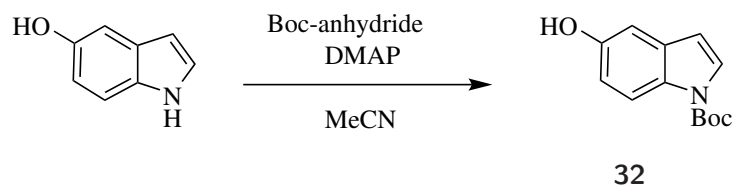


mp/ $^{\circ}\text{C}$ 209-210. ¹H NMR (500 MHz, CDCl₃) δ_{H} 8.70 (dd, $J = 7.4, 1.1$ Hz, 2H), 8.36 (dd, $J = 7.7, 1.3$ Hz, 2H), 7.69 (td, $J = 7.4, 1.3$ Hz, 2H), 7.45 (td, $J = 7.6, 1.2$ Hz, 2H), 2.17 (s, 3H). ¹³C{¹H} NMR (126 MHz, CDCl₃) δ_{C} 184.3, 179.6, 141.1, 136.0, 135.3, 128.8, 128.6, 22.6. IR (ATR): $\tilde{\nu} = 2956, 2923, 2852, 1726, 1615, 1594, 1462, 1440, 1373, 1304, 1289, 1254, 1133, 1086, 1070, 1011, 762, 740, 677, 588, 565$. HRMS calcd. for C₁₂H₈BiO₂S⁺: 425.0049 [M-OAc]⁺; found (ESI⁺): 425.0053. Rf: (MeOH/HOAc, 98/2) 0.6. Yield: 42.2 mg (91%).

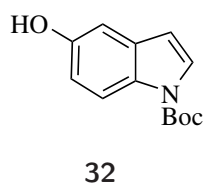
Recycling 5,5-dioxido-10H-dibenzo[b,e][1,4]thiabismine-10-yl acetate **22g**

The crude 5,5-dioxido-10H-dibenzo[b,e][1,4]thiabismine-10-yl acetate product was telescoped for the transmetallation using K_2CO_3 (17.4 mg, 126 μmol) and 4-fluorophenyl boronic acid (12.9 mg, 92.9 μmol) in a mixture of toluene (2.00 mL) and water (0.01 mL) that was allowed to stir at 60 °C for 2 h. The reaction mixture was subsequently dried (MgSO_4), filtered through a cotton plug and dried *in vacuo* resulting in the pure desired product (42 mg, 96%)

Boc Protection of 1H-indole-5-ol

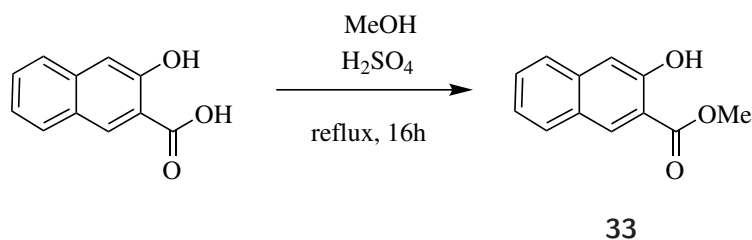


Boc-anhydride (2.50 g, 11.3 mmol) was added to a solution of 1H-Indole-5-ol (500 mg, 3.76 mmol) and DMAP (45.9 mg, 376 μmol) in MeCN (10 mL) at room temperature and stirred for 1 h. Subsequently the solvent was removed *in vacuo*, CH_2Cl_2 (10 mL) was added and washed with H_2O (10 mL \times 3). The organic layer was separated, dried (MgSO_4) and removed *in vacuo*. The crude product was dissolved in MeOH (10 mL) and K_2CO_3 (1.6 g, 19 mmol) was added resulting in a suspension, that was stirred for 2 h. The reaction mixture was then filtered, dried (MgSO_4) and concentrated *in vacuo*. The crude was purified by flash column chromatography, giving a clear colourless oil.

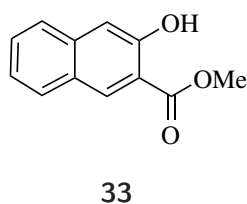
tert-Butyl 5-hydroxy-1H-indole-1-carboxylate **32**

^1H NMR (500 MHz, CDCl_3) δ_{H} 7.99 (s, 1H), 7.56 (d, $J = 3.7$ Hz, 1H), 6.98 (d, $J = 2.5$ Hz, 1H), 6.83 (dd, $J = 8.9, 2.6$ Hz, 1H), 6.46 (d, $J = 3.7$ Hz, 1H), 4.72 (s, 1H), 1.66 (s, 9H). $^{13}\text{C}\{^1\text{H}\}$ NMR (126 MHz, CDCl_3) δ_{C} 151.6, 149.9, 131.8, 130.2, 127.0, 116.0, 113.1, 107.0, 106.1, 83.7, 28.4. IR (ATR): $\tilde{\nu} = 3420, 1731, 1703, 1619, 1589, 1450, 1369, 1279, 1162, 1122, 1082, 1025, 842, 809, 760, 721$. HRMS calcd. for $\text{C}_{13}\text{H}_{14}\text{NO}_3^-$: 232.0979 $[\text{M}-\text{H}]^-$; found (ESI $^-$): 232.0976. Rf: (petrol/ Et_2O , 5/2) 0.3. Yield: 829 mg (95%). In accordance with literature values.²⁵⁸

Esterification of methyl 3-hydroxy-2-naphthoate

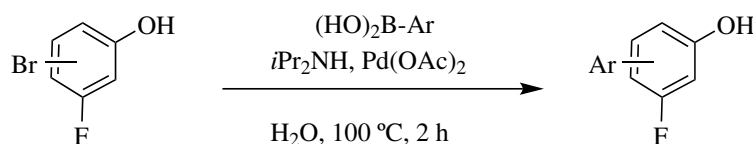


3-Hydroxy-2-naphthoic acid (1.00 g, 5.30 mmol) was added to MeOH (20 mL) and a few drops of conc. H_2SO_4 . The reaction mixture was heated at reflux for 16 h before EtOAc (20 mL) was added and the reaction mixture washed with KHCO_3 (aq.). The organic phase was dried (MgSO_4), filtered and subsequently concentrated *in vacuo* to afford the desired product.

Methyl 3-hydroxy-2-naphthoate **33**

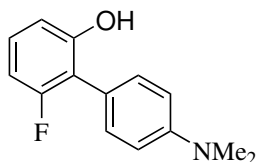
mp/ $^{\circ}\text{C}$ 72-74. $^1\text{H NMR}$ (500 MHz, CDCl_3) δ_{H} 10.43 (s, 1H), 8.50 (s, 1H), 7.80 (dd, $J = 8.3, 1.2$ Hz, 1H), 7.69 (dd, $J = 8.5, 1.1$ Hz, 1H), 7.50 (ddd, $J = 8.2, 6.8, 1.3$ Hz, 1H), 7.39 – 7.29 (m, 2H), 4.03 (s, 3H). $^{13}\text{C}\{^1\text{H}\}$ NMR (126 MHz, CDCl_3) δ_{C} 170.4, 156.4, 138.1, 132.6, 129.4, 129.3, 127.2, 126.5, 124.1, 114.3, 111.8, 52.7. IR (ATR): $\tilde{\nu} = 3244, 1683, 1517, 1508, 1463, 1440, 1325, 1285, 1215, 1146, 1075, 952, 913, 872, 841, 810, 788, 747, 682, 668$. HRMS calcd. for $\text{C}_{13}\text{H}_{14}\text{NO}_3^-$: 201.0557 $[\text{M}-\text{H}]^-$; found (ESI $^-$): 201.0587. Rf: (petrol/ Et_2O , 5/2) 0.18. Yield: 984 mg (92%). In accordance with with literature values²⁵⁹

Preparation of Authentic Samples of Arylation Products Obtained as Mixtures



General protocol: Bromo-3-fluorophenol (485 μmol), boronic acid (727 μmol), diisopropyl amine (136 μL , 970 μmol) and $\text{Pd}(\text{OAc})_2$ (10.8 mg, 48.5 μmol) were added to a microwave vial and the vial was sealed. After evacuating and back-filling with N_2 the vial, degassed H_2O (2 mL) was added and the reaction heated to 100 $^{\circ}\text{C}$. After 2 h the reaction mixture was extracted with CH_2Cl_2 , the organic phase was dried (MgSO_4) and concentrated *in vacuo* and purified by column chromatography.

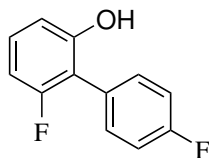
4'-(Dimethylamino)-6-fluoro-[1,1'-biphenyl]-2-ol 30a



30a

mp/°C 155-157. $^1\text{H NMR}$ (500 MHz, CDCl_3) δ_{H} 7.31 – 7.24 (m, 2H), 7.15 (td, $J = 8.2, 6.4$ Hz, 1H), 6.88 – 6.81 (m, 2H), 6.79 (dt, $J = 8.2, 1.1$ Hz, 1H), 6.71 (ddd, $J = 9.3, 8.3, 1.1$ Hz, 1H), 5.29 (s, 1H), 3.02 (s, 6H). $^{13}\text{C}\{^1\text{H}\}$ NMR (126 MHz, CDCl_3) δ_{C} 160.5 (d, $J = 244.2$ Hz), 154.5 (d, $J = 5.4$ Hz), 150.7, 131.1, 128.6 (d, $J = 10.5$ Hz), 116.9 (d, $J = 19.1$ Hz), 116.7, 113.1, 110.9 (d, $J = 2.9$ Hz), 107.6 (d, $J = 23.1$ Hz), 40.5. $^{19}\text{F NMR}$ (126 MHz, CDCl_3) δ_{F} -115.58 (dd, $J = 9.0, 6.5$ Hz). IR (ATR): $\tilde{\nu} = 3148, 1610, 1585, 1525, 1494, 1458, 1348, 1306, 1294, 1254, 1198, 1138, 1001, 931, 825, 784, 737, 581$. HRMS calcd. for $\text{C}_{14}\text{H}_{13}\text{FNO}^-$: 230.0987 [M-H] $^-$; found (ESI $^-$): 230.0985. Rf: (petrol/ Et_2O , 5/1) 0.26. Yield: 110 mg (98%).

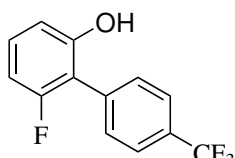
4',6-Difluoro-[1,1'-biphenyl]-2-ol 30b



30b

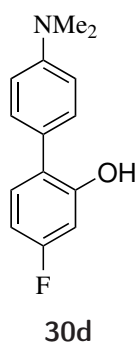
mp/°C 71-72. $^1\text{H NMR}$ (500 MHz, CDCl_3) δ_{H} 7.44 – 7.36 (m, 2H), 7.25 – 7.17 (m, 3H), 6.80 (dt, $J = 8.2, 1.1$ Hz, 1H), 6.75 (ddd, $J = 9.3, 8.3, 1.1$ Hz, 1H), 5.00 (s, 1H). $^{13}\text{C}\{^1\text{H}\}$ NMR (126 MHz, CDCl_3) δ_{C} 162.9 (d, $J = 248.7$ Hz), 160.3 (d, $J = 245.6$ Hz), 154.1 (d, $J = 5.5$ Hz), 132.4 (d, $J = 8.3$ Hz), 129.6 (d, $J = 10.5$ Hz), 126.0 (d, $J = 3.5$ Hz), 116.5 (d, $J = 21.5$ Hz), 115.9 (d, $J = 18.9$ Hz), 111.5 (d, $J = 3.1$ Hz), 107.9 (d, $J = 22.7$ Hz). $^{19}\text{F NMR}$ (126 MHz, CDCl_3) δ_{F} -112.67 (tt, $J = 8.6, 5.5$ Hz), -115.31 (dd, $J = 9.2, 6.4$ Hz). IR (ATR): $\tilde{\nu} = 3546, 1625, 1601, 1579, 1517, 1463, 1404, 1329, 1294, 1228, 1178, 1159, 999, 837, 785, 734, 574, 524, 501$. HRMS calcd. for $\text{C}_{12}\text{H}_7\text{F}_2\text{O}^-$: 205.0470 [M-H] $^-$; found (ESI $^-$): 205.0510. Rf: (petrol/ Et_2O , 5/1) 0.3. Yield: 162 mg (85%).

6-Fluoro-4'-(trifluoromethyl)-[1,1'-biphenyl]-2-ol 30c

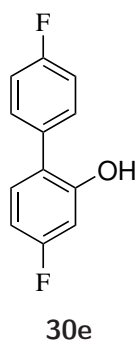


30c

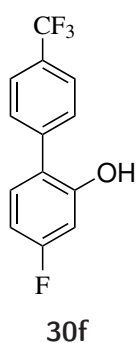
mp/°C 83-85. $^1\text{H NMR}$ (500 MHz, CDCl_3) δ_{H} 7.77 (d, $J = 8.1$ Hz, 2H), 7.58 (d, $J = 8.0$ Hz, 2H), 7.30 – 7.16 (m, 1H), 6.84 – 6.72 (m, 2H), 4.97 (s, 1H). $^{13}\text{C}\{^1\text{H}\}$ NMR (126 MHz, CDCl_3) δ_{C} 160.2 (d, $J = 246.2$ Hz), 153.9 (d, $J = 5.7$ Hz), 134.4, 131.06, 130.7 (d, $J = 32.7$ Hz), 130.1 (d, $J = 10.6$ Hz), 126.1 (q, $J = 3.8$ Hz), 124.1 (q, $J = 272.5$ Hz), 115.7 (d, $J = 18.6$ Hz), 111.8 (d, $J = 3.2$ Hz), 108.2 (d, $J = 22.7$ Hz). $^{19}\text{F NMR}$ (126 MHz, CDCl_3) δ_{F} -62.75, -115.23 (dd, $J = 9.2, 6.5$ Hz). IR (ATR): $\tilde{\nu} = 3308, 2927, 1645, 1586, 1465, 1405, 1324, 1293, 1246, 1165, 1118, 1067, 1000, 844, 786, 724, 611$. HRMS calcd. for $\text{C}_{13}\text{H}_7\text{F}_4\text{O}^-$: 255.0439 [M-H] $^-$; found (ESI $^-$): 255.0444. Rf: (petrol/ Et_2O , 5/1) 0.20. Yield: 98 mg (79%).

4'-(Dimethylamino)-4-fluoro-[1,1'-biphenyl]-2-ol **30d**

mp/°C 113-114. $^1\text{H NMR}$ (500 MHz, CDCl_3) δ_H 7.27 (m, 2H), 7.14 (dd, $J = 8.4, 6.6$ Hz, 1H), 6.87 – 6.78 (m, 2H), 6.73 – 6.61 (m, 2H), 5.54 – 5.22 (m, 1H), 3.01 (s, 6H). $^{13}\text{C}\{^1\text{H}\}$ NMR (126 MHz, CDCl_3) δ_C 162.8 (d, $J = 244.6$ Hz), 153.9 (d, $J = 12.2$ Hz), 150.4, 130.9 (d, $J = 9.8$ Hz), 129.9, 124.6 (d, $J = 3.1$ Hz), 123.4, 113.3, 107.6 (d, $J = 21.3$ Hz), 103.0 (d, $J = 24.9$ Hz), 40.6. $^{19}\text{F NMR}$ (126 MHz, CDCl_3) δ_F -113.80 – -114.01 (m). IR (ATR): $\tilde{\nu} = 3414, 2927, 1610, 1504, 1321, 1281, 1264, 1226, 1187, 1154, 1133, 1099, 970, 843, 802$. HRMS calcd. for $\text{C}_{14}\text{H}_{13}\text{FNO}^-$: 230.0987 [M-H] $^-$; found (ESI $^-$): 230.0977. Rf: (petrol/ Et_2O , 5/1) 0.26. Yield: 91 mg (81%).

4',4-Difluoro-[1,1'-biphenyl]-2-ol **30e**

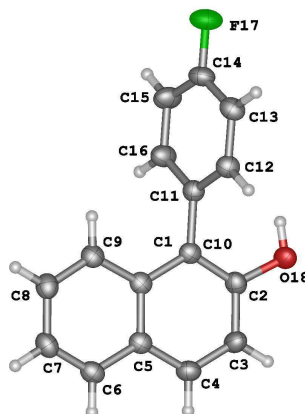
mp/°C 95-96. $^1\text{H NMR}$ (500 MHz, CDCl_3) δ_H 7.42 – 7.36 (m, 2H), 7.22 – 7.13 (m, 2H), 7.15 (dd, $J = 9.2, 6.5$ Hz, 1H), 6.73 – 6.69 (m, 2H), 5.12 (d, $J = 1.2$ Hz, 1H). $^{13}\text{C}\{^1\text{H}\}$ NMR (126 MHz, CDCl_3) δ_C 163.3 (d, $J = 246.2$ Hz), 162.7 (d, $J = 247.9$ Hz), 153.7 (d, $J = 12.0$ Hz), 132.3 (d, $J = 3.5$ Hz), 131.3 (d, $J = 9.9$ Hz), 131.1 (d, $J = 8.1$ Hz), 123.5 (d, $J = 3.2$ Hz), 116.5 (d, $J = 21.7$ Hz), 108.1 (d, $J = 21.7$ Hz), 103.6 (d, $J = 24.9$ Hz). $^{19}\text{F NMR}$ (126 MHz, CDCl_3) δ_F -112.41 (ddd, $J = 9.1, 9.1, 6.8$ Hz), -113.73 (tt, $J = 8.6, 5.3$ Hz). IR (ATR): $\tilde{\nu} = 3323, 2361, 2342, 2332, 1601, 1498, 1293, 1275, 1244, 1222, 1182, 1161, 1139, 1105, 1094, 970, 840, 816, 801$. HRMS calcd. for $\text{C}_{12}\text{H}_7\text{F}_2\text{O}^-$: 205.0470 [M-H] $^-$; found (ESI $^-$): 205.0496. Rf: (petrol/ Et_2O , 5/1) 0.3. Yield: 177 mg (93%).

4-Fluoro-4'-(trifluoromethyl)-[1,1'-biphenyl]-2-ol **30f**

mp/°C 85-86. $^1\text{H NMR}$ (500 MHz, CDCl_3) δ_H 7.74 (d, $J = 8.0$ Hz, 2H), 7.58 (d, $J = 8.0$ Hz, 2H), 7.21 (dd, $J = 8.5, 6.4$ Hz, 1H), 6.82 – 6.64 (m, 2H), 5.25 (s, 1H). $^{13}\text{C}\{^1\text{H}\}$ NMR (126 MHz, CDCl_3) δ_C 163.6 (d, $J = 247.4$ Hz), 153.7 (d, $J = 11.6$ Hz), 140.4, 131.5 (d, $J = 9.9$ Hz), 130.1 (q, $J = 32.7$ Hz), 129.7, 126.2 (q, $J = 3.9$ Hz), 124.2 (q, $J = 272.1$ Hz), 123.3 (d, $J = 3.3$ Hz), 108.5 (d, $J = 21.7$ Hz), 103.9 (d, $J = 24.8$ Hz). $^{19}\text{F NMR}$ (126 MHz, CDCl_3) δ_F -62.61, -111.47 (ddd, $J = 9.9, 8.2, 6.3$ Hz). IR (ATR): $\tilde{\nu} = 3401, 1618, 1496, 1402, 1321, 1289, 1163, 1123, 1100, 1068, 1021, 1009, 970, 846, 805, 709, 612$. HRMS calcd. for $\text{C}_{13}\text{H}_7\text{F}_4\text{O}^-$: 255.0439 [M-H] $^-$; found (ESI $^-$): 255.0442. Rf: (petrol/ Et_2O , 5/1) 0.20. Yield: 118 mg (95%).

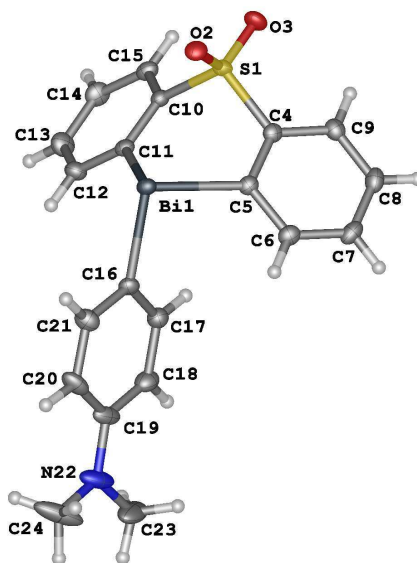
Crystallographic Information

Crystallographic data for 11c



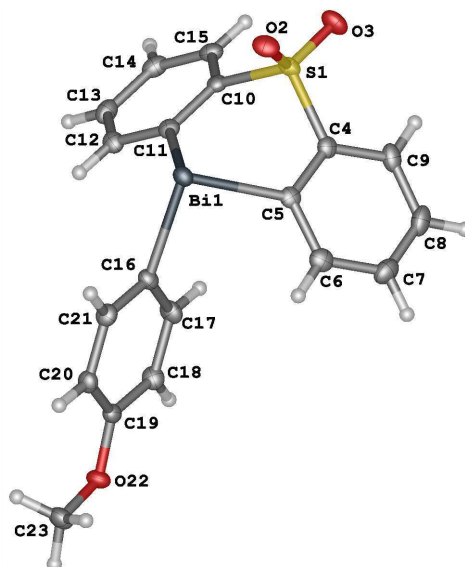
Empirical formula	C ₁₆ H ₁₁ OF
Formula weight	238.25
Temperature/K	120(2)
Crystal system	monoclinic
Space group	I2/a
a/Å	28.1724(10)
b/Å	7.7034(3)
c/Å	22.1866(7)
α/°	90
β/°	93.141(3)
γ/°	90
Volume/Å ³	4807.8(3)
Z	16
ρ _{calc} g/cm ³	1.317
μ/mm ⁻¹	0.748
F(000)	1984.0
Crystal size/mm ³	0.329 × 0.049 × 0.028
Radiation	CuKα (λ = 1.54184)
2 θ range for data collection/°	6.284 to 148.986
Index ranges	-34 ≤ h ≤ 35, -6 ≤ k ≤ 9, -27 ≤ l ≤ 27
Reflections collected	19506
Independent reflections	4825 [R _{int} = 0.0412, R _{sigma} = 0.0300]
Data/restraints/parameters	4825/0/331
Goodness-of-fit on F ²	1.034
Final R indexes [I >= 2σ (I)]	R ₁ = 0.0454, wR ₂ = 0.1158
Final R indexes [all data]	R ₁ = 0.0577, wR ₂ = 0.1273
Largest diff. peak/hole / e Å ⁻³	0.22/-0.28

Crystallographic data for 21a



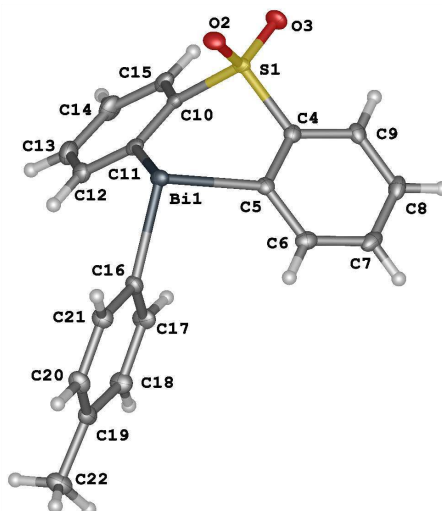
Empirical formula	C ₂₀ H ₁₈ BiNO ₂ S
Formula weight	545.39
Temperature/K	120(2)
Crystal system	monoclinic
Space group	C2/c
a/Å	12.1935(4)
b/Å	11.5939(4)
c/Å	13.2791(4)
α/°	90
β/°	95.950(3)
γ/°	90
Volume/Å ³	1867.16(11)
Z	4
ρ _{calc} g/cm ³	1.940
μ/mm ⁻¹	9.567
F(000)	1040.0
Crystal size/mm ³	0.257 × 0.093 × 0.041
Radiation	MoKα (λ = 0.71073)
2 θ range for data collection/°	5.94 to 61.058
Index ranges	-16 ≤ h ≤ 17, -16 ≤ k ≤ 16, -18 ≤ l ≤ 18
Reflections collected	41030
Independent reflections	5410 [R _{int} = 0.0386, R _{sigma} = 0.0239]
Data/restraints/parameters	5410/0/228
Goodness-of-fit on F ²	1.025
Final R indexes [I ≥ 2σ (I)]	R ₁ = 0.0188, wR ₂ = 0.0368
Final R indexes [all data]	R ₁ = 0.0245, wR ₂ = 0.0388
Largest diff. peak/hole / e Å ⁻³	0.83/-0.75

Crystallographic data for 21b



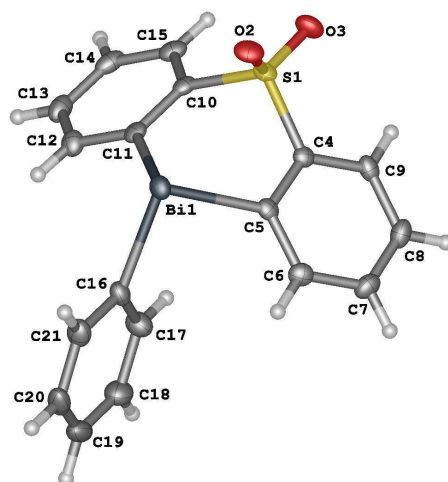
Empirical formula	$C_{19}H_{15}O_3S\text{Bi}$
Formula weight	532.35
Temperature/K	120(2)
Crystal system	monoclinic
Space group	$C2/c$
$a/\text{\AA}$	21.2431(8)
$b/\text{\AA}$	13.3554(5)
$c/\text{\AA}$	11.8685(5)
$\alpha/^\circ$	90
$\beta/^\circ$	98.048(4)
$\gamma/^\circ$	90
Volume/ \AA^3	3334.1(2)
Z	8
$\rho_{\text{calc}}/\text{g cm}^{-3}$	2.121
μ/mm^{-1}	10.715
F(000)	2016.0
Crystal size/ mm^3	$0.396 \times 0.066 \times 0.05$
Radiation	$\text{MoK}\alpha$ ($\lambda = 0.71073$)
2θ range for data collection/ $^\circ$	6.102 to 60.814
Index ranges	$-28 \leq h \leq 28, -18 \leq k \leq 18, -16 \leq l \leq 16$
Reflections collected	36123
Independent reflections	4778 [$R_{\text{int}} = 0.0374, R_{\text{sigma}} = 0.0240$]
Data/restraints/parameters	4778/0/218
Goodness-of-fit on F^2	1.032
Final R indexes [$I \geq 2\sigma(I)$]	$R_1 = 0.0184, wR_2 = 0.0344$
Final R indexes [all data]	$R_1 = 0.0243, wR_2 = 0.0362$
Largest diff. peak/hole / $e \text{\AA}^{-3}$	0.82/-0.64

Crystallographic data for 21c



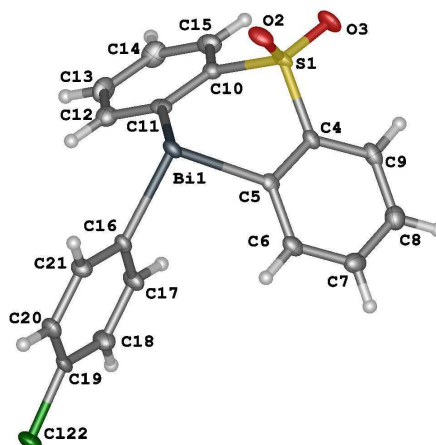
Empirical formula	$C_{19}H_{15}O_2S Bi$
Formula weight	516.35
Temperature/K	120(2)
Crystal system	monoclinic
Space group	$C2/c$
$a/\text{\AA}$	21.4472(9)
$b/\text{\AA}$	12.2454(5)
$c/\text{\AA}$	12.5804(5)
$\alpha/^\circ$	90
$\beta/^\circ$	101.038(4)
$\gamma/^\circ$	90
Volume/ \AA^3	3242.9(2)
Z	8
ρ_{calc} g/cm^3	2.115
μ/mm^{-1}	11.009
F(000)	1952.0
Crystal size/ mm^3	$0.302 \times 0.167 \times 0.136$
Radiation	$\text{MoK}\alpha$ ($\lambda = 0.71073$)
2θ range for data collection/ $^\circ$	6.6 to 60.822
Index ranges	$-28 \leq h \leq 30, -16 \leq k \leq 17, -17 \leq l \leq 17$
Reflections collected	31036
Independent reflections	4645 [$R_{int} = 0.0372, R_{sigma} = 0.0241$]
Data/restraints/parameters	4645/0/209
Goodness-of-fit on F^2	1.072
Final R indexes [$I \geq 2\sigma(I)$]	$R_1 = 0.0189, wR_2 = 0.0389$
Final R indexes [all data]	$R_1 = 0.0220, wR_2 = 0.0400$
Largest diff. peak/hole / $e \text{\AA}^{-3}$	0.57/-1.03

Crystallographic data for 21e



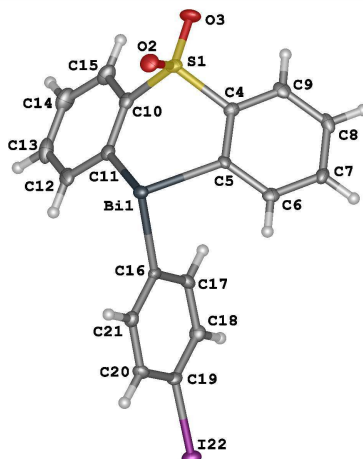
Empirical formula	C ₁₈ H ₁₃ O ₂ SBi
Formula weight	502.32
Temperature/K	120(2)
Crystal system	monoclinic
Space group	C2/c
a/Å	21.8215(8)
b/Å	12.1031(4)
c/Å	12.1806(5)
α/°	90
β/°	101.103(4)
γ/°	90
Volume/Å ³	3156.8(2)
Z	8
ρ _{calc} g/cm ³	2.114
μ/mm ⁻¹	11.306
F(000)	1888.0
Crystal size/mm ³	0.219 × 0.104 × 0.071
Radiation	MoKα (λ = 0.71073)
2 θ range for data collection/°	6.628 to 61.11
Index ranges	-30 ≤ h ≤ 30, -17 ≤ k ≤ 17, -16 ≤ l ≤ 17
Reflections collected	33904
Independent reflections	4527 [R _{int} = 0.0372, R _{sigma} = 0.0240]
Data/restraints/parameters	4527/0/199
Goodness-of-fit on F ²	1.075
Final R indexes [I ≥ 2σ (I)]	R ₁ = 0.0198, wR ₂ = 0.0351
Final R indexes [all data]	R ₁ = 0.0262, wR ₂ = 0.0370
Largest diff. peak/hole / e Å ⁻³	0.74/-0.98

Crystallographic data for 21g



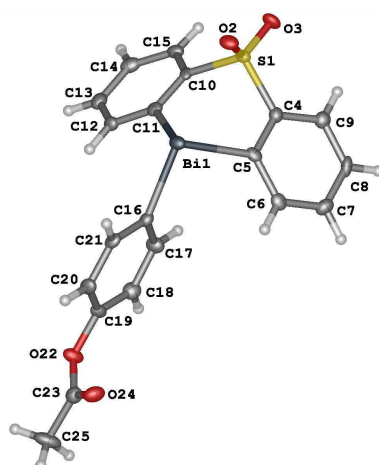
Empirical formula	$C_{18}H_{12}O_2SCiBi$
Formula weight	536.77
Temperature/K	120(2)
Crystal system	triclinic
Space group	P - 1
a/Å	7.6168(4)
b/Å	9.9489(6)
c/Å	11.7916(7)
$\alpha/^\circ$	66.908(6)
$\beta/^\circ$	81.921(5)
$\gamma/^\circ$	86.564(5)
Volume/Å ³	813.79(9)
Z	2
ρ_{calc} g/cm ³	2.191
μ/mm^{-1}	11.131
F(000)	504.0
Crystal size/mm ³	0.303 × 0.174 × 0.076
Radiation	MoK α ($\lambda = 0.71073$)
2 Θ range for data collection/ $^\circ$	6.19 to 60.84
Index ranges	-10 ≤ h ≤ 10, -13 ≤ k ≤ 13, -16 ≤ l ≤ 16
Reflections collected	16591
Independent reflections	4446 [$R_{int} = 0.0390$, $R_{sigma} = 0.0386$]
Data/restraints/parameters	4446/0/208
Goodness-of-fit on F ²	1.033
Final R indexes [$I \geq 2\sigma(I)$]	$R_1 = 0.0228$, $wR_2 = 0.0417$
Final R indexes [all data]	$R_1 = 0.0265$, $wR_2 = 0.0433$
Largest diff. peak/hole / e Å ⁻³	1.00/-1.26

Crystallographic data for 21i



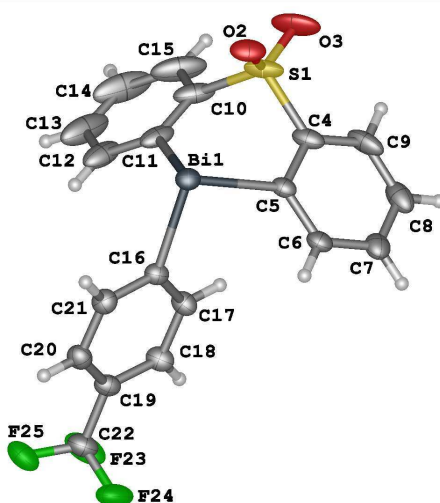
Empirical formula	C ₁₈ H ₁₂ O ₂ SIBi
Formula weight	628.22
Temperature/K	120(2)
Crystal system	monoclinic
Space group	P2 ₁ /n
a/Å	14.4080(5)
b/Å	13.6513(5)
c/Å	18.2200(8)
α/°	90
β/°	104.078(4)
γ/°	90
Volume/Å ³	3476.0(2)
Z	8
ρ _{calc} g/cm ³	2.401
μ/mm ⁻¹	12.046
F(000)	2304.0
Crystal size/mm ³	0.218 × 0.037 × 0.025
Radiation	MoKα (λ = 0.71073)
2 θ range for data collection/°	5.83 to 61.094
Index ranges	-20 ≤ h ≤ 20, -19 ≤ k ≤ 19, -25 ≤ l ≤ 25
Reflections collected	79236
Independent reflections	9936 [R _{int} = 0.0604, R _{sigma} = 0.0447]
Data/restraints/parameters	9936/0/415
Goodness-of-fit on F ²	1.045
Final R indexes [I ≥ 2σ (I)]	R ₁ = 0.02913, wR ₂ = 0.0423
Final R indexes [all data]	R ₁ = 0.0509, wR ₂ = 0.0473
Largest diff. peak/hole / e Å ⁻³	1.28/-0.99

Crystallographic data for 21j



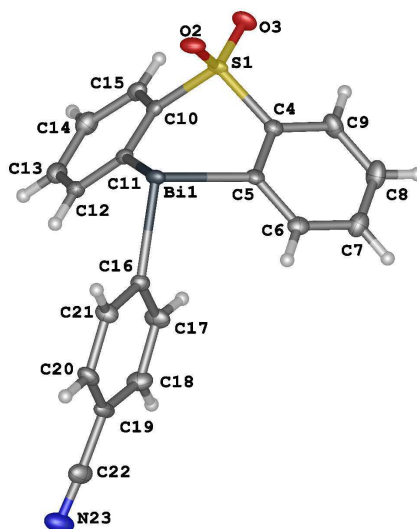
Empirical formula	C ₂₀ H ₁₅ BiO ₄ S
Formula weight	560.36
Temperature/K	120(2)
Crystal system	orthorhombic
Space group	Fdd2
a/Å	43.5802(9)
b/Å	43.1692(8)
c/Å	7.93329(13)
α/°	90
β/°	90
γ/°	90
Volume/Å ³	14925.1(5)
Z	32
ρ _{calc} g/cm ³	1.995
μ/mm ⁻¹	9.584
F(000)	8512.0
Crystal size/mm ³	0.683 × 0.04 × 0.019
Radiation	MoKα (λ = 0.71073)
2 θ range for data collection/°	5.926 to 61.014
Index ranges	-56 ≤ h ≤ 56, -60 ≤ k ≤ 57, -11 ≤ l ≤ 11
Reflections collected	76545
Independent reflections	10447 [R _{int} = 0.0741, R _{sigma} = 0.0474]
Data/restraints/parameters	10447/1/471
Goodness-of-fit on F ²	1.014
Final R indexes [I ≥ 2σ (I)]	R ₁ = 0.0293, wR ₂ = 0.0554
Final R indexes [all data]	R ₁ = 0.03685, wR ₂ = 0.0580
Largest diff. peak/hole / e Å ⁻³	2.38/-1.11
Flack parameter	-0.039(3)

Crystallographic data for 21k



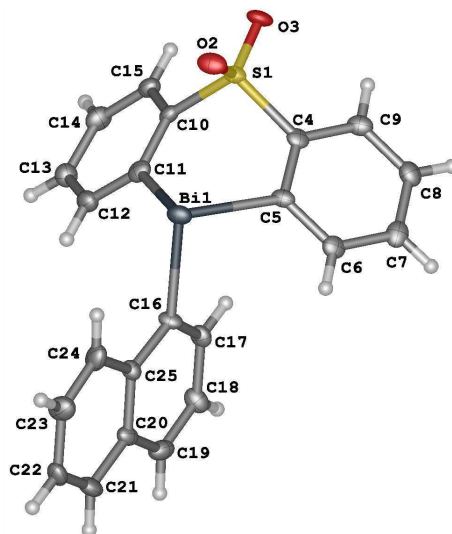
Empirical formula	C ₁₉ H ₁₂ O ₂ F ₃ SBi
Formula weight	570.33
Temperature/K	120(2)
Crystal system	monoclinic
Space group	P2 ₁ /n
a/Å	11.7322(3)
b/Å	11.6423(3)
c/Å	25.9048(8)
α/°	90
β/°	91.866(3)
γ/°	90
Volume/Å ³	3536.46(17)
Z	8
ρ _{calc} g/cm ³	2.142
μ/mm ⁻¹	10.129
F(000)	2144.0
Crystal size/mm ³	0.25 × 0.104 × 0.081
Radiation	MoKα (λ = 0.71073)
2 θ range for data collection/°	5.77 to 61.092
Index ranges	-16 ≤ h ≤ 16, -16 ≤ k ≤ 16, -33 ≤ l ≤ 36
Reflections collected	77048
Independent reflections	10134 [R _{int} = 0.0374, R _{sigma} = 0.0246]
Data/restraints/parameters	10134/144/497
Goodness-of-fit on F ²	1.054
Final R indexes [I >= 2σ (I)]	R ₁ = 0.0270, wR ₂ = 0.0442
Final R indexes [all data]	R ₁ = 0.0364, wR ₂ = 0.0471
Largest diff. peak/hole / e Å ⁻³	2.96/-3.53

Crystallographic data for 211



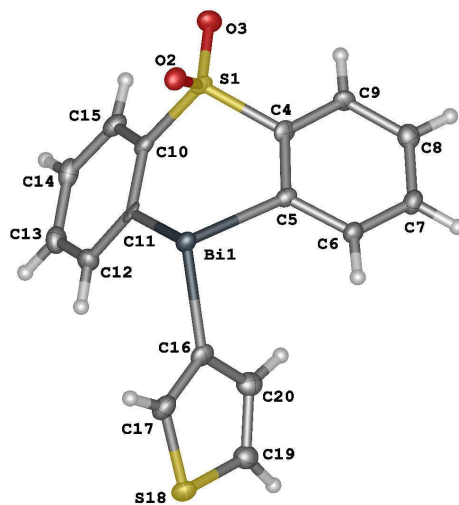
Empirical formula	$C_{19}H_{12}BiNO_2S$
Formula weight	527.34
Temperature/K	120(2)
Crystal system	triclinic
Space group	P - 1
a/Å	7.8209(4)
b/Å	9.8105(6)
c/Å	11.7472(7)
$\alpha/^\circ$	67.789(6)
$\beta/^\circ$	80.887(5)
$\gamma/^\circ$	86.588(5)
Volume/Å ³	823.91(9)
Z	2
ρ_{calc} g/cm ³	2.126
μ /mm ⁻¹	10.837
F(000)	496.0
Crystal size/mm ³	0.247 × 0.19 × 0.043
Radiation	MoK α ($\lambda = 0.71073$)
2 Θ range for data collection/ $^\circ$	6.614 to 61.1
Index ranges	-10 ≤ h ≤ 10, -13 ≤ k ≤ 13, -16 ≤ l ≤ 15
Reflections collected	17270
Independent reflections	4515 [$R_{int} = 0.0392$, $R_{sigma} = 0.0385$]
Data/restraints/parameters	4515/0/217
Goodness-of-fit on F ²	1.045
Final R indexes [$I \geq 2\sigma(I)$]	$R_1 = 0.0224$, $wR_2 = 0.0430$
Final R indexes [all data]	$R_1 = 0.0257$, $wR_2 = 0.0445$
Largest diff. peak/hole / e Å ⁻³	0.65/-1.03

Crystallographic data for 21m



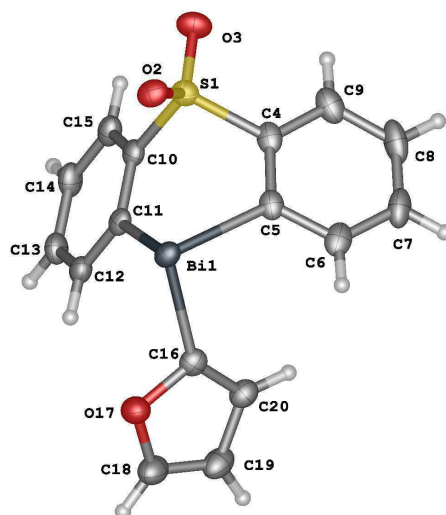
Empirical formula	C ₂₂ H ₁₅ O ₂ SBi
Formula weight	552.38
Temperature/K	120(2)
Crystal system	monoclinic
Space group	Cc
a/Å	11.8066(5)
b/Å	20.3287(9)
c/Å	7.5104(3)
α/°	90
β/°	99.129(4)
γ/°	90
Volume/Å ³	1779.75(13)
Z	4
ρ _{calc} g/cm ³	2.062
μ/mm ⁻¹	20.647
F(000)	1048.0
Crystal size/mm ³	0.239 × 0.152 × 0.094
Radiation	CuKα (λ = 1.54184)
2 θ range for data collection/°	8.7 to 147.522
Index ranges	-14 ≤ h ≤ 14, -25 ≤ k ≤ 24, -9 ≤ l ≤ 9
Reflections collected	13057
Independent reflections	3536 [R _{int} = 0.0434, R _{sigma} = 0.0311]
Data/restraints/parameters	3536/2/235
Goodness-of-fit on F ²	1.055
Final R indexes [I >= 2σ (I)]	R ₁ = 0.0439, wR ₂ = 0.1113
Final R indexes [all data]	R ₁ = 0.0440, wR ₂ = 0.1114
Largest diff. peak/hole / e Å ⁻³	0.60/-1.61
Flack parameter	0.00(2)

Crystallographic data for 21s



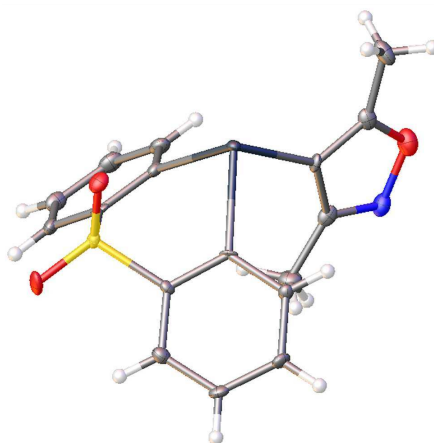
Empirical formula	$C_{16}H_{11}O_2S_2Bi$
Formula weight	508.35
Temperature/K	120(2)
Crystal system	monoclinic
Space group	$P2_1/n$
a/Å	11.2231(6)
b/Å	8.0328(5)
c/Å	33.365(2)
$\alpha/^\circ$	90
$\beta/^\circ$	94.310(6)
$\gamma/^\circ$	90
Volume/Å ³	2999.4(3)
Z	8
ρ_{calc} g/cm ³	2.251
μ/mm^{-1}	12.034
F(000)	1904.0
Crystal size/mm ³	0.154 × 0.116 × 0.027
Radiation	MoK α ($\lambda = 0.71073$)
2 Θ range for data collection/ $^\circ$	6.262 to 61.156
Index ranges	$-14 \leq h \leq 15$, $-11 \leq k \leq 11$, $-40 \leq l \leq 44$
Reflections collected	18516
Independent reflections	7652 [$R_{int} = 0.0471$, $R_{sigma} = 0.0658$]
Data/restraints/parameters	7652/706/417
Goodness-of-fit on F^2	1.034
Final R indexes [$I \geq 2\sigma(I)$]	$R_1 = 0.0393$, $wR_2 = 0.0712$
Final R indexes [all data]	$R_1 = 0.0571$, $wR_2 = 0.0793$
Largest diff. peak/hole / e Å ⁻³	1.35/-1.76

Crystallographic data for 21t



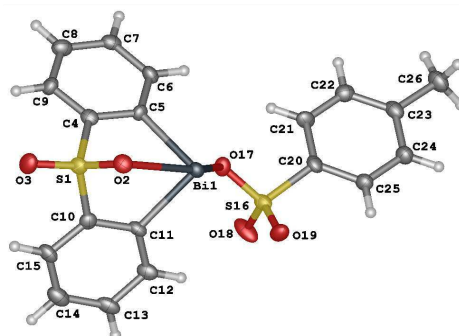
Empirical formula	C ₁₆ H ₁₁ BiO ₃ S
Formula weight	492.29
Temperature/K	120(2)
Crystal system	triclinic
Space group	P - 1
a/Å	8.2553(3)
b/Å	9.0358(4)
c/Å	10.8435(4)
α/°	71.021(4)
β/°	77.946(3)
γ/°	71.901(4)
Volume/Å ³	721.80(5)
Z	2
ρ _{calc} g/cm ³	2.265
μ/mm ⁻¹	12.364
F(000)	460.0
Crystal size/mm ³	0.186 × 0.104 × 0.081
Radiation	MoKα (λ = 0.71073)
2 θ range for data collection/°	6.174 to 60.918
Index ranges	-11 ≤ h ≤ 10, -12 ≤ k ≤ 12, -15 ≤ l ≤ 15
Reflections collected	14908
Independent reflections	3977 [R _{int} = 0.0388 R _{sigma} = 0.0354]
Data/restraints/parameters	3977/0/190
Goodness-of-fit on F ²	1.034
Final R indexes [I ≥ 2σ (I)]	R ₁ = 0.0233, wR ₂ = 0.0445
Final R indexes [all data]	R ₁ = 0.0268, wR ₂ = 0.0459
Largest diff. peak/hole / e Å ⁻³	2.13/-1.40

Crystallographic data for 21w



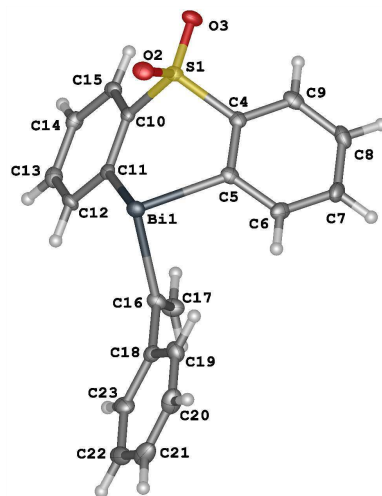
Empirical formula	C ₁₇ H ₁₄ NO ₃ SBi
Formula weight	521.33
Temperature/K	120(2)
Crystal system	orthorhombic
Space group	P2 ₁ 2 ₁ 2 ₁
a/Å	7.22400(10)
b/Å	11.3972(2)
c/Å	19.2691(2)
α/°	90
β/°	90
γ/°	90
Volume/Å ³	1586.49(4)
Z	4
ρ _{calc} g/cm ³	2.183
μ/mm ⁻¹	23.169
F(000)	984.0
Crystal size/mm ³	0.168 × 0.123 × 0.088
Radiation	CuKα (λ = 1.54184)
2 θ range for data collection/°	9.014 to 149.012
Index ranges	-9 ≤ h ≤ 9, -14 ≤ k ≤ 13, -24 ≤ l ≤ 24
Reflections collected	56480
Independent reflections	3223 [R _{int} = 0.0574, R _{sigma} = 0.0595]
Data/restraints/parameters	3223/0/210
Goodness-of-fit on F ²	1.215
Final R indexes [I >= 2σ (I)]	R ₁ = 0.0154, wR ₂ = 0.0404
Final R indexes [all data]	R ₁ = 0.0154, wR ₂ = 0.0404
Largest diff. peak/hole / e Å ⁻³	0.47/-2.14
Flack parameter	-0.021(3)

Crystallographic data for 22c



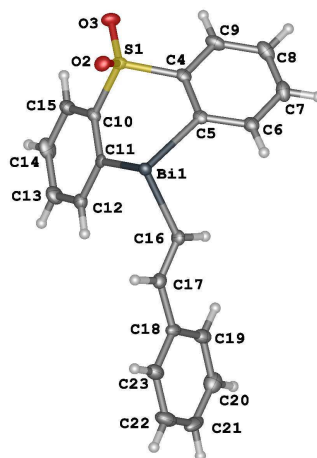
Empirical formula	$C_{19}H_{15}O_5S_2Bi$
Formula weight	596.41
Temperature/K	120(2)
Crystal system	monoclinic
Space group	$P2_1/n$
a/Å	15.6742(3)
b/Å	7.07136(14)
c/Å	17.3321(4)
$\alpha/^\circ$	90
$\beta/^\circ$	108.521(2)
$\gamma/^\circ$	90
Volume/Å ³	1821.55(7)
Z	4
ρ_{calc} g/cm ³	2.175
μ /mm ⁻¹	21.405
F(000)	1136.0
Crystal size/mm ³	0.506 × 0.049 × 0.027
Radiation	CuK α ($\lambda = 1.54184$)
2 Θ range for data collection/ $^\circ$	9.204 to 156.298
Index ranges	-19 ≤ h ≤ 19, -5 ≤ k ≤ 89, -22 ≤ l ≤ 21
Reflections collected	9373
Independent reflections	3762 [$R_{int} = 0.0614$, $R_{sigma} = 0.0568$]
Data/restraints/parameters	3762/0/245
Goodness-of-fit on F ²	1.075
Final R indexes [$I \geq 2\sigma(I)$]	$R_1 = 0.0602$, $wR_2 = 0.1642$
Final R indexes [all data]	$R_1 = 0.0616$, $wR_2 = 0.1665$
Largest diff. peak/hole / e Å ⁻³	5.24/-2.08

Crystallographic data for 23a



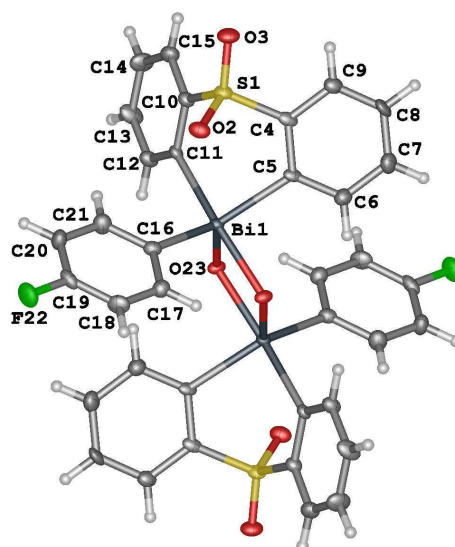
Empirical formula	$C_{20}H_{15}BiO_2S$
Formula weight	528.36
Temperature/K	120(2)
Crystal system	triclinic
Space group	P-1
a/Å	8.5629(4)
b/Å	9.9321(5)
c/Å	11.2385(5)
$\alpha/^\circ$	107.961(4)
$\beta/^\circ$	106.537(4)
$\gamma/^\circ$	97.144(4)
Volume/Å ³	847.71(8)
Z	2
ρ_{calc} g/cm ³	2.070
μ /mm ⁻¹	10.531
F(000)	500.0
Crystal size/mm ³	0.245 × 0.084 × 0.026
Radiation	MoK α (λ = 0.71073)
2 Θ range for data collection/ $^\circ$	5.93 to 61.35
Index ranges	-12 ≤ h ≤ 12, -14 ≤ k ≤ 13, -15 ≤ l ≤ 15
Reflections collected	16403
Independent reflections	4604 [R_{int} = 0.0574, R_{sigma} = 0.0595]
Data/restraints/parameters	4604/1/217
Goodness-of-fit on F ²	1.037
Final R indexes [$I \geq 2\sigma(I)$]	$R_1 = 0.0315$, $wR_2 = 0.0556$
Final R indexes [all data]	$R_1 = 0.0388$, $wR_2 = 0.0593$
Largest diff. peak/hole / e Å ⁻³	1.69/-1.50

Crystallographic data for 23b



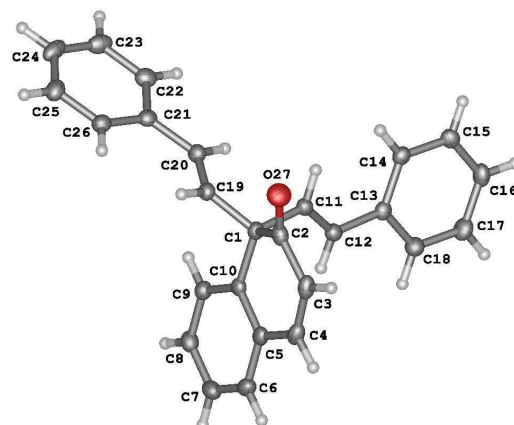
Empirical formula	$C_{20}H_{15}BiO_2S$
Formula weight	528.36
Temperature/K	120(2)
Crystal system	orthorhombic
Space group	$Pca2_1$
a/Å	18.5016(7)
b/Å	9.9202(4)
c/Å	9.6287(4)
$\alpha/^\circ$	90
$\beta/^\circ$	90
$\gamma/^\circ$	90
Volume/Å ³	1767.25(12)
Z	4
ρ_{calc} g/cm ³	1.986
μ/mm^{-1}	10.103
F(000)	1000.0
Crystal size/mm ³	0.251 × 0.052 × 0.042
Radiation	MoK α ($\lambda = 0.71073$)
2 Θ range for data collection/ $^\circ$	6.022 to 61.144
Index ranges	$-26 \leq h \leq 25$, $-14 \leq k \leq 13$, $-13 \leq l \leq 12$
Reflections collected	37312
Independent reflections	5053 [$R_{int} = 0.0596$, $R_{sigma} = 0.0441$]
Data/restraints/parameters	5053/1/217
Goodness-of-fit on F ²	1.066
Final R indexes [$I \geq 2\sigma(I)$]	$R_1 = 0.0277$, $wR_2 = 0.0437$
Final R indexes [all data]	$R_1 = 0.0430$, $wR_2 = 0.0485$
Largest diff. peak/hole / e Å ⁻³	2.13/-1.00
Flack parameter	-0.047(4)

Crystallographic data for 25a



Empirical formula	$C_{40}H_{30}Bi_2F_2N_2O_6S_2$
Formula weight	1154.74
Temperature/K	120(2)
Crystal system	monoclinic
Space group	$P2_1/n$
a/Å	8.4209(5)
b/Å	14.4753(9)
c/Å	15.3747(9)
$\alpha/^\circ$	90
$\beta/^\circ$	94.706(6)
$\gamma/^\circ$	90
Volume/Å ³	1867.80(19)
Z	2
ρ_{calc} g/cm ³	2.053
μ/mm^{-1}	9.581
F(000)	1096.0
Crystal size/mm ³	0.119 × 0.064 × 0.033
Radiation	MoK α ($\lambda = 0.71073$)
2 Θ range for data collection/ $^\circ$	6.016 to 61.19
Index ranges	$-12 \leq h \leq 11, -18 \leq k \leq 19, -21 \leq l \leq 21$
Reflections collected	18410
Independent reflections	5102 [$R_{int} = 0.0500, R_{sigma} = 0.0549$]
Data/restraints/parameters	5102/0/245
Goodness-of-fit on F^2	1.047
Final R indexes [$I \geq 2\sigma(I)$]	$R_1 = 0.0313, wR_2 = 0.0492$
Final R indexes [all data]	$R_1 = 0.0467, wR_2 = 0.0538$
Largest diff. peak/hole / e Å ⁻³	1.14/-0.92

Crystallographic data for 26y



Empirical formula	C ₂₆ H ₂₀ O
Formula weight	348.42
Temperature/K	120(2)
Crystal system	monoclinic
Space group	P2 ₁ /n
a/Å	12.0802(3)
b/Å	10.9189(4)
c/Å	13.8347(4)
α/°	90
β/°	94.602(3)
γ/°	90
Volume/Å ³	1818.95(9)
Z	4
ρ _{calc} g/cm ³	1.272
μ/mm ⁻¹	0.584
F(000)	736.0
Crystal size/mm ³	0.473 × 0.374 × 0.245
Radiation	CuKα (λ = 1.54184)
2 θ range for data collection/°	9.354 to 149.212
Index ranges	-15 ≤ h ≤ 14, -13 ≤ k ≤ 13, -17 ≤ l ≤ 16
Reflections collected	32893
Independent reflections	36973 [R _{int} = 0.0305, R _{sigma} = 0.0134]
Data/restraints/parameters	3697/0/244
Goodness-of-fit on F ²	1.033
Final R indexes [I ≥ 2σ (I)]	R ₁ = 0.0370, wR ₂ = 0.0923
Final R indexes [all data]	R ₁ = 0.0402, wR ₂ = 0.0949
Largest diff. peak/hole / e Å ⁻³	0.21/-0.21

Bibliography

- [1] D. H. R. Barton, N. Y. Bhatnagar, J.-C. Blazejewski, B. Charpiot, J.-P. Finet, D. J. Lester, W. B. Motherwell, M. T. B. Papoula, S. P. Stanforth, *J. Chem. Soc. Perkin Trans. 1* **1985**, 2657–2665.
- [2] R. B. Teponno, S. Kusari, M. Spiteller, *Nat. Prod. Rep.* **2016**, *33*, 1044–1092.
- [3] S. R. Ibrahim, G. A. Mohamed, *Fitoterapia* **2015**, *106*, 194–225.
- [4] W. Hoffmeister, *Ann. der Chem. und Pharm.* **1871**, *159*, 191–217.
- [5] R. Hirsch, *Ber. Dtsch. Chem. Ges.* **1890**, *23*, 3705–3710.
- [6] A. Kralj, E. Kurt, N. Tschammer, M. R. Heinrich, *ChemMedChem* **2014**, *9*, 151–168.
- [7] C. Pearson, D.; Wysong, D., Breder, *J. Org. Chem.* **1967**, *32*, 2358–2360.
- [8] R. Long, X. Yan, Z. Wu, Z. Li, H. Xiang, X. Zhou, *Org. Biomol. Chem.* **2015**, *13*, 3571–3574.
- [9] X. Zhao, C. S. Yeung, V. M. Dong, *J. Am. Chem. Soc.* **2010**, *132*, 5837–5844.
- [10] R. B. Bedford, R. L. Webster, C. J. Mitchell, *Org. Biomol. Chem.* **2009**, *7*, 4853–4857.
- [11] B. Xiao, Y. Fu, J. Xu, T. J. Gong, J. J. Dai, J. Yi, L. Liu, *J. Am. Chem. Soc.* **2010**, *132*, 468–469.
- [12] L. Ackermann, E. Diers, A. Manvar, *Org. Lett.* **2012**, *14*, 1154–1157.
- [13] S. Gu, C. Chen, W. Chen, *J. Org. Chem.* **2009**, *74*, 7203–7206.
- [14] S. Oi, S.-i. Watanabe, S. Fukita, Y. Inoue, *Tetrahedron Lett.* **2003**, *44*, 8665–8668.
- [15] R. B. Bedford, S. J. Coles, M. B. Hursthouse, M. E. Limmert, *Angew. Chem. Int. Ed.* **2003**, *42*, 112–114.
- [16] T. Truong, O. Daugulis, *Chem. Sci.* **2013**, *4*, 531–535.
- [17] H. Alinezhad, S. M. Tavakkoli, F. Salehian, *Synth. Commun.* **2010**, *40*, 3226–3232.
- [18] R. J. Tang, T. Milcent, B. Crousse, *J. Org. Chem.* **2018**, *83*, 930–938.
- [19] J. E. Baldwin, C. G. Carter, *J. Am. Chem. Soc.* **1978**, *100*, 3942–3944.
- [20] M. Boukachabia, N. Vriamont, D. Lambin, O. Riant, L. Aribi-Zouioueche, *Comptes Rendus Chim.* **2014**, *17*, 403–412.
- [21] L. Bougdid, A. Heynderickx, S. Delbaere, C. Moustrou, *Tetrahedron* **2007**, *63*, 8242–8249.

- [22] J. J. Boruah, S. P. Das, R. Borah, S. R. Gogoi, N. S. Islam, *Polyhedron* **2013**, *52*, 246–254.
- [23] N. Miyaura, A. Suzuki, *Chem. Rev.* **1995**, *95*, 2457–2483.
- [24] A. J. Lennox, G. C. Lloyd-Jones, *Chem. Soc. Rev.* **2014**, *43*, 412–443.
- [25] C. Cordovilla, C. Bartolomé, J. M. Martínez-Irarduya, P. Espinet, *ACS Catal.* **2015**, *5*, 3040–3053.
- [26] P. Espinet, A. M. Echavarren, *Angew. Chem. Int. Ed.* **2004**, *43*, 4704–4734.
- [27] A. Zernickel, W. Du, S. A. Ghorpade, D. N. Sawant, A. A. Makki, N. Sekar, J. Eppinger, *J. Org. Chem.* **2018**, *83*, 1842–1851.
- [28] T. Konakahara, Y. Kiran, Y. Okuno, R. Ikeda, N. Sakai, *Tetrahedron Lett.* **2010**, *51*, 2335–2338.
- [29] G. A. Molander, S. L. J. Trice, S. M. Kennedy, S. D. Dreher, M. T. Tudge, *J. Am. Chem. Soc.* **2012**, *134*, 11667–11673.
- [30] K. Mori, T. Itakura, T. Akiyama, *Angew. Chem. Int. Ed.* **2016**, *55*, 11642–11646.
- [31] C. Cazorla, T. S. De Vries, E. Vedejs, *Org. Lett.* **2013**, *15*, 984–987.
- [32] D. H. Barton, B. Charpiot, W. B. Motherwell, *Tetrahedron Lett.* **1982**, *23*, 3365–3368.
- [33] D. H. Barton, N. Yadav-Bhatnagar, J.-P. Finet, J. Khamsi, W. B. Motherwell, S. P. Stanforth, *Tetrahedron* **1987**, *43*, 323–332.
- [34] R. Mohan, *Nat. Chem.* **2010**, *2*, 336–336.
- [35] Z. Huang, J.-P. Lumb, *ACS Catal.* **2019**, *9*, 521–555.
- [36] H. Suzuki, N. Komatsu, T. Ogawa, T. Murafuji, T. Ikegami, Y. Matano, *Organobismuth Chemistry*, Elsevier Science, Amsterdam, **2001**.
- [37] D. R. Lide, *Handb. Chem. Phys.* **2003**, *53*, 2616.
- [38] J. M. Bothwell, S. W. Krabbe, R. S. Mohan, *Chem. Soc. Rev.* **2011**, *40*, 4649–4707.
- [39] C. S. Anderson, *Miner. Commod. Summ. 2016* **2016**, *21*, 36–37.
- [40] D. M. Keogan, D. M. Griffith, *Molecules* **2014**, *19*, 15258–15297.
- [41] Y. E. L. Jesse O. Betterton, *Pat. US 1989734 A* **1940**, 1–2.
- [42] W. Kroll, *Pat. 410533* **1925**, 1–2.
- [43] A. G. Betts, *Art or process of refining lead by electrolysis*, **1901**.
- [44] P. de Marcillac, N. Coron, G. Dambier, J. Leblanc, J.-P. Moalic, *Nature* **2003**, *422*, 876–878.
- [45] T. E. Sox, C. A. Olson, *Antimicrob. Agents Chemother.* **1989**, *33*, 2075–2082.
- [46] M. Waugh, *Sex. Transm. Infect.* **2017**, *93*, 202–202.
- [47] K. Iuchi, Y. Hatano, T. Yagura, *Biochem. Pharmacol.* **2008**, *76*, 974–986.

- [48] H. Gilman, H. L. Yale, *Chem. Rev.* **1942**, *30*, 281–320.
- [49] R. J. Schwamm, M. Lein, M. P. Coles, C. M. Fitchett, *Chem. Commun.* **2018**, *54*, 916–919.
- [50] L. Lempenauer, E. Duñach, G. Lemièrre, *Org. Lett.* **2016**, *18*, 1326–1329.
- [51] A. L. Silva, J. C. Bordado, *Catal. Rev.* **2004**, *46*, 31–51.
- [52] S. S. Bhat, *Two-part moisture curable polyurethane adhesive*, **1997**.
- [53] C. Löwig, E. Schweizer, *Ann. der Chem. und Pharm.* **1850**, *75*, 315–355.
- [54] A. Marquardt, *Ber. Dtsch. Chem. Ges.* **1887**, *20*, 1516–1523.
- [55] K. Urgin, C. Aubé, C. Pichon, M. Pipelier, V. Blot, C. Thobie-Gautier, E. Léonel, D. Dubreuil, S. Condon, *Tetrahedron Lett.* **2012**, *53*, 1894–1896.
- [56] R. De Ketelaere, F. Delbeke, G. Van Der Kelen, *J. Organomet. Chem.* **1971**, *30*, 365–368.
- [57] S. L. Benjamin, L. Karagiannidis, W. Levason, G. Reid, M. C. Rogers, *Organometallics* **2011**, *30*, 895–904.
- [58] H. J. Breunig, D. Müller, *Zeitschrift für Naturforsch. B* **1983**, *38*, 125–129.
- [59] S. Schulz, A. Kuczkowski, D. Bläser, C. Wölper, G. Jansen, R. Haack, *Organometallics* **2013**, *32*, 5445–5450.
- [60] J. Emsley, *The Elements*, Oxford : Clarendon Press, 3rd ed., **1998**.
- [61] A. N. Sobolev, V. K. Belsky, I. P. Romm, N. Y. Chernikova, E. N. Guryanova, *Acta Crystallogr. Sect. C Cryst. Struct. Commun.* **1985**, *41*, 967–971.
- [62] H. Kooijman, A. L. Spek, K. J. C. van Bommel, W. Verboom, D. N. Reinhoudt, *Acta Crystallogr. Sect. C Cryst. Struct. Commun.* **1998**, *54*, 1695–1698.
- [63] M. ul Haque, H. A. Tayim, J. Ahmed, W. Horne, *J. Crystallogr. Spectrosc. Res.* **1985**, *15*, 561–571.
- [64] E. A. Adams, J. W. Kolis, W. T. Pennington, *Acta Crystallogr. Sect. C Cryst. Struct. Commun.* **1990**, *46*, 917–919.
- [65] D. M. Hawley, G. Ferguson, *J. Chem. Soc. A Inorganic Phys. Theor.* **1968**, 2059 – 2063.
- [66] H. Gilman, H. L. Yablunsky, *J. Am. Chem. Soc.* **1941**, *63*, 207–211.
- [67] F. Challenger, *J. Chem. Soc. Trans.* **1914**, *105*, 2210–2218.
- [68] S. Faleschini, P. Zanella, L. Doretto, G. Faraglia, *J. Organomet. Chem.* **1972**, *44*, 317–323.
- [69] H. Hartmann, G. Habenicht, W. Reiss, *Z. Anorg. Allg. Chem.* **1962**, *317*, 54–62.
- [70] I. V. Egorova, V. V. Zhidkov, I. P. Grinishak, *Russ. J. Gen. Chem.* **2015**, *85*, 1692–1697.
- [71] G. Deacon, W. Jackson, J. Pfeiffer, *Aust. J. Chem.* **1984**, *37*, 527–535.

- [72] Y. Matano, T. Miyamatsu, H. Suzuki, *Organometallics* **1996**, *15*, 1951–1953.
- [73] L. K. Rasmussen, M. Begtrup, T. Ruhland, *J. Org. Chem.* **2004**, *69*, 6890–6893.
- [74] L. D. Freedman, G. O. Doak, *Chem. Rev.* **1982**, *82*, 15–57.
- [75] I. V. Egorova, V. V. Zhidkov, I. P. Grinishak, A. A. Rezvanova, *Russ. J. Gen. Chem.* **2014**, *84*, 1374–1377.
- [76] H. Suzuki, T. Murafuji, N. Azuma, *J. Chem. Soc. Perkin Trans. 1* **1992**, *53*, 1593–1600.
- [77] A. Schmuck, K. Seppelt, *Chem. Ber.* **1989**, *122*, 803–808.
- [78] J.-P. Finet, A. Y. Fedorov, *J. Organomet. Chem.* **2006**, *691*, 2386–2393.
- [79] S. Combes, J.-P. Finet, *Tetrahedron* **1998**, *54*, 4313–4318.
- [80] H. Suzuki, T. Ikegami, Y. Matano, N. Azuma, *J. Chem. Soc. Perkin Trans. 1* **1993**, *4*, 2411–2415.
- [81] C. A. Hunter, K. N. Houk, J.-M. Lehn, M. J. Krische, M. Olivucci, S. V. Ley, M. Venturi, J. Thiem, H. Yamamoto, C.-H. Wong, H. Wong, *Bismuth-Mediated Organic Reactions, Vol. 311*, Springer Berlin Heidelberg, **2012**.
- [82] Y. Matano, *Organometallics* **2000**, *19*, 2258–2263.
- [83] Y. Matano, S. A. Begum, T. Miyamatsu, H. Suzuki, *Organometallics* **1998**, *17*, 4332–4334.
- [84] Y. Matano, T. Suzuki, T. Iwata, T. Shinokura, H. Imahori, *Bull. Chem. Soc. Jpn.* **2008**, *81*, 1621–1628.
- [85] Y. Matano, N. Azuma, H. Suzuki, *J. Chem. Soc. Perkin Trans. 1* **1995**, 2543–2549.
- [86] H. Suzuki, T. Ikegami, N. Azuma, *J. Chem. Soc. Perkin Trans. 1* **1997**, 1609–1616.
- [87] Y. Matano, N. Azuma, H. Suzuki, *Tetrahedron Lett.* **1993**, *34*, 8457–8460.
- [88] Y. Matano, *J. Chem. Soc. Perkin Trans. 1* **1994**, *19*, 2703–2709.
- [89] Y. Matano, M. Yoshimune, H. Suzuki, *Tetrahedron Lett.* **1995**, *36*, 7475–7478.
- [90] Y. Matano, M. Yoshimune, N. Azuma, H. Suzuki, *J. Chem. Soc. Perkin Trans. 1* **1996**, 1971–1977.
- [91] Y. Matano, *Chem. Commun.* **2000**, *1*, 2233–2234.
- [92] Y. Matano, T. Miyamatsu, H. Suzuki, *Chem. Lett.* **1998**, 127–128.
- [93] Y. Matano, S. Begum, H. Suzuki, *Synthesis* **2004**, *2001*, 1081–1085.
- [94] D. H. R. Barton, B. Charpiot, E. T. H. Dau, W. B. Motherwell, C. Pascard, C. Pichon, *Helv. Chim. Acta* **1984**, *67*, 586–599.
- [95] G. Wittig, K. Clauß, *Liebigs Ann.* **1952**, *578*, 136–146.
- [96] A. F. M. Mustafizur Rahman, T. Murafuji, M. Ishibashi, Y. Miyoshi, Y. Sugihara, *J. Organomet. Chem.* **2004**, *689*, 3395–3401.

- [97] K. Matoba, S.-i. Motofusa, C. Sik Cho, K. Ohe, S. Uemura, *J. Organomet. Chem.* **1999**, *574*, 3–10.
- [98] S. K. Kang, H. C. Ryu, J. W. Kim, *Synth. Commun.* **2001**, *31*, 1021–1026.
- [99] S. K. Kang, H. C. Ryu, S. W. Lee, *Synth. Commun.* **2001**, *31*, 1027–1034.
- [100] S. Shimada, M. L. N. Rao in *Top. Curr. Chem., Vol. 311*, Springer, Berlin, Heidelberg, **2011**, pp. 199–228.
- [101] D. H. Barton, J.-P. Finet, J. Khamsi, *Tetrahedron Lett.* **1988**, *29*, 1115–1118.
- [102] S. A. Lermontov, I. M. Rakov, N. S. Zefirov, P. Stang, *Tetrahedron Lett.* **1996**, *37*, 4051–4054.
- [103] M. P. Permashwar, K. K. Banerji, *Aust. J. Chem.* **1976**, *29*, 1939–1945.
- [104] D. J. Upadhyaya, S. D. Samant, *Catal. Today* **2013**, *208*, 60–65.
- [105] D. H. Barton, J.-P. Finet, W. B. Motherwell, C. Pichon, *Tetrahedron* **1986**, *42*, 5627–5636.
- [106] F. Challenger, O. V. Richards, *J. Chem. Soc.* **1934**, 405–411.
- [107] Y. Mitsumoto, M. Nitta, *Bull. Chem. Soc. Jpn.* **2003**, *76*, 1029–1034.
- [108] Y. Matano, H. Nomura, *Angew. Chem. Int. Ed.* **2002**, *41*, 3028–3031.
- [109] Y. Matano, T. Hisanaga, H. Yamada, S. Kusakabe, H. Nomura, H. Imahori, *J. Org. Chem.* **2004**, *69*, 8676–8680.
- [110] C. F. de Graauw, J. A. Peters, H. van Bekkum, J. Huskens, *Synthesis* **1994**, *1994*, 1007–1017.
- [111] D. B. Dess, J. C. Martin, *J. Org. Chem.* **1983**, *48*, 4155–4156.
- [112] R. A. Abramovitch, D. H. Barton, J.-P. Finet, *Tetrahedron* **1988**, *44*, 3039–3071.
- [113] D. H. Barton, N. Ozbalik, M. Ramesh, *Tetrahedron* **1988**, *44*, 5661–5668.
- [114] J. P. Finet, *Chem. Rev.* **1989**, *89*, 1487–1501.
- [115] T. Arnauld, D. H. Barton, E. Doris, *Tetrahedron* **1997**, *53*, 4137–4144.
- [116] T. Arnauld, D. H. R. Barton, J. F. Normant, E. Doris, *J. Org. Chem.* **1999**, *64*, 6915–6917.
- [117] T. Ooi, R. Goto, K. Maruoka, *J. Am. Chem. Soc.* **2003**, *125*, 10494–10495.
- [118] P. K. Koech, M. J. Krische, *J. Am. Chem. Soc.* **2004**, *126*, 5350–5351.
- [119] P. N. Riley, M. G. Thorn, J. S. Vilaro, M. A. Lockwood, P. E. Fanwick, I. P. Rothwell, *Organometallics* **1999**, *18*, 3016–3024.
- [120] D. H. Barton, J.-P. Finet, C. Giannotti, F. Halley, *Tetrahedron* **1988**, *44*, 4483–4494.
- [121] S. David, A. Thiéffry, *Tetrahedron Lett.* **1981**, *22*, 2885–2888.
- [122] J. C. Anderson, R. Cubbon, M. Harding, D. S. James, *Tetrahedron Asymmetry* **1998**, *9*, 3461–3490.

- [123] K. Ikegai, Y. Nagata, T. Mukaiyama, *Bull. Chem. Soc. Jpn.* **2006**, *79*, 761–767.
- [124] M. Goswami, A. Ellern, N. L. B. Pohl, *Angew. Chem. Int. Ed.* **2013**, *52*, 8441–8445.
- [125] A. Y. Fedorov, J. P. Finet, *J. Chem. Soc. Trans. 1* **2000**, 3775–3778.
- [126] W.-Q. Zhang, X.-L. Wang, G.-C. Liu, L. Chen, Y.-Z. Wang, *RSC Adv.* **2016**, *6*, 84284–84293.
- [127] P. I. O’Daniel, Z. Peng, H. Pi, S. A. Testero, D. Ding, E. Spink, E. Leemans, M. A. Boudreau, T. Yamaguchi, V. A. Schroeder, W. R. Wolter, L. I. Llarrull, W. Song, E. Lastochkin, M. Kumarasiri, N. T. Antunes, M. Espahbodi, K. Lichtenwalter, M. A. Suckow, S. Vakulenko, S. Mobashery, M. Chang, *J. Am. Chem. Soc.* **2014**, *136*, 3664–3672.
- [128] B. Sreedhar, R. Arundhathi, P. L. Reddy, M. L. Kantam, *J. Org. Chem.* **2009**, *74*, 7951–7954.
- [129] S. Verma, N. Kumar, S. L. Jain, *Tetrahedron Lett.* **2012**, *53*, 4665–4668.
- [130] D. Saberi, M. Sheykhan, K. Niknam, A. Heydari, *Catal. Sci. Technol.* **2013**, *3*, 2025.
- [131] M. Palucki, S. L. Buchwald, *J. Am. Chem. Soc.* **1997**, *119*, 11108–11109.
- [132] X. Liao, Z. Weng, J. F. Hartwig, *J. Am. Chem. Soc.* **2008**, *130*, 195–200.
- [133] D. A. Culkin, J. F. Hartwig, *Acc. Chem. Res.* **2003**, *36*, 234–245.
- [134] M. Matsushita, K. Kamata, K. Yamaguchi, N. Mizuno, *J. Am. Chem. Soc.* **2005**, *127*, 6632–6640.
- [135] T. Sakamoto, H. Yonehara, C. Pac, *J. Org. Chem.* **1994**, *59*, 6859–6861.
- [136] Y. Zhang, Y. Lv, X. Wang, A. Peng, K. Zhang, X. Jie, J. Huang, Z. Tian, *Anal. Chem.* **2018**, *90*, 5481–5488.
- [137] P. B. Arockiam, C. Bruneau, P. H. Dixneuf, *Chem. Rev.* **2012**, *112*, 5879–5918.
- [138] X. Qian, J. Han, L. Wang, *Tetrahedron Lett.* **2016**, *57*, 607–610.
- [139] D. H. R. Barton in *Ligand Coupling React. with Heteroatomic Compd.* (Ed.: Finet), Elsevier Science, 1st ed., **1998**, Chapter 6, pp. 159–204.
- [140] K. Ohkata, S. Takemoto, M. Ohnishi, K.-Y. Akiba, *Tetrahedron Lett.* **1989**, *30*, 4841–4844.
- [141] T. Fuchigami, M. Miyazaki, *Electrochim. Acta* **1997**, *42*, 1979–1984.
- [142] N. G. Connelly, W. E. Geiger, *Chem. Rev.* **1996**, *96*, 877–910.
- [143] G. Gritzner, J. Kuta, *Pure Appl. Chem.* **1984**, *56*, 955–966.
- [144] D. A. C. Brownson, C. E. Banks in *Handb. Graphene Electrochem.*, Springer London, London, **2014**, pp. 23–77.
- [145] A. McKillop, W. R. Sanderson, *Tetrahedron* **1995**, *51*, 6145–6166.
- [146] D. H. R. Barton, J.-P. Finet, C. Giannotti, F. Halley, *J. Chem. Soc. Perkin Trans. 1* **1987**, 241.

- [147] C. Hansch, A. Leo, R. W. Taft, *Chem. Rev.* **1991**, *91*, 165–195.
- [148] D. H. R. Barton, J.-C. Blazejewski, B. Charpiot, J.-P. Finet, W. B. Motherwell, M. T. B. Papoula, S. P. Stanforth, *J. Chem. Soc. Perkin Trans. 1* **1985**, 2667–2675.
- [149] D. H. R. Barton, J. Finet, *Pure Appl. Chem.* **1987**, *59*, 937–946.
- [150] A. Fedorov, S. Combes, J. P. Finet, *Tetrahedron* **1999**, *55*, 1341–1352.
- [151] W. Clegg, R. J. Errington, G. A. Fisher, D. C. R. Hockless, N. C. Norman, A. G. Orpen, S. E. Stratford, *J. Chem. Soc. Dalt. Trans.* **1992**, *671*, 1967–1974.
- [152] C. C. Carres, S. Guccione, *Organometallics* **2008**, *27*, 747–752.
- [153] M. Khodadadi-Moghaddam, A. Habibi-Yangjeh, M. R. Gholami, *J. Mol. Catal. A Chem.* **2009**, *306*, 11–16.
- [154] M. Sheehan, P. Sharratt, *Org. Process Res. Dev.* **1999**, *3*, 471–475.
- [155] G. Cainelli, P. Galletti, D. Giacomini, *Chem. Soc. Rev.* **2009**, *38*, 990–1001.
- [156] G. I. Elliott, J. P. Konopelski, *Tetrahedron* **2001**, *57*, 5683–5705.
- [157] D. H. R. Barton, J.-C. Blazejewski, B. Charpiot, D. J. Lester, W. B. Motherwell, M. T. B. Papoula, *J. Chem. Soc. Chem. Commun.* **1980**, 827–829.
- [158] D. H. R. Barton, J.-P. Finet, W. B. Motherwell, C. Pichon, *J. Chem. Soc. Perkin Trans. 1* **1987**, *43*, 251.
- [159] F. Challenger, J. F. Wilkinson, *J. Chem. Soc. Trans.* **1922**, *121*, 91.
- [160] A. D. Beveridge, G. S. Harris, *J. Chem. Soc.* **1966**, 520.
- [161] R. D. Shannon, *Acta Crystallogr. Sect. A* **1976**, *32*, 751–767.
- [162] F. Eckert, I. Leito, I. Kaljurand, A. Kütt, A. Klamt, M. Diedenhofen, *J. Comput. Chem.* **2009**, *30*, 799–810.
- [163] I. Ugi, D. Marquarding, H. Klusacek, P. Gillespie, F. Ramirez, *Acc. Chem. Res.* **1971**, *4*, 288–296.
- [164] R. G. Pearson, *Inorg. Chem.* **1988**, *27*, 734–740.
- [165] L. K. Rasmussen, M. Begtrup, T. Ruhland, *J. Org. Chem.* **2006**, *71*, 1230–1232.
- [166] Y. Matano, S. A. Begum, T. Miyamatsu, H. Suzuki, *Organometallics* **1999**, *18*, 5668–5681.
- [167] V. Stavila, J. H. Thurston, D. Prieto-Centurión, K. H. Whitmire, *Organometallics* **2007**, *26*, 6864–6866.
- [168] L. Dostál, R. Jambor, A. Růžicka, R. Jirásko, A. Lyčka, J. Beckmann, S. Ketkov, *Inorg. Chem.* **2015**, *54*, 6010–6019.
- [169] B. P. Carrow, J. F. Hartwig, *J. Am. Chem. Soc.* **2011**, *133*, 2116–2119.
- [170] J. J. Dunsford, E. R. Clark, M. J. Ingleson, *Dalton Trans.* **2015**, *44*, 20577–83.
- [171] M. Carraro, M. Gardan, A. Sartorel, C. Maccato, M. Bonchio, *Dalton Trans.* **2016**, *45*, 14544–14548.

- [172] H. Weingärtner, *Angew. Chem. Int. Ed.* **2008**, *47*, 654–670.
- [173] C. M. Alder, J. D. Hayler, R. K. Henderson, A. M. Redman, L. Shukla, L. E. Shuster, H. F. Sneddon, *Green Chem.* **2016**, *18*, 3879–3890.
- [174] G. Faraglia, *J. Organomet. Chem.* **1969**, *20*, 99–104.
- [175] W. Clegg, R. J. Errington, G. A. Fisher, R. J. Flynn, N. C. Norman, *J. Chem. Soc. Dalt. Trans.* **1993**, *608*, 637.
- [176] G. Stavber, M. Zupan, M. Jereb, S. Stavber, *Org. Lett.* **2004**, *6*, 4973–4976.
- [177] X. S. Xue, Y. Wang, M. Li, J. P. Cheng, *J. Org. Chem.* **2016**, *81*, 4280–4289.
- [178] P. T. Cleve, *Ber. Dtsch. Chem. Ges.* **1888**, *21*, 891–896.
- [179] H. E. Armstrong, E. C. Rossiter, *Chem. News J. Ind. Sci.* **1889**, *59*, 225–226.
- [180] Z. Lu, Q. Li, M. Tang, P. Jiang, H. Zheng, X. Yang, *Chem. Commun.* **2015**, *51*, 14852–14855.
- [181] M. D. Cowart, P. A. Bhatja, J. F. . Daanen, A. Stewart, M. Patel, T. Kolasa, J. D. . Brioni, J. Rohde, K. M. Engstrom, *Benzimidazoles that are useful in treating sexual dysfunction*, **2003**.
- [182] K. V. Rajendran, D. J. Carr, D. G. Gilheany, *Tetrahedron Lett.* **2011**, *52*, 7113–7115.
- [183] T. Arnauld, D. H. Barton, E. Doris, *Tetrahedron Lett.* **1997**, *38*, 365–366.
- [184] I. Kumar, P. Bhattacharya, K. H. Whitmire, *Organometallics* **2014**, *33*, 2906–2909.
- [185] A. E. Wendlandt, S. S. Stahl, *Angew. Chem. Int. Ed.* **2015**, *54*, 14638–14658.
- [186] S. Fukuzumi, K. Ohkubo, *Org. Biomol. Chem.* **2014**, *12*, 6059–6071.
- [187] A. Yoshimura, V. V. Zhdankin, *Chem. Rev.* **2016**, *116*, 3328–3435.
- [188] A. Toma, C. I. Raț, A. Silvestru, T. Rüffer, H. Lang, M. Mehring, *J. Organomet. Chem.* **2016**, *806*, 5–11.
- [189] J. Luan, L. Zhang, Z. Hu, *Molecules* **2011**, *16*, 4191–4230.
- [190] M. Minoura, Y. Kanamori, A. Miyake, K.-y. Akiba, *Chem. Lett.* **1999**, *28*, 861–862.
- [191] N. Sakurai, T. Mukaiyama, *Chem. Lett.* **2007**, *36*, 928–929.
- [192] J. P. Finet, A. Y. Fedorov, *Russ. Chem. Bull.* **2004**, *53*, 1488–1495.
- [193] D. V. Moiseev, Y. B. Malysheva, A. S. Shavyrin, Y. a. Kurskii, A. V. Gushchin, *J. Organomet. Chem.* **2005**, *690*, 3652–3663.
- [194] C. J. Carmalt, A. H. Cowley, A. Decken, Y. G. Lawson, N. C. Norman, *Organometallics* **1996**, *15*, 887–890.
- [195] A. Schmuck, K. Seppelt, *Chem. Ber.* **1989**, *122*, 803–808.
- [196] S. Shimada, O. Yamazaki, T. Tanaka, Y. Suzuki, M. Tanaka, *J. Organomet. Chem.* **2004**, *689*, 3012–3023.
- [197] H. Suzuki, T. Murafuji, N. Azuma, *J. Chem. Soc. Perkin Trans. 1* **1992**, *377*, 1593.

- [198] T. Murafuji, K. Kitagawa, D. Yoshimatsu, K. Kondo, K. Ishiguro, R. Tsunashima, I. Miyakawa, Y. Mikata, *Eur. J. Med. Chem.* **2013**, *63*, 531–535.
- [199] B. T. Worrell, S. P. Ellery, V. V. Fokin, *Angew. Chem. Int. Ed.* **2013**, *52*, 13037–13041.
- [200] G. Becker, J. Egner, M. Meiser, O. Mundt, J. Weidlein, *Z. Anorg. Allg. Chem.* **1997**, *623*, 941–956.
- [201] S. Sasaki, K. Sutoh, F. Murakami, M. Yoshifuji, *J. Am. Chem. Soc.* **2002**, *124*, 14830–14831.
- [202] A. M. Preda, W. B. Schneider, M. Rainer, T. Ruffer, D. Schaarschmidt, H. Lang, M. Mehring, *Dalton Trans.* **2017**, *46*, 8269–8278.
- [203] P. J. Sinclair, J. Goulet, F. Wong, M. Goulet, W. H. Parsons, M. J. Wyvratt, *D-heteroaryl, O-alkylheteroaryl, O-alkenylheteroaryl and O-alkynylheteroarylmacrolides having immunosuppressive activity*, **1993**.
- [204] P. Petiot, A. Gagnon, *Eur. J. Org. Chem.* **2013**, 5282–5289.
- [205] M. M. Nad, T. K. Kozminskaya, K. A. Kocheshkov, *Russ. J. Appl. Chem.* **1946**, *16*, 897 – 900.
- [206] S. Shimada, J. Maruyama, Y. K. Choe, T. Yamashita, *Chem. Commun.* **2009**, *54*, 6168–6170.
- [207] A. J. Lennox, G. C. Lloyd-Jones, *Angew. Chem. Int. Ed.* **2013**, *52*, 7362–7370.
- [208] A. A. Thomas, S. E. Denmark, *Science* **2016**, *352*, 329–332.
- [209] Y. Yamamoto, H. Matsubara, H. Yorimitsu, A. Osuka, *ChemCatChem* **2016**, *8*, 2317–2320.
- [210] H. Chen, J. F. Hartwig, *Angew. Chem. Int. Ed.* **1999**, *38*, 3391–3393.
- [211] M. Murata, T. Oyama, S. Watanabe, Y. Masuda, *J. Org. Chem.* **2000**, *65*, 164–168.
- [212] J. W. B. Fyfe, N. J. Fazakerley, A. J. B. Watson, *Angew. Chem. Int. Ed.* **2017**, *56*, 1249–1253.
- [213] C. C. C. Johansson Seechurn, M. O. Kitching, T. J. Colacot, V. Snieckus, *Angew. Chem. Int. Ed.* **2012**, *51*, 5062–5085.
- [214] J. P. Wan, L. Gan, Y. Liu, *Org. Biomol. Chem.* **2017**, *15*, 9031–9043.
- [215] J. C. Colbert, R. M. Lacy, *J. Am. Chem. Soc.* **1946**, *68*, 270–271.
- [216] H.-F. Hou, R. K. Peddinti, C.-C. Liao, *Org. Lett.* **2002**, *4*, 2477–2480.
- [217] A. Ozanne-Beaudenon, S. Quideau, *Angew. Chem. Int. Ed.* **2005**, *44*, 7065–7069.
- [218] G. K. S. Prakash, T. Mathew, C. Panja, G. a. Olah, *J. Org. Chem.* **2007**, *72*, 5847–5850.
- [219] H. Suzuki, T. Ikegami, Y. Matano, *Tetrahedron Lett.* **1994**, *35*, 8197–8200.
- [220] Y. Matano, H. Nomura, T. Hisanaga, H. Nakano, M. Shiro, H. Imahori, *Organometallics* **2004**, *23*, 5471–5480.

- [221] H.-J. Gais, *Organosulfur Chemistry in Asymmetric Synthesis*, Wiley, **2008**, pp. 375–398.
- [222] J. Z. Wang, J. Zhou, C. Xu, H. Sun, L. Kürti, Q. L. Xu, *J. Am. Chem. Soc.* **2016**, *138*, 5202–5205.
- [223] J. Luo, S. Preciado, I. Larrosa, *J. Am. Chem. Soc.* **2014**, *136*, 4109–4112.
- [224] L. Wan, N. Dastbaravardeh, G. Li, J.-Q. Yu, *J. Am. Chem. Soc.* **2013**, *135*, 18056–18059.
- [225] M. Wada, S. Natsume, S. Suzuki, U. Akira, M. Nakamura, S. Hayase, T. Erabi, *J. Organomet. Chem.* **1997**, *548*, 223–227.
- [226] A. M. Preda, M. Krasowska, L. Wrobel, P. Kitschke, P. C. Andrews, J. G. MacLellan, L. Mertens, M. Korb, T. Rüffer, H. Lang, A. A. Auer, M. Mehring, *Beilstein J. Org. Chem.* **2018**, *14*, 2125–2145.
- [227] C. Ludwig, M. Dolny, H.-J. Götze, *Spectrochim. Acta Part A Mol. Biomol. Spectrosc.* **1997**, *53*, 2363–2372.
- [228] N. Riemer, C. Coswig, M. Shipman, B. Schmidt, *Synlett* **2018**, *29*, 2427–2431.
- [229] T.-H. Lee, J. Jayakumar, C.-H. Cheng, S.-C. Chuang, *Chem. Commun.* **2013**, *49*, 11797–11799.
- [230] M. Bourgotte, J.-F. Delhomel, M. Dubernet, M.-H. Gouy, *Derivatives of 6-substituted triazolopyridazines as REV-ERB agonists*, **2013**.
- [231] Z. Gao, Y. H. Lim, M. Tredwell, L. Li, S. Verhoog, M. Hopkinson, W. Kaluza, T. L. Collier, J. Passchier, M. Huiban, V. Gouverneur, *Angew. Chem. Int. Ed.* **2012**, *51*, 6733–6737.
- [232] K. Manabe, S. Ishikawa, *Synthesis* **2008**, *2008*, 2645–2649.
- [233] J. Hofmann, T. Clark, M. R. Heinrich, *J. Org. Chem.* **2016**, *81*, 9785–9791.
- [234] X. Bao, Y. Jin, X. Liu, H. Liao, L. Zhang, T. Pang, *RSC Adv.* **2014**, *4*, 6761.
- [235] E. Buck, Z. J. Song, D. Tschaen, P. G. Dormer, R. P. Volante, P. J. Reider, *Org. Lett.* **2002**, *4*, 1623–1626.
- [236] L. Liu, J. Tang, J. Qiang, J. Li, M. He, *J. Chem. Res.* **2016**, *40*, 261–264.
- [237] H. Zeng, D. Cao, Z. Qiu, C.-J. Li, *Angew. Chem. Int. Ed.* **2018**, *57*, 3752–3757.
- [238] D. Best, M. Jean, P. Van De Weghe, *J. Org. Chem.* **2016**, *81*, 7760–7770.
- [239] L. Navarro, M. D. Pujol, *Tetrahedron Lett.* **2015**, *56*, 1812–1815.
- [240] S. K. Dayal, R. W. Taft, *J. Am. Chem. Soc.* **1973**, *95*, 5595–5604.
- [241] M. Pichette Drapeau, T. Ollevier, M. Taillefer, *Chem. - A Eur. J.* **2014**, *20*, 5231–5236.
- [242] Q. Zhang, D. Wang, X. Wang, K. Ding, *J. Org. Chem.* **2009**, *74*, 7187–7190.
- [243] J. Chen, X. Wang, X. Zheng, J. Ding, M. Liu, H. Wu, *Tetrahedron* **2012**, *68*, 8905–8907.

- [244] I. W. Davies, J. F. Marcoux, J. T. Kuethe, M. D. Lankshear, J. D. O. Taylor, N. Tsou, P. G. Dormer, D. L. Hughes, K. N. Houk, V. Guner, *J. Org. Chem.* **2004**, *69*, 1298–1308.
- [245] H. Keipour, A. Hosseini, A. Afsari, R. Oladee, M. A. Khalilzadeh, T. Ollevier, *Can. J. Chem.* **2016**, *94*, 95–104.
- [246] Y. F. Wong, Z. Wang, J. Sun, *Org. Biomol. Chem.* **2016**, *14*, 5751–5754.
- [247] E. R. Biehl, A. R. Deshmukh, M. Dutt, *Synthesis* **1993**, *1993*, 885–888.
- [248] D. Verga, C. Percivalle, F. Doria, A. Porta, M. Freccero, *J. Org. Chem.* **2011**, *76*, 2319–2323.
- [249] H.-M. Kuo, I. Chu-Hsuan, H.-S. Sheu, C. K. Lai, *Tetrahedron* **2013**, *69*, 4226–4235.
- [250] T. Müller, K. Djanashvili, J. A. Peters, I. W. Arends, U. Hanefeld, *Zeitschrift für Naturforsch. B* **2015**, *70*, 587–595.
- [251] A. J. Lennox, G. C. Lloyd-Jones, *J. Am. Chem. Soc.* **2012**, *134*, 7431–7441.
- [252] R. Shintani, S. Isobe, M. Takeda, T. Hayashi, *Angew. Chem. Int. Ed.* **2010**, *49*, 3795–3798.
- [253] A. Tarui, E. Miyata, A. Tanaka, K. Sato, M. Omote, A. Ando, *Synlett* **2015**, *26*, 55–58.
- [254] Y. Yamamoto, M. Takizawa, X. Q. Yu, N. Miyaura, *Angew. Chem. Int. Ed.* **2008**, *47*, 928–931.
- [255] A. F. Asachenko, K. R. Sorochkina, P. B. Dzhevakov, M. A. Topchiy, M. S. Nechaev, *Adv. Synth. Catal.* **2013**, *355*, 3553–3557.
- [256] H. Weidmann, H. Jr K. Z Immerman, *Liebigs Ann.* **1958**, *619*, 28–35.
- [257] S. Asghar, S. B. Tailor, D. Elorriaga, R. B. Bedford, *Angew. Chem. Int. Ed.* **2017**, *56*, 16367–16370.
- [258] N. Amishiro, T. Atumi, T. Nakazato, H. Umehara, H. Fujihara, F. Shinohara, J. Funahashi, J. Yamamoto, K. Yagi, *JAK Inhibitor*, **2009**.
- [259] N. Krogsgaard-Larsen, C. G. Delgar, K. Koch, P. M. G. E. Brown, C. Møller, L. Han, T. H. V. Huynh, S. W. Hansen, B. Nielsen, D. Bowie, D. S. Pickering, J. S. Kastrop, K. Frydenvang, L. Bunch, *J. Med. Chem.* **2017**, *60*, 441–457.